RMIT UNIVERSITY

The Rheological Behaviour of Aerated Sludge

A thesis submitted in fulfilment of the requirements for the degree of Doctor of Philosophy by

Veena Bobade

School of Engineering

College of Science, Engineering and Health

RMIT University

December 2018

DECLARATION

I certify that except where due acknowledgement has been made, the work is that of the author alone; the work has not been submitted previously, in whole or in part, to qualify for any other academic award; the content of the thesis is the result of work which has been carried out since the official commencement date of the approved research program; any editorial work, paid or unpaid, carried out by a third party is acknowledged; and, ethics procedures and guidelines have been followed.

I acknowledge the support I have received for my research through the provision of an Australian Government Research Training Program Scholarship.

Veena Bobade
13/12/18

ACKNOWLEDGEMENTS

Firstly, I would like to express my sincere and deep gratitude to my principal supervisor, A/Prof. Nicky Eshtiaghi, who gave me the opportunity to do a PhD and provided critical feedback and dedicated support at every stage of my PhD. I am also grateful to Prof. Geoffrey Evans (Newcastle University) and Dr Jean-Christophe Baudez (IRSTEA, France), my co-supervisors, for their insightful comments, thoughtful advice and positive criticism. My research would not have been accomplished without the continuous support of each and every member of my supervisory team.

I am grateful for the support I received from an Australian Government Research Training Program Scholarship, which made completing this project and thesis possible.

I would also like to thank the laboratory staff – Mr Mike Allan, Dr Babu Iyer, Dr Muthu Pannirselvam, Dr Zeyad Nasa, Mr Cameron Crombie and Mrs Peggy Chang – of RMIT's College of Science, Engineering and Health. Throughout my research program, they assisted me ably with various technical instruments and chemicals. I would like to extend my special thanks to Mr. James Barker from Scientex Australia for guiding me and helping me to set up the correct procedure for the surface tension measurement.

Many thanks to my fellow colleagues and former postgraduate students, Dr Ehsan Farno, Dr Biplob Pramanik, Kevin Hii, Deverpiran Vishak, Samira Miryahyaei, Pooja Takkalkar, Shruti Sakarka and Zubayeda Zahan, whose friendship and companionship helped to create an inspiring and fun environment in which to learn and grow.

Dr Campbell Aitken provided professional editing services in accordance with the Institute of Professional Editors' *Guidelines for editing research theses*.

I wish to offer my deepest gratitude to my parents and in-laws, who have loved me and motivated me continually. I would like to thank my husband, Vineet Bobade, to whom this thesis is dedicated. He knows that he is the person behind my success. I am indebted to his sacrifice and understanding. Last but not least, I would like to acknowledge the understanding and sacrifice of my son Vedant Bobade, which enabled me to complete my PhD on time. I am determined to make you proud and happy through my care, love and achievements.

PUBLICATIONS AND PRESENTATIONS DURING CANDIDATURE

JOURNAL PUBLICATIONS

1. **Bobade, V.,** Evans, G., Baudez, J.C. and Eshtiaghi, N. (2018) Impact of gas injection on physicochemical properties of waste activated sludge: A linear relationship between the change of viscoelastic properties and the change of other physiochemical properties. Water Research 144, 246-253 (*Top 5% in Water Science and Technology, 5Y-IF: 7.62, Q1 rank*)

2. **Bobade, V.**, Cheetham, M., Hashim, J. and Eshtiaghi, N. (2018) Influence of gas injection on viscous and viscoelastic properties of Xanthan gum. Water Research 134, 86-91 (*Top 5% in Water Science and Technology, 5Y-IF: 7.62, Q1 rank*)

3. **Bobade, V**., Baudez, J.-C., Evans, G. and Eshtiaghi, N. (2017) Impact of gas injection on the apparent viscosity and viscoelastic property of waste activated sewage sludge. Water Research 114, 296-307 (*Top 5% in Water Science and Technology, 5Y-IF: 7.62, Q1 rank*)

4. **Bobade, V.**, Evans, G. and Eshtiaghi, N. (2019) Bubble rise velocity and bubble size in thickened waste activated sludge: utilising electrical resistance tomography (ERT). Chemical Engineering Research and Design I 48, 119-128 (*5Y-IF: 3.08, Q1 rank*)

PEER-REVIEWED CONFERENCE PAPERS

1. **Bobade. V,** Baudez, J.-C., Evans, G. and Eshtiaghi, N. (2017) Estimation of change in Waste activated sludge rheological properties and sludge surface properties at different gas flow rates. Asian Pacific Confederation of Chemical Engineering (APCChE & Chemeca 2017), Melbourne, 23–28 July.

2. **Bobade, V**., Baudez, J.-C., Evans, G. and Eshtiaghi, N. (2016), Impact of gas injection on the viscosity of waste activated sludge. Chemical Engineering – Regeneration, Recovery and Reinvention (Chemeca 2016), Adelaide, 25–28 September.

CONFERENCE PRESENTATIONS

1. Eshtiaghi, N., **Bobade, V.**, Baudez, J.-C. and Evans, G. (2016) Real time monitoring of the sludge rheology during gas mixing using commercial rheometer. Specialized Conference on Small Water and Wastewater Systems 2016, Athens, 14–16 September.
2. **Bobade, V.**, Baudez, J.-C., Evans, G. and Eshtiaghi, N. (2016) Impact of gas injection on the liquid and solid behaviour of waste activated sewage sludge. WETT HDR Symposium, 25th November, Melbourne.
3. Eshtiaghi, N., **Bobade. V.**, Baudez, J.-C. and Evans, G. (2017) The effect of aeration intensity on sludge rheological properties. IWA World Conference on Anaerobic Digestion 2017, Beijing, 17–20 October.
4. **Bobade, V.**, Baudez, J.-C., Evans, G. and Eshtiaghi, N. (2017) Monitoring elasticity of sludge as a measure for the changes in sludge physical properties. 9th Australian–Korean Rheology Conference, Sydney, 29 November – 1 December.
5. **Bobade, V.**, Baudez, J.-C., Evans, G. and Eshtiaghi, N. (2018) Monitoring rheology as a tool for measuring the effective shear rate in the bubble columns. 6th International Conference on Sustainable Solid Waste Management 2018, Naxos, 13–16 June.
6. Eshtiaghi, N., **Bobade, V.**, Baudez, J.-C. and Evans, G. (2018) Impact of gas injection on flow and physicochemical properties of municipal sewage sludge. 7th International Symposium on Energy from Biomass and Waste 2018, Venice, 15–18 October.
7. **Bobade V**, Baudez, J.-C., Evans, G. and Eshtiaghi, N. (2018) Impact of gas injection on flow, physicochemical and gas phase characteristics of municipal sewage sludge. WETT HDR Symposium, 14th November, Melbourne. (*Best Oral Presentation Award*).

NOMENCLATURE

C_D	Drag coefficient
COD	Chemical Oxygen Demand (mg/L)
CMC	Carboxy methyl cellulose
d_b	Bubble diameter (mm)
dh	Bubble horizontal diameter (mm)
DAS	Data acquisition system
DGD	Dynamic gas disengagement
DO	Dissolved Oxygen (mg/L)
Ec	cohesion energy
ECT	Electrical capacitance tomography
EIT	Electrical impedance tomography
EPS	Extracellular polymeric substances
ERT	Electrical resistance tomography
ESEM	Environmental scanning electron microscope
G	Young's modulus (Pa)
G'	Storage modulus (Pa)
G"	Loss modulus (Pa)
H	Height of the column (m)
HB	Herschel–Bulkley
mN/m	Unit of surface tension (mill newton / meter)
K	Consistency index ($Pa.s^n$)
kcps	Unit of intensity of beam (kilo counts per second)

LB-EPS	Loosely bound EPS
LPM	Unit of gas flow rate (litre per minute)
LVE	Linear viscoelastic region
M	Torque (N.m)
n	Flow behaviour index
P	Power input (W)
Pa	Pascal
psi	pounds per square inch
R_e	Reynolds number
rpm	Revolutions per minute
sCOD	Soluble chemical oxygen demand (mg/L)
sMBR	Submerged membrane bioreactor
SMP	Soluble microbial products
SRT	Sludge retention time
SVI	Sludge volume index
t	Time (s)
Torr	Unit of pressure (1 Torr = 133.32Pa)
TS	Total solids (g/L) & (wt%)
TSS	Total suspended solids (mg/L)
u_b	Bubble rise velocity (m/s)
u_g	Gas superficial velocity (m/s)
v	Volume (m^3)
WAS	Waste activated sludge

Greek Letters

ρ	Density kg/m3
τ	Shear stress (Pa)
τ_o	Yield stress (Pa)
γ	Strain (%)
$\dot{\gamma}$	Shear rate (s^{-1})
Ω	Angular velocity (rad/s)
$\sigma_{imposed}$	Stress imposed by gas injection (Pa)
μ	Viscosity (Pa.s)
μ_{eff}	Effective viscosity (Pa.s)
g	Acceleration due to gravity, 9.81 m/s^2
ε_g	Gas holdup (-)
σ_1	Conductivity of continuous phase (µS/cm)
σ_2	Conductivity of dispersed phase (µS/cm)
σ_{mc}	Average reconstructed conductivity by ERT measurements (µS/cm)
ζ	Zeta potential (mv)
Tan (δ)	Tan delta (ratio of G"/G') (-)

SUMMARY

Sludge is the semi-solid residual material from wastewater treatment. Biological activated sludge treatment is the most widely used wastewater treatment process, due to numerous benefits such as high efficiency and low operating cost. During activated sludge treatment, the sludge feed is mixed with aerobic microorganisms in an aeration tank. Air provides oxygen to the microorganism to help it to break down complex organic compounds into carbon dioxide and water, thereby reducing sludge volume. Gas bubbles rising through the liquid improve mixing in the treatment tank and enhance biological reactions. This reduction in inhomogeneity, in turn, increases efficiency and reduces energy consumption.

In an aeration tank in a conventional process, the typical solids content range is 1.5–5.0 g/L. However, population growth and improved living standards have driven exponential growth in wastewater production, necessitating treatment of waste with higher solids content. This study was designed to reveal how gas injection affects concentrated sludge rheology in a solids content range of 30–55 g/L, and whether any relationship between the rheology and physicochemical properties of sludge and gas phase characteristics exists.

Waste activated sludge (WAS) is composed of water, microorganisms, and macromolecules grouped in bioflocs. Hence its structure depends on many factors; it can change substantially when exposed to shear stress and is known to exhibit shear thinning behaviour. Consequently, rheology plays a crucial role in optimising and designing aeration systems. Aeration causes fluctuations in shear that affects sludge rheology and mixing hydrodynamics and oxygen transfer. Thus, it is essential to understand the effect of shear induced by gas injection on sludge characteristics to optimise both the reactors and separators, and how and why the rheology of waste activated sludge changes during gas injection with regard to variation in gas flow rate and concentration, both in the non-linear (flow) regime and in the linear viscoelastic regime. Moreover, rising bubbles, gas holdup, bubble rise velocity and bubble size affect oxygen transfer efficiency in the aeration tank. Therefore, it is also important to know how the change in gas flow rate affects the gas holdup, bubble size distribution and bubble rise velocity in waste activated

sludge with different solid content so that waste activated sludge treatment can be optimised.

In the first study within this PhD project (study 1), the objective was to understand how the rheology of waste activated sludge in the non-linear region (the change of apparent viscosity vs shear rate) changes during gas injection with regard to variation in gas flow rate and solid concentration of sludge. To understand the impact of gas injection on flow behaviour, a flow curve was measured for sludge with a total solids content of 30 g/L and with a gas flow rate of 0.5 L/min and 3 L/min before and after gas injection. The flow curve measurement was carried out using both in situ (while injecting the gas) and after sparging methods (after 20 mins of gas injection). The impact of gas injection on the apparent viscosity of sludge was investigated because viscosity is closely related to mass transfer efficiency in the aeration tank. The result showed that the in situ method of yield stress fluid analysis is inappropriate, because it only allows measurement at the interface, not within the material, because gas cushioning causes slippage that leads to inaccurate rheological data. However, the after sparging method proved more reliable, showed negligible impact of gas injection on the apparent viscosity of the sludge. For example, the apparent viscosity of 30 g/L of total solids content, for a shear rate range of 0.1 s^{-1} to 50 s^{-1} for no gas and after sparging gas at 0.5 L/min and 3 L/min, was in the range of 0.3 Pa.s to 44 Pa.s for no gas and after injecting gas.

Since gas injection had negligible impact on apparent viscosity, it was essential to understand its effect on the viscoelastic properties of sludge. Therefore, in study 2 the researcher aimed to understand how rheology of waste activated sludge in the linear viscoelastic region changes during gas injection with regard to variation in gas flow rate and concentration. The impact of gas injection on the viscoelastic properties (storage modulus and loss modulus) of sludge was measured by carrying out creep tests and time sweep measurement of sludge for no gas and after gas injection for 20 mins at very low stress and strain (at 1 Hz frequency). Experiments were performed using 42 g/L total solids of waste activated sludge at gas flow rates of 0.5 L/min and 1.5 L/min. The creep test result showed that increasing gas injection from no gas to 0.5 L/min increased the strain by 40%. Further increase in the gas injection rate to 1.5 L/min increased the strain by 84% over the no gas creep curve, indicating the structure was weakening with gas injection.

Similarly, the time sweep test result showed that increasing gas injection reduced the elastic modulus of sludge by 23% at 0.5 L/min and by 35% at 1.5 L/min compared to the no gas time sweep. This change in an elastic property of the fluid is an indication of the change in sludge structure due to gas injection, which was further evident through environmental scanning electron microscope (ESEM) images as cracks appearing in the sludge structure. To evaluate the stress imposed by gas injection, the successive creep and dynamic measurement (time sweep) of non-aerated 42 g/L sludge was repeated with a broader stress (1 to1.5Pa) and strain (0.1 to 0.5%) range at 1 Hz frequency. The researcher compared the response of aerated and unaerated sludge samples (42 g/L total solids concentration of WAS) through creep and time sweep tests and determined the extent of additional stress induced by gas injection. Analysis of creep and time sweep data showed that gas injection rates of 0.5 L/min and 1.5 L/min imposed stress of 0.1 Pa and 0.3 Pa, respectively. Thus, a technique for finding an unaerated simulant to an aerated system with a similar elastic property was established. Overall, the results suggested that although gas bubbling induces extra shear, it does not break down the sludge's structure sufficiently to reduce apparent viscosity significantly. However, the effect of bubbles on the viscoelastic property of sludge is substantial.

It was hypothesised that the rheological changes in the viscoelastic region induced by gas injection occur due to change in suspended solids, organic matter solubilisation (sCOD), surface tension and zeta potential. In study three, the researcher sought to understand the correlation between the imposed stress and the physical properties of sludge. Suspended solids, zeta potential, surface tension, sCOD and the viscoelastic property of sludge were measured at different concentrations of WAS (30 to 55 g/L) and different gas flow rates (1 to 7 L/min). The results showed that the imposed stress increases with the increase in gas flow rate but decreases with the increase in the solid concentration of sludge. The stress imposed by gas injection also showed a direct relationship with gas velocity. Moreover, a linear correlation between the percentage changes in physical properties (suspended solids, zeta potential, surface tension and sCOD) and imposed stress was observed, confirming the hypothesis. A simple model based on sludge concentration and gas velocity was developed to predict the extra stress induced by gas injection.

The work to this point was mainly performed on sludge, which is an opaque system and hinders estimation of bubble behaviour (gas phase characteristics). Furthermore, the rheological behaviour of sludge changes over time because of ageing and microbial

activity. This cause variation in sludge viscosity and hampers process optimisation. Rheological properties affect the design parameters of treatment equipment and thus – potentially – energy consumption and operational costs. Thus, the objective of study 4 was to understand the behaviour of a simulating model fluid for sludge during gas injection. To understand the impact of gas injection on the model fluid (Xanthan gum), the rheological properties of Xanthan gum were measured using flow curves, time sweep and creep tests. Different concentrations of Xanthan gum (3 g/L to 6 g/L) and gas flow rates (0.5 L/min to 2 L/min) were used. The results showed that, in the flow region, increased gas flow rate caused negligible change in the apparent viscosity of Xanthan gum solution. However, in the linear viscoelastic region, the creep test and time sweep test proved that gas injection increases the storage and loss modulus, indicating the strengthening of molecular structure. Thus, for the first time, it was shown that, although Xanthan gum behaves similarly to sludge in the liquid regime, its behaviour is unlike that of sludge in the solid regime. This means Xanthan gum is unsuitable as a model fluid for sludge under gas injection below the yield stress point.

Following on from study 4, the objective of study 5 was to learn how and why the change in gas flow rate and concentration affects the gas holdup, bubble size and bubble rise velocity (and hence the oxygen transfer efficiency in the aeration tank) in waste activated sludge. The gas phase characteristics of thickened sludge with total solids content of 30 g/L and 55 g/L at gas flow rates of 1–7 L/min were measured using electrical resistance tomography (ERT) and a dynamic gas disengagement method. The results showed that gas holdup, bubble rise velocity, and bubble size have natural log, linear, and exponential relationships (respectively) to the stress imposed by gas injection.

The outcomes of this research give new insight into the design and optimisation of the WAS aeration process as reducing energy consumption, optimising loading rate and increasing process performance through better oxygen transfer efficiency are closely linked to the gas phase characteristics of sludge. This work is novel and has considerable potential for use in the design of wastewater treatment plants.

TABLE OF CONTENTS

LIST OF FIGURES

LIST OF TABLES

CHAPTER 1: INTRODUCTION

1.1 PROJECT BACKGROUND

Growing awareness about the environment and increasingly stringent environmental regulations, population and global economic growth, industrial development and urbanisation have resulted in an increasing volume of sludge and intensification of current wastewater treatment plant. Finding ways to improve our ability to treat sludge at higher solid concentration is therefore increasingly important.

Sludge is generated in wastewater treatment plants as settled solids and biological cell mass, produced during primary treatment and secondary treatment respectively. Secondary treatment processes (i.e. membrane bioreactor and conventional activated sludge systems) experience considerable fluctuations in shear through fine bubble aeration (De Temmerman et al. 2015). The resulting instabilities in shear may affect sludge rheology (e.g. viscosity) and therefore the efficiency of sludge pumping (i.e. recycle flows), bioreactor hydrodynamics (i.e. mixing), oxygen transfer, secondary settler (or separator) hydrodynamics, membrane filtration and sludge dewaterability (Ratkovich et al. 2013). Thus, it is crucial to understand the effect of shear induced by gas injection on sludge characteristics to optimise both the bioreactors and separators.

Seyssiecq et al. (2008) considered the effect of aeration rate on the apparent viscosity of waste activated sludge (WAS) when performing an in situ rheological characterisation of sludge in aeration bioreactors with total solids (TS) ranging from 10 to 35g/L. The experiment demonstrated an overall decrease in the shear-thinning properties of aerated sludge compared to non-aerated sludge, with a plateau at a high aeration rate. This suggests that gas injection strongly influences the rheological behaviour of sludge. Although there are some studies on the impact of concentration, temperature (Farno et al. 2015a, Hii et al. 2017), pH (Hong et al. 2016, Tixier et al. 2003b), and change in pH (Tixier et al. 2003b) on the rheology of waste activated and digested sludge, little research has been conducted on the effect of gas injection on waste activated sludge rheology. Furthermore, few researchers have studied the influence of gas injection on gas holdup, bubble rise velocity and bubble size in sludge at low concentrations ($\leq 2\%$) (Babaei et al. 2015a, b), and no work has been done on concentrated sludge.

Knowledge of bubble properties, including bubble rise velocity, bubble size and gas holdup, is vital for the proper design and operation of bubble columns in wastewater treatment plants. Moreover, they have a crucial role in enabling calculation of the mass transfer rates (Anastasiou et al. 2013) and contact times of the gas and liquid phases, which impact on the performance of the equipment. However, the measurement of bubble size and bubble velocity in two and three-phase systems has always been a challenging problem (Ishkintana and Bennington 2010, Jin et al. 2007).

The primary objective of this research was to better understand the impact of gas injection on sludge rheology in both the linear viscoelastic region and non-linear region (flow region). In addition to the rheological investigation, changes in the physicochemical properties of the sludge were investigated to understand the reason for the change in sludge rheology with aeration and how it links to the physicochemical properties of sludge. The secondary objective of this study was to measure the gas phase properties in concentrated waste activated sludge and to investigate whether the rheological changes can be used to predict the gas phase properties and vice versa.

1.2 SCIENTIFIC OBJECTIVES AND RESEARCH QUESTIONS

This study focused on the rheology of waste activated sludge at different gas injection flow rates and different solids concentrations of sludge to understand its relationships with gas holdup, bubble rise velocity and bubble size. Its scientific and technological objectives were to:

1. Understand how and why the rheology of secondary sludge changes during gas injection with regard to variation in gas flow rate and concentration
2. Measure the extent of stress imposed by gas injection
3. Understand the influence of varying gas flow rates on sludge physicochemical properties at different solid concentrations
4. Determine the influence of varying gas flow rates and concentrations on gas holdup, bubble rise velocity and bubble size
5. Develop a mathematical model correlating the change in rheology with sludge physicochemical properties and gas phase characteristics (gas holdup, bubble rise velocity and bubble size) with regard to the change in sludge concentration and gas flow rate.

To achieve the abovementioned objectives, the research questions addressed in this thesis were:

1. How does a varying gas flow rate affect the rheology of waste activated sludge? What are the causes of these changes – are sludge structures modified due to gas injection?
2. How do changes in gas flow rate and concentration affect the physical characteristics of sludge?
3. Can a model fluid for sludge be used for visualisation and calculation of bubble rise velocity and bubble size and its correlations with the stress imposed by gas injection?
4. How and why does the change in gas flow rate and solid concentration of sludge affect gas holdup, bubble size and bubble rise velocity in waste activated sludge?
5. What type of model can predict the rheology of aerated sludge and its link to changes in physicochemical properties of sludge?

1.3 THESIS OUTLINE

Following this introductory chapter, chapter 2 presents a detailed review of the literature on rheology, sludge types, sludge treatment, and gas phase characteristics. It has specific emphasis on the impact of gas injection on sludge physicochemical properties, including rheology and gas phase properties.

Chapter 3 describes the materials and methods used in this project. It has three experimental design sections. The first section describes the experimental setup and procedure used for rheological measurements. The second section describes the experimental procedures used for measurement of physicochemical properties. The third section outlines the experimental procedure and setup used for gas phase characteristic (gas holdup, bubble rise velocity and bubble size) measurement. Following this, model development for calculation of effective shear rate is discussed.

Chapter 4 describes how gas injection affects the apparent viscosity and viscoelastic properties of waste activated sludge at two concentrations and gas flow rates. In addition, this chapter illustrates a new technique for finding an unaerated simulant of an aerated system using viscoelastic properties, thereby addressing research question 1. This chapter was published in Water Research in 2017 (volume 114, pp. 296-307).

Chapter 5 addresses research questions 2 and 5 in describing research on the impact of gas injection on the physicochemical properties of sludge. The chapter outlines the impact of four gas flow rates on the physicochemical properties of four concentrations of waste activated sludge. It describes the linear relationship between percentage changes in physicochemical and viscoelastic properties. In addition, it details a model developed for the stress imposed by gas injection based on sludge solids concentration and gas velocity. This chapter was published in Water Research in 2018 (volume 144, pp. 246-253).

Chapter 6 describes the research outcomes in relation to a model fluid of sludge (research question 3). Sludge is an opaque fluid, which hinders visual-based measurement; a transparent model fluid offers a way to understand its gas phase characteristics. The researcher sought to understand the change in Xanthan gum's rheological properties and determine its suitability as a simulant for aerated sludge. The impact of four gas flow rates on four concentrations of Xanthan gum is presented and discussed. This chapter was published in Water Research in 2018 (volume 134, pp. 86-91).

Chapter 7 addresses research question 4, describing the researcher's use of electrical resistance tomography for two concentrations of waste activated sludge and four gas flow rates. This chapter presents, for the first time, calculation of gas phase characteristics (bubble rise velocity, effective shear rate, and bubble diameter) using the Herschel-Bulkley model. The chapter also describes a direct relationship between the stress imposed and bubble rise velocity and bubble diameter. This chapter was published in Chemical Engineering Research and Design in 2019 (volume 48, pp. 119-128)

Chapter 8 highlights the potential for application of the knowledge developed in this project to industrial waste water treatment plants.

Chapter 9 provides the conclusions drawn from this study and recommendations for further work.

1.4 REFERENCES

Anastasiou, A.D., Passos, A.D. and Mouza, A.A. (2013) Bubble columns with fine pore sparger and non-Newtonian liquid phase: Prediction of gas holdup. Chemical Engineering Science 98, 331-338.

Babaei, R., Bonakdarpour, B. and Ein-Mozaffari, F. (2015a) Analysis of gas phase characteristics and mixing performance in an activated sludge bioreactor using electrical resistance tomography. Chemical Engineering Journal 279, 874-884.

Babaei, R., Bonakdarpour, B. and Ein-Mozaffari, F. (2015b) The use of electrical resistance tomography for the characterization of gas holdup inside a bubble column bioreactor containing activated sludge. Chemical Engineering Journal 268, 260-269.

De Temmerman, L., Maere, T., Temmink, H., Zwijnenburg, A. and Nopens, I. (2015) The effect of fine bubble aeration intensity on membrane bioreactor sludge characteristics and fouling. Water Research 76, 99-109.

Farno, E., Baudez, J.C., Parthasarathy, R. and Eshtiaghi, N. (2015) Impact of temperature and duration of thermal treatment on different concentrations of anaerobic digested sludge: Kinetic similarity of organic matter solubilisation and sludge rheology. Chemical Engineering Journal 273(0), 534-542.

Hii, K., Parthasarathy, R., Baroutian, S., Gapes, D.J. and Eshtiaghi, N. (2017) Rheological measurements as a tool for monitoring the performance of high pressure and high temperature treatment of sewage sludge. Water Research 114, 254-263.

Hong, E., Yeneneh, A.M., Kayaalp, A., Sen, T.K., Ang, H.M. and Kayaalp, M. (2016) Rheological characteristics of municipal thickened excess activated sludge (TEAS): impacts of pH, temperature, solid concentration and polymer dose. Research on Chemical Intermediates 42(8), 6567-6585.

Ishkintana, L.K. and Bennington, C.P.J. (2010) Gas holdup in pulp fibre suspensions: Gas voidage profiles in a batch-operated sparged tower. Chemical Engineering Science 65(8), 2569-2578.

Jin, H., Wang, M. and Williams, R.A. (2007) Analysis of bubble behaviors in bubble columns using electrical resistance tomography. Chemical Engineering Journal 130(2–3), 179-185.

Ratkovich, N., Horn, W., Helmus, F.P., Rosenberger, S., Naessens, W., Nopens, I. and Bentzen, T.R. (2013) Activated sludge rheology: A critical review on data collection and modelling. Water Research 47(2), 463-482.

Seyssiecq, I., Marrot, B., Djerroud, D. and Roche, N. (2008) In situ triphasic rheological characterisation of activated sludge, in an aerated bioreactor. Chemical Engineering Journal 142(1), 40-47.

Tixier, N., Guibaud, G. and Baudu, M. (2003) Effect of ph and ionic environment changes on interparticle interactions affecting activated sludge flocs: A rheological approach. Environmental Technology 24(8), 971-978.

CHAPTER 2: LITERATURE REVIEW

2.1 RHEOLOGY

Rheology is the scientific study of the flow behaviour of matter (solids, liquids and gases) and its time-dependent behaviour under the influence of stress (Barnes 2004, Mezger 2011). Rheological research has contributed much towards the improvement of sludge treatment and our understanding of the nature of colloidal systems (Chang 2016, Ratkovich et al. 2013).

2.1.1 FLUID FLOW BEHAVIOUR

The flow behaviour of fluids is governed by their physicochemical properties. An increase in solute concentration will increase the viscosity of a solution and change the flow behaviour. On the other hand, an increase in the shear rate increases the friction among the molecules and decreases entanglement; as a result, viscosity decreases and we observe a change in flow behaviour. The flow behaviour of fluids can be categorised in the following ways.

Ideally viscous fluids

An ideal viscous fluid, or Newtonian fluid, is a fluid in which the shear stress is directly proportional to the shear strain (Barnes et al. 1989). Examples of ideally viscous fluids are pure solvent, and water.

Shear-thinning fluids

Shear-thinning fluid is a fluid in which viscosity decreases with increasing shear stress (Barnes et al. 1989). These fluids are also known as pseudoplastic fluids and are mostly complex fluids such as blood, milk or mayonnaise. Shear thinning fluid sometimes shows a plateau of zero shear viscosity at low shear rate.

The behaviour of shear thinning fluids can be approximated by various mathematical models. However, the most commonly used models are as follows.

The simple power-law or Ostwald model (Eq. 2.1) (Eshtiaghi et al. 2013, Moeller and Torres 1997), applicable for a wide range of shear rates:

$$\tau = k\dot{\gamma}^n \qquad (2.1)$$

The Bingham model (Eq. 2.2) (Eshtiaghi et al. 2013, Guibaud et al. 2004):

$$\tau = \tau_o + \mu\dot{\gamma} \quad (2.2)$$

The Sisko model (Eq. 2.3) (Mori et al. 2006, Pollice et al. 2007):

$$\tau = k\dot{\gamma}^n + \mu_\infty\dot{\gamma} \quad (2.3)$$

The Herschel Bulkley model (Eq. 2.4) (Baroutian et al. 2013, Baudez and Coussot 2001):

$$\tau = \tau_o + k\dot{\gamma}^n \quad (2.4)$$

The Casson model (Eq. 2.5) (Barnes et al. 1989, Chhabra and Richardson 2008):

$$\tau = \sqrt{\tau_{Cy}} + \sqrt{\mu}\dot{\gamma} \quad (2.5)$$

The cross-viscosity fluid model (Eq. 2.6) (Eshtiaghi et al. 2012):

$$\mu = \frac{\mu_o}{1 + k\,\dot{\gamma}^n} \quad (2.6)$$

Where, τ is the shear stress (Pa), μ is the viscosity of the fluid (Pa.s), k is the consistency index (Pa.s^n), n is the flow behaviour index (n < 1), μ_o is zero shear viscosity (Pa.s), μ_∞ is infinite shear viscosity (Pa.s), τ_{Cy} is the Casson yield point (Pa), and τ_o is the yield stress of the fluid.

Shear-thickening fluids

In shear-thickening fluids, viscosity increases with increasing shear stress. These fluids are also known as dilatant fluids (n > 1) (Boersma et al. 1990). Colloidal suspensions, such as corn starch in water, are examples of shear thickening fluids.

Viscoelastic fluid

Fluids that show both liquid (viscous) and solid (elastic) behaviour simultaneously are called viscoelastic fluids. Viscoelastic fluids also display time-dependent behaviour. They include amorphous polymers, semicrystalline polymers, biopolymers and metals (Barnes et al. 1989, Baudez et al. 2013a).

Elasticity is defined as elastic deformation of a material due to applied stress; that is, the deformation can be completely recovered once the applied stress is removed. An ideal viscoelastic fluid will flow under applied stress and will stop flowing when the stress is removed. The theory of elasticity applicable for viscoelastic fluids is described by Hooke's law (Eq.2. 7), with the constant of proportionality known as Young's modulus, G (Chhabra and Richardson 2008).

$$\tau = -G\frac{dx}{dy} = G\gamma \quad (2.7)$$

Where *dx* is described as the shear displacement of two elements and *dy* is the distance between the two elements.

Viscoelastic fluid properties are generally measured using oscillatory measurements where oscillatory strain (γ) is applied, and in response the elastic and viscous characteristics of fluid are determined (Coussot 2005). Thus, the storage (elastic) modulus G' and loss (viscous) modulus G" are determined. G' and G" often depend on the stress (or strain) amplitude and frequency, and can be determined by applying a frequency and varying the deformation and stress amplitude or by applying a stress or amplitude and varying the frequency. Such measurements describe the behaviour of materials in linear viscoelastic region (Chhabra and Richardson 2008).

2.1.2 RHEOMETERS AND MEASURING SYSTEMS

A rheometer is an instrument used to monitor the response of a fluid to the applied force. There are two main types of rheometers: a strain control rheometer allows the user to define the shear strain and measure the resulting shear stress, and a stress control rheometer is used to define the shear stress and measure the resulting shear strain. However, hybrid rheometers are now available which allow direct strain control and direct stress control and normal force measurement.

The main geometries that are available with the hybrid rheometer are the concentric cylinder, cone and plate, and parallel plate. The concentric cylinder's geometry consists of an inner cylinder (bob) and an outer cylinder (cup). These cylinder-shaped components

have the same axis of symmetry or rotation if mounted in the working position. The concentric cylinder's geometry can be classified as large gap or small gap. It is mainly suitable for low-viscosity fluids, dispersion or any liquid that is pourable in the cup. The large gap is more suitable for bulk materials with larger particulates; however, small-gap geometry is suitable for materials with limited stability or prone to edge failure or rapid solvent evaporation (Barnes et al. 1989, Mezger 2011). Special geometries such as grooved bob, vane and helical geometries are used to overcome the error caused due to slip at the material/geometry interface.

A cone and plate setup consists of a circular cone and a plate. The cone is generally the upper rotating part and the plate the bottom stationary part. Cone geometries are available in various sizes (diameters) and cone angles. The measurable range of stress and strain or shear rate can be varied to capture the widest range of material properties by changing size and cone angle; for example, with a cone angle of 1°, at a rotational speed of $n = 100\ min^{-1}$, the resulting shear rate is $\dot{\gamma} = 600s^{-1}$. However, with a cone angle of 2° at the same speed, $\dot{\gamma} = 300s^{-1}$ will be achieved (Mezger 2011).

Parallel plate geometry consists of two parallel plates. Its application is similar to that of the cone and plate setup. However, the gap size in cone and plate has a very limited range, but the gap size between parallel plates can be changed substantially.

The advantages of using parallel plate or cone and plate setups over a concentric cylinder are that the sample required is small, and by reducing the gap size, most of the air bubbles trapped inside the sample can be pressed out before the test. However, the disadvantages of using the parallel plate and cone and plate over the concentric cylinder are that there is a limit to the maximum shear rate applied due to the risk of expelling or edge failure For samples that may exhibit edge drying in a cone plate or parallel plate approach, concentric cylinders are useful (Farno 2016, Mezger 2011).

2.2 WHAT IS SLUDGE?

Sludge is the semi-solid residual material left behind after the treatment of wastewater. It mainly consist of microorganisms, organic and inorganic chemical substances, and metals (Ratkovich et al. 2013). Sludge is mainly classified as primary sludge (generated from primary settling of untreated wastewater), secondary sludge (generated from secondary

clarification during an activated sludge process or in a membrane bioreactor), or digested sludge (generated from an anaerobic digestion process).

2.3 SLUDGE TREATMENT METHODS

Contaminants are removed from municipal waste water using physical, chemical and biological processes. After primary treatment (see below), water (effluent) is safe enough to release into the environment. The by-product formed during this process is a semi-solid waste known as sewage sludge, which needs further treatment before being suitable for disposal (Droste and Gehr 2018).

Sewage or waste water treatment normally comprises of three stages: primary, secondary and tertiary treatment. In primary treatment, the waste water flows through settling and sedimentation tanks. The aim of primary treatment is to remove large objects, skim off oil and grease, and settle out solids to collect and send for further treatment. Secondary treatment is mainly used to degrade the biological content of the sewage. Most treatment plants use an aerobic biological process to treat settled sewage after primary treatment (Chagnon and Harleman 2005, Liu 2003). Aeration is the key to the aerobic biological process, because air provides oxygen to the bacteria to break down complex organic matter into carbon dioxide and water, thereby reducing sludge volume. Moreover, it helps to maintain the homogenous condition within the reactor and increase oxygen transfer efficiency, which reduces energy consumption. (Nonetheless, aeration typically accounts for 60 -75% of the total energy consumption of a treatment plant (Seyssiecq et al. 2008).) The settled solids from the secondary treatment then undergo tertiary treatment, called sludge anaerobic digestion. During the digestion process, the solids are degraded to form water, carbon dioxide and biogas. The final products from the digester, such as dried sludge and biogas, can be used as fuel in the agricultural or household sectors (Droste and Gehr 2018, Farno 2016, Greene 2014).

2.4 SLUDGE FLOC STRUCTURE AND PHYSICAL PROPERTIES

2.4.1 WHAT IS FLOC?

Sludge flocs are formed through a process of complex organisation of heterogeneous materials such as bacteria, detritus and mucilage of macromolecules (Andreadakis 1993). Sludge solids are rarely found as separate particles in water, but practically always as

agglomerate particles called flocs. These flocs hold water within their structures and act as single particles hydrodynamically (Sanin et al. 2011). In the biological process, settling of sludge floc, not the individual sludge particles, is important. However, the sludge floc is full of water and hence the behaviour of floc is related to how the water in the floc is attached to solids. If the water is trapped in the crevices and or interstitial spaces of the floc, and if the floc is destroyed, it becomes free water, that is, water which is not associated with the suspended solids particles (Sanin et al. 2011).

Numerous morphological and surface characteristics of floc exert direct or indirect influence on sludge settlement problems. For example, poor clarification and turbid effluents during wastewater treatment are caused by either the inability of small clumps of bacteria to flocculate (dispersed growth) or the break-up of larger flocs and formation of small compact flocs that do not settle well (Andreadakis 1993). Thus, the microbial activity within the sludge is a crucial factor in the activated sludge process (Li and Bishop 2004). Similarly, extracellular polymeric substances (EPS) are very important for floc properties of the activated sludge (Wilen et al. (2003). Bo and Lant (2004) studied the hydrodynamics, floc size distribution and settleability and compressibility of activated sludge in a bubble column reactor. They reported that in highly turbulent flow, the floc structure disintegrated and generated a large quantity of smaller and looser flocs. Other authors reported that by increasing aeration intensity and shear, EPS from flocs were released into the surrounding environment (Meng et al. 2008, Menniti et al. 2009, Park et al. 2005). De Temmerman et al. (2015) reported that breakage due to aeration inevitably led to higher concentrations of very small floc fragments in the bulk liquid. Although flocs that are continuously exposed to low shear grow into loose and weak flocs, exposing flocs to a continuous high shear breaks them down into Kolmogorov scales, the smallest scale in the turbulent flow at which viscosity dominates.

2.4.2 TOTAL SOLIDS AND TOTAL SUSPENDED SOLIDS

Total solids (TS) are defined as the sum of total suspended solids (TSS) and total dissolved solids. Total solids concentration is the main parameter affecting sludge rheology (Lotito et al. 1997). Many researchers have shown that the viscosity of sludge increases with solids content (Eshtiaghi et al. 2013, Forster 1981, Markis et al. 2014, Ratkovich et al. 2013, Tixier et al. 2003a). An increase in TS concentration also increases the apparent viscosity, yield stress and fluid consistency of sludge (Markis et al. 2014).

Additionally, Pollice et al. (2007) showed that an increase in solids concentration also increases the energy demand for mixing in an activated sludge process. Fang et al. (2015), Meng et al. (2009), Trussell et al. (2007) showed that the total solids content of sludge also affects the physical properties of sludge such as soluble chemical oxygen demand (sCOD), zeta potential and EPS content.

Total suspended solids refers to that portion of the total solids that is retained on a fiberglass filter paper of approximately 0.22 microns pore size. Suspended solids mostly consist of colloidal and particulate particles (Meng et al. 2017, Trussell et al. 2007). Zhang et al. (2004) found that TSS gradually decreases with increasing aeration intensity. This reduction in TSS due to aeration intensity is the consequence of the floc breaking and releasing EPS present inside the floc structure into liquor (Chang et al. 2002), which decreases the oxygen transfer efficiency due to an increase in the food-to-microorganism ratio (Houghton and Quarmby 1999, Meng et al. 2006, Wilén et al. 2003). Moreover, an increase in TSS decreases the gas holdup, oxygen transfer effeciency and increases sCOD (Babaei et al. 2015a, Durán et al. 2016, Khalili et al. 2018b).

2.4.3 SOLUBLE COD

Chemical oxygen demand is defined as the amount of oxygen required to oxidise the organic matter and inorganic chemicals present in the wastewater measured by chemical reaction (Pisarevsky et al. 2005). Thus, total COD is the sum of total biodegradable COD and total non-biodegradable COD. These fractions are further divided into soluble and particulate fractions because they are subject to different biochemical reactions (Karia and Christian 2013). The soluble fraction is defined as possesing a characteristic dimension of less than 1 nm, whereas the particulate fraction is defined as possesing a chracteristic dimension of between 1 nm and 1μm (Hu et al. 2002).

The sCOD is a critical parameter for estimation and optimisation of the performance of the biological treatment process (Hayet et al. 2016). sCOD content is also used to determine the amount of oxygen required for biodegradation in the aeration tank (Henze and Henze 1997). An increase in sCOD clearly indicates the disintegration of floc structure (Farno et al. 2014, 2015b, Grönroos et al. 2005, Hii et al. 2017). Similarly, aereation intensity has a significant impact on sCOD; for example, (Meng et al. 2008) found that an increase in aereation intensity from 150 L/hr to 400 L/hr increased sCOD

from 4.64% to 6.51% because the shear induced by gas injection led to floc breakage. Azami et al. (2012), Ladewig and Al-Shaeli (2016), Meng et al. (2006) have also highlighted the role of soluble microbial products (SMP), characterised as sCOD, on the kinetic activity, flocculating and settling properties of sludge.

2.4.4 *SURFACE TENSION*

Surface tension is the elastic tendency of a fluid (Speight 2017), that is, the cohesive forces between the fluid–solid or fluid–fluid interface. Surface tension is closely related to the carbohydrate and protein content of EPS; they are amphiphobic molecules and can change the surface tension of the fluid (Sheng et al. 2010). There exists a direct relationship between surface tension and the cohesive energy of the molecule, according to Schonhorn (1965). Moreover, the cohesion of sludge increases with an increasing polysaccharide content of EPS (Ahimou et al. 2007). In addition, there is a direct relationship between the interfacial surface tension and bioflocculation; that is, when fine dispersed particles clump together to form a large agglomerated floc, settling of organic matter takes place and reduces the interfacial surface tension (Liss and Droppo 2005).

Knowledge of surface tension and gas flow rate at a given concentration helps us to understand the orientation and growth times of bubbles (Kulkarni and Joshi 2005). During the bubble formation and detachment process, dynamic and static surface tension forces act on a bubble. In the initial growth phase, the surface tension is dynamic because its contact angle with the orifice changes continuously; in the later part, it reaches a constant contact angle, approaching a static condition. Thus, although the surface tension forces are small, they vary significantly with gas flow rates and influence bubble formation. Bubble characteristics (notably shape and size) depends on the surface tension of the fluid, and bubble rise velocity depend on the viscous property of the fluid (Sikorski et al. 2009).

2.4.5 *ZETA POTENTIAL*

The zeta potential, which measures the electrostatic interactions between particles, represents the potential drop between the diffuse double layers of the surface of a fluid. Measurement of the zeta potential enables detailed insight into the cause of dispersion, aggregation, flocculation and sedimentation (Hunter 1981, Vold 1982, Yuan et al. 2011). A reduction in zeta potential, that is, a negative value, indicates that the sludge is

becoming more stable and the repulsive force is increasing more than the attractive force; therefore the resistance to aggregation is increasing (Vold 1982). At a constant aeration rate (e.g. 0.2 m^3/h, as Meng et al. (2006) observed), the zeta potential value becomes less negative with an increase in solid concentration. Meng et al. (2006) also showed that zeta potential is inversely correlated to membrane fouling.

In a broader perspective, the change in zeta potential is associated with the EPS concentration of the sludge, that is, the greater the concentration of EPS, the more negative the zeta potential of the sludge (Meng et al. (2006), Wilén et al. (2003)). However, Sutherland (2001) also showed that EPS plays a crucial role in defining the stability of the system. Therefore, a more negative surface charge of sludge indicates an increased solubilisation of loosely bound EPS (LB-EPS) (Zhang et al. 2013).

2.5 RHEOLOGICAL BEHAVIOUR OF SLUDGE

Rheology plays a significant role in the design and optimisation of wastewater treatment processes (Barnes et al. 1989, Krishnan et al. 2010). Dentel (1997) also showed that consistent rheological characterisation of sludge is important for practical applications in sludge treatment plants. Few studies have focused on the rheological behaviour of primary sludge, probably because it is the most difficult sludge to handle due to its complex flow behaviour, particularly at low temperature and high concentrations (Bhattacharya 1981). Two samples of primary sludge of the same total solid concentration but of different organic composition will exhibit different rheological behaviour; it is therefore very important that the physical and chemical characteristics of primary sludge are properly determined in order to make meaningful use of the rheological data in process design (Bhattacharya 1981). Moeller and Torres (1997) studied the rheological and physicochemical characteristics of sludge, and concluded that there is no direct relationship between them, except for an inverse relationship between TSS and flow index(n); however, other authors have shown that the yield stress of fluid increases with increased concentration (Hasara et al. 2004, Markis et al. 2014).

Secondary sludge is generated after secondary treatment. It has complex rheological properties that evolve with time due to ageing and microbial activity (Baudez and Coussot 2001). The time-dependent nature of secondary sludge complicates measurement of its physical parameters (Seyssiecq. et al. 2003). Sanin (2002) studied the change in

secondary sludge rheology with respect to the effect of variables such as pH, conductivity and solids concentration, and noted that the power law model was the best fit to the rheograms obtained for 2% concentration. Hasara et al. (2004) studied the rheological properties of waste activated sludge in a submerged membrane bioreactor (sMBR), and concluded that Ostwald de Vaele is the most suitable model for measuring the flow properties of sludge in that context. Later, Laera et al. (2007) found that the Bingham model and Ostwald model were equally good fits for the sludge in an sMBR. Guibaud et al. (2004) characterised the rheology of activated sludge originating from different aeration tanks and from laboratory-scale plants using a rheometer, and stated that Bingham's parameters Viscosity and shear stress are strongly influenced by the TSS content of the sludge. As mentioned in section 1.1, Seyssiecq et al. (2008) considered the effect of aeration rate on the viscosity of activated sludge when performing an in situ rheological characterisation of sludge in aeration bioreactors with TSS ranging from 10 to 35g/L. The experiment demonstrated an overall decrease in the shear-thinning properties of aerated sludge compared to non-aerated sludge, with a plateau at a high aeration rate. The implications are that gas injection strongly influences the rheological behaviour of sludge, or that gas injection causes slippage; these findings require verification. Although some researchers have studied the impact of concentration, temperature, pH and conductivity on secondary sludge rheology, research on the impact of gas injection on activated sludge rheology to date is very limited.

Digested sludge is the sludge resulting from an anaerobic digestion process. Baudez et al. (2011) determined the rheological properties of digested sludge at different concentrations, and concluded that qualitatively digested sludge behaviour is identical at different solids concentrations, and depends only on the yield stress and Bingham viscosity, both parameters being closely related to solids concentration. They also developed a master curve that reveals the rheological behaviour of digested sludge at any concentration. Jiang et al. (2014) studied the rheological characteristics of highly concentrated anaerobic digested sludge with TS content more than 8% while they varied temperature between 35^{o}C and 70^{o}C. They concluded that the Herschel–Bulkley model fit the experimental data well, and observed shear-thinning behaviour with a yield stress for flow measurement. They also concluded that an increase in TS content increases the yield stress value, as well as cohesion energy (Ec), with a power law relationship. To understand the increasing complexity of sludge with increase in concentration and

overcome the difficulties of measuring its rheological properties, Eshtiaghi et al. (2012) identified model fluids such as carboxymethyl cellulose (CMC), Carbopol® gel and Laponite clay suspension that can be used to study the rheological behaviour of sludge at high shear rates, over short time periods and where time dependency is dominant, respectively. Dieude-Fauvel et al. (2014) attempted to create an electrical fingerprint of digested sludge as a tool for in-situ rheological measurement. Dai, Gai and Dong (2014) also investigated the rheology of sludge with respect to the sludge retention time (SRT) and temperature in an anaerobic digestion reactor with TS content of 16.16%, and found that the flowability of sludge from a thermophilic anaerobic digestion reactor – even at high concentration – was better than from mesophilic anaerobic digestion reactors. Baudez, Slatter and Eshtiaghi (2013b) studied the impact of temperature on digested sludge rheology and concluded that sludge became progressively more fluid when the temperature was increased, and that Bingham viscosity decreased with increasing temperature, indicating that thermal agitation had a major influence.

2.6 GAS PHASE CHARACTERISTICS IN VISCOELASTIC FLUIDS

2.6.1 GAS HOLDUP

Holdup is the relative space occupied by a phase in a flow conduit (Cheremisinoff 1986). Gas holdup is one of the major characteristics associated with multiphase flow. The holdup determines the residence time of the gas in the liquid, and in combination with the bubble size, it controls the gas–liquid interfacial area available for mass transfer. It also predetermines wastewater treatment reactor design, because the total volume of the reactor for any range of operating conditions depends on the maximum holdup that must be accommodated (Yusuf and Murray 1988). Esmaeili et al. (2015) studied the effect of liquid phase rheology on the hydrodynamics of bubble column reactor, and observed that the elasticity of the operating liquid reduced bubble chord length and increased the total gas holdup. They evaluated the gas holdup using Equation 2.8, varying the gas velocity between 0.02m/s and 0.22 m/s for 0.5wt% CMC and 0.5wt% Xanthan gum solutions.

$$\varepsilon_g = 1 - \frac{1}{\rho_l g}\left(\frac{\Delta P}{\Delta Z}\right) \quad (2.8)$$

Where, ε_g = Gas holdup (-), ρ_l = liquid density (kg/m^3), g = gravity (m/s^2), ΔP = pressure gradient (Pa) measure by pressure transducer, and ΔZ = height difference (m) (change in height of the liquid due to gas injection).

Bajón Fernández et al. (2015) studied the impact of viscosity and superficial gas velocity on the hydrodynamics of the bubble column while studying the gas to liquid mass transfer in rheologically complex fluids like CMC (0.5 to 1.5 wt%) and glycerol (0 to 90 wt%). They injected carbon dioxide gas at velocities of 0.0016–0.037m/s, and found that the hydrodynamics of the bubble column strongly influence the mass transfer, and stated that there is a need for a better understanding of the relationship between hydrodynamics and apparent viscosity and rheological variations during gas injection.

Fransolet et al. (2005) evaluated the influence of liquid rheology on the gas flow pattern in a bubble column reactor. They determined the average gas holdup for five different concentrations of Xanthan gum (0 to 5 g/L) with compressed air velocity ranging from 0 to 1.5 m/s using pressure probes and EMT, and concluded that gas holdup values at any superficial velocity decrease as the concentration is increased. They used Equation 2.9 to calculate gas holdup data.

$$\varepsilon_g = a u_g^b \mu^{-c} \quad (2.9)$$

Where, εg = Gas holdup (-), a = Fitting Parameter (0.26), b = Fitting Parameter (0.54), c = Fitting Parameter (0.147), u_g = Gas superficial velocity (m/s), μ = Apparent liquid viscosity (Pa s).

Hofmeester (1988) stated that gas holdup is an important parameter in the fermentation industry; if the gas holdup is too low or too high it may adversely affect the end product. He elaborated the measurement technique of gas holdup in the bioreactor by visualising the dispersion of liquid level. Gas holdup is strongly influenced by superficial gas velocity and the viscosity of the fluid. High viscosity diminishes the bubble rise velocity, that is, hinders the escape of bubbles, which leads to high gas holdup and a decrease in the difference in mean density between the gas and fluid (Wang and McNeil (1996). Anastasiou et al. (2013) formulated a generalised model (Equation 2.10) for predicting the average gas holdup in bubble columns using Xanthan gum (0.22 to 0.35 wt%) as a non-Newtonian shear thinning fluid, and stated that the equation is in very good agreement

(± 10%) with all the available data, because the dimensionless numbers incorporate the effects of both gas superficial velocity and liquid phase properties.

$$\varepsilon_g = 2.2\,[Fr^{1.07} Ar^{0.84}\, Eo^{0.19} \left(\frac{d_s}{d_c}\right)^{1.16} \left(\frac{d_p}{d_s}\right)^{2.86}]^{0.264} \quad (2.10)$$

Where, ε_g = Gas holdup, Fr = Froude number =$Fr = \frac{u_g^2}{d_c g}$, Ar =Archimedes number = $Ar = \frac{d_c^3 \rho_L^2 g}{\mu_L^2}$, Eo = Eotvos number = $Eo = \frac{d_c^2 \rho_L g}{\sigma_L}$, u_g= Superficial gas Velocity (m/s), μ_L = Viscosity of liquid (Pa s), ρ_L= Density of liquid (kg/m^3), σ_L= Surface tension (N/m), d_s = Sparger diameter (m), d_p= Pore diameter (μm), d_c= Column diameter (m).

As part of research into the hydrodynamics and oxygen mass transfer in aqueous solutions of polysaccharides, Eickenbusch et al. (1995) studied the effect of column diameter (0.19m to 0.60m) on the gas holdup of highly viscous fluids (Xanthan gum and hydropropyl guar) and reported that the diameter effect on gas holdup was negligible and that it was only effective for highly viscous fluids in smaller columns. Recently, Babaei et al. (2015b) used electrical resistance tomography (ERT) for the quantitative analysis of gas holdup and its distribution in activated sludge bioreactors. ERT is an advanced and non-invasive flow visualisation technique which is suitable for opaque fluids and enables online measurements in different axial and radial locations within the reactor. Babaei et al. (2015b) used Equation 2.11 to calculate the overall gas holdup and Equation 2.12 to calculate the apparent viscosity of activated sludge as a function of TSS concentration and superficial gas velocity.

$$\varepsilon_g, overall = \frac{0.02558 u_g^{1.249} \phi}{0.01147 + \phi + 0.3276\phi^2} \quad (2.11)$$

Where, ϕ = Ln ($0.5197 u_g^{0.4136} \mu_{app}$), and

$$\mu_{app} = 6.613 \exp(0.1289(\text{TSS})^{0.9375}) \times \left(28 * u_g\right)^{\left(0.02436\,(TSS)^{\,0.5947} - 0.3688\right)} \quad (2.12)$$

ε_g,overall = Overall gas holdup (-), μ_{app} = Apparent viscosity (Pa.s), TSS = Total suspended solid concentration (g/L), u_g= Gas superficial velocity (cm/s).

Giuseppe et al. (2013) studied the combined effect of surface tension and viscosity on bubble column hydrodynamics and reported that gas holdup changes with the surface tension and viscosity of the fluid. They also reported that the surface tension of the liquid determines the bubble shape and bubble rise velocity. Kulkarni and Joshi (2005) previously found that the surface tension of the liquid also determines the orientation/growth time of the bubbles. Chhabra (2012) reported that surface tension, along with Reynolds number, determines the sphericity of bubbles; however, the shape also depends on the size (volume) of the bubble and the physical properties of the continuous phase. Chhabra (2012) also observed shape transitions from spherical (A) to prolate-tear (B), then to oblate cusped (C), and finally to Davies–Taylor-type spherical caps (D), as shown in Figure 2.1. Chhabra (2012) mentioned that, depending upon the physical properties of the continuous and dispersed phase, dissimilar shapes are observed in rheologically complex liquids. Thus, the measurement of surface tension is important, because it affects bubble shape, drag force, bubble velocity and thereby gas holdup, as Zuber and Findlay (1965) had found.

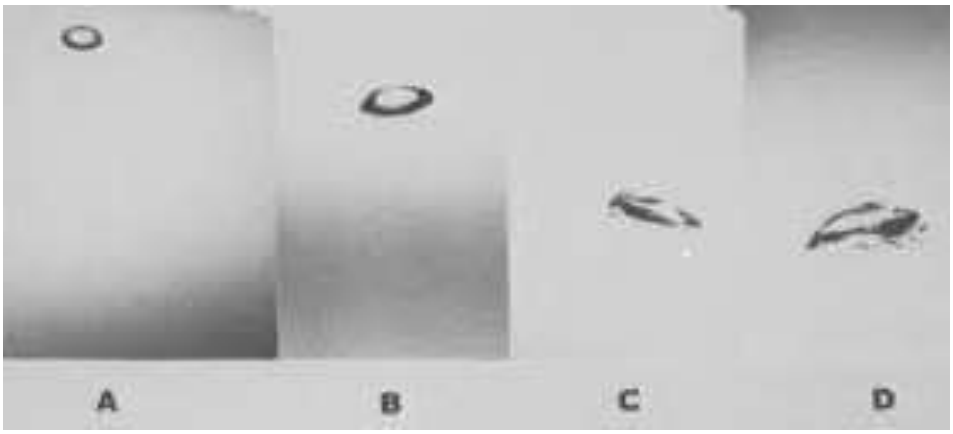

Figure 2.1: bubble shape transition in non-Newtonian fluid (Chhabra, 2012), a) spherical, b) prolate-tear, c) oblate cusped, d) Davies–Taylor type spherical caps

2.6.2 BUBBLE RISE VELOCITY AND BUBBLE SIZE

In addition to gas holdup, the bubble rise velocity is an important phenomenon in the hydrodynamics of the bubble column because it determines the operation time of the column and the contact time of the gas and liquid phase. The main forces which act on a bubble's rise during its motion in liquid are gravity, buoyancy, drag, surface tension, viscous forces, added mass force, history force (arising out of the unequal distribution of vorticity), and lift force (unsteadiness of the flow) (Kulkarni and Joshi 2005). Amirnia et

al. (2013) studied the rise velocity of air bubbles in non-Newtonian biopolymer solutions (Xanthan gum and CMC) as a function of bubble volume. They reported that the terminal rise velocity of the bubbles increased as a power law function with bubble volume in small-sized bubbles (i.e. bubbles of equivalent diameter up to 0.5 cm) in a Stokes flow regime. The rise in velocity for larger bubbles was independent of both bubble volume and the properties of the solution. Dziubiński et al. (2003) commented that because of the complex flow mechanism, which depends on the various process parameters, the typical approach to calculate the gas bubble flow velocity is based on empirical correlations or a classical concept of drag coefficient. They calculated the drag coefficient correlation (Equation 2.13), originally proposed by Dewsbury et al. (1999), and found that the Reynolds number calculated using Equation 2.14 (used in equation 2.13) has a minimum ± 40% error, but the horizontal bubble diameter had no significant effect on the error with which the drag coefficient was calculated.

$$Cd = \frac{16}{Re_h}\left(1 + 0.173Re_h^{0.657}\right) + \left[\frac{0.413}{\left(1 + 16.3Re_h^{-1.09}\right)}\right] \quad (2.13)$$

$$Re_h = \frac{u^{2-n} d_h^n \rho_L}{k} \quad (2.14)$$

Where, Cd = Drag coefficient, Re_h = Reynolds number, u = Terminal velocity of the gas bubble in an unbound[1]medium (m/s), n= Flow behaviour index in power law model (-), d_h = The horizontal bubble diameter (m), ρ_L = Liquid density (kg/m^3), k= Consistency index in the power law model (Pa.s^n)

Tran et al. (2015) proposed Equation 2.15 for the drag coefficient for bubbles in yield stress fluid, and stated that bubbles in yield stress fluid are less mobile than those in power law fluid.

$$C_D = \frac{5\left(1 + \frac{3R_e^*}{16}\right)}{R_e^*} \quad (2.15)$$

Where, C_D = Drag coefficient (-), Re^* = Generalised Reynolds number = $\frac{\rho_l u_t d^*}{X(n)\mu_{eff}}$, $X(n)$= Correction factor = 1.38(-), ρ_l= Density of liquid (kg/m^3), d* = Equivalent spherical

[1] Unbound medium: when the bubble is flowing with some arbitrary but Stokesian velocity distribution.

diameter of the bubble (m), μ_{eff}= Effective viscosity $= \frac{\tau}{u_t/d^*}$, u_t= Terminal velocity of the bubble (m/s).

According to Cheremisinoff (1986), with considerations of non-Newtonian effects (viscosity and surface tension), the drag coefficient can be given as

$$C_D = \frac{24Y}{2^n Re_0} \quad (2.16)$$

$$Re_0 = \frac{\rho U^{2-n} a^n}{K} \quad (2.17)$$

$$Y = \frac{2^n 3^{\frac{n-3}{2}}(13 + 4n - 8n^2)}{(2n+1)(n+2)} \quad (2.18)$$

Where Re_0 = Reynolds number, Y = Correction factor for the drag coefficient, ρ = Density (kg/m^3), U= Terminal velocity of gas bubble (m/s), a= Radius of bubble (m), n= Flow behaviour index in the power law model (-), k = Consistency index in the power law model (Pa.s^n)

Cheremisinoff (1986) also developed a generalised bubble rise model by considering the effects of the interaction of forces such as buoyancy and viscous, inertial and interfacial tension forces. The following force ratios were considered: buoyancy/viscous, buoyancy/inertia and buoyancy/interfacial tension. The air bubble rise velocity in non-Newtonian fluid, considering all the above ratios, is given in Equation 2.19:

$$U \infty (g\Delta\rho)^A [KF(n')]^B (\sigma)^c (\rho)^D (d)^E \quad (2.19)$$

Where, g = gravitational acceleration (m/s^2), Δρ = Density difference (kg/m^3), K= consistency index (Pa.s^n), n' = Pseudoplasticity index (-), F(n′) = a correction term (-), σ = surface tension (N/m), d = bubble equivalent spherical diameter (m), A = (3n) / (3+ (4n - 1) (n′ - 1)), B = - (4n - 1) / (3 + (4n - 1) (n′ - 1)),C = - (n – 1) / (3 + (4n – 1) (n′ - 1)), D = 2(n – 1) / (3 + (4n – 1) (n′ - 1)), E = (4n – 1) (n′ + 1) / (3 + (4n – 1) (n′ - 1))

By substituting n = 1 (n is the index for the flow regime and when equal to one corresponds to a laminar viscous regime; n = 0.25 corresponds to a turbulent regime in

which the viscosity becomes negligible) in A to E and then substituting the values of A to E in Equation 2.19 and rearranging the equation, the Stokes drag formula was obtained for non-Newtonian fluid behaviour as shown in Equation 2.20.

$$C_D \propto F(n')\left(\frac{\rho u^{2-n'} d^{n'}}{K}\right) \quad (2.20)$$

Where C_D = Drag coefficient (-), u = rise velocity (m/s)

At large Reynolds numbers (>10^4) and for n = 0.4375 (transition regime), and $1 \geq n' \geq 0.5$, where the bubble velocity (u) becomes less sensitive to fluid rheology (Krishnan et al. 2010), Equation 2.19 is approximated as $u \propto \sqrt{\mathrm{gd}}$, as in the Mendelson wave analogy equation (1967) and Davies–Taylor theory (1950).

Babaei et al. (2015a) studied gas phase characteristics (gas holdup, bubble rise velocity and bubble size) using ERT combined with the dynamic gas disengagement (DGD) technique, in which the gas behaviour inside the column is recorded by measuring the gas holdup over the defined time period after turning off the gas flow. The gas phase characteristics have a powerful effect on the oxygen mass transfer rate. Babaei et al. (2015a) used the correlations (Equation 2.21) developed by Margaritis et al. (1999) to calculate the drag coefficient for substitution in Equation 2.23 for calculating the bubble diameter. In addition, for systems with different bubble size, Babaei et al. (2015a) explained the calculation of a bubble's Sauter mean diameter and its relation to gas velocity and bubble coalescence phenomena. So far, all the empirical equations that have been used in the literature to calculate the average bubble size are based on the power-law model-based dimensionless equations (Babaei et al. 2015a, Fransolet et al. 2005, Jamshidi and Mostoufi 2017, Lind and Phillips 2010).

$$C_{D,\infty} = \frac{16}{Re}(1 + 0.173Re^{0.657}) + \frac{0.413}{1 + 16300Re^{-1.09}} \quad (Re < 60) \quad (2.21)$$

$$C_{D,\infty} = 0.95 \quad (Re > 60) \quad (2.22)$$

Where, $C_{D,\infty}$ = Drag coefficient of a single bubble (-), Re = Reynolds number = $\frac{\rho_l d_h^n u_b^{2-n}}{K}$, ρ_l = Density of liquid (kg/m^3), n = Flow index (-), K = Consistency index (Pa.s^n).

$$d_b = \sqrt[3]{\frac{C_{D,\infty} d_h^2 u_b^2}{4g}} \quad (2.23)$$

Where, d_h = Horizontal diameter of bubble (m), u_b = Bubble rise velocity (m/s), g = Gravitational constant (m/s^2).

Babaei et al. (2015a) developed a model for an aerated activated sludge system that relates the mean bubble diameter to superficial gas velocity and rheological properties. It is presented in Equation 2.24 based on the best fit to their data.

$$ds = \frac{0.03918 u_g^{0.09543}(x^2 - 3.765x + 8.661)}{x^2 + 0.4958x + 11.94} \quad (2.24)$$

Where, d_s = Sauter mean diameter of bubble (m), u_g = Superficial gas velocity (m/s),

$$x = 11.1\phi + 0.6239 \quad (2.25)$$

$$\phi = \ln\left(0.5197 u_g^{0.4136} \mu_l\right) \quad (2.26)$$

Where, μ_l = apparent viscosity of the liquid (Pa.s)

The correlations for phase interactions in multiphase flow are usually based on a single bubble; however, some modifications are required to take into account the effect of volume fraction or mass fraction of the dispersed phase. The most important parameter in multi-phase flow is the drag force acting on each bubble, since it reflects two-phase flow effects (i.e. resistance or friction caused by both the liquid phase and the gaseous phase) in determining the flow fields of the dispersed and continuous phases.

Other studies of the hydrodynamics of bubble columns incorporating non-Newtonian fluids describe factors influencing bubble rise velocity/bubble motion. SHAH Y.T et al. (1982) suggested that gas holdup and mass transfer coefficient are the most important parameters for design and scale-up of bubble columns. However, since bubble dynamics and flow regime indirectly influence a bubble column's efficiency, these authors also studied bubble behaviour with change in concentration of organic matter and salts. They reported that the bubble coalescences depending on the concentration, and that increase in concentration of organic matter or salt increases bubble coalescence. Moreover, Denis Funfschilling (2001) proposed that two competing mechanisms – negative wake and residual stresses that reduce the local fluid viscosity – are responsible for bubble interaction and coalescence in non-Newtonian and viscoelastic fluids. Bubble coalescence

is related to viscosity and bubble rise velocity because the bubble contact time increases monotonously with fluid viscosity, as Orvalho et al. (2015) explained.

To understand the correlation between the gas flow rate and viscosity and volumetric mass transfer coefficients, Gomezdiaz et al. (2009) measured the gas liquid interfacial area under differing operating conditions. They observed an increased concentration of liquid phase decreases in the gas–liquid interfacial area, producing large bubbles even at a high gas flow rate.

However, the elasticity of fluid plays a major role in determining the length to radius aspect ratio of bubbles, and bubble motion can only be observed if the yield force to buoyant force ratio is greater than or equal to 0.50 ± 0.04, as Sikorski et al. (2009) reported. Dimakopoulos et al. (2013), Lind and Phillips (2010) also proved that the elasticity of fluid influences the bubble characteristics. In addition, Jin et al. (2012) and Jamshidi and Mostoufi (2017) observed a linear correlation between gas flow rate and bubble rise velocity.

2.7 MODEL FLUIDS FOR SLUDGE

Sludge rheology is complex and changes with time due to ageing and microbial activity. Therefore, sludge cannot be used as a reference material for industrial process design or controlled experiments because the results obtained are unique to each batch (Eshtiaghi et al. 2012). To overcome this problem, researchers have sought to identify and characterise a suitable transparent model fluid that mimics the behaviour of sludge (Baudez et al. 2013a, Cao et al. 2016, Eshtiaghi et al. 2012). Curran et al. (2002), Spinosa and Lotito (2003) studied kaolin suspension and Carbopol® gel respectively as proxy materials for yield stress fluids such as sewage sludge. Low molecular weight polymeric gels can be used to mimic sludge flocculation and sludge dewatering (Legrand et al. 1998). Polystyrene latex particles of size similar to that of bacteria can be used to simulate extracellular polymers (Sanin and Vesilind 1996). Similarly, researchers have used transparent viscous fluid Xanthan gum as a model for sludge by measuring and comparing its rheological parameters in flow regimes (Cao et al. 2017, Cao et al. 2016, Fransolet et al. 2005, Haque et al. 1986, Kennedy et al. 2018) for applications of wastewater treatment processes such as mixing and gas holdup measurement.

2.8 GAP IN KNOWLEDGE AND RESEARCH QUESTION

2.8.1 GAP IN KNOWLEDGE

The review of the literature presented in this chapter showed that the change in sludge rheology during gas injection has not been studied in detail. Only Seyssiecq et al. (2008) have investigated the impact of different flow rates of gas injection on the viscosity of secondary sludge by carrying out in situ measurements. Seyssiecq et al. (2008) used a torque meter rather than a commercial rheometer, a method that requires many assumptions, such as considering a power law fluid to calculate shear stress, and the shear rate five times of the superficial gas velocity. Moreover, no published work addresses the impact of gas injection on both the viscous and viscoelastic properties of concentrated waste activated sludge, and no method has been developed to calculate the stress the gas flow imposes on the sludge. The literature contains no research measuring the impact of gas injection on the rheological properties of a model fluid.

The review of the literature on the physicochemical properties of sludge showed that change in physicochemical properties and gas injection has been studied to understand its impact on membrane fouling resistance (Meng et al. 2007, Meng et al. 2008, Meng et al. 2017, Menniti et al. 2009). However, no published work concerns the impact of gas injection on the physicochemical properties of concentrated waste activated sludge and its relation to the stress imposed by gas injection. Moreover, no study has discovered the relationship between sludge rheology and physiochemical properties.

Additionally, most of the studies involving the measurement of gas holdup, bubble rise velocity and bubble size in waste activated sludge are based on using transparent model fluids, because sludge is an opaque and complex fluid. In the few studies that have been performed with sludge, the concentration of waste activated sludge used was 0.02 to 1.5wt%, a range that does not capture the expected increase in the solid content of WAS (Babaei et al. 2015a, b, Jamshidi and Mostoufi 2017). Thus, the impacts of gas injection on gas holdup, bubble rise velocity and bubble size in concentrated waste activated sludge have not yet been investigated sufficiently to understand the impact of sludge rheology on gas phase properties. More work is needed to better understand the impact of gas injection on sludge rheology and the impact of sludge rheology on gas phase characteristics as well as sludge physicochemical properties.

2.8.2 RESEARCH QUESTIONS

The following research questions were formulated based on the gaps in knowledge outlined above.

1. How does a varying gas flow rate affect the rheology of waste activated sludge? What are the causes of these changes – are sludge structure modified due to gas injection?
2. How do changes in gas flow rate and concentration affect the physiochemical characteristics of sludge?
3. Can a model fluid for sludge be used for calculation of bubble rise velocity and bubble size and for calculating the stress imposed by gas injection?
4. How & why the change in gas flow rate and concentration affects gas holdup, bubble size distribution and bubble rise velocity in waste activated sludge?
5. What type of model can predict the rheology of aerated sludge and its relationship with physiochemical properties of sludge as well as gas phase characteristic?

2.9 REFERENCES

Ahimou, F., Semmens, M.J., Haugstad, G. and Novak, P.J. (2007) Effect of protein, polysaccharide, and oxygen concentration profiles on biofilm cohesiveness. Applied and environmental microbiology 73(9), 2905-2910.

Amirnia, S., de Bruyn, J.R., Bergougnou, M.A. and Margaritis, A. (2013) Continuous rise velocity of air bubbles in non-Newtonian biopolymer solutions. Chemical Engineering Science 94, 60-68.

Anastasiou, A.D., Passos, A.D. and Mouza, A.A. (2013) Bubble columns with fine pore sparger and non-Newtonian liquid phase: Prediction of gas holdup. Chemical Engineering Science 98, 331-338.

Andreadakis, A.D. (1993) Physical and chemical properties of activated sludge floc. Water Research 27(12), 1707-1714.

Azami, H., Sarrafzadeh, M.H. and Mehrnia, M.R. (2012) Soluble microbial products (SMPs) release in activated sludge systems: a review. Iranian Journal of Environmental Health Science & Engineering 9(1), 30-30.

Babaei, R., Bonakdarpour, B. and Ein-Mozaffari, F. (2015a) Analysis of gas phase characteristics and mixing performance in an activated sludge bioreactor using electrical resistance tomography. Chemical Engineering Journal 279, 874-884.

Babaei, R., Bonakdarpour, B. and Ein-Mozaffari, F. (2015b) The use of electrical resistance tomography for the characterization of gas holdup inside a bubble column bioreactor containing activated sludge. Chemical Engineering Journal 268, 260-269.

Bajón Fernández, Y., Cartmell, E., Soares, A., McAdam, E., Vale, P., Darche-Dugaret, C. and Jefferson, B. (2015) Gas to liquid mass transfer in rheologically complex fluids. Chemical Engineering Journal 273, 656-667.

Barnes, H.A. (2004) Interface Science and Technology. Petsev, D.N. (ed), pp. 721-759, Elsevier.

Barnes, H.A., Hutton, J.F. and Walters, K. (1989) An introduction to rheology, Elsevier : Distributors for the U.S. and Canada, Elsevier Science Pub. Co., Amsterdam.

Baroutian, S., Eshtiaghi, N. and Gapes, D.J. (2013) Rheology of a primary and secondary sewage sludge mixture: Dependency on temperature and solid concentration. Bioresource Technology 140, 227-233.

Baudez, J.-C., Gupta, R.K., Eshtiaghi, N. and Slatter, P. (2013a) The viscoelastic behaviour of raw and anaerobic digested sludge: Strong similarities with soft-glassy materials. Water Research 47(1), 173-180.

Baudez, J.C. and Coussot, P. (2001) Rheology of aging, concentrated, polymeric suspensions: Application to pasty sewage sludges. Journal of Rheology 45(5), 1123-1140.

Baudez, J.C., Markis, F., Eshtiaghi, N. and Slatter, P. (2011) The rheological behaviour of anaerobic digested sludge. Water Research 45(17), 5675-5680.

Baudez, J.C., Slatter, P. and Eshtiaghi, N. (2013b) The impact of temperature on the rheological behaviour of anaerobic digested sludge. Chemical Engineering Journal 215-216, 182-187.

Bhattacharya, S.N. (1981) Flow characteristics of primary and digested sewage sludge. Rheologica Acta 20, 288- 298.

Bo, J. and Lant, P. (2004) Flow regime, hydrodynamics, floc size distribution and sludge properties in activated sludge bubble column, air-lift and aerated stirred reactors. Chemical Engineering Science 59(12), 2379-2388.

Boersma, W.H., Laven, J. and Stein, H.N. (1990) Shear thickening (dilatancy) in concentrated dispersions. AIChE Journal 36(3), 321-332.

Cao, X., Yuan, H., Zhao, Z. and Ding, H. (2017) Analysis on xanthan gum solution to simulate flow performance of digestion sludge. Transactions of the Chinese Society of Agricultural Engineering 33(15), 260-265.

Cao, X., Zhao, Z., Cheng, L. and Yin, W. (2016) Evaluation of a Transparent Analog Fluid of Digested Sludge: Xanthan Gum Aqueous Solution. Procedia Environmental Sciences 31(Supplement C), 735-742.

Chagnon, F.J. and Harleman, D.R. (2005) Chemically Enhanced Primary Treatment of Wastewater. Water Encyclopedia 1, 659-660.

Chang, I.-S., Le Clech, P., Jefferson, B. and Judd, S. (2002) Membrane fouling in membrane bioreactors for wastewater treatment.(Abstract). Journal of Environmental Engineering 128(11), 1018.

Chang, Q. (2016) Colloid and Interface Chemistry for Water Quality Control. Chang, Q. (ed), pp. 61-77, Academic Press.

Cheremisinoff, N.P. (1986) Encyclopedia of fluid mechanics, Gulf Pub. Co., Book Division, Houston.

Chhabra, R.P. (2012) Bubbles, Drops, and Particles in Non-Newtonian Fluids, Second Edition, Taylor and Francis, Hoboken.

Chhabra, R.P. and Richardson, J.F. (2008) Non-Newtonian Flow and Applied Rheology (Second Edition), pp. 56-109, Butterworth-Heinemann, Oxford.

Coussot, P. (2005) Experimental procedures and problems in paste viscometry. Rheometry of pastes, suspensions, and granular materials: applications in industry and environment. John Wiley & Sons, Inc, Hoboken. https://doi. org/10.1002/0471720577. ch3.

Curran, S.J., Hayes, R.E., Afacan, A., Williams, M.C. and Tanguy, P.A. (2002) Properties of Carbopol Solutions as Models for Yield-Stress Fluids. Journal of Food Science 67(1), 176-180.

Dai, X., Gai, X. and Dong, B. (2014) Rheology evolution of sludge through high-solid anaerobic digestion. Bioresour Technology 174, 6-10.

Davies, R.M. and Taylor, S.G. (1950) The mechanics of large bubbles rising through extended liquids and through liquids in tubes. Proceedings of the Royal Society of London. Series A, Mathematical and Physical Sciences 200, 375-390.

De Temmerman, L., Maere, T., Temmink, H., Zwijnenburg, A. and Nopens, I. (2015) The effect of fine bubble aeration intensity on membrane bioreactor sludge characteristics and fouling. Water Research 76, 99-109.

Denis Funfschilling, H.Z.L. (2001) Flow of non-Newtonian fluids around bubbles: PIV measurements andbirefringence visualisation. Chemical Engineering Science 56, 1137-1141.

Dentel, S.K. (1997) Evaluation and role of rheological properties in sludge management. Water Science and Technology 36(11), 1-8.

Dewsbury, K., Karamanev, D. and Margaritis, A. (1999) Hydrodynamic characteristics of free rise of light solid particles and gas bubbles in non-Newtonian liquids. Chemical Engineering Science 54(21), 4825-4830.

Dieude-Fauvel, E., Heritier, P., Chanet, M., Girault, R., Pastorelli, D., Guibelin, E. and Baudez, J.C. (2014) Modelling the rheological properties of sludge during anaerobic digestion in a batch reactor by using electrical measurements. Water Research 51, 104-112.

Dimakopoulos, Y., Pavlidis, M. and Tsamopoulos, J. (2013) Steady bubble rise in Herschel–Bulkley fluids and comparison of predictions via the Augmented Lagrangian Method with those via the Papanastasiou model. Journal of Non-Newtonian Fluid Mechanics 200(0), 34-51.

Droste, R.L. and Gehr, R.L. (2018) Theory and practice of water and wastewater treatment, John Wiley & Sons.

Durán, C., Fayolle, Y., Pechaud, Y., Cockx, A. and Gillot, S. (2016) Impact of suspended solids on the activated sludge non-newtonian behaviour and on oxygen transfer in a bubble column. Chemical Engineering Science 141, 154-165.

Dziubiński, M., Orczykowska, M. and Budzyński, P. (2003) Comments on bubble rising velocity in non-Newtonian liquids. Chemical Engineering Science 58(11), 2441-2443.

Eickenbusch, H., Brunn, P.O. and Schumpe, A. (1995) Mass transfer into viscous pseudoplastic liquid in large-diameter bubble columns. Chemical Engineering and Processing 34, 479-485.

Eshtiaghi, N., Markis, F., Yap, S.D., Baudez, J.C. and Slatter, P. (2013) Rheological characterisation of municipal sludge: A review. Water Research 47(15), 5493-5510.

Eshtiaghi, N., Yap, S.D., Markis, F., Baudez, J.-C. and Slatter, P. (2012) Clear model fluids to emulate the rheological properties of thickened digested sludge. Water Research 46(9), 3014-3022.

Esmaeili, A., Guy, C. and Chaouki, J. (2015) The effects of liquid phase rheology on the hydrodynamics of a gas–liquid bubble column reactor. Chemical Engineering Science 129, 193-207.

Fang, W., Zhang, P., Ye, J., Wu, Y., Zhang, H., Liu, J., Zhu, Y. and Zeng, G. (2015) Physicochemical properties of sewage sludge disintegrated with high pressure homogenization. International Biodeterioration & Biodegradation 102, 126-130.

Farno, E. (2016) Rheological modification of muncipal sewage sludge by thermal treatment (Anaerobic digested sludge and waste activated sludge), RMIT university, Australia.

Farno, E., Baudez, J.C., Parthasarathy, R. and Eshtiaghi, N. (2014) Rheological characterisation of thermally-treated anaerobic digested sludge: Impact of temperature and thermal history. Water Research 56, 156-161.

Farno, E., Baudez, J.C., Parthasarathy, R. and Eshtiaghi, N. (2015a) Impact of temperature and duration of thermal treatment on different concentrations of anaerobic digested sludge: Kinetic similarity of organic matter solubilisation and sludge rheology. Chemical Engineering Journal 273(0), 534-542.

Farno, E., Baudez, J.C., Parthasarathy, R. and Eshtiaghi, N. (2015b) Impact of temperature and duration of thermal treatment on different concentrations of anaerobic digested sludge: Kinetic similarity of organic matter solubilisation and sludge rheology. Chemical Engineering Journal 273, 534-542.

Forster, C.F. (1981) Preliminary studies on the relationship between sewage sludge viscosities and the nature of the surfaces of the component particles. Biotechnology Letters 3(12), 707-712.

Fransolet, E., Crine, M., Marchot, P. and Toye, D. (2005) Analysis of gas holdup in bubble columns with non-Newtonian fluid using electrical resistance tomography and dynamic gas disengagement technique. Chemical Engineering Science 60(22), 6118-6123.

Giuseppe, O., Silvio, G., Gerardino, D.E., Antonio, M., Marek, R. and Piero, S. (2013) Preliminary assessments of combined effects of surface tension and viscosity on bubble column hydrodynamics. Chemical Engineering Transactions 32, 1579 - 1584.

Gomezdiaz, D., Navaza, J., Quintansriveiro, L. and Sanjurjo, B. (2009) Gas absorption in bubble column using a non-Newtonian liquid phase. Chemical Engineering Journal 146(1), 16-21.

Greene, P. (2014) Anaerobic_Digestion_and_Biogas.

Grönroos, A., Kyllönen, H., Korpijärvi, K., Pirkonen, P., Paavola, T., Jokela, J. and Rintala, J. (2005) Ultrasound assisted method to increase soluble chemical oxygen demand (SCOD) of sewage sludge for digestion. Ultrasonics Sonochemistry 12(1), 115-120.

Guibaud, G., Dollet, P., Tixier, N., Dagot, C. and Baudu, M. (2004) Characterisation of the evolution of activated sludges using rheological measurements. Process Biochemistry 39, 1803–1810.

Haque, M.W., Nigam, K.D.P. and Joshi, J.B. (1986) Hydrodynamics and mixing in highly viscous pseudo-plastic non-newtonian solutions in bubble columns. Chemical Engineering Science 41(9), 2321-2331.

Hasara, H., Kinacib, C., Unlua, A., Togrul, H. and Ipek, U. (2004) Rheological properties of activated sludge in a sMBR. Biochemical Engineering Journal 20, 1–6.

Hayet, C., Saida, B.-A., Youssef, T. and Hédi, S. (2016) Study of biodegradability for municipal and industrial Tunisian wastewater by respirometric technique and batch reactor test. Sustainable Environment Research 26(2), 55-62.

Henze, M.A. and Henze, M. (1997) Wastewater treatment : biological and chemical processes, Springer, Berlin, Heidelberg, [Germany].

Hii, K., Parthasarathy, R., Baroutian, S., Gapes, D.J. and Eshtiaghi, N. (2017) Rheological measurements as a tool for monitoring the performance of high pressure and high temperature treatment of sewage sludge. Water Research 114, 254-263.

Hofmeester, J.J.M. (1988) Gas hold-up measurements in bioreactors. Trends in Biotechnology 6(1), 19-22.

Hong, E., Yeneneh, A.M., Kayaalp, A., Sen, T.K., Ang, H.M. and Kayaalp, M. (2016) Rheological characteristics of municipal thickened excess activated sludge (TEAS): impacts of pH, temperature, solid concentration and polymer dose. Research on Chemical Intermediates 42(8), 6567-6585.

Houghton, J.I. and Quarmby, J. (1999) Biopolymers in wastewater treatment. Current Opinion in Biotechnology 10(3), 259-262.

Hu, Z., Chandran, K., Smets, B.F. and Grasso, D. (2002) Evaluation of a rapid physical–chemical method for the determination of extant soluble COD. Water Research 36(3), 617-624.

Hunter, R.J. (1981) Zeta Potential in Colloid Science, pp. 1-10, Academic Press.

Ishkintana, L.K. and Bennington, C.P.J. (2010) Gas holdup in pulp fibre suspensions: Gas voidage profiles in a batch-operated sparged tower. Chemical Engineering Science 65(8), 2569-2578.

Jamshidi, N. and Mostoufi, N. (2017) Measurement of bubble size distribution in activated sludge bubble column bioreactor. Biochemical Engineering Journal 125(Supplement C), 212-220.

Jiang, J., Wu, J., Poncin, S. and Li, H.Z. (2014) Rheological characteristics of highly concentrated anaerobic digested sludge. Biochemical Engineering Journal 86, 57-61.

Jin, H.-R., Lim, D.H., Lim, H., Kang, Y., Jung, H. and Kim, S.D. (2012) Demarcation of large and small bubbles in viscous slurry bubble columns. Industrial & Engineering Chemistry Research 51(4), 2062-2069.

Jin, H., Wang, M. and Williams, R.A. (2007) Analysis of bubble behaviors in bubble columns using electrical resistance tomography. Chemical Engineering Journal 130(2–3), 179-185.

Karia, G. and Christian, R. (2013) Wastewater treatment: concepts and design approach, PHI Learning Pvt. Ltd.

Kennedy, S., Bhattacharjee, P.K., Bhattacharya, S.N., Eshtiaghi, N. and Parthasarathy, R. (2018) Control of the mixing time in vessels agitated by submerged recirculating jets, p. 171037.

Khalili, F., Nasr, M.J., Kazemzadeh, A. and Ein- Mozaffari, F. (2018) Analysis of gas holdup and bubble behavior in a biopolymer solution inside a bioreactor using tomography and dynamic gas disengagement techniques. Journal of Chemical Technology & Biotechnology 93(2), 340-349.

Krishnan, J.M., Deshpande, A.P., Murali, K.J. and Sunil, K.P.B. (2010) Rheology of complex *f*luids, Springer, Dordrecht, New York.

Kulkarni, A.A. and Joshi, J.B. (2005) Bubble formation and bubble rise velocity in gas-liquid systems -A Review. Industrial & Engineering Chemistry Research 44, 5873 - 5931.

Ladewig, B. and Al-Shaeli, M.N.Z. (2016) Fundamentals of Membrane Bioreactors: Materials, Systems and Membrane Fouling, Springer, Singapore, singapore.

Laera, G., Giordano, C., Pollice, A., Saturno, D. and Mininni, G. (2007) Membrane bioreactor sludge rheology at different solid retention times. Water Research 41(18), 4197-4203.

Legrand, V., Hourdet, D., Audebert, R. and Snidaro, D. (1998) Deswelling and flocculation of gel networks: application to sludge dewatering. Water Research 32(12), 3662-3672.

Li, B. and Bishop, P.L. (2004) Micro-profiles of activated sludge floc determined using microelectrodes. Water Res 38(5), 1248-1258.

Lind, S.J. and Phillips, T.N. (2010) The effect of viscoelasticity on a rising gas bubble. Journal of Non-Newtonian Fluid Mechanics 165, 852-865.

Liss, S.N. and Droppo, I.G. (2005) Flocculation in natural and engineered environmental systems, CRC Press, Boca Raton.

Liu, Y. (2003) Chemically reduced excess sludge production in the activated sludge process. Chemosphere 50(1), 1-7.

Lotito, V., Spinosa, L., Mininni, G. and Antonacci, R. (1997) The rheology of sewage sludge at different steps of treatment. Water Science and Technology 36(11), 79-85.

Margaritis, A., Te Bokkel, D.W. and Karamanev, D.G. (1999) Bubble rise velocities and drag coefficients in non-Newtonian polysaccharide solutions. Biotechnology and Bioengineering 64(3), 257-266.

Markis, F., Baudez, J.-C., Parthasarathy, R., Slatter, P. and Eshtiaghi, N. (2014) Rheological characterisation of primary and secondary sludge: Impact of solids concentration. Chemical Engineering Journal 253, 526-537.

Mendelson, H.D. (1967) The prediction of bubble terminal velocities from wave theory. AIChE Journal 13(2), 250-253.

Meng, F., Chae, S.-R., Drews, A., Kraume, M., Shin, H.-S. and Yang, F. (2009) Recent advances in membrane bioreactors (MBRs): Membrane fouling and membrane material. Water Research 43(6), 1489-1512.

Meng, F., Shi, B., Yang, F. and Zhang, H. (2007) New insights into membrane fouling in submerged membrane bioreactor based on rheology and hydrodynamics concepts. Journal of Membrane Science 302(1–2), 87-94.

Meng, F., Yang, F., Shi, B. and Zhang, H. (2008) A comprehensive study on membrane fouling in submerged membrane bioreactors operated under different aeration intensities. Separation and Purification Technology 59(1), 91-100.

Meng, F., Zhang, H., Yang, F., Zhang, S., Li, Y. and Zhang, X. (2006) Identification of activated sludge properties affecting membrane fouling in submerged membrane bioreactors. Separation and Purification Technology 51(1), 95-103.

Meng, F., Zhang, S., Oh, Y., Zhou, Z., Shin, H.-S. and Chae, S.-R. (2017) Fouling in membrane bioreactors: An updated review. Water Research 114(Supplement C), 151-180.

Menniti, A., Kang, S., Elimelech, M. and Morgenroth, E. (2009) Influence of shear on the production of extracellular polymeric substances in membrane bioreactors. Water Research 43(17), 4305-4315.

Mezger, T.G. (2011) The rheology handbook : for users of rotational and oscillatory rheometers, Vincentz Network, Hanover, Germany.

Moeller, G. and Torres, L.G. (1997) Rheological characterization of primary and secondary sludges treated by both aerobic and anaerobic digestion. Bioresource Technology 61(3), 207-211.

Mori, M., Seyssiecq, I. and Roche, N. (2006) Rheological measurements of sewage sludge for various solids concentrations and geometry. Process Biochemistry 41(7), 1656-1662.

Orvalho, S., Ruzicka, M.C., Olivieri, G. and Marzocchella, A. (2015) Bubble coalescence: Effect of bubble approach velocity and liquid viscosity. Chemical Engineering Science 134, 205-216.

Park, J.-S., Yeon, K.-M. and Lee, C.-H. (2005) Hydrodynamics and microbial physiology affecting performance of a new MBR, membrane-coupled high-performance compact reactor. Desalination 172(2), 181-188.

Pisarevsky, A., Polozova, I. and Hockridge, P. (2005) Chemical Oxygen Demand. Russian Journal of Applied Chemistry 78(1), 101-107.

Pollice, A., Giordano, C., Laera, G., Saturno, D. and Mininni, G. (2007) Physical characteristics of the sludge in a complete retention membrane bioreactor. Water Research 41(8), 1832-1840.

Ratkovich, N., Horn, W., Helmus, F.P., Rosenberger, S., Naessens, W., Nopens, I. and Bentzen, T.R. (2013) Activated sludge rheology: A critical review on data collection and modelling. Water Research 47(2), 463-482.

Sanin, F.D. (2002) Effect of solution physical chemistry on the rheological properties of activated sludge. Water Research South Africa 28(02), 207-212.

Sanin, F.D., Clarkson, W.W. and Vesilind, P.A. (2011) Sludge engineering: the treatment and disposal of wastewater sludges, DEStech Publications, Inc, United states of America.

Sanin, F.D. and Vesilind, P.A. (1996) Synthetic Sludge: A physical/chemical model in understanding bioflocculation. Water Environment Research 68(5), 927-933.

Schonhorn, H. (1965) Theoretical relationship between surface tension and cohesive energy density. The Journal of Chemical Physics 43(6), 2041-2043.

Seyssiecq, I., Marrot, B., Djerroud, D. and Roche, N. (2008) In situ triphasic rheological characterisation of activated sludge, in an aerated bioreactor. Chemical Engineering Journal 142(1), 40-47.

Seyssiecq., Ferrasse and Roche (2003) State-of-the-art: rheological characterisation of wastewater treatment sludge. Biochemical Engineering Journal 16(1), 41-56.

SHAH Y.T, KELKAR B.G, GODBOLE S.P and W.D, D. (1982) Design Parameters Estimations for Bubble Column Reactors. AlChE Journal 28(353-379).

Sheng, G.-P., Yu, H.-Q. and Li, X.-Y. (2010) Extracellular polymeric substances (EPS) of microbial aggregates in biological wastewater treatment systems: A review. Biotechnology Advances 28(6), 882-894.

Sikorski, D., Tabuteau, H. and de Bruyn, J.R. (2009) Motion and shape of bubbles rising through a yield-stress fluid. Journal of Non-Newtonian Fluid Mechanics 159(1-3), 10-16.

Speight, J.G. (2017) Environmental Organic Chemistry for Engineers. Speight, J.G. (ed), pp. 203-261, Butterworth-Heinemann.

Spinosa, L. and Lotito, V. (2003) A simple method for evaluating sludge yield stress. Advances in Environmental Research 7(3), 655-659.

Sutherland, I.W. (2001) Exopolysaccharides in biofilms, flocs and related structures. Water Science and Technology 43(6), 77.

Tixier, N., Guibaud, G. and Baudu, M. (2003a) Determination of some rheological parameters for the characterization of activated sludge. Bioresource Technology 90(2), 215-220.

Tixier, N., Guibaud, G. and Baudu, M. (2003b) Effect of ph and ionic environment changes on interparticle interactions affecting activated sludge flocs: A rheological approach. Environmental Technology 24(8), 971-978.

Tran, A., Rudolph, M.L. and Manga, M. (2015) Bubble mobility in mud and magmatic volcanoes. Journal of Volcanology and Geothermal Research 294, 11-24.

Trussell, R.S., Merlo, R.P., Hermanowicz, S.W. and Jenkins, D. (2007) Influence of mixed liquor properties and aeration intensity on membrane fouling in a submerged membrane bioreactor at high mixed liquor suspended solids concentrations. Water Research 41(5), 947-958.

Vold, M.J. (1982) Zeta potential in colloid science. Principles and applications. Journal of Colloid and Interface Science 88(2), 608.

Wang, Y. and McNeil, B. (1996) A study of gas hold-up, liquid velocity, and mixing time in a complex high viscosity, fermentation fluid in an airlift bioreactor. Chem. Eng. Technol. 19(2), 143-153.

Wilén, B.-M., Jin, B. and Lant, P. (2003) The influence of key chemical constituents in activated sludge on surface and flocculating properties. Water Research 37(9), 2127-2139.

Wilen, B.M., Jin, B. and Lant, P. (2003) Relationship between flocculation of activated sludge and composition of extracellular polymeric substances. Water Sci Technol 47(12), 95-103.

Yuan, H., Zhu, N. and Song, F. (2011) Dewaterability characteristics of sludge conditioned with surfactants pretreatment by electrolysis. Bioresource Technology 102(3), 2308-2315.

Yusuf, C. and Murray, M.-Y. (1988) Gas holdup behaviour in fermentation broths and other non-Newtonian fluids in pneumatically agitated reactors. The Chemical Engineering Journal 39, B31-B36.

Zhang, Y., Zhang, P., Guo, J., Ma, W., Fang, W., Ma, B. and Xu, X. (2013) Sewage sludge solubilization by high-pressure homogenization. Water Science and Technology 67(11), 2399-2405.

Zhang, Z., Zhu, J. and Park, K.J. (2004) Effects of duration and intensity of aeration on solids decomposition in pig slurry for odour control. Biosystems Engineering 89(4), 445-456.

Zuber, N. and Findlay, J.A. (1965) Average volumetric concentration in two-phase flow systems Journal of Heat Transfer 87(4), 453-468.

CHAPTER 3: MATERIALS AND METHODS

3.1 SAMPLE PREPARATION

Waste activated sludge was studied in this project. WAS mainly consists of organic matter, microorganisms and bacteria dissolved in water; that is, the biomass that settles out in the secondary clarifier. Since WAS is mainly a microbial cell mass, it is a complex material which is difficult to handle (Baroutian et al. 2013, Baudez and Coussot 2001).

Waste activated sludge at a total solid concentration of 3.0% was collected from a waste water treatment plant in Victoria, Australia. The microbial activity inside the sludge was reduced by storing it at 4^{o}C for 30 days. This procedure improves the stability of samples, resulting in reproducible data (Curvers et al. 2009). To enable preparation of different concentrations of WAS samples, the sludge was thickened to higher solid concentration (6%) using a centrifuge at 7^{o}C and 8000 rpm (i.e. 12,200 maximum relative centrifugal force) for 30 minutes. It was then mixed with the original sludge sample (liquor) using a benchtop overhead stirrer at a speed of 250 rpm at room temperature to prepare homogeneous samples of the desired concentrations (3%, 4%, 5% and 5.5%).

The sludge sample was heated to 105^{o}C in the oven for at least 24 hours, and the sludge concentration calculated using the difference in weight (Rice et al. 2012), as shown in equation 3.1.

$$\%\ concentration = \left[\frac{m_{(dry\ sludge+dish)} - m_{(dish,empty)}}{m_{(wet\ sludge+dish)} - m_{(dish,empty)}}\right] * 100 \quad (3.1)$$

3.2 RHEOLOGICAL MEASUREMENTS

A hybrid shear stress controlled rheometer (HR3) from TA Instruments was used for all rheological tests. The HR3 enables measurement of properties such as viscosity and shear stress, as well as viscoelastic properties like storage and loss modulus, strain, and phase angle. The rheological measurement process involves measuring the response of a material to an applied deformation. The deformation, or strain, can be applied in different ways to establish a relationship between material properties and the stress, strain and time conditions; only relatively simple shear conditions can be used (Brownsey 1998). Rheology can be measured in two different regimes: the linear viscoelastic region (in

which the material behaves as solid over the applied deformation without destroying the sample structure) and the non-linear viscoelastic region (in which the material behaves as liquid over the applied deformation and the sample structure fully destroyed) (Mezger 2011).

3.2.1 MEASUREMENT GEOMETRY AND APPARATUS

There are several geometries available for the stress controlled rheometer. A concentric cylinder is recommended for measuring structured fluids (materials which contain more than one phase, such as solid particles dispersed in a liquid, gas particles in foam or an emulsion of immiscible liquids) (Baudez et al. 2011, Eshtiaghi et al. 2013). This study employed a specially designed plexiglass cup (inner diameter: 100 mm, length: 100 mm) with a stainless steel porous disk (outer diameter: 100 mm, thickness: 1.6 mm, porosity: 40%, from SINTEC Australia) at the bottom for the gas sparging and stainless steel grooved bob geometry with outer diameter of 14.9 mm and length 42 mm, as shown in Figure 3.1. The gas flow rate used was in the range on 0.5LPM to 7 LPM which corresponds to the gas superficial velocity of 0.00091 m/s to 0.01274 m/s.

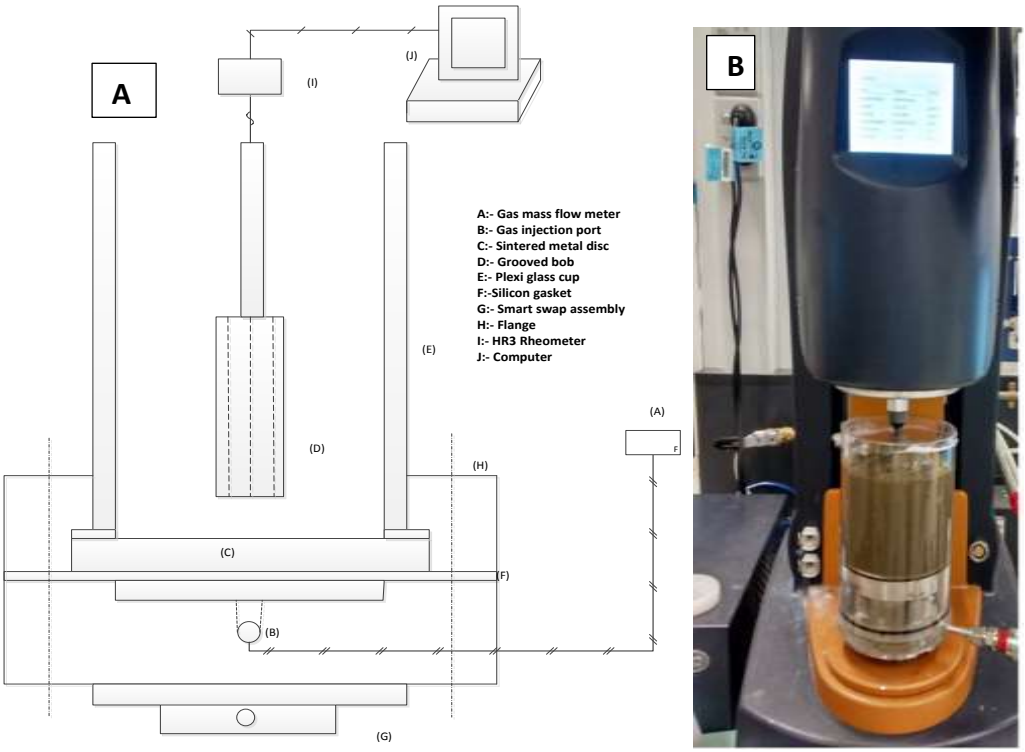

Figure 3.1: (A) Schematic drawing of experimental setup, (B) actual experimental setup

3.2.2 RHEOLOGICAL MEASUREMENTS IN NON-LINEAR VISCOELASTIC REGION

In the non-linear region, flow behaviour is the most important rheological measurement. Viscosity, an important flow behaviour parameter, is measured as a function of the shear rate. The obtained data can be plotted as viscosity v/s shear rate (viscosity curve) or shear stress v/s shear rate (flow curve). Thus, flow curve measurement makes it possible to understand the viscosity at different shear rates, which is important for optimising technical processes such as pumping or spraying.

In this study, to analyse the impact of gas injection on the flow behaviour of sludge, the flow curve of a 3% solid concentration of WAS measured using in situ and after sparging. For in situ measurement, the flow curve was obtained while injecting the gas at 0.5 LPM to 3 LPM. However, in the after sparging method the gas was first sparged at 0.5 LPM to 3 LPM for 20 minutes through sludge before obtaining the flow curve. Before each flow curve measurement, the sample was pre-sheared at high shear rate (400 s^{-1}; the maximum shear rate without turbulence in this cup is 401 s^{-1}) for 900 s and then allowed to rest for 120 s to obtain an identical sludge sample before each flow curve measurement. The viscosity of the sample was then measured over the shear rate range of 0.001 s^{-1} to100 s^{-1}. The stepwise procedure used to measure sample viscosity is shown in Figure 3.2. To select the appropriate geometry for the experiment and to validate the viscosity values, a comparison of flow curves obtained with different gap sizes (42.55 mm and 35 mm) and geometries (large vane: d = 30 mm, h = 65 mm; small vane: d = 28 mm, h = 42 mm; grooved bob: d = 14.9 mm, h = 42 mm; smooth bob: d = 28 mm, h = 42 mm) was performed as shown in Figure 3.3.

From Figure 3.3 it is clear that the smooth bob produces lower viscosity values at low shear rate due to slippage (Barnes 1995). However, all the other geometries used produced exactly the same viscosity values. Hence it was feasible to use the small vane, large vane, and grooved bob geometries for viscosity measurement.

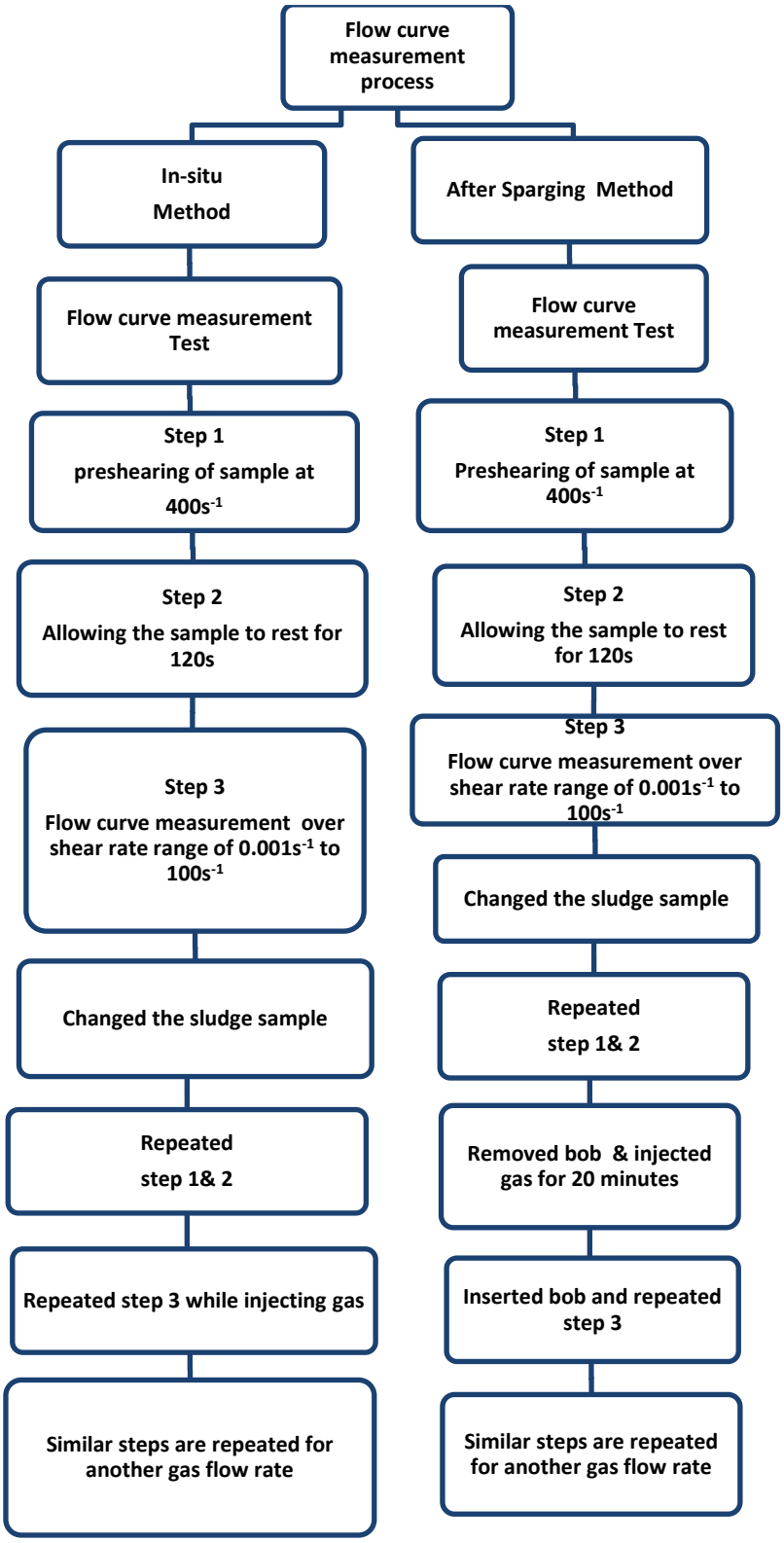

Figure 3.2: Schematic of experimental procedure for flow curve measurement for both In situ and after sparging methods

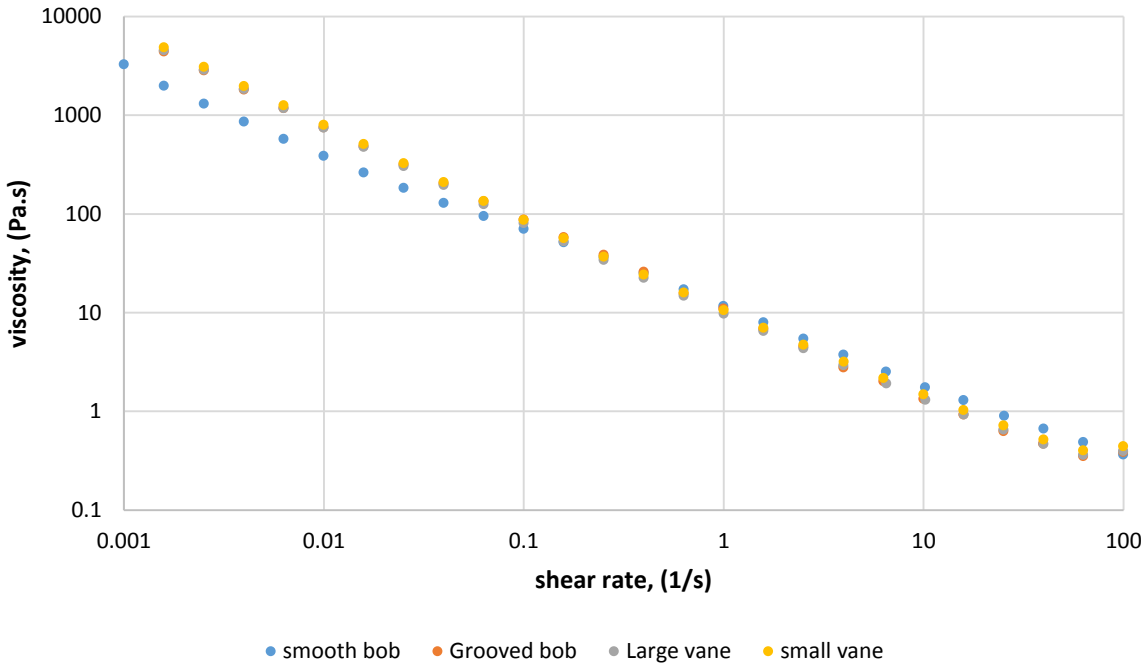

Figure 3.3: Comparison of viscosity curves for waste activated sludge containing 3% total solids, without gas, using four geometries

Grooved bob geometry with a wide gap (42.55 mm) was chosen for the rheological measurements. The flow curves were recalculated using Equations 3.2 and 3.3 (Estellé et al. 2008, Markis et al. 2014, Mezger 2011).

$$\tau_{Ri} = \frac{M}{(2\pi H R_i^2)} \quad (3.2)$$

$$\dot{\gamma} = 2M \frac{d\Omega}{dM}, \tau_c \leq \tau_y \leq \tau_b \quad (3.3)$$

Where M is the torque (N·m), H is the height of the bob (m), R_i is the radius of the rotating bob (m), Ω is angular velocity (rad/s), derivative dΩ/dM is calculated as ($\Omega_j - \Omega_{j-1}$) / ($M_j - M_{j-1}$), and τ_y, τ_c, τ_b are yield stress and stress at the cup and bob respectively (Pa).

Equation 3.3 can be used for three different types of fluids (Herschel–Bulkley (HB) fluid, power law fluid or Casson fluid) and is applicable to any gap size. Additionally the extra stresses induced by secondary flow or turbulence flow was checked by using Taylor

number and Reynolds number (Mezger 2011). The data collected was well within the stable region of laminar flow.

To understand the impact of different methods of sparging on rheological measurement and to select the correct method for further experiments, the flow curve measurements obtained from both the in situ method and after sparging method using different geometries were compared, as shown in Figure 3.4. Figure 3.4A shows the flow curve measurements using the in situ method; for the same sample and at the same shear rate, different geometries produce different viscosities. The differences between viscosity values generated with different geometries increase as the shear rate decreases. However, the viscosity curve obtained using the after sparging method (Figure 3.4B) shows that the viscosity measured at the same shear rate is same.

To determine the reason for the massive difference in viscosity values at low shear rate for the same sludge sample due to different geometries, change in torque against shear rate was plotted for both the in situ and after sparging method, as shown in Figure 3.5.

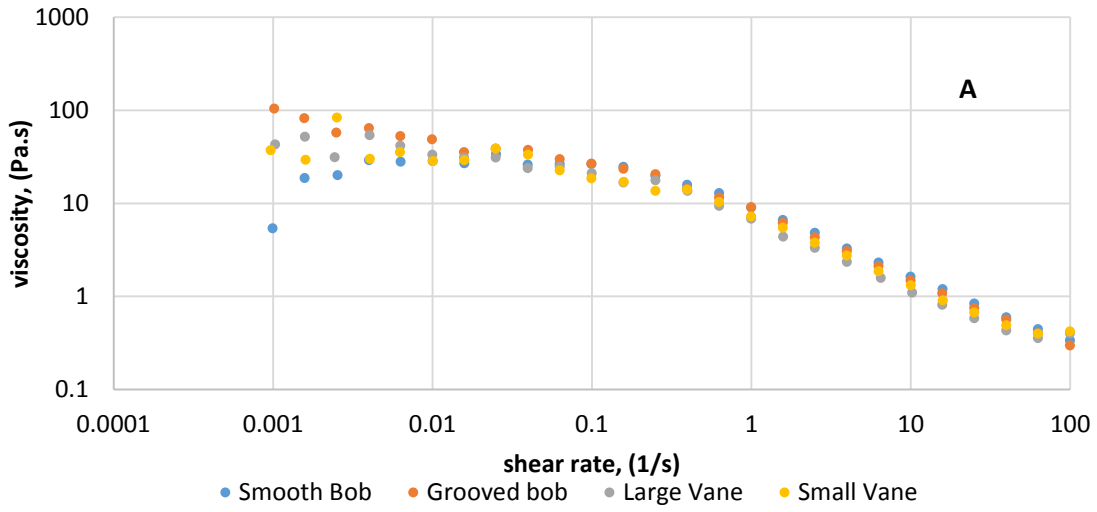

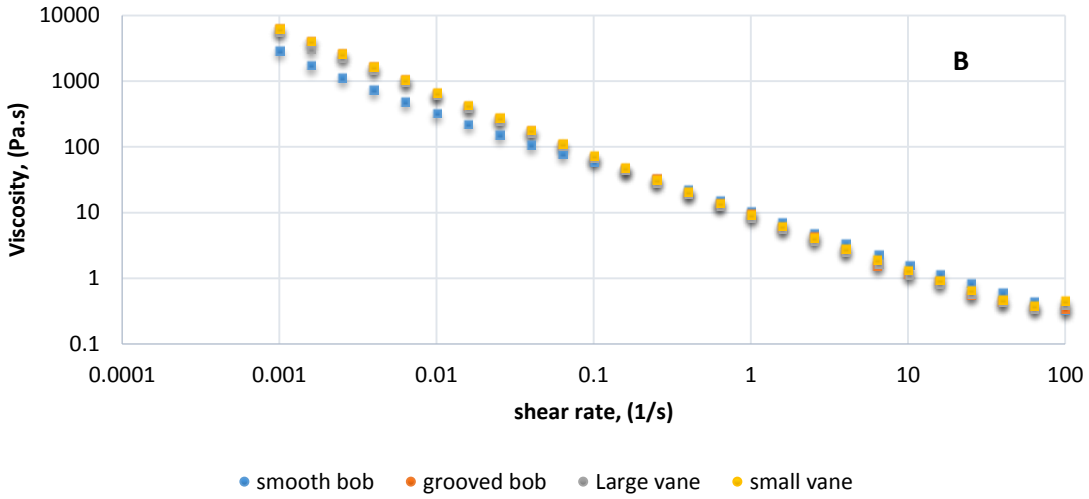

Figure 3.4: Comparison of viscosity curves for waste activated sludge containing 3% total solids at 0.5 LPM of gas flow rate using four geometries, (A) In situ and (B) After sparging

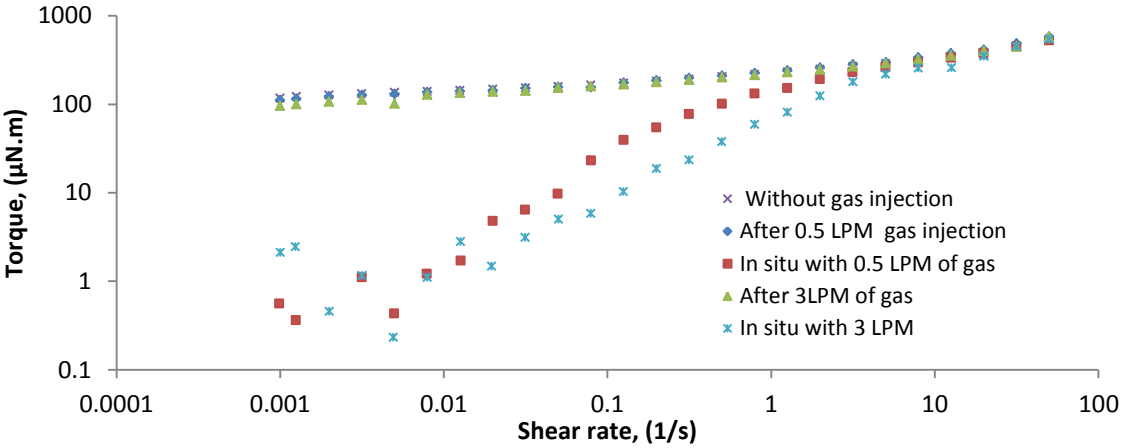

Figure 3.5: Comparing impact of gas injection at two gas flow rate of 0.5 LPM and 3.0 LPM through two different methods of in situ and after sparging on torque

Figure 3.5 shows that with the in situ method, torque data are scattered in the low shear rate zone, but there is no variation at high shear rates. Moreover, the torque curve for the after sparging method appears smooth throughout the entire shear rate range and is irrespective of gas flow rate. Thus, scattering of torque data during the application of the in situ method in the low shear rate zone must occur due to the presence of gas. This means that at low shear rate gas injection affects torque strongly in the in situ method, and hence huge viscosity drops are only observed in the low shear rate range. Thus, the lower viscosity values in the low shear rate range obtained from the in situ method are not because of change in material characteristics, but because slippage is occurring due to

channelling of gas through the sample at centre of sample around rotating bob . At the higher shear rate the torque is so high that gas bubble presence close to the bob does not affect torque measurement. Hence, the torque, displacement and viscosity curves at high shear rates show the same value irrespective of the method used. Consequently, the after sparging method is more reliable for rheological measurement, and further experiments were based on this method only.

3.2.3 RHEOLOGICAL MEASUREMENTS IN THE LINEAR VISCOELASTIC REGION

Rheological properties in the LVE are important to gain a complete picture of how a material undergoes structural rearrangement with the applied deformation. To understand the LVE of a sample, a strain sweep is carried out at very low frequency and by changing the strain rate from low to high. The material behaves independent of strain up to a critical strain level, above which the material falls in the non-linear region and the storage modulus starts decreasing, as shown in Figure 3.6. Using the strain applicable to the LVE (i.e. the strain below the critical strain threshold), tests such as creep and time sweep can be performed.

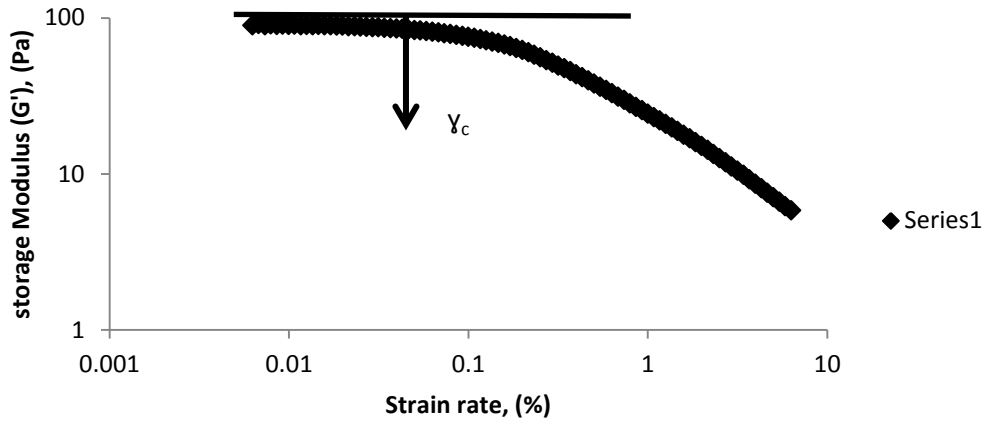

Figure 3.6: Sludge strain sweep at a frequency of 1 Hz

Oscillatory time sweep

Oscillatory time sweeps are important when testing materials such as dispersions and structured fluids that may undergo macro- or micro-structural rearrangement with time that affects their rheological behaviour. In this study, time sweep tests were performed to improve understanding of the impact of gas injection on sludge structure by measuring storage and loss modulus.

The storage modulus G' (G prime, in Pa) represents the elastic portion of the viscoelastic behavior, which describes the solid-state behavior of the sample. The loss modulus G" (G double prime, in Pa) characterizes the viscous portion of the viscoelastic behavior, which can be seen as the liquid-state behavior of the sample.

Viscous behavior arises from the internal friction between the components in a flowing fluid, thus between molecules and particles. This friction converts the deformation energy into heat energy which is absorbed by the surrounding. This loss of energy is also called energy dissipation. In contrast, the elastic portion of energy is stored in the deformed material; i.e. by extending and stretching the internal superstructures without overstressing the interactions and without destroying the material. When the material is later released, this unused stored energy acts like a driving force for reforming the structure into its original shape (Mezger 2011).

The experimental procedure for the time sweep test was carried out as follows. The sludge was pre-sheared at a high shear rate (400 s^{-1}) for 900 s. This step helps to ensure that identical condition is achieved in all samples. Final shear stress was monitored carefully while pre-shearing. The sludge was then kept at rest for a short period (120 s) without causing any further disturbance (i.e. without removing the bob) (Baudez 2008, Markis et al. 2014). Following the pre-shearing step, to understand the structural deformation of sludge, a time sweep test corresponding to a constant strain of 0.09% and frequency (1 Hz), well within the LVE, was performed at different solids concentrations of sludge for 1500 s. After repeating the pre-shearing stage, the bob was removed and nitrogen gas at four different flow rates from 1 LPM to 7 LPM which corresponds to superficial gas velocities of 0.00182 m/s to 0.01274 m/s was sparged for 1200 s. After this step, the bob was reinserted, and a time sweep test was performed on aerated sludge sample at 0.09% strain and 1 Hz frequency. The same procedure was carried out for other gas flow rates.

Creep test

Creep and creep recovery tests were used to analyse viscoelastic behaviour while performing two shear stress steps. This method is mostly used to examine chemically unlinked and unfilled polymers (melts and solutions), but it is also suitable to evaluate the behavior of chemically cross-linked polymers, gels and dispersions showing a physical chemical network of forces. To make sure the structural changes in the sludge due to gas

injection were because of physical changes in the network of forces, creep tests were carried out in this study for 4.2% sludge concentration at two gas flow rates.

The experimental procedure for the creep test was carried out in the following way. The sludge was pre-sheared at a high shear rate (400 s^{-1}) for 900 s to ensure that an identical condition was achieved. Final shear stress was monitored carefully while pre-shearing. The sludge was then kept at rest for a short period (120 s) without removing the bob (Baudez 2008, Markis et al. 2014). Following the pre-shearing step, to understand the physical changes in the network (i.e. elastic deformation of the sludge), a creep test corresponding to constant stress of 0.89 Pa (well within the LVE) was performed with a 4.2% solids concentration of WAS for a duration of 900 s. In the next step, to account for all the structural and shearing changes that may occur during the test due to the removal and insertion of the bob, the bob was removed immediately after the pre-shearing step, and the sludge was allowed to rest for 900 s (the same duration as for the time sweep test). After 900 s rest, the bob was reinserted and the creep test Pa was repeated with the same stress of 0.89. This enabled measurement of the impact of removing and replacing the bob on sludge structure after a long rest time.

After repeating the pre-shearing stage and removing the bob, nitrogen gas at flow rates of 0.5 LPM and 1.5 LPM was sparged for 1500 s. After this step, the bob was reinserted, and a creep test was performed on the aerated sludge sample at 0.89 Pa stress. To calculate the shear induced only by gas injection, the extra shear imposed by removing and replacing the bob was deducted from the obtained data at this step. The same procedure was carried out for other gas flow rates. A detailed stepwise procedure for both the time sweep test and creep test is shown in Figure 3.7A.

Further successive creep and dynamic measurements (time sweep) of non-aerated sludge with broader stress and strain % ranges (at 1 Hz frequency) were performed to calculate the shear stress induced by gas injection. For example, a strain % of greater than 0.09% was applied to the non-aerated sludge sample to achieve the same response as in aerated sludge at 0.09% strain. The difference showed the amount of induced shear due to gas injection, as detailed in Figure 3.7B.

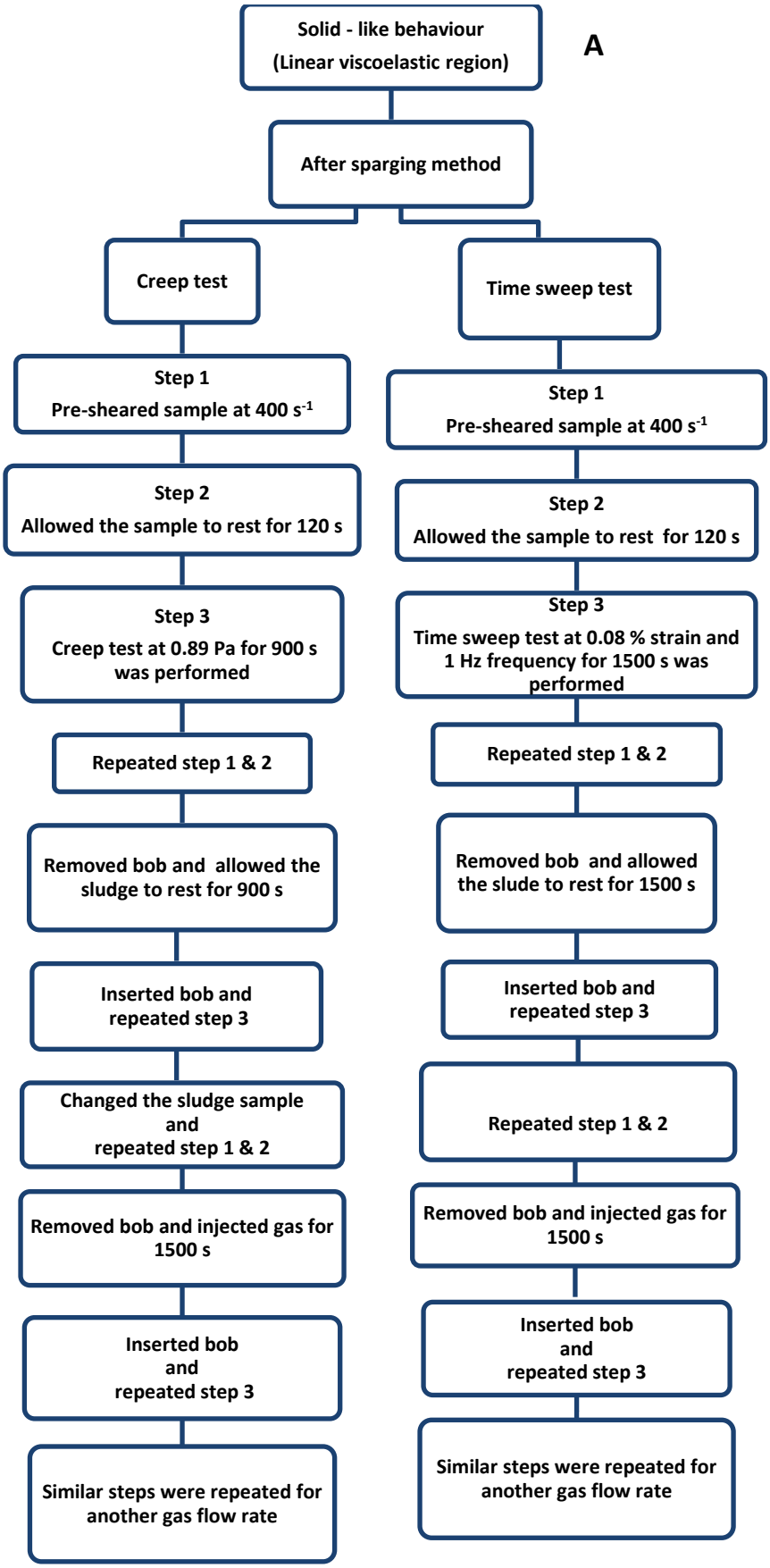

Figure 3.7: (A) Schematic of experimental procedure for both creep test & time sweep test

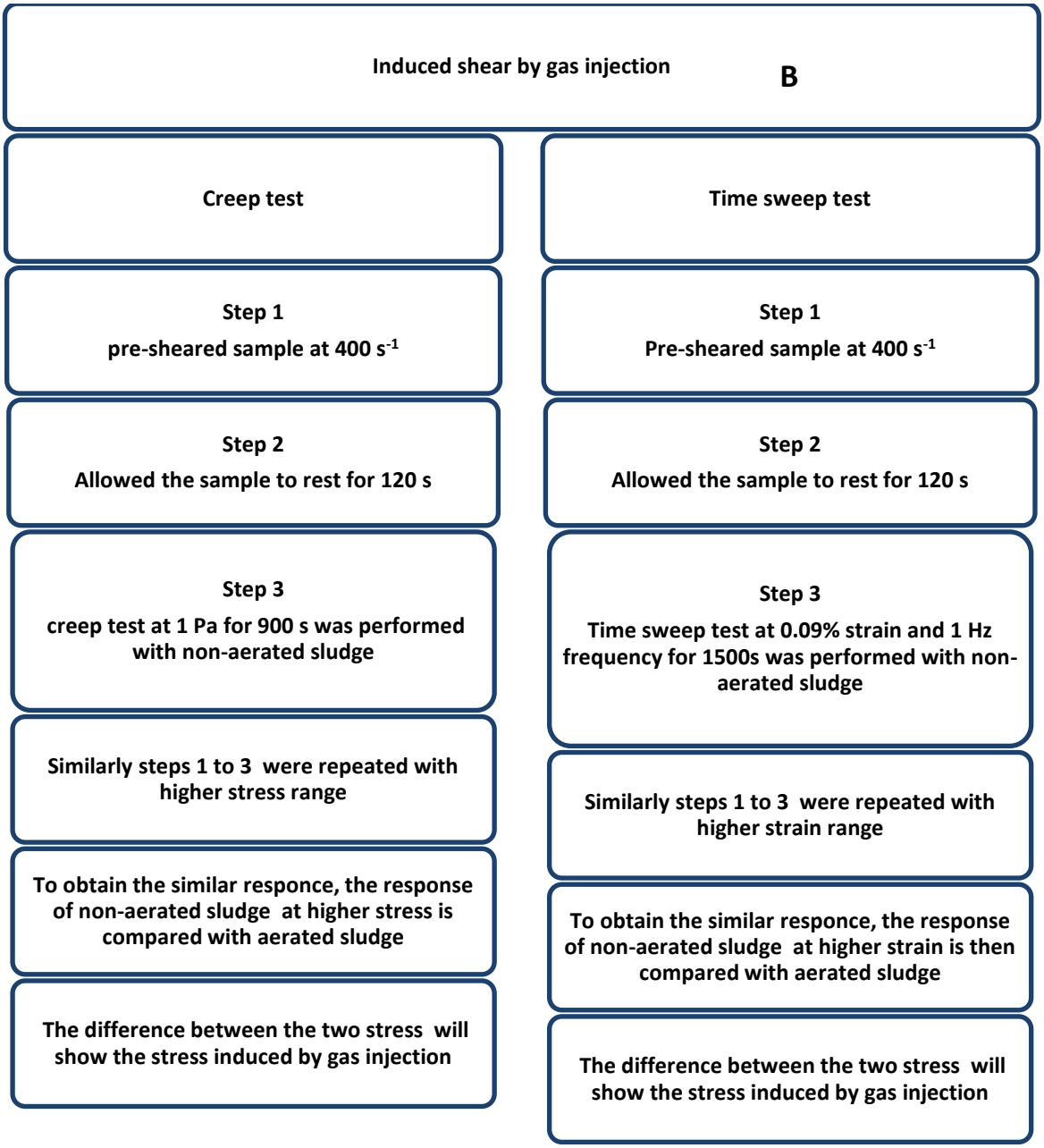

Figure 3.7: (B) Schematic of experimental procedure for extra stress imposed by gas injection in both Creep test & Time sweep test

3.3 PHYSICO-CHEMICAL PROPERTIES

Knowledge of the physico-chemical properties of matter are important to engineers for the efficient design and operation of unit processes. To understand the impact of gas injection on sludge physico-chemical properties and its correlation with sludge rheology, properties such as TSS, zeta potential, sCOD and surface tension must be measured.

3.3.1 TOTAL SUSPENDED SOLIDS

Total suspended solids consist of organic and inorganic materials of size larger than 2 microns (Branigan 2013). In waste water treatment, measuring the concentration of suspended solids regularly is important to ensure that the process runs efficiently, and it also gives a much clearer picture of what is actually going on in the process. If the suspended solids are at high concentration, the system can become overloaded, increasing the oxygen requirement and wasting energy. If the suspended solids are at low concentration then the microorganisms will run out of "food" and start to die, decreasing the efficiency of the digestion process. To understand the impact of gas injection on WAS, TSS was measured using the following process.

A known quantity (g) of sludge was dissolved with 5 ml of water with the help of a magnetic stirrer. The diluted sample was then filtered completely using 1.5µm ProWeigh® Original binderless glass fibre filters. The weight of the filter paper and the filtered separated solids was measured and noted. The filter paper and solids was then dried in an oven at 80^{oC} for 4–6 hours, and the dry mass recorded. Because it is difficult to measure the exact volume of thick sludge, assuming the density is same as that of water at $1g/cm^3$, and $1g/cm^3$ of water = 1 g/ml, the TSS in g/ml can be calculated as

$$TSS\left(\frac{g}{l}\right) = \frac{(dry\ weight\ of\ residue\ and\ filter(g) - dry\ weight\ of\ filter\ alone(g)}{\frac{weight\ of\ sludge\ sample(g)}{density\ of\ water\ (\frac{g}{cm^3})}} * 1000$$

For aerated samples, the gas was injected for 20 mins at the desired flow rate and the above procedure was repeated to measure TSS. The procedure was repeated for all concentrations and gas flow rates.

3.3.2 SOLUBLE COD

The sCOD of sludge was measured under the same gas injection conditions as in the rheological characterisation, using a Hach procedure (involving COD high range plus reagents, a DR6000 spectrophotometer and a Hach DRB200 reactor). The sludge samples were centrifuged at 10,000 rpm (i.e. 20913 maximum relative centrifugal force) for 20 min to separate the liquor and solids. The small quantity of separated liquor was filtered through mixed cellulose ester membranes (porosity of 0.45 µm) for sCOD measurement.

The 2 µml of filtered sample was added to the COD reagent (HR+) and placed in the COD digester (DRB200 reactor) at 150^{o}C for 120 mins. The reacted sample was allowed to cool until room temperature was achieved. The sCOD was measured by placing the reacted sample vial in the DR6000 Spectrophotometer.

3.3.3 ZETA POTENTIAL

Zeta potential measurement provides insight about the causes of dispersion, aggregation, flocculation and sedimentation. Zeta potential also affects the size and density of the flocs formed. The zeta potential, measured as the surface charge/electrostatic interaction between the particles, represents the potential drop between the diffuse double layers of the surface. This measurement improves understanding of the stability of the fluid and its sedimentation and flocculation process (Hunter 1981, Vold 1982, Yuan et al. 2011).

The zeta potential is determined by introducing fine particles in an electric field and measuring their mobility, by light scattering method. Particle mobility is related to the zeta potential (ζ) at the interface using the Smoluchowski equation.

$$\nu_E = \frac{\zeta \varepsilon}{\mu}$$

Where, µ= viscosity of the fluid (Pa.s), ζ = zeta potential of the fluid (mv), ν_E = particle mobility in electrical field (cm^2/mv.s), and Ɛ = the electrical permittivity (Coulombs (C) ^{2} / Pa.cm^2).

The intensity of the scattered light and the unscattered laser light (reference beam) is then compared and displayed in the log sheet. The minimum required intensity of the reference beam (count rate) is 20 kcps. If the count rate falls below 20 kcps, the measurement fails to complete. Therefore, the sample used for measurement of zeta potential has to be optically clear.

The sludge used in this process was concentrated WAS. In order to obtain an accurate zeta potential measurement, the sludge samples were centrifuged at 10,000 rpm (i.e. 20913 maximum relative centrifugal force) for 20 min to separate the liquor from the solids.

Zeta potential measurement was performed using a Zetasizer Nano Range from Malvern Instruments and disposable folded capillary cells (DTS 1070). When the conductivity of

the sludge was greater than 5ms/cm, the measurement was taken in monomodal mode in order to reduce sample/electrode degradation due to high conductivity. The measurement was carried out at 20^{o}C, with an interval of 10 s between each set of readings. Each measurement was duplicated. The standard maximum deviation allowed was ±5%.

3.3.4 SURFACE TENSION

The surface tension of a fluid changes with any change in formulation at the molecular level. Measurements of surface tension help us understand the dispersion and adhesion of the fluid. For example, if there is a decrease in the surface tension of sludge, the first sign is foam formation, representing the presence of surfactants or a high volatile fatty acid concentration that prevents the sludge settling. However, if the surface tension increases, this indicates an increase in salt content, which can lead to entrainment of air within the solids/floc structure of sludge (Davies and Rideal 1963). It was important to measure the surface tension of the sludge in order to understand the impact of gas injection on the sludge's structure.

Surface tension was measured for all the sludge samples and at each gas velocity using a surface tension meter (Kruss, Germany). Since sludge contains both cations and anions, the standard platinum plate is not recommended; the sludge sticks to the plate, increasing the tension on the plate and biasing the surface tension measurement. To overcome this issue, a microscope cover glass (18 x 18 x 0.1 mm) & microscope glass slide (26 x 76 x 1 mm) was used to measure the surface tension (refer to Figure 3.8). The standard process of activation, using an oxygen flame, was carried out before each measurement. The activation process is important to get rid of any dust particles attached to the plate that might affect measurement.

Sludge is a complex liquid consisting of both organic and inorganic material in the form of bio-floc. It was observed that steady-state surface tension was not achieved at a standard time of 60 s because, the viscosity of raw sludge is much higher than that of water it takes more time to achieve a stable surface tension reading. Since, surface tension is related to cohesion energy, that is, the attraction of the liquid molecules to each other rather than to molecules in the air that is adhesion. Sludge being a complex mixture of solid and liquid phase; the attraction between the liquid molecules in sludge is less than that of water. Hence, surface tension is measured with both the microscope glass slide and

glass cover at different depths and time to choose the optimum depth and time of measurement of sludge surface tension. The two plates (the microscope slide and cover) were first calibrated by measuring the surface tension of water at different depths and comparing these figures with the surface tension of water measured with a standard platinum plate, as shown in Table 3.1. We can see that the surface tension measured using the microscope cover slide at different depths varies only minimally from the surface tension measured using the standard platinum plate, unlike the surface tension measured using the slide. Thus, the microscope cover slide was chosen as a plate to use in finding a suitable depth and duration for sludge surface tension measurement (refer to Table 3.2). Eventually, the standard 2 mm depth and measurement time of 1200s were chosen to achieve the steady state measurement of raw sludge.

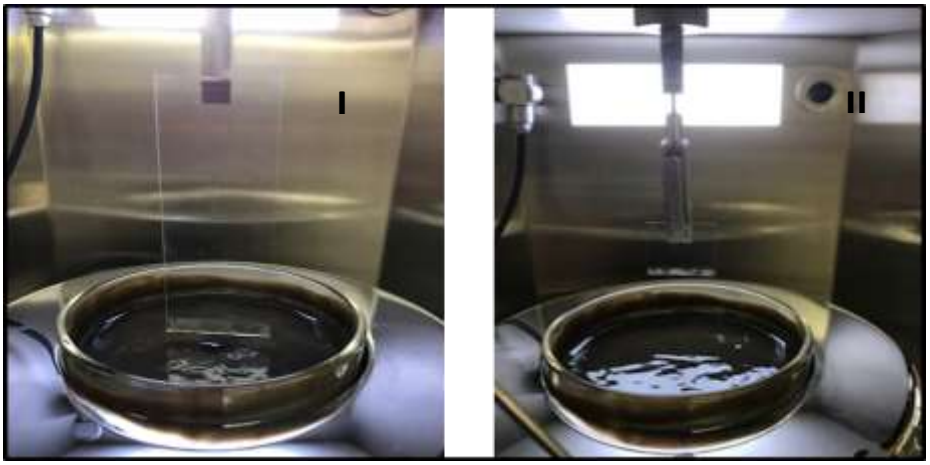

Figure 3.8: Surface tension measurement using (I) microscope glass slide & (ii) microscope cover slide

Table 3.1 Surface tension of water measured using three plates for calibration

Water			
Immersion depth	Platinum plate (mN/m)	Microscope slide (mN/m)	Cover slide (mN/m)
10 mm	72.55	61.64	71.09
5 mm	73.03	62.07	70.23
2 mm	73.29	55.12	70.5

Table 3.2. Surface tension comparison of sludge at different depths and time using cover glass

Sludge sample without gas		
Time (s)	Immersion depth (mm)	Surface tension (mN/m)
100	10mm	102.47
200	10 mm	97.32
350	10 mm	94.61
600	10 mm	90.35
600	5 mm	80.9
600	5 mm	80.3
600	5mm	79.06
600	3mm	77.29
800	3mm	75.46
600	2mm	61.10
800	2mm	51.89
1200	2mm	46.04

3.3.5 *MICROSCOPE ANALYSIS OF FLOC STRUCTURE*

To verify the impact of gas injection on the sludge structure, microscopic analysis was performed using a conventional environmental scanning electron microscope (FEI QUANTA 200) at a magnification of 200. The temperature and pressure were maintained at 4^{o}C and 5.20 Torr for all samples during imaging.

3.4 GAS PHASE CHARACTERISATION

3.4.1 *ERT MEASUREMENT TECHNIQUE*

Electrical resistance tomography was used to measure the conductivity distribution across different sensor planes. Four sensor planes were located across the cup (see Figure 3.9). Each plane was mounted with 16 equally spaced rectangular electrodes (10 x 7 mm). The major components of ERT are the data acquisition system (DAS) and an image reconstruction system. The electrodes are connected to the DAS using coaxial cables. The DAS applies a current between the two adjacent electrodes and measures the returning voltage between all other electrode pairs. This procedure was repeated for the remaining combinations of adjacent electrode pairs. A frequency of 9600 Hz and injection current of 15 mA was use in all experiments. The DAS was connected to a computer which processed the data using an image reconstruction algorithm, as shown in Figure 3.9. Total 316 pixels of non-invasive conductivity measurements were obtained in each plane per frame.

The conductivity distribution measured by ERT was then used to determine the gas phase distribution in the column. The Maxwell equation was used to convert the conductivity data into the gas holdup (Babaei et al. 2015b).

$$\varepsilon_g = \frac{2\sigma_1 + \sigma_2 - 2\sigma_{mc} - \frac{\sigma_{mc}\sigma_2}{\sigma_1}}{\sigma_{mc} - \frac{\sigma_2}{\sigma_1}\sigma_{mc} + 2(\sigma_1 - \sigma_2)} \quad (3.4)$$

Where ε_g = Gas holdup, σ_1 = Conductivity of continuous phase (µS/cm), σ_2 = Conductivity of dispersed phase (µS/cm), and σ_{mc} = average of reconstructed conductivity by ERT measurements (µS/cm).

Since the gas phase (nitrogen) is non-conductive, substituting $\sigma_2 = 0$ in Equation 3.4 modifies Equation 3.4 as shown in Equation 3.5.

$$\varepsilon_g = \frac{2(\sigma_1 - \sigma_{mc})}{2\sigma_1 + \sigma_{mc}} \quad (3.5)$$

The sludge concentration was varied from 3% to 5.5% and the gas injection rate was varied from 1 LPM to 7 LPM. All the experiments were carried out at room temperature.

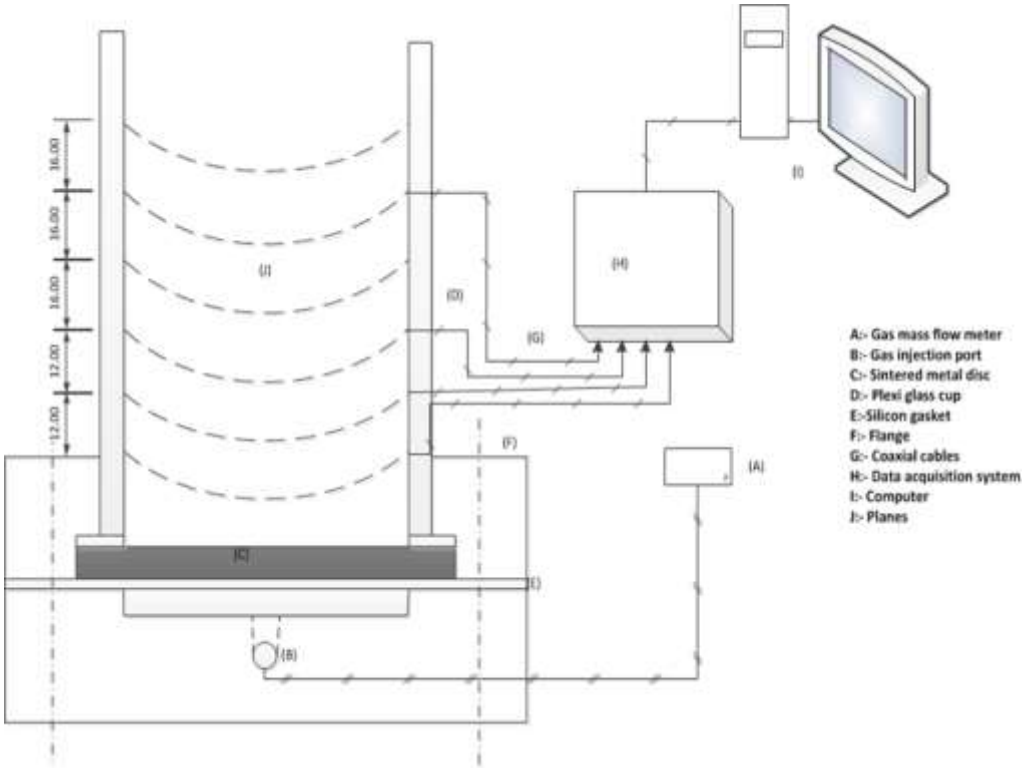

Figure 3.9: Schematic drawing of experimental setup with ERT system

3.4.2 DYNAMIC GAS DISENGAGEMENT TECHNIQUE

Dynamic gas disengagement (DGD) technique was used to measure the bubble rise velocity inside the bubble column and to understand the bubble size classes within the column. The DGD process used was as follows.

1) Start measuring the conductivity distribution using ERT
2) At frame 10 start injecting the gas at desired gas flow rate for 20 mins
3) After 20 mins stop the gas flow rate
4) Continue to measure the conductivity distribution for another 20 mins
5) Calculate the gas holdup for an average of 20 frames
6) Plot the gas holdup against time required for 20 frames (as shown in Figure 3.10).

The bubble rise velocity for different bubble size class is calculated using Equations 3.6 and 3.7, where the large size bubbles disengage first (t_2) and the small size bubbles

disengage last (t_3), and the average bubble rise velocity is calculated as shown in Equation 3.8 (Babaei et al. 2015a). For the range of concentrations and gas flow rates that were used in this study, the change in liquid height was minimal. The maximum difference between using actual liquid height and initial liquid height will be 7%. Hence initial liquid height (68 mm) is considered for all the calculations.

$$u_{b,\text{small}} = \frac{H_{liquid}}{(t_3 - t_1)} \quad (3.6), \quad \&$$

$$u_{b,large} = \frac{H_{liquid}}{(t_2 - t_1)} \quad (3.7)$$

$$u_{b,average} = \frac{\sum_1^N \varepsilon_{g,i} * ub_{,i}}{\varepsilon_g overall} \quad (3.8)$$

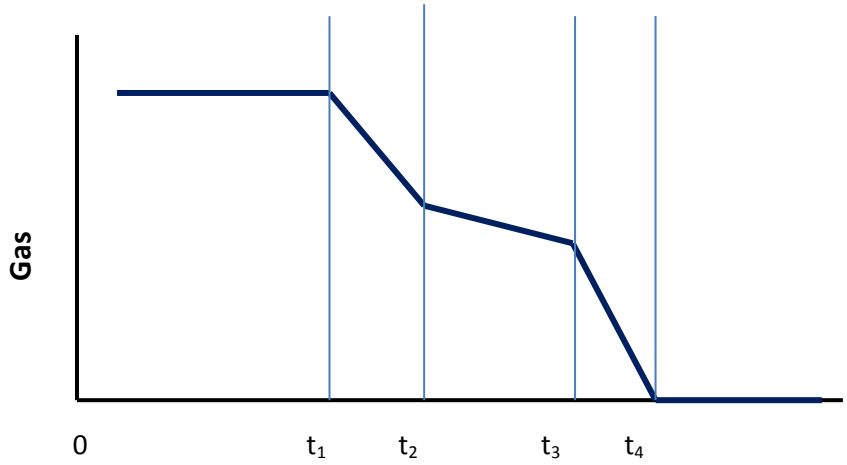

Figure 3.10: Theoretical representation of dynamic gas disengagement technique

3.4.3 EFFECTIVE SHEAR RATE CALCULATION

Effective viscosity (μ_{eff}) is one of the most widely used design parameters in the literature for correlating mass transfer and hydrodynamic parameters for viscous non-Newtonian systems. There are many disagreements in the literature regarding the effective viscosity and effective shear rate of a non-Newtonian fluid (Al-Masry and Chetty 1997). In most of the literature the power law model is used to calculate the effective shear rate of non-Newtonian fluid (Babaei et al. 2015b, Fransolet et al. 2005). However, WAS is well known to best fit the HB model (Eshtiaghi et al. 2013). The effective shear rate can be calculated using the HB model as shown below.

The energy dissipation rate in a stirred tank (Sánchez Pérez et al. 2006) is given as

$$\frac{P}{v} = \tau\dot{\gamma} \quad (3.9)$$

Where, P = Power Input (W), v = Volume (m^3), τ = Shear Stress (Pa), $\dot{\gamma}$ = Shear rate (s^{-1}).

Further, the viscosity of a fluid is the ratio of shear stress to shear rate, that is:

$$\mu = \frac{\tau}{\dot{\gamma}} \quad (3.10)$$

Where μ = Viscosity (Pa s).

Therefore, rearranging Equation 3.10, we get

$$\tau = \mu\dot{\gamma} \quad (3.11)$$

Substituting τ from Equation 3.11 into Equation 3.9, Equation 3.9 can be written as:

$$\frac{p}{v} = \mu\dot{\gamma}^2 \quad (3.12)$$

Or

$$\dot{\gamma} = \left(\frac{1}{\mu}\frac{p}{v}\right)^{\frac{1}{2}} \quad (3.13)$$

For fluids obeying the HB model, shear stress is calculated as:

$$\tau = \tau_o + K\dot{\gamma}^n \quad (3.14)$$

Where, τ_o = yield stress of the material (Pa), K = consistency index (Pa s^n), and n = flow index (-).

Therefore substituting τ from Equation 3.14 into Equation 3.10, we get:

$$\mu = \frac{\tau_o + K\dot{\gamma}^n}{\dot{\gamma}} \quad (3.15)$$

Now substituting μ from Equation 3.15 into Equation 3.13, we get:

$$\dot{\gamma} = \left(\frac{1}{\frac{\tau_o + K\dot{\gamma}^n}{\dot{\gamma}}} \frac{p}{v} \right)^{\frac{1}{2}} \quad (3.16)$$

Therefore by rearranging equation 3.16, we get:

$$\frac{p}{v} = \dot{\gamma} \left(\tau_o + K\dot{\gamma}^n \right) \quad (3.17)$$

However, the bubble column's power energy dissipation rate (Sánchez Pérez et al. 2006) is given as:

$$\frac{p}{v} = g\rho u_g \quad (3.18)$$

Where g = acceleration due to gravity force = 9.81 (m/s^2), and u_g= gas superficial velocity (m/s).

The superficial velocity (u_g)of the gas is calculated as follows:

$$u_g = \frac{volumetric\ flowrate}{Area}$$

As mentioned above, the diameter of the membrane is 108 mm and its thickness is 1.6 mm.

$$\therefore A = \pi * (0.054)^2 = 0.009160\ m^2$$

Thus for 1 LPM of gas flow rate (0.000017 m^3/s), the gas superficial velocity is:

$$u_g = \frac{0.000017}{0.009160} = 0.00182 \frac{m}{s}$$

Therefore substituting $\frac{p}{v}$ from Equation 3.18 to Equation 3.17 and rearranging the equation, we get:

$$\dot{\gamma} = \frac{g\rho u_g}{(\tau_o + K\dot{\gamma}^n)} \quad (3.19)$$

Since, the shear rate is on both the sides of equation, solving Equation 3.19 using a trial and error method and by substituting the HB parameters to get RHS = LHS, the effective shear rate is calculated.

3.4.4 BUBBLE SIZE CALCULATION

Bubble size plays an important role in gas–liquid contact in the bubble columns. However, all the empirical equations that have been used in the literature to calculate the average bubble size are based on the power law model and use dimensionless equations that incorporate several assumptions (Babaei et al. 2015a, Fransolet et al. 2005, Jamshidi and Mostoufi 2017, Lind and Phillips 2010). To avoid reliance on the power law model and the aforementioned assumptions, the HB model can used to calculate bubble size as follows.

From Equation 3.15, we know that:

$$\mu = \frac{\tau_o}{\dot{\gamma}} + K\dot{\gamma}^{n-1}$$

Also, Margaritis et al. (1999) reported that shear rate is the ratio of bubble rise velocity to bubble horizontal diameter, as shown in Equation 3.20.

$$\dot{\gamma} = \frac{u_b}{d_h} \quad (3.20)$$

Where u_b = bubble rise velocity (m/s), d_h = bubble horizontal diameter (m).

Thus, the bubble horizontal diameter d_h is calculated using Equation 3.20.

Reynolds number, Re, for the HB model is calculated using Equation 3.21 (Madlener et al. 2009).

$$R_e = \frac{\rho {u_b}^{2-n} {d_h}^{n}}{\left(\frac{\tau_o}{8}\right)\left(\frac{d_h}{u_b}\right)^{n} + K\,(\frac{3m+1}{4m})^{n}\, 8^{n-1}} \quad (3.21)$$

Where:

$$m = \frac{nK(\frac{8u_b}{d_h})^{n}}{\tau_o + K(\frac{8u_b}{d_h})^{n}}$$

For non-Newtonian shear-thinning fluids, the drag coefficient, C_D (White and McDougall) is calculated using Equation 3.22 or 3.23 (Margaritis et al. 1999). Equation 3.22 was proved to be the best fit for Re values less than 3.30 by (Wenyuan et al. 2010).

$$C_D = \frac{24}{R_e}\left(1 + 0.173\, {R_e}^{0.657}\right) + \frac{0.413}{1 + 16300 {R_e}^{-1.09}} \quad (R_e < 60) \quad (3.22)$$

$$C_D = 0.95 \quad (R_e > 60) \quad (3.23)$$

Now assuming $C_{D\infty} = C_D$, the bubble size is calculated as:

$$d_b = \sqrt[3]{\frac{3\, C_{D\infty}\, {d_h}^2 {u_b}^2}{4g}} \quad (3.24)$$

Where g = Acceleration due to gravity (9.81 m/s^2) and d_b = Average bubble size in the column (m).

3.5 REFERENCES

Ahimou, F., Semmens, M.J., Haugstad, G. and Novak, P.J. (2007) Effect of protein, polysaccharide, and oxygen concentration profiles on biofilm cohesiveness. Applied and environmental microbiology 73(9), 2905-2910.

Al-Masry, W.A. and Chetty, M. (1997) On the estimation of effective shear rate in external loop airlift reactors: non-Newtonian fluids*. Studies in Environmental Science 66, 153-166.

Amirnia, S., de Bruyn, J.R., Bergougnou, M.A. and Margaritis, A. (2013) Continuous rise velocity of air bubbles in non-Newtonian biopolymer solutions. Chemical Engineering Science 94, 60-68.

Anastasiou, A.D., Passos, A.D. and Mouza, A.A. (2013) Bubble columns with fine pore sparger and non-Newtonian liquid phase: Prediction of gas holdup. Chemical Engineering Science 98, 331-338.

Andreadakis, A.D. (1993) Physical and chemical properties of activated sludge floc. Water Research 27(12), 1707-1714.

Azami, H., Sarrafzadeh, M.H. and Mehrnia, M.R. (2012) Soluble microbial products (SMPs) release in activated sludge systems: a review. Iranian Journal of Environmental Health Science & Engineering 9(1), 30-30.

Babaei, R., Bonakdarpour, B. and Ein-Mozaffari, F. (2015a) Analysis of gas phase characteristics and mixing performance in an activated sludge bioreactor using electrical resistance tomography. Chemical Engineering Journal 279, 874-884.

Babaei, R., Bonakdarpour, B. and Ein-Mozaffari, F. (2015b) The use of electrical resistance tomography for the characterization of gas holdup inside a bubble column bioreactor containing activated sludge. Chemical Engineering Journal 268, 260-269.

Bajón Fernández, Y., Cartmell, E., Soares, A., McAdam, E., Vale, P., Darche-Dugaret, C. and Jefferson, B. (2015) Gas to liquid mass transfer in rheologically complex fluids. Chemical Engineering Journal 273, 656-667.

Barnes, H.A. (2004) Interface Science and Technology. Petsev, D.N. (ed), pp. 721-759, Elsevier.

Barnes, H.A., Hutton, J.F. and Walters, K. (1989) An introduction to rheology, Elsevier : Distributors for the U.S. and Canada, Elsevier Science Pub. Co., Amsterdam/New York.

Barnes, H. A. (1995). A review of the slip (wall depletion) of polymer solutions, emulsions and particle suspensions in viscometers: its cause, character, and cure. *Journal of Non-Newtonian Fluid Mechanics*, *56*(3), 221-251.

Baroutian, S., Eshtiaghi, N. and Gapes, D.J. (2013) Rheology of a primary and secondary sewage sludge mixture: Dependency on temperature and solid concentration. Bioresource Technology 140, 227-233.

Baudez, J.-C., Gupta, R.K., Eshtiaghi, N. and Slatter, P. (2013a) The viscoelastic behaviour of raw and anaerobic digested sludge: Strong similarities with soft-glassy materials. Water Research 47(1), 173-180.

Baudez, J.C. (2008) Physical aging and thixotropy in sludge rheology. Applied Rheology 18(1), 13495-13491-13495-13498.

Baudez, J.C. and Coussot, P. (2001) Rheology of aging, concentrated, polymeric suspensions: Application to pasty sewage sludges. Journal of Rheology 45(5), 1123-1140.

Baudez, J.C., Markis, F., Eshtiaghi, N. and Slatter, P. (2011) The rheological behaviour of anaerobic digested sludge. Water Research 45(17), 5675-5680.

Baudez, J.C., Slatter, P. and Eshtiaghi, N. (2013b) The impact of temperature on the rheological behaviour of anaerobic digested sludge. Chemical Engineering Journal 215-216, 182-187.

Bhattacharya, S.N. (1981) Flow characteristics of primary and digested sewage sludge. Rheologica Acta 20, 288- 298.

Bo, J. and Lant, P. (2004) Flow regime, hydrodynamics, floc size distribution and sludge properties in activated sludge bubble column, air-lift and aerated stirred reactors. Chemical Engineering Science 59(12), 2379-2388.

Boersma, W.H., Laven, J. and Stein, H.N. (1990) Shear thickening (dilatancy) in concentrated dispersions. AIChE Journal 36(3), 321-332.

Branigan, J. (2013) Development of a Field Test for Total Suspended Solids Analysis, University of Nebraska, Lincoln, NE.

Brownsey, G.J. (1998) Rheological Measurement. Collyer, A.A. and Clegg, D.W. (eds), pp. 427-452, Springer Netherlands, Dordrecht.

Cao, X., Yuan, H., Zhao, Z. and Ding, H. (2017) Analysis on xanthan gum solution to simulate flow performance of digestion sludge. Transactions of the Chinese Society of Agricultural Engineering 33(15), 260-265.

Cao, X., Zhao, Z., Cheng, L. and Yin, W. (2016) Evaluation of a Transparent Analog Fluid of Digested Sludge: Xanthan Gum Aqueous Solution. Procedia Environmental Sciences 31(Supplement C), 735-742.

Chagnon, F.J. and Harleman, D.R. (2005) Chemically Enhanced Primary Treatment of Wastewater. Water Encyclopedia 1, 659-660.

Chang, I.-S., Le Clech, P., Jefferson, B. and Judd, S. (2002) Membrane fouling in membrane bioreactors for wastewater treatment.(Abstract). Journal of Environmental Engineering 128(11), 1018.

Chang, Q. (2016) Colloid and Interface Chemistry for Water Quality Control. Chang, Q. (ed), pp. 61-77, Academic Press.

Cheremisinoff, N.P. (1986) Encyclopedia of fluid mechanics, Gulf Pub. Co., Book Division, Houston.

Chhabra, R.P. (2012) Bubbles, Drops, and Particles in Non-Newtonian Fluids, Second Edition, Taylor and Francis, Hoboken.

Chhabra, R.P. and Richardson, J.F. (2008) Non-Newtonian Flow and Applied Rheology (Second Edition), pp. 56-109, Butterworth-Heinemann, Oxford.

Coussot, P. (2005) Experimental procedures and problems in paste viscometry. Rheometry of pastes, suspensions, and granular materials: applications in industry and environment. John Wiley & Sons, Inc, Hoboken. https://doi. org/10.1002/0471720577. ch3.

Curran, S.J., Hayes, R.E., Afacan, A., Williams, M.C. and Tanguy, P.A. (2002) Properties of Carbopol Solutions as Models for Yield-Stress Fluids. Journal of Food Science 67(1), 176-180.

Curvers, D., Saveyn, H., Scales, P.J. and Van der Meeren, P. (2009) A centrifugation method for the assessment of low pressure compressibility of particulate suspensions. Chemical Engineering Journal 148(2-3), 405-413.

Dai, X., Gai, X. and Dong, B. (2014) Rheology evolution of sludge through high-solid anaerobic digestion. Bioresour Technology 174, 6-10.

Davies, J.T. and Rideal, E.K. (1963) Interfacial phenomena, Academic Press, New York.

Davies, R.M. and Taylor, S.G. (1950) The mechanics of large bubbles rising through extended liquids and through liquids in tubes. Proceedings of the Royal Society of London. Series A, Mathematical and Physical Sciences 200, 375-390.

De Temmerman, L., Maere, T., Temmink, H., Zwijnenburg, A. and Nopens, I. (2015) The effect of fine bubble aeration intensity on membrane bioreactor sludge characteristics and fouling. Water Research 76, 99-109.

Denis Funfschilling, H.Z.L. (2001) Flow of non-Newtonian fluids around bubbles: PIV measurements andbirefringence visualisation. Chemical Engineering Science 56, 1137-1141.

Dentel, S.K. (1997) Evaluation and role of rheological properties in sludge management. Water Science and Technology 36(11), 1-8.

Dewsbury, K., Karamanev, D. and Margaritis, A. (1999) Hydrodynamic characteristics of free rise of light solid particles and gas bubbles in non-Newtonian liquids. Chemical Engineering Science 54(21), 4825-4830.

Dieude-Fauvel, E., Heritier, P., Chanet, M., Girault, R., Pastorelli, D., Guibelin, E. and Baudez, J.C. (2014) Modelling the rheological properties of sludge during anaerobic digestion in a batch reactor by using electrical measurements. Water Research 51, 104-112.

Dimakopoulos, Y., Pavlidis, M. and Tsamopoulos, J. (2013) Steady bubble rise in Herschel–Bulkley fluids and comparison of predictions via the Augmented Lagrangian Method with those via the Papanastasiou model. Journal of Non-Newtonian Fluid Mechanics 200(0), 34-51.

Droste, R.L. and Gehr, R.L. (2018) Theory and practice of water and wastewater treatment, John Wiley & Sons.

Durán, C., Fayolle, Y., Pechaud, Y., Cockx, A. and Gillot, S. (2016) Impact of suspended solids on the activated sludge non-newtonian behaviour and on oxygen transfer in a bubble column. Chemical Engineering Science 141, 154-165.

Dziubiński, M., Orczykowska, M. and Budzyński, P. (2003) Comments on bubble rising velocity in non-Newtonian liquids. Chemical Engineering Science 58(11), 2441-2443.

Eickenbusch, H., Brunn, P.O. and Schumpe, A. (1995) Mass transfer into viscous pseudoplastic liquid in large-diameter bubble columns. Chemical Engineering and Processing 34, 479-485.

Eshtiaghi, N., Markis, F., Yap, S.D., Baudez, J.C. and Slatter, P. (2013) Rheological characterisation of municipal sludge: A review. Water Research 47(15), 5493-5510.

Eshtiaghi, N., Yap, S.D., Markis, F., Baudez, J.-C. and Slatter, P. (2012) Clear model fluids to emulate the rheological properties of thickened digested sludge. Water Research 46(9), 3014-3022.

Esmaeili, A., Guy, C. and Chaouki, J. (2015) The effects of liquid phase rheology on the hydrodynamics of a gas–liquid bubble column reactor. Chemical Engineering Science 129, 193-207.

Estellé, P., Lanos, C. and Perrot, A. (2008) Processing the Couette viscometry data using a Bingham approximation in shear rate calculation. Journal of Non-Newtonian Fluid Mechanics 154(1), 31-38.

Fang, W., Zhang, P., Ye, J., Wu, Y., Zhang, H., Liu, J., Zhu, Y. and Zeng, G. (2015) Physicochemical properties of sewage sludge disintegrated with high pressure homogenization. International Biodeterioration & Biodegradation 102, 126-130.

Farno, E. (2016) Rheological modification of muncipal sewage sludge by thermal treatment (Anaerobic digested sludge and waste activated sludge), RMIT university, Australia.

Farno, E., Baudez, J.C., Parthasarathy, R. and Eshtiaghi, N. (2014) Rheological characterisation of thermally-treated anaerobic digested sludge: Impact of temperature and thermal history. Water Research 56, 156-161.

Farno, E., Baudez, J.C., Parthasarathy, R. and Eshtiaghi, N. (2015a) Impact of temperature and duration of thermal treatment on different concentrations of anaerobic digested sludge: Kinetic similarity of organic matter solubilisation and sludge rheology. Chemical Engineering Journal 273(0), 534-542.

Farno, E., Baudez, J.C., Parthasarathy, R. and Eshtiaghi, N. (2015b) Impact of temperature and duration of thermal treatment on different concentrations of anaerobic digested sludge: Kinetic similarity of organic matter solubilisation and sludge rheology. Chemical Engineering Journal 273, 534-542.

Forster, C.F. (1981) Preliminary studies on the relationship between sewage sludge viscosities and the nature of the surfaces of the component particles. Biotechnology Letters 3(12), 707-712.

Fransolet, E., Crine, M., Marchot, P. and Toye, D. (2005) Analysis of gas holdup in bubble columns with non-Newtonian fluid using electrical resistance tomography and dynamic gas disengagement technique. Chemical Engineering Science 60(22), 6118-6123.

Giuseppe, O., Silvio, G., Gerardino, D.E., Antonio, M., Marek, R. and Piero, S. (2013) Preliminary assessments of combined effects of surface tension and viscosity on bubble column hydrodynamics. Chemical Engineering Transactions 32, 1579 - 1584.

Gomezdiaz, D., Navaza, J., Quintansriveiro, L. and Sanjurjo, B. (2009) Gas absorption in bubble column using a non-Newtonian liquid phase. Chemical Engineering Journal 146(1), 16-21.

Greene, P. (2014) Anaerobic_Digestion_and_Biogas. Electronic Book

Grönroos, A., Kyllönen, H., Korpijärvi, K., Pirkonen, P., Paavola, T., Jokela, J. and Rintala, J. (2005) Ultrasound assisted method to increase soluble chemical oxygen demand (SCOD) of sewage sludge for digestion. Ultrasonics Sonochemistry 12(1), 115-120.

Guibaud, G., Dollet, P., Tixier, N., Dagot, C. and Baudu, M. (2004) Characterisation of the evolution of activated sludges using rheological measurements. Process Biochemistry 39, 1803–1810.

Haque, M.W., Nigam, K.D.P. and Joshi, J.B. (1986) Hydrodynamics and mixing in highly viscous pseudo-plastic non-newtonian solutions in bubble columns. Chemical Engineering Science 41(9), 2321-2331.

Hasara, H., Kinacib, C., Unlua, A., Togrul, H. and Ipek, U. (2004) Rheological properties of activated sludge in a sMBR. Biochemical Engineering Journal 20, 1–6.

Hayet, C., Saida, B.-A., Youssef, T. and Hédi, S. (2016) Study of biodegradability for municipal and industrial Tunisian wastewater by respirometric technique and batch reactor test. Sustainable Environment Research 26(2), 55-62.

Henze, M.A. and Henze, M. (1997) Wastewater treatment : biological and chemical processes, Springer, Berlin, Heidelberg, [Germany].

Hii, K., Parthasarathy, R., Baroutian, S., Gapes, D.J. and Eshtiaghi, N. (2017) Rheological measurements as a tool for monitoring the performance of high pressure and high temperature treatment of sewage sludge. Water Research 114, 254-263.

Hofmeester, J.J.M. (1988) Gas hold-up measurements in bioreactors. Trends in Biotechnology 6(1), 19-22.

Hong, E., Yeneneh, A.M., Kayaalp, A., Sen, T.K., Ang, H.M. and Kayaalp, M. (2016) Rheological characteristics of municipal thickened excess activated sludge (TEAS): impacts

of pH, temperature, solid concentration and polymer dose. Research on Chemical Intermediates 42(8), 6567-6585.

Houghton, J.I. and Quarmby, J. (1999) Biopolymers in wastewater treatment. Current Opinion in Biotechnology 10(3), 259-262.

Hu, Z., Chandran, K., Smets, B.F. and Grasso, D. (2002) Evaluation of a rapid physical–chemical method for the determination of extant soluble COD. Water Research 36(3), 617-624.

Hunter, R.J. (1981) Zeta Potential in Colloid Science, pp. 1-10, Academic Press.

Ishkintana, L.K. and Bennington, C.P.J. (2010) Gas holdup in pulp fibre suspensions: Gas voidage profiles in a batch-operated sparged tower. Chemical Engineering Science 65(8), 2569-2578.

Jamshidi, N. and Mostoufi, N. (2017) Measurement of bubble size distribution in activated sludge bubble column bioreactor. Biochemical Engineering Journal 125(Supplement C), 212-220.

Jiang, J., Wu, J., Poncin, S. and Li, H.Z. (2014) Rheological characteristics of highly concentrated anaerobic digested sludge. Biochemical Engineering Journal 86, 57-61.

Jin, H.-R., Lim, D.H., Lim, H., Kang, Y., Jung, H. and Kim, S.D. (2012) Demarcation of large and small bubbles in viscous slurry bubble columns. Industrial & Engineering Chemistry Research 51(4), 2062-2069.

Jin, H., Wang, M. and Williams, R.A. (2007) Analysis of bubble behaviors in bubble columns using electrical resistance tomography. Chemical Engineering Journal 130(2–3), 179-185.

Karia, G. and Christian, R. (2013) Wastewater treatment: concepts and design approach, PHI Learning Pvt. Ltd.

Kennedy, S., Bhattacharjee, P.K., Bhattacharya, S.N., Eshtiaghi, N. and Parthasarathy, R. (2018) Control of the mixing time in vessels agitated by submerged recirculating jets, p. 171037.

Khalili, F., Nasr, M.J., Kazemzadeh, A. and Ein- Mozaffari, F. (2018) Analysis of gas holdup and bubble behavior in a biopolymer solution inside a bioreactor using tomography and dynamic gas disengagement techniques. Journal of Chemical Technology & Biotechnology 93(2), 340-349.

Krishnan, J.M., Deshpande, A.P., Murali, K.J. and Sunil, K.P.B. (2010) Rheology of complex *f*luids, Springer, Dordrecht, New York.

Kulkarni, A.A. and Joshi, J.B. (2005) Bubble formation and bubble rise velocity in gas-liquid systems -A Review. Industrial & Engineering Chemistry Research 44, 5873 - 5931.

Ladewig, B. and Al-Shaeli, M.N.Z. (2016) Fundamentals of Membrane Bioreactors: Materials, Systems and Membrane Fouling, Springer, Singapore, singapore.

Laera, G., Giordano, C., Pollice, A., Saturno, D. and Mininni, G. (2007) Membrane bioreactor sludge rheology at different solid retention times. Water Research 41(18), 4197-4203.

Legrand, V., Hourdet, D., Audebert, R. and Snidaro, D. (1998) Deswelling and flocculation of gel networks: application to sludge dewatering. Water Research 32(12), 3662-3672.

Li, B. and Bishop, P.L. (2004) Micro-profiles of activated sludge floc determined using microelectrodes. Water Res 38(5), 1248-1258.

Lind, S.J. and Phillips, T.N. (2010) The effect of viscoelasticity on a rising gas bubble. Journal of Non-Newtonian Fluid Mechanics 165, 852-865.

Liss, S.N. and Droppo, I.G. (2005) Flocculation in natural and engineered environmental systems, CRC Press, Boca Raton.

Liu, Y. (2003) Chemically reduced excess sludge production in the activated sludge process. Chemosphere 50(1), 1-7.

Lotito, V., Spinosa, L., Mininni, G. and Antonacci, R. (1997) The rheology of sewage sludge at different steps of treatment. Water Science and Technology 36(11), 79-85.

Madlener, K., Frey, B. and Ciezki, H.K. (2009) Generalized reynolds number for non-newtonian fluids. EUCASS Proceedings Series – Advances in AeroSpace Sciences 1, 237-250.

Margaritis, A., Te Bokkel, D.W. and Karamanev, D.G. (1999) Bubble rise velocities and drag coefficients in non-Newtonian polysaccharide solutions. Biotechnology and Bioengineering 64(3), 257-266.

Markis, F., Baudez, J.-C., Parthasarathy, R., Slatter, P. and Eshtiaghi, N. (2014) Rheological characterisation of primary and secondary sludge: Impact of solids concentration. Chemical Engineering Journal 253, 526-537.

Mendelson, H.D. (1967) The prediction of bubble terminal velocities from wave theory. AIChE Journal 13(2), 250-253.

Meng, F., Chae, S.-R., Drews, A., Kraume, M., Shin, H.-S. and Yang, F. (2009) Recent advances in membrane bioreactors (MBRs): Membrane fouling and membrane material. Water Research 43(6), 1489-1512.

Meng, F., Shi, B., Yang, F. and Zhang, H. (2007) New insights into membrane fouling in submerged membrane bioreactor based on rheology and hydrodynamics concepts. Journal of Membrane Science 302(1–2), 87-94.

Meng, F., Yang, F., Shi, B. and Zhang, H. (2008) A comprehensive study on membrane fouling in submerged membrane bioreactors operated under different aeration intensities. Separation and Purification Technology 59(1), 91-100.

Meng, F., Zhang, H., Yang, F., Zhang, S., Li, Y. and Zhang, X. (2006) Identification of activated sludge properties affecting membrane fouling in submerged membrane bioreactors. Separation and Purification Technology 51(1), 95-103.

Meng, F., Zhang, S., Oh, Y., Zhou, Z., Shin, H.-S. and Chae, S.-R. (2017) Fouling in membrane bioreactors: An updated review. Water Research 114(Supplement C), 151-180.

Menniti, A., Kang, S., Elimelech, M. and Morgenroth, E. (2009) Influence of shear on the production of extracellular polymeric substances in membrane bioreactors. Water Research 43(17), 4305-4315.

Mezger, T.G. (2011) The rheology handbook : for users of rotational and oscillatory rheometers, Vincentz Network, Hanover, Germany.

Moeller, G. and Torres, L.G. (1997) Rheological characterization of primary and secondary sludges treated by both aerobic and anaerobic digestion. Bioresource Technology 61(3), 207-211.

Mori, M., Seyssiecq, I. and Roche, N. (2006) Rheological measurements of sewage sludge for various solids concentrations and geometry. Process Biochemistry 41(7), 1656-1662.

Orvalho, S., Ruzicka, M.C., Olivieri, G. and Marzocchella, A. (2015) Bubble coalescence: Effect of bubble approach velocity and liquid viscosity. Chemical Engineering Science 134, 205-216.

Park, J.-S., Yeon, K.-M. and Lee, C.-H. (2005) Hydrodynamics and microbial physiology affecting performance of a new MBR, membrane-coupled high-performance compact reactor. Desalination 172(2), 181-188.

Pisarevsky, A., Polozova, I. and Hockridge, P. (2005) Chemical Oxygen Demand. Russian Journal of Applied Chemistry 78(1), 101-107.

Pollice, A., Giordano, C., Laera, G., Saturno, D. and Mininni, G. (2007) Physical characteristics of the sludge in a complete retention membrane bioreactor. Water Research 41(8), 1832-1840.

Ratkovich, N., Horn, W., Helmus, F.P., Rosenberger, S., Naessens, W., Nopens, I. and Bentzen, T.R. (2013) Activated sludge rheology: A critical review on data collection and modelling. Water Research 47(2), 463-482.

Rice, E.W., Bridgewater, L., Association, A.P.H., Association, A.W.W. and Federation, W.E. (2012) Standard methods for the examination of water and wastewater., Washington, D.C. American Water Works Association, 2012. .

Sánchez Pérez, J.A., Rodríguez Porcel, E.M., Casas López, J.L., Fernández Sevilla, J.M. and Chisti, Y. (2006) Shear rate in stirred tank and bubble column bioreactors. Chemical Engineering Journal 124(1–3), 1-5.

Sanin, F.D. (2002) Effect of solution physical chemistry on the rheological properties of activated sludge. Water Research South Africa 28(02), 207-212.

Sanin, F.D., Clarkson, W.W. and Vesilind, P.A. (2011) Sludge engineering: the treatment and disposal of wastewater sludges, DEStech Publications, Inc, United states of America.

Sanin, F.D. and Vesilind, P.A. (1996) Synthetic Sludge: A physical/chemical model in understanding bioflocculation. Water Environment Research 68(5), 927-933.

Schonhorn, H. (1965) Theoretical relationship between surface tension and cohesive energy density. The Journal of Chemical Physics 43(6), 2041-2043.

Seyssiecq, I., Marrot, B., Djerroud, D. and Roche, N. (2008) In situ triphasic rheological characterisation of activated sludge, in an aerated bioreactor. Chemical Engineering Journal 142(1), 40-47.

Seyssiecq., Ferrasse and Roche (2003) State-of-the-art: rheological characterisation of wastewater treatment sludge. Biochemical Engineering Journal 16(1), 41-56.

SHAH Y.T, KELKAR B.G, GODBOLE S.P and W.D, D. (1982) Design Parameters Estimations for Bubble Column Reactors. AlChE Journal 28(353-379).

Sheng, G.-P., Yu, H.-Q. and Li, X.-Y. (2010) Extracellular polymeric substances (EPS) of microbial aggregates in biological wastewater treatment systems: A review. Biotechnology Advances 28(6), 882-894.

Sikorski, D., Tabuteau, H. and de Bruyn, J.R. (2009) Motion and shape of bubbles rising through a yield-stress fluid. Journal of Non-Newtonian Fluid Mechanics 159(1-3), 10-16.

Speight, J.G. (2017) Environmental Organic Chemistry for Engineers. Speight, J.G. (ed), pp. 203-261, Butterworth-Heinemann.

Spinosa, L. and Lotito, V. (2003) A simple method for evaluating sludge yield stress. Advances in Environmental Research 7(3), 655-659.

Sutherland, I.W. (2001) Exopolysaccharides in biofilms, flocs and related structures. Water Science and Technology 43(6), 77.

Tixier, N., Guibaud, G. and Baudu, M. (2003a) Determination of some rheological parameters for the characterization of activated sludge. Bioresource Technology 90(2), 215-220.

Tixier, N., Guibaud, G. and Baudu, M. (2003b) Effect of ph and ionic environment changes on interparticle interactions affecting activated sludge flocs: A rheological approach. Environmental Technology 24(8), 971-978.

Tran, A., Rudolph, M.L. and Manga, M. (2015) Bubble mobility in mud and magmatic volcanoes. Journal of Volcanology and Geothermal Research 294, 11-24.

Trussell, R.S., Merlo, R.P., Hermanowicz, S.W. and Jenkins, D. (2007) Influence of mixed liquor properties and aeration intensity on membrane fouling in a submerged membrane bioreactor at high mixed liquor suspended solids concentrations. Water Research 41(5), 947-958.

Vold, M.J. (1982) Zeta potential in colloid science. Principles and applications. Journal of Colloid and Interface Science 88(2), 608.

Wang, Y. and McNeil, B. (1996) A study of gas hold-up, liquid velocity, and mixing time in a complex high viscosity, fermentation fluid in an airlift bioreactor. Chem. Eng. Technol. 19(2), 143-153.

Wenyuan, F., Youguang, M., Shaokun, J., Ke, Y. and Huaizhi, L. (2010) An Experimental Investigation for Bubble Rising in Non-Newtonian Fluids and Empirical Correlation of Drag Coefficient. Journal of Fluids Engineering 132(2), 021305-021305-021307.

White, P. and McDougall, F.R. (2001) Integrated solid waste management : a life cycle inventory, Blackwell Science, Oxford, UK ; Malden, MA.

Wilén, B.-M., Jin, B. and Lant, P. (2003) The influence of key chemical constituents in activated sludge on surface and flocculating properties. Water Research 37(9), 2127-2139.

Wilen, B.M., Jin, B. and Lant, P. (2003) Relationship between flocculation of activated sludge and composition of extracellular polymeric substances. Water Sci Technol 47(12), 95-103.

Yuan, H., Zhu, N. and Song, F. (2011) Dewaterability characteristics of sludge conditioned with surfactants pretreatment by electrolysis. Bioresource Technology 102(3), 2308-2315.

Yusuf, C. and Murray, M.-Y. (1988) Gas holdup behaviour in fermentation broths and other non-Newtonian fluids in pneumatically agitated reactors. The Chemical Engineering Journal 39, B31-B36.

Zhang, Y., Zhang, P., Guo, J., Ma, W., Fang, W., Ma, B. and Xu, X. (2013) Sewage sludge solubilization by high-pressure homogenization. Water Science and Technology 67(11), 2399-2405.

Zhang, Z., Zhu, J. and Park, K.J. (2004) Effects of duration and intensity of aeration on solids decomposition in pig slurry for odour control. Biosystems Engineering 89(4), 445-456.

Zuber, N. and Findlay, J.A. (1965) Average volumetric concentration in two-phase flow systems Journal of Heat Transfer 87(4), 453-468.

CHAPTER 4: IMPACT OF GAS INJECTION ON THE APPARENT VISCOSITY AND VISCOELASTIC PROPERTIES OF WASTE ACTIVATED SEWAGE SLUDGE

This chapter was published in Water Research

(Vol: 114, P: 296-307, 2017)

Keywords: Triphasic rheological characterisation; Waste activated sludge; creep test; Time sweep; viscosity curve; ESEM image

Bobade, V., Baudez, J.C., Evans, G. and Eshtiaghi, N. "Impact of gas injection on the apparent viscosity and viscoelastic property of waste activated sewage sludge". Water Research 114 (2017) 296-307.

Graphical Abstract

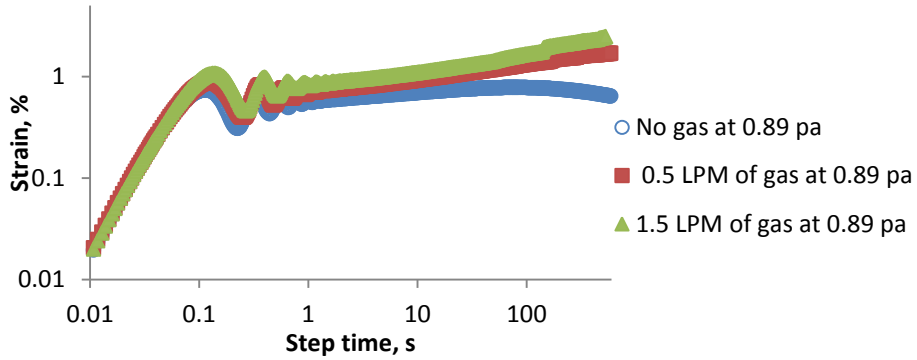

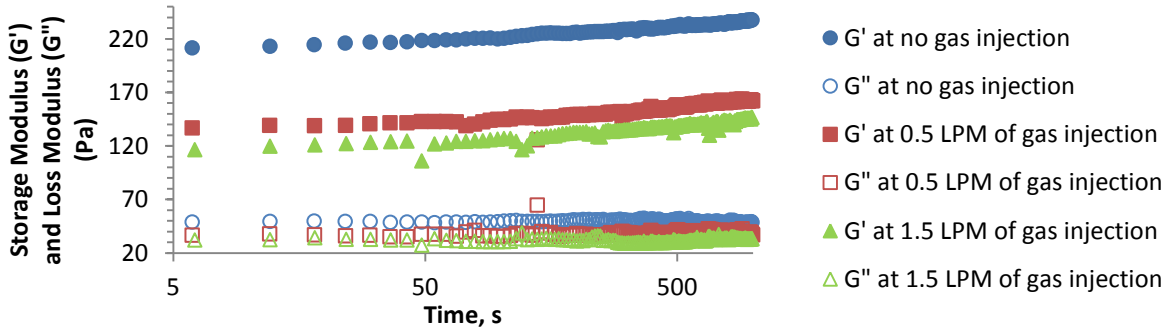

4.1 ABSTRACT

Gas injection is known to play a major role on the particle size of the sludge, the oxygen transfer rate, as well as the mixing efficiency of membrane bioreactors and aeration basins in the waste water treatment plants. The rheological characteristics of sludge are closely related to the particle size of the sludge floc. However, particle size of sludge floc depends partly on the shear induced in the sludge and partly on physico-chemical nature of the sludge.

The objective of this work is to determine the impact of gas injection on both the apparent viscosity and viscoelastic property of sludge. The apparent viscosity of sludge was investigated by two methods: in-situ and after sparging. Viscosity curves obtained by in-situ measurement showed that the apparent viscosity decreases significantly from 4000 Pa.s to 10 Pa.s at low shear rate range (below 10 s^{-1}) with an increase in gas flow rate (0.5 LPM to 3 LPM); however the after sparging flow curve analysis showed that the reduction in apparent viscosity throughout the shear rate range is negligible to be displayed. Torque and displacement data at low shear rate range revealed that the obtained lower apparent viscosity in the in-situ method is not the material characteristics, but the slippage effect due to a preferred location of the bubbles close to the bob, causing an inconsistent decrease of torque and increase of displacement at low shear rate range.

In linear viscoelastic regime, the elastic and viscous modulus of sludge was reduced by 33% & 25%, respectively, due to gas injection because of induced shear. The amount of induced shear measured through two different tests (creep and time sweep) were the same. The impact of this induced shear on sludge structure was also verified by microscopic images.

4.2 INTRODUCTION

Rheological behavior of sludge is of crucial importance in sludge management concerning design, optimisation and operation of the treatment process (Baroutian et al. 2013, Eshtiaghi et al. 2013, Ratkovich et al. 2013, Seyssiecq. et al. 2003, Slatter 1997) The rheological behavior of sludge, in general, is reported as a non-Newtonian pseudoplastic with shear thinning behaviour (Baudez 2008, Seyssiecq et al. 2008) , which evolves with time due to microbial activity (Baudez et al. 2001). In fact the rheological properties of sludge also change with sludge treatment processes and operating parameters as a result

of changing sludge composition (Dieude-Fauvel et al. 2014, Hao et al. 2016, Monteiro 1997, Tixier et al. 2003a). However, the change in rheological properties with shear rate is because of change in internal structure (Baudez 2008, Baudez and Coussot 2001, Ruiz-Hernando et al. 2015) .

Recent studies on aerated waste activated sludge mainly focused on the impact of changing rheological behaviour of sludge on energy consumption, mixing efficiency, membrane fouling, mass transfer, floc structure, and process control (Ratkovich et al. 2013, Seyssiecq et al. 2008). The importance of optimising and modelling of aeration and settling tanks in wastewater treatment plants considering the impact of sludge rheology on the process parameters studied by Seyssiecq. et al. (2003). The mass transfer rate decreases with an increase in the solid concentration of waste activated sludge and strongly influences the performance of membrane bioreactor (Rosenberger et al. 2002). The reason for decreasing mass transfer rate with increasing solid concentration is due to an increase in viscosity and changes in system hydrodynamics as a result of the variation of bubble buoyancy, bubble shape and turbulence (Bajón Fernández et al. 2015).

The mixing time in the bubble column which is an important parameter for design and scale up is significantly affected by fluid rheology (Brannock et al. 2010, Meng et al. 2007). Wang and McNeil (1996) found that mixing time of the fermentation fluid for the same superficial gas velocity increases with increasing viscosity because of the poor radial gas dispersion due to gas bubble coalesce. Similarly, with the use of electrical resistance tomography (ERT) technique, Babaei et al. (2015a) reported that the mixing time of activated sludge decreases with an increase in superficial gas velocity and increases with an increase in the solid concentration of sludge. The bubble rise velocity and bubble size, which were considered the main parameter influencing the mixing time, both are impacted by the fluid characteristics i.e. sludge rheology.

Aeration intensity also has a significant impact on the physicochemical and biological properties of activated sludge in a membrane bioreactor (MBR), which also consequently influences the sludge rheology (Menniti et al. 2010). The particle size distribution, submicron particle concentration and organic carbon fractions of sludge can be affected as a result of shear induced by aeration intensity (De Temmerman et al. (2015). Zhang et al. (2015) also observed the particle size reduction and formation of micro flocs due to breakage of larger particles under high aeration.

Seyssiecq et al. (2008) had reported that by increasing gas flow rate the apparent viscosity of activated sludge is strongly lowered at low shear rate because of shearing caused by air bubbles. Whereas, no change in the apparent viscosity was observed with increasing gas flow rates at high shear rates range as mechanical shearing had a dominant impact compared to impact of gas injection.

Although few studies have been done on the impact of gas injection on different process parameters (Babaei et al. 2015a, Ratkovich et al. 2013, Seyssiecq et al. 2015, Seyssiecq et al. 2008), not only the comparison between them is difficult, due to variation of sparger type, experimental setup and assumptions made for calculation, but there is no study on the impact of aeration on sludge rheological properties. So, this study aims to systematically investigate the impact of gas injection on sludge rheological properties.

The first part of this paper is devoted to examining the impact of gas injection on sludge apparent viscosity (nonlinear viscoelastic region) by using two different methods: in-situ and after sparging. In the second part, the impact of gas injection on the linear viscoelastic region of waste activated sludge is investigated by using creep and dynamic time sweep tests. The extent of induced shear by gas via different methods will be compared for accuracy purpose.

4.3 MATERIALS AND METHODS

4.3.1 SAMPLE PREPARATION

Waste activated sludge at a total solid concentration of 3.0% was collected from one of waste water treatment plant in Victoria, Australia. The impact of microbial activities inside the sludge was reduced, by storing the sludge at 4^{o}C for 30 days. This procedure helps with the stability of samples which results in reproducible data (Curvers et al. 2009). To prepare different concentration of sludge samples, the sludge was thickened to higher concentration (6%) using a centrifuge at 7^{o}C and 8000 rpm (i.e. at 12,200 maximum relative centrifugal force) for 30 minutes and mixed with original sludge sample to prepare the homogeneous sample of desired concentrations.

The sludge sample was heated to 105^{o}c in the oven for at least 24 hours, to measure the sludge concentration through the weight difference between before and after placing it in the oven for 24 hours (Rice et al. 2012).

4.3.2 APPARATUS

Rheological measurements were performed using a commercially available hybrid stress controlled (HR3) rheometer from TA Instruments. A custom designed plexi glass cup (inner diameter: 100 mm, length: 100 mm) with a stainless steel porous disk (outer diameter: 100 mm, thickness: 1.6 mm, porosity: 40%, from SINTEC Australia) at the bottom for the gas sparging and grooved bob geometry with outer diameter of 14.9 mm, and 42 mm length as shown in Figure 4.1 is used. The gas flow rate was varied from 0.5 LPM to 4 LPM using a gas mass flow meter from AALBORG at a pressure of 10 psi.

4.3.3 RHEOMETRIC TECHNIQUE

The flow curve of 3wt% solid concentration of sludge was measured using two different methods: in-situ and after sparging. For in-situ measurement, flow curve was obtained while continuously injecting the gas at 0.5 LPM and 3 LPM. However, in after sparging method the gas was first sparged at 0.5 LPM and 3 LPM for 20 minutes through sludge and then the flow curve was determined after stopping gas. Before each flow curve measurement the sample was pre-sheared at high shear rate (400 s^{-1}) [as the maximum shear rate without turbulence in this cup with used grooved bob geometry is 401 s^{-1}] for 900 s and then allowed to rest for 120 s to obtain an identical sludge sample before each flow curve measurement (Baudez 2008). The viscosity of the sample was then measured over the shear rate range of 0.001 s^{-1} to 100 s^{-1}. To check whether slippage occurred, flow curves were obtained for different gap sizes (42.55 mm & 35 mm) & different geometries (large vane: d=30 mm, *h*= 65 mm; small vane: d= 28 mm, h= 42 mm; grooved bob: d= 14.9 mm, h= 42 mm; smooth bob: d= 28 mm, h= 42 mm).

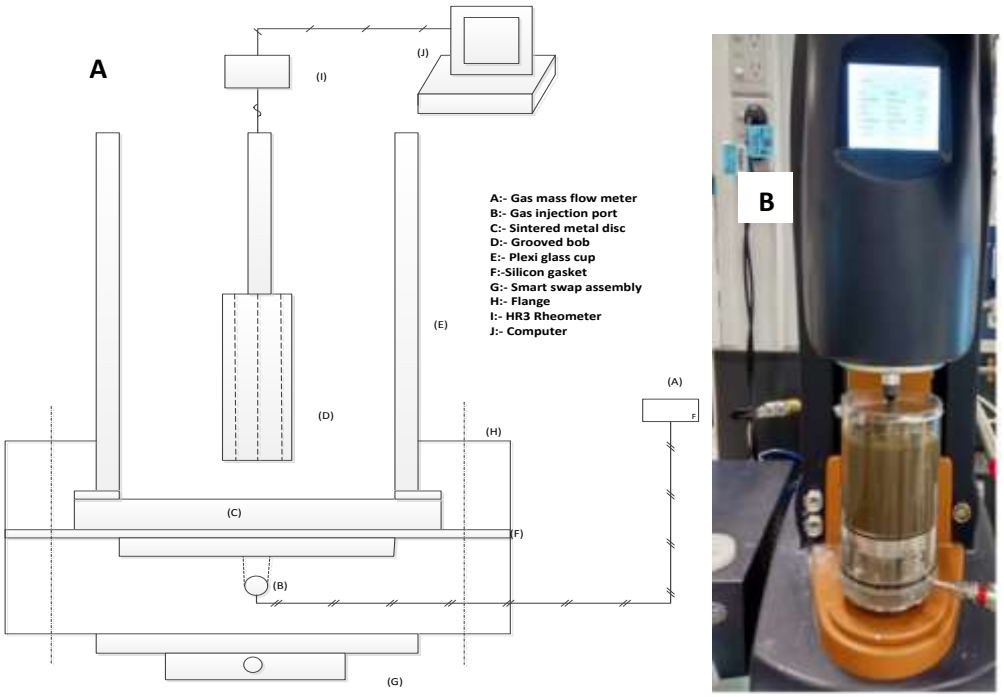

Figure 4.1: (A) Schematic drawing of experimental setup, (B) actual experimental setup

Since a grooved bob geometry with a wide gap (42.55 mm) was used, the flow curves were recalculated using Equations 4.1 and 4.2 (Estellé et al. 2008).

$$\tau_{Ri} = \frac{M}{(2\pi HR_i^2)} \quad (4.1)$$

$$\dot{\gamma} = 2M \frac{d\Omega}{dM}, \tau_c \leq \tau_y \leq \tau_b \quad (4.2)$$

Where, M is the torque (N.m), H is the height of the Bob (m), R_i and R_o are the radius of the rotating Bob and the cup, Ω is angular velocity (rad/s), derivative dΩ/dM is calculated as of $(\Omega_j - \Omega_{j-1}) / (M_j - M_{j-1})$ and τ_y, τ_c, τ_b are yield stress and stress at the cup and bob respectively (Pa).

To highlight gas injection induces extra shear on sludge, both creep test and dynamic measurement (time sweep) test were carried out to calculate induced additional shear via two different methods for comparison on a single solid concentration of sludge (4.2%). The experimental procedure for creep and time sweep test was carried out in the following pattern: Pre-sheared the sludge at high shear rate (400 s^{-1}) for 900 s. This step helps to ensure that an identical condition is achieved before each step. Final shear stress was monitored carefully while preshearing to confirm the same condition is achieved. The

sludge was then kept at rest for a short period (120 s) without causing any further disturbance (i.e. without removing the Bob) to start the test in the same condition (Baudez 2008, Markis et al. 2014). Following the preshearing step, to understand the elastic deformation of sludge, a constant stress of 0.89 Pa which is well within the linear viscoelastic range was applied for the duration of 900 s and the corresponding strain was recorded over time. In the next step for careful consideration of all the structural and shearing changes that may occur during the test due to removing and insertion of Bob; Bob was removed immediately after the preshearing step, and sludge was allowed to rest for 900 s (the same duration of creep test). After 900 s rest, Bob was reinserted and the creep test with the same stress of 0.89 Pa was repeated. Thus the major impact of removing and replacing the bob after allowing the long rest time on sludge structure was monitored and taken into account in the following.

After repeating preshearing stage and removing bob, Nitrogen gas at two different flow rates of 0.5 LPM and 1.5 LPM was sparged for 1500 s. After this step, the Bob was reinserted, and a creep test was performed at 0.89 Pa stress. To calculate the shear-induced only by gas injection, the extra shear imposed by removing and replacing the Bob was deducted from obtained data at this step. Similar to the abovementioned procedure time sweep test was also carried out at a very low shear strain (0.08%) and frequency (1 Hz) to remain in the linear viscoelastic region (LVE) for the duration of the 1500 s. A detailed stepwise procedure is shown in Figure 4.2A.

Then the successive creep and dynamic measurement (time sweep) of non-aerated 4.2% sludge with a broader stress and strain % (at 1 Hz frequency) range was repeated to evaluate the shear stress induced by gas injection. For example, a higher stress more than 0.89 Pa was applied to non-aerated sludge sample to achieve the same response of aerated sludge to 0.89 Pa stress. The difference will show the amount of induced shear due to gas injection as detailed in Figure 4.2B.

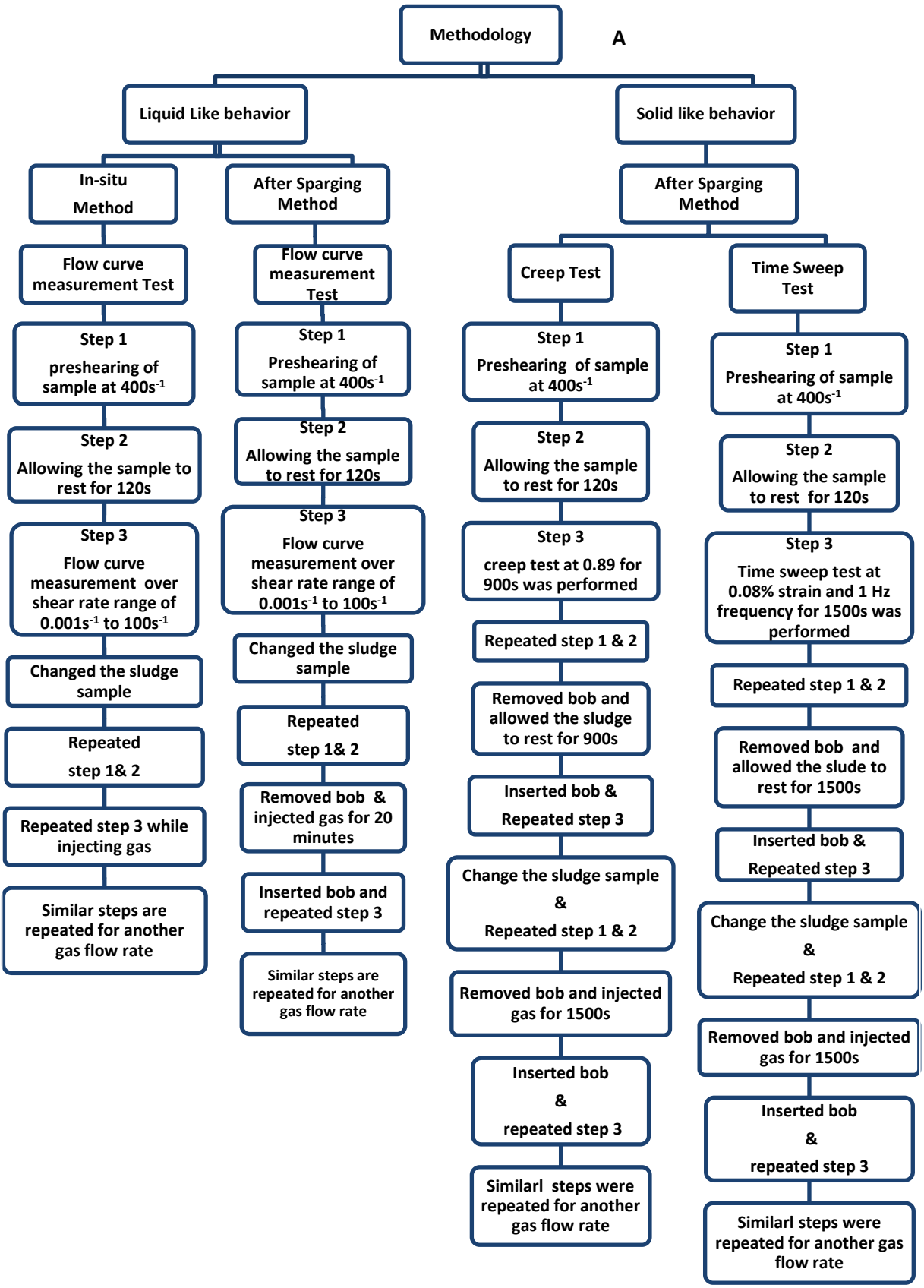
Methodology
A
Liquid Like behavior
Solid like behavior
In-situ Method
After Sparging Method
After Sparging Method
Flow curve measurement Test
Flow curve measurement Test
Creep Test
Time Sweep Test
Step 1 preshearing of sample at 400s-1
Step 2 Allowing the sample to rest for 120s
Step 3 Flow curve measurement over shear rate range of 0.001s-1 to 100s-1
Changed the sludge sample
Repeated step 1& 2
Repeated step 3 while injecting gas
Similar steps are repeated for another gas flow rate
Step 1 Preshearing of sample at 400s-1
Step 2 Allowing the sample to rest for 120s
Step 3 Flow curve measurement over shear rate range of 0.001s-1 to 100s-1
Changed the sludge sample
Repeated step 1& 2
Removed bob & injected gas for 20 minutes
Inserted bob and repeated step 3
Similar steps are repeated for another gas flow rate
Step 1 Preshearing of sample at 400s-1
Step 2 Allowing the sample to rest for 120s
Step 3 creep test at 0.89 for 900s was performed
Repeated step 1 & 2
Removed bob and allowed the sludge to rest for 900s
Inserted bob & Repeated step 3
Change the sludge sample & Repeated step 1 & 2
Removed bob and injected gas for 1500s
Inserted bob & repeated step 3
Similarl steps were repeated for another gas flow rate
Step 1 Preshearing of sample at 400s-1
Step 2 Allowing the sample to rest for 120s
Step 3 Time sweep test at 0.08% strain and 1 Hz frequency for 1500s was performed
Repeated step 1 & 2
Removed bob and allowed the slude to rest for 1500s
Inserted bob & Repeated step 3
Change the sludge sample & Repeated step 1 & 2
Removed bob and injected gas for 1500s
Inserted bob & repeated step 3
Similarl steps were repeated for another gas flow rate

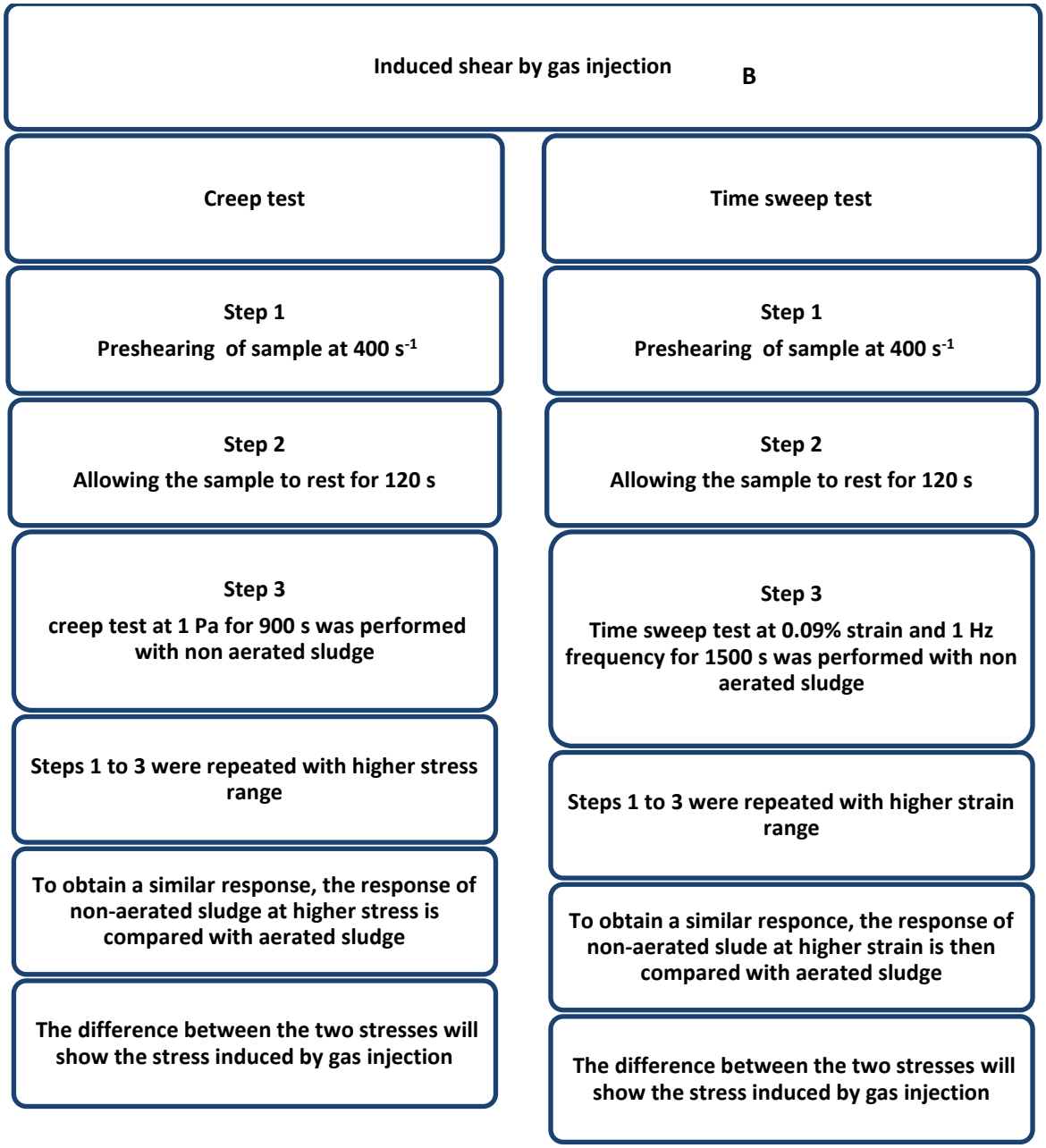

Figure 4.2: Schematic of experimental procedure for (A) liquid-like and (B) solid-like behavior for induced stress measurement

4.3.4 MICROSCOPICAL ANALYSIS

To verify the impact of gas injection on sludge structure, microscopic analysis was performed. Microscopic analysis was carried out under conventional environmental scanning electron microscope (FEI QUANTA 200) at a magnification of 200. The temperature and pressure were maintained at 4^{o}C and 5.20 Torr for all the samples during imaging to keep sludge structure in the same environmental conditions before imaging.

4.4 RESULTS AND DISCUSSION

4.4.1 IMPACT OF GAS INJECTION ON THE APPARENT VISCOSITY OF WAS

The viscosity curves of 3% solid concentration at 0.5 LPM and 3 LPM of gas flow rates with both in-situ and after sparging method revealed that during in-situ measurement the viscosity of sludge at low shear rate region (< 1 s^{-1}) decreased sharply (more than 3 decades) but inconsistently whereas, above 1 s^{-1} a similar trend for viscosities were observed (refer Figure 4.3A). Although a similar reduction in the viscosity of sludge due to gas injection was reported by Seyssiecq et al. (2008) using a torque meter, scattered data at the low shear rate range and a massive reduction of viscosity (~600 Pa drop in a second) via in-situ measurement was not satisfactory; so the after sparging method was implemented. Through after sparging method, the decrease in viscosity was consistent throughout the shear rate range (Figure 4.3B). Similar viscosity curves were also obtained at higher solid concentrations of sludge as well (data not shown for 4 & 5% solid concentration).

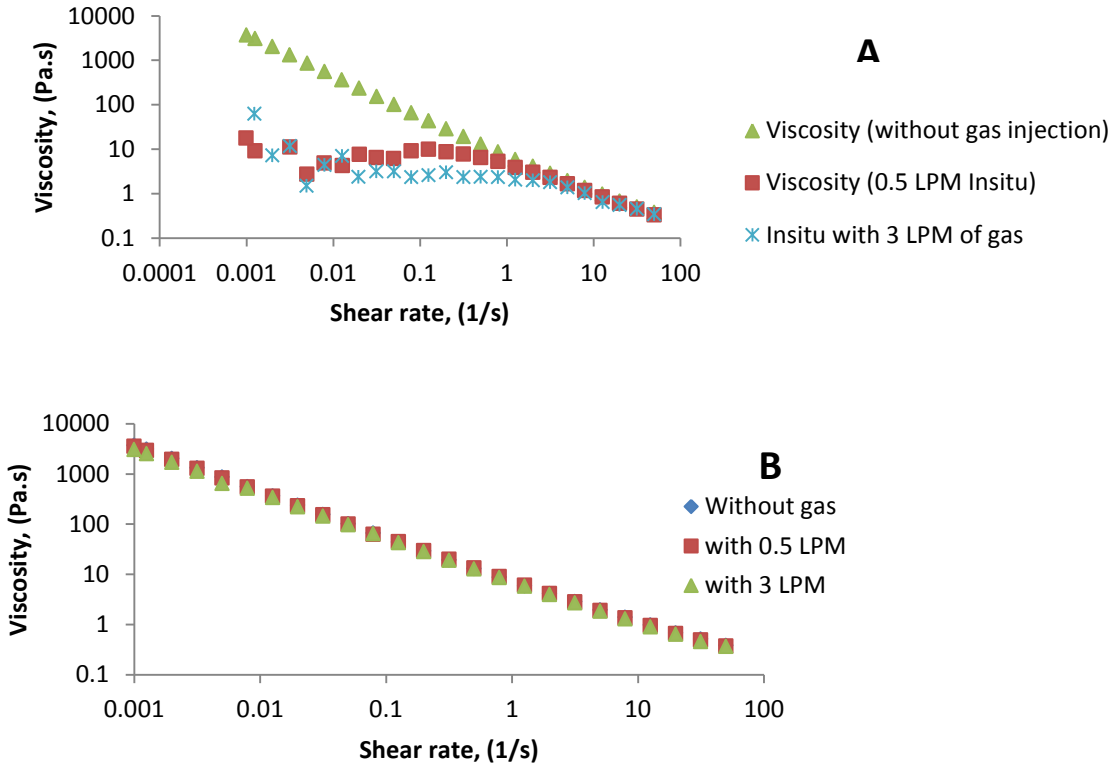

Figure 4.3: Impact of gas injection on the viscosity of 3% total solid concentration WAS at two different gas flow rate of 0.5 LPM, and 3 LPM measured through (A) in-situ method and (B) after sparging method

The comparison of viscosity curves of 3% WAS at 0.5 LPM for both methods indicated that the viscosity value above the shear rate of 1 s^{-1} is independent of the method used; however, enormous change in viscosity value exists below the shear rate of 1 s^{-1}(Figure 4.4).

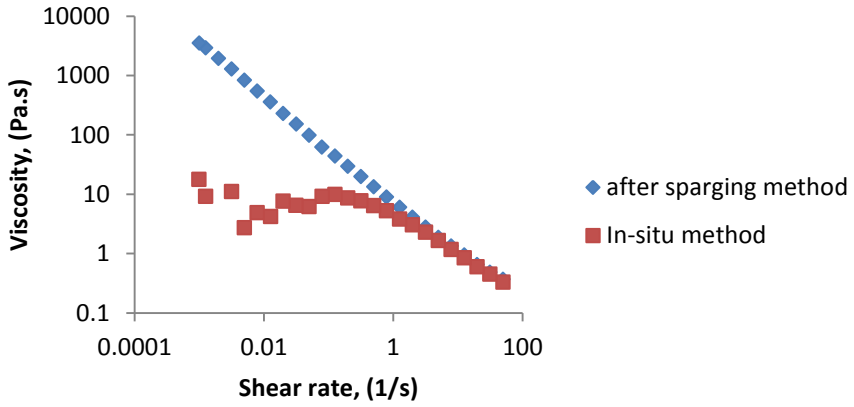

Figure 4.4: Comparison of viscosity curve for 3% total solid concentration WAS at 0.5 LPM of gas flow rate with after sparging method and in-situ method

The reason for the massive difference in viscosity values in the low shear rate at same condition for the same sludge sample was evaluated by plotting changes in torque against shear rate for both in-situ and after sparging (Figure 4.5). The torque data showed scattering in the low shear rate zone due to the presence of gas. This means at low shear rate gas injection impacts on torque measurement in an in-situ method and hence the huge viscosity drops was only observed in low shear rate range. In fact, bubbles rise where the viscosity is the lowest close to the Bob (Orvalho et al. 2015). This induces a dramatic change at the interface between bob and sludge, possibly causing slippage.

To investigate whether slippage occurs, the viscosity curves were plotted for different geometries and gap sizes of aerated and non-aerated sludge samples (Figure 4.6). For without gas injection, slippage occurs only with smooth bob below the critical shear rate of 0.1 s^{-1}(Figure 4.6A). Tabuteau et al. (2004) also reported slippage at low shear rate with smooth surfaces for sewage sludge. On the contrary for an in-situ method the viscosity value for the same sludge sample and at the same 0.5 LPM gas flow rates, the viscosity curve is different for different geometries and gap sizes (Figure 4.6B). However, in after sparging method the viscosity value for different gap sizes and geometries appears to be same except for smooth bob below critical shear rate. (Figure 4.6B inset). Thus the

lower viscosity value at low shear rate range obtained from the in-situ method is not because of change in material characteristics, but because slippage is occurring.

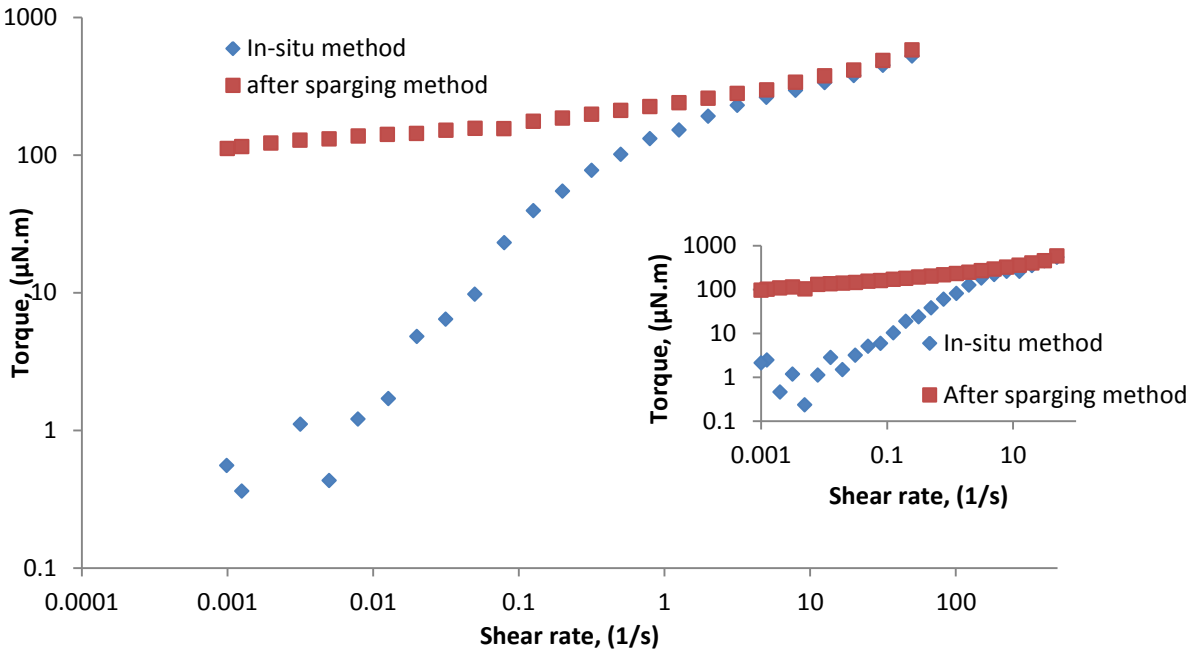

Figure 4.5: Comparing impact of gas injection at two gas flow rate of 0.5 LPM and 3.0 LPM (inset) through two different methods of in-situ and after sparging on torque

At the higher shear rate the torque is so high that gas bubble presence close to bob does not impact on torque measurement. Hence the torque, displacement and viscosity curve at high shear rate shows the same value irrespective of the method used.

Consequently, the results obtained from after sparging method are reliable, and the decrease in viscosity at a low shear rate with increasing gas flow rate reported by Seyssiecq et al. (2008), seems to be erratic, because we did not observe a distinctive effect of gas injection on sludge viscosity in non-linear viscoelastic region. The same behaviour was also observed at higher concentrations as well (data not shown).

Bubble coalescence caused by high viscosity of sludge can be the reason behind the negligible decrease in viscosity at different gas flow rates. Fransolet et al. (2005) reported that in a non-Newtonian fluid a viscosity value above 0.04 Pa.s causes the bubble coalescence and a decrease in gas holdup. In our experimental works, not only sludge viscosity is higher than 0.04 Pa.s but also the actual stress imposed by gas injection is very low as shown in section 3.2, and hence there is a negligible decrease in viscosity throughout the shear rate range. Thus the in-situ method of analysis for the rheological

properties of yield stress fluid as shown by the Seyssiecq et al. (2008) becomes inappropriate for rheological measurement as it only allows to measure what is going on at the interface and not within the material. Additionally, this information will bring new insights on increasing the mass transfer and preventing membrane fouling as it is closely related to sludge viscosity and aeration intensity.

Mass transfer rate increases by decreasing the bubble plume diameter while bubble size linearly increases by increasing viscosity during aeration process. In addition, the change in bubble size with changing viscosity will impact on oxygen transfer efficiency as well as turbulence in bubble column as the contact time between the gas and liquid decreases (Fabiyi and Novak 2008).

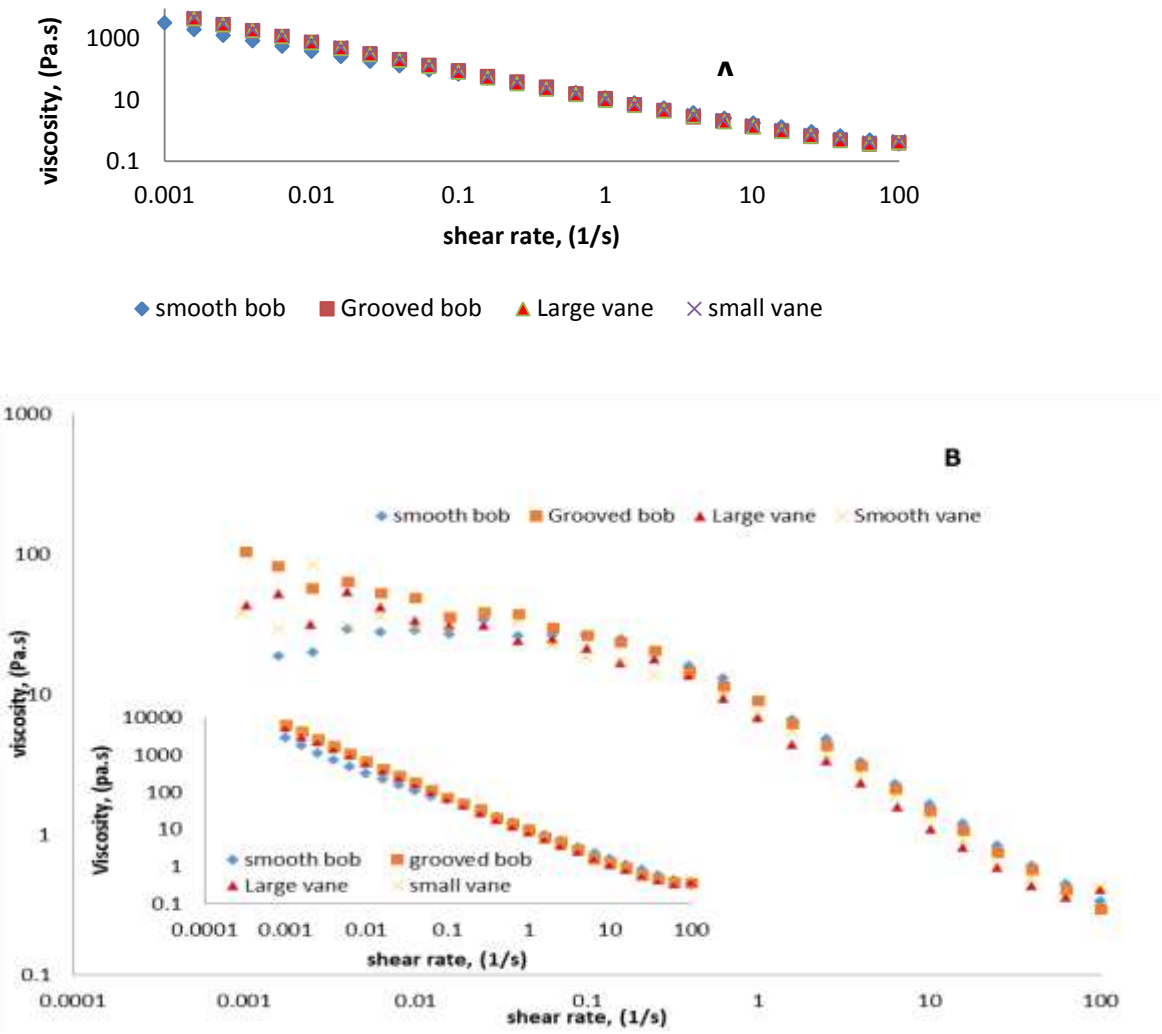

Figure 4.6: Comparison of viscosity curve for 3% total solid concentration of WAS with different geometries (A) without gas; (B)at 0.5 LPM of gas flow rate via in-situ method and after sparging method (inset)

4.4.2 IMPACT OF GAS INJECTION ON VISCOELASTIC PROPERTY OF SLUDGE

The examination of the influence of gas injection on viscoelastic property of sludge in linear viscoelastic region was carried out by both (1) creep test, and (2) dynamic time sweep test. The influence of gas injection at two gas flow rates of 0.5 LPM and 1.5 LPM on 4.2% solids concentration of waste activated sludge was reported in Figure 4.7. Figure 4.7A shows that by increasing gas injection, there is a growth in strain% within the observed time frame of creep test than that of without gas, which indicates that structure is becoming weaker with gas injection. The increased in strain% confirms that gas injection induces an extra shear. During the experiment, it was observed that the tan δ (G"/G') increases approximately by 14% with gas injection but remains less than 1 means still the sludge behave as a solid and does not flow (Figure 4.8). Tan delta (tan δ) less than 1 indicates that the extra shear induced by gas injection is not sufficient to completely change the material characteristics. However, the increase in tan δ for the same solid concentration suggests that the particles are dissociating as they disaggregate, deform and elongate (Mezger 2011). Furthermore, Figure 4.7B also shows that by increasing gas injection, both elastic and viscous modulus of sludge reduces over the entire time frame due to induced shear by gas injection. However, it is worth to notice that still G' is greater than G" which means the applied force is smaller than the molecular or inter-particle forces and the material is behaving similar to a solid. Similarly, as shown in Figure 4.7B the decrease in G' (elastic modulus) with gas injection is around 70 Pa and the decrease in G" (viscous modulus) with gas injection is around 10 Pa. It means that the elastic behaviour of sludge has been remarkably modified by gas injection. However, the viscous behavior of the sludge had minor changes compared to non-aerated sludge. Thus aeration has a significant impact on elastic behavior as compared to viscous behavior. The similar change of elastic and viscous modulus by increasing gas volume fraction in a yield stress fluids was also observed by Ducloué et al. (2015). Duclouée has added different gas volume fraction (Nitrogen and fluoro hexane) to a concentrated silicon and water emulsion having yield stress between 10 and 40 Pa. They observed that the deformation of bubbles in yield stress fluid takes place differently depending on the stress applied to the fluid. The elastic and viscous modulus of the suspending fluid solely depends on gas volume fraction and is linked to the capillary number. A capillary number is the dimensionless number representing the effect of viscous forces versus surface tension across the gas-liquid interface.

Since, there is a notable impact of gas injection on the viscoelastic property of sludge, it is necessary to consider this impact on the design and efficient operation of pumps, aeration systems, mixers and valves. The friction factor and head loss in the pipe and pumping system are calculated based on elasticity of the fluid (Jones and Sanks 2008, Ratkovich et al. 2013). In addition, pumping and air lift operation in a membrane filtration process or membrane bioreactors is required to reduce fouling on the membrane surface by creating cross flow.

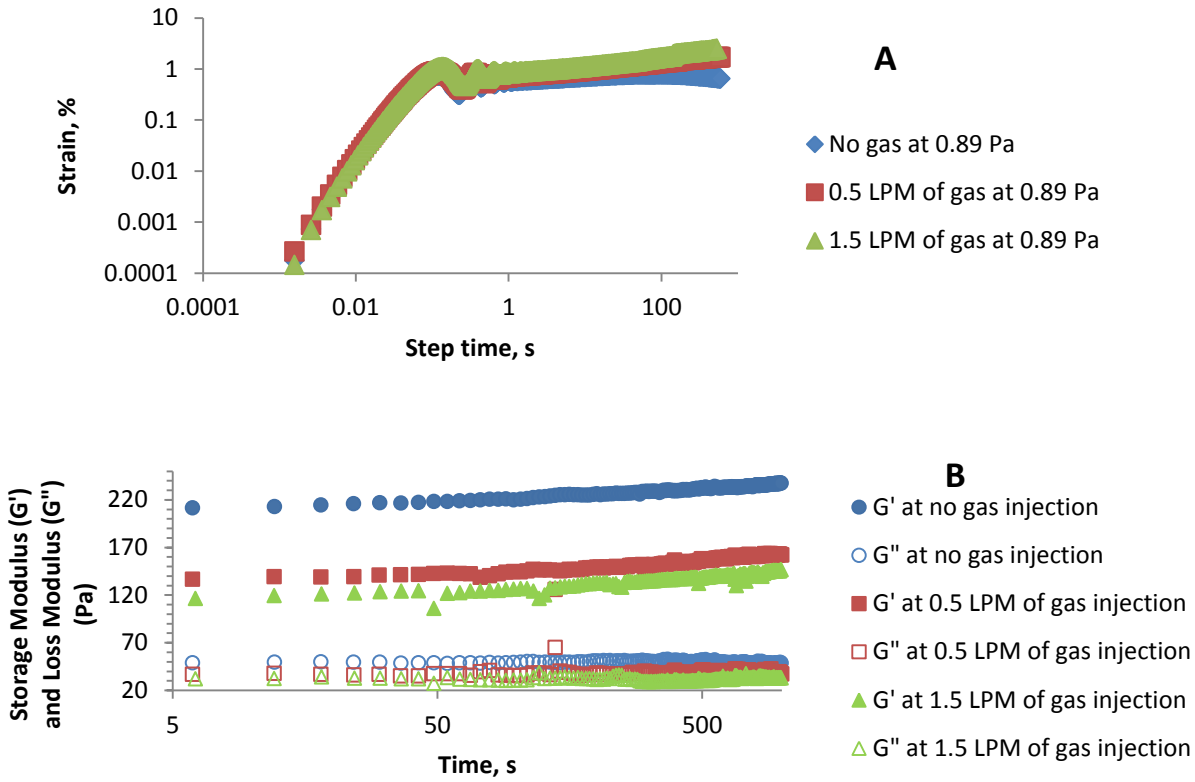

Figure 4.7: Impact of gas injection on 4.2% total solid concentrations WAS at two different gas flow rate of 0.5 LPM and 1.5 LPM measured through (A) creep test and (B) time sweep test

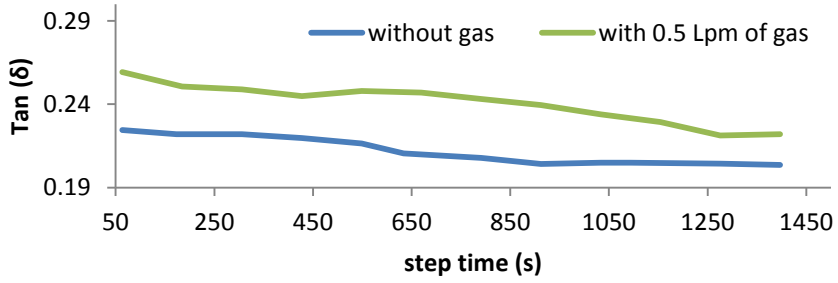

Figure 4.8: Increase in tan (delta) value of 4.2% sludge with gas injection at 0.5 LPM flow rate

4.4.3 ESTIMATION OF THE AMOUNT OF SHEAR INDUCED BY GAS INJECTION

In this part by comparing the response of aerated and un-aerated sludge samples (4.2% total solids concentration of WAS) through creep and time sweep tests, the extent of additional stress induced by gas injection was determined. The creep response of un-aerated sludge sample imposing 1 Pa stress is equivalent to the impact of imposing 0.89 Pa on a sludge sample which aerates with 0.5 LPM for 900 s. The difference between these two stresses indicates gas injection have a similar effect that an additional stress of 0.11 Pa (Figure 4.9A). Likewise the results of creep test for the same sludge without gas injection and aerated sludge sample with 1.5 LPM for 900 s indicates that 0.31 Pa stress was imposed by injecting gas when the initial stress imposed is 0.89 Pa for aerated sludge (Figure 4.9A inset).

Time sweep was carried out, to double check the accuracy of the calculated extra stress imposed due to gas injection, (Figure 4.9B). The elastic response of 4.2% solid concentration un-aerated WAS to 0.2% deformation is the same as the elastic response of aerated sample at 0.5 LPM for 900 s at 0.08% deformation. The difference between two deformations means that during gas injection sludge an extra 0.12% strain (deformation) was imposed on the sludge sample when the gas was injected at a rate of 0.5 LPM. The amount of imposed strain was also increased to 0.22% by increasing the gas flow rate to 1.5 LPM (Figure 4.9B inset).

To be able to calculate what is the equivalent stress for this strain (deformation) induced by gas, Metzger (2011)'s equation was used as presented in Equation 4.3.

$$\tau = \frac{strain}{100} \text{ x } G^* \quad (4.3)$$

Where $\tau\tau$ is stress (Pa), strain (%) and G* (Pa) is the complex modulus obtained from the amplitude sweep test (data not shown). The complex modulus of un-aerated 4.2% WAS at the strain range between 0 and 0.4% was 144 Pa.

Table 4.1 compares the calculated stress via two distinct methods of creep test and time sweep test. It shows that the calculated stress imposed by gas injection via two different methods is the same for two gas flow rates (0.5 LPM and 1.5 LPM) tested in this work. These results clearly prove that injecting gas induces extra shear on sludge.

Furthermore, the technique that we established for calculating the stress induced by gas injection can be used for selecting a suitable un-aerated simulant with the equivalent elastic behaviour of aerated sludge samples. This will bring an opportunity to study an aerated system without interfering air bubbles in the experimental works.

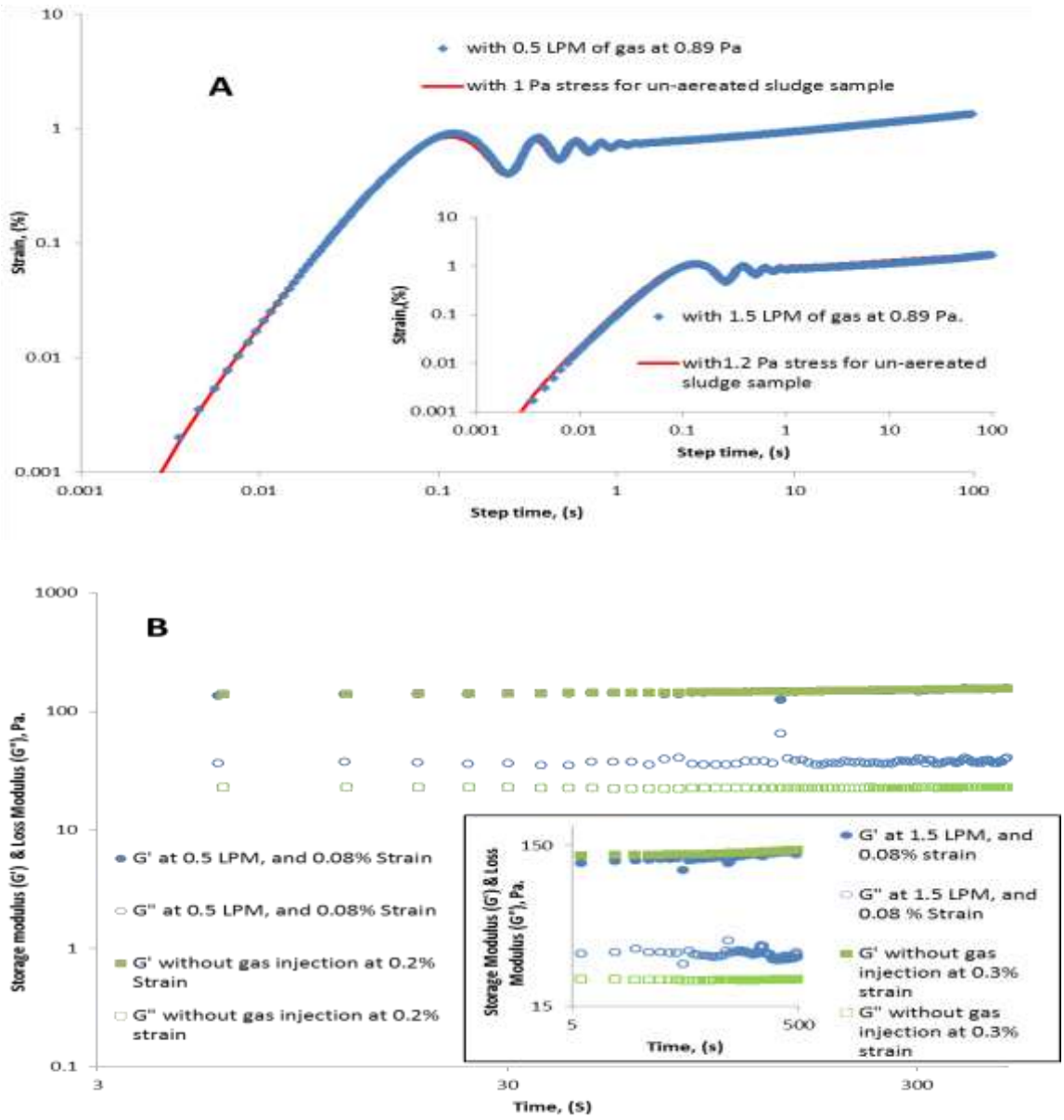

Figure 4.9: Comparison of equivalent stress (strain) induced by gas injection at two gas flow rates of 0.5 LPM and 1.5 LPM (inset) on 4.2% WAS via two different experiments (A) creep test and (B) time sweep

Table 4.1. The calculated stress imposed by gas injection on 4.2% was via two different tests (creep and time sweep) at two gas flow rates of 0.5 LPM and 1.5 LPM for 900 s

Creep test				
Gas flow rate (LPM)	Applied stress for aerated sludge (Pa)	Applied stress for un-aerated (Pa)	stress imposed by the gas (Pa)	
0.5	0.89	1	1-0.89 = **0.11**	
1.5	0.89	1.2	1.2-0.89 = **0.31**	
Time sweep test				
Gas flow rate (LPM)	Applied strain for aerated sludge (%)	Applied strain for un-aerated sludge (%)	Strain imposed by the gas (%)	Equivalent stress imposed by the gas (Pa)
0.5	0.08	0.2	0.2-0.08= 0.12	(0.12/100)*144 = **0.17**
1.5	0.08	0.3	0.3 – 0.08= 0.22	(0.22/100)*144 = **0.32**

4.4.4 IMPACT OF GAS INJECTION ON SLUDGE STRUCTURE

The investigation of ESEM images of the impact of gas injection on sludge structure showed that as the gas injection increases, the sludge structures become weaker (Figure 4.10). The images showed that for without gas injection the floc structure appears to be strongly associated, and a smooth plain structure of sludge is seen. However, with gas injection rate of 0.5 LPM the floc structure appears to be slightly porous in nature, and with further increase in the gas flow rate to 4.0 LPM, the floc structure seems to be more permeable. Thus the images clearly showed that gas injection changed sludge floc

structure. Menniti et al. (2009) have reported that an increase in shear increased the release of soluble EPS through the erosion of floc structure. Menniti et al. (2010) explained that the reduction in floc size in the low shear environment is because of the influence of aeration on worms which is responsible for the release of more soluble EPS. Thus, the gas injection modifies the sludge floc structure which its consequences was observed in the reduction of G' and G" with gas injection.

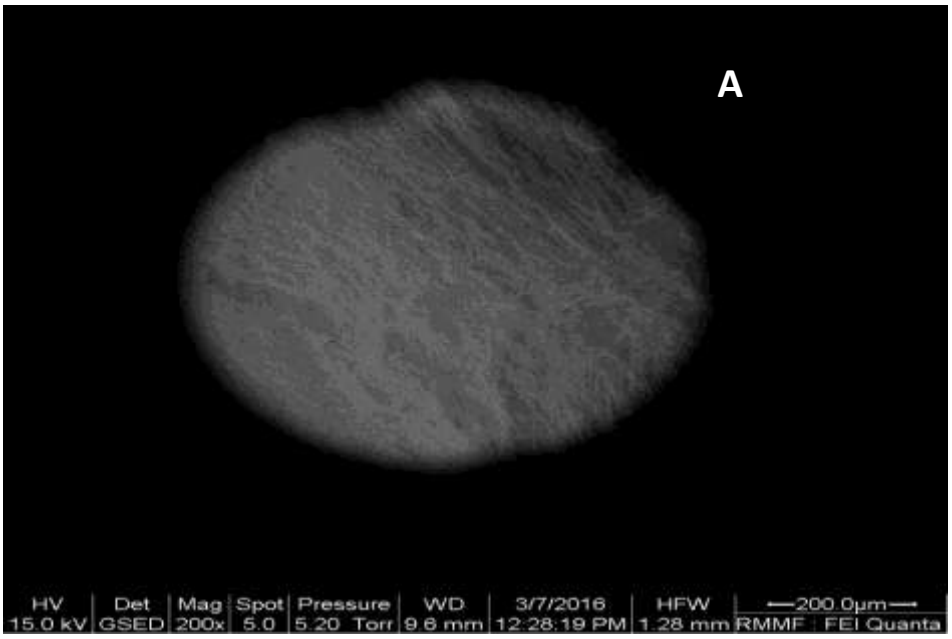

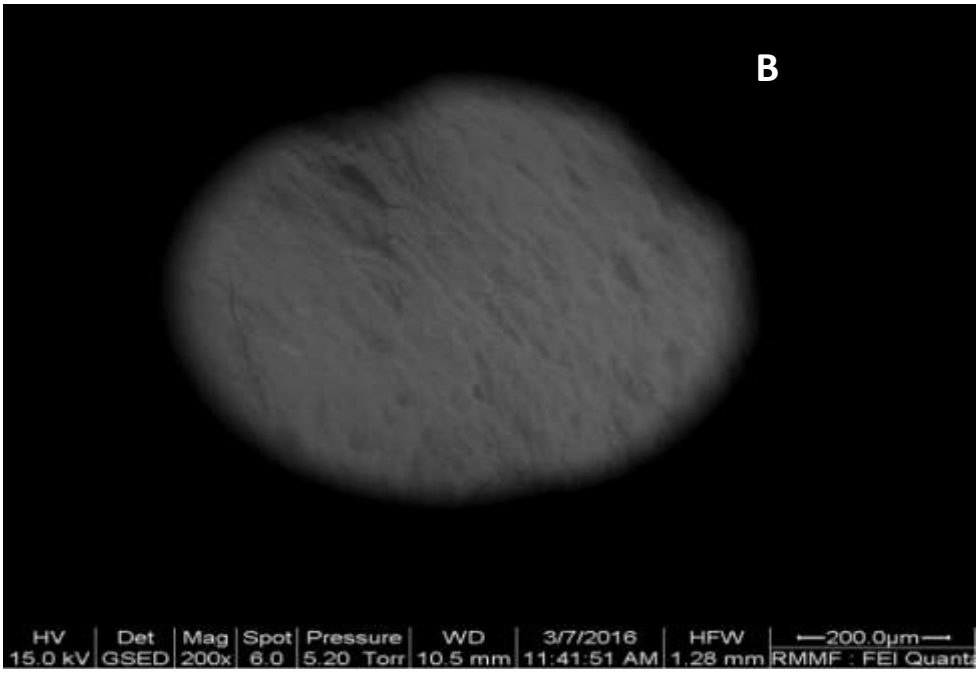

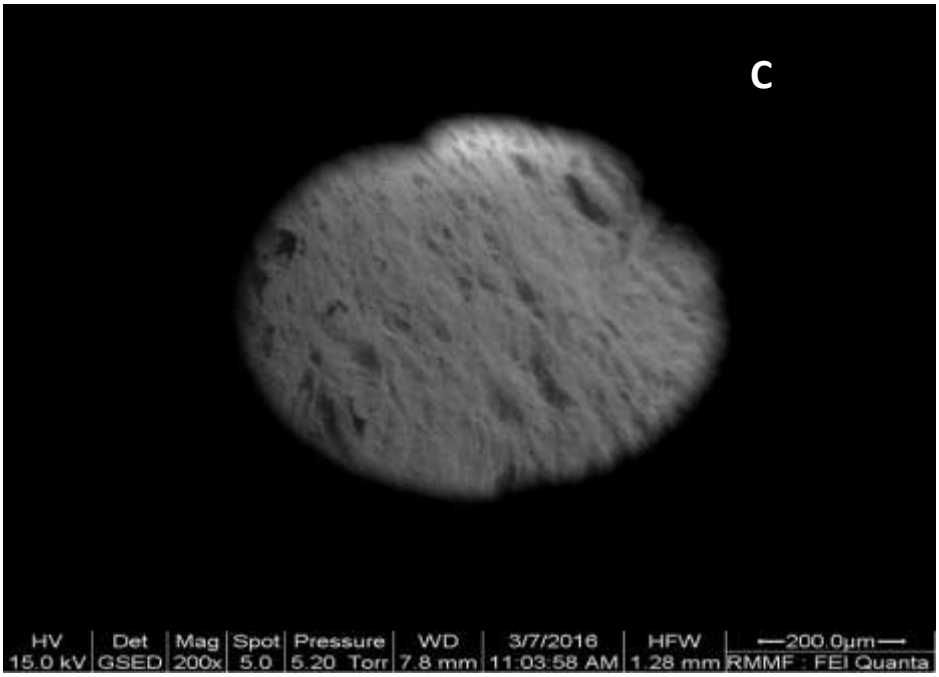

Figure 4.10: Microscopic image of 3% sludge floc structure (A) without gas, (B) with 0.5 LPM of gas, and (c) with 4 LPM of gas

4.5 CONCLUSION

The present study investigated how the gas injection affects the apparent viscosity and viscoelastic properties of waste activated sludge. The viscosity curve of two different methods in-situ and after sparging measurement showed a huge difference in viscosity values at low shear rate range. The rising gas bubbles close to the rotating bob causes slippage and causes very low viscosity in in-situ method compared to after sparging method.

Creep test and dynamic measurement (time sweep) proved that the gas injection induces shear in sludge. The increase in tan (delta) and the decrease in the elastic and viscous modulus of sludge by increasing gas flow rate is an indication of weakening sludge structure. This was also proved by ESEM images of sludge, where bubbling modified the sludge structure.

Our results suggest that although gas bubbling induces extra shear, it is not enough to breakdown the structure completely and to show a considerable impact on the viscosity of sludge. However, the impact of bubbles on the viscoelastic property of sludge is notable.

Also, a technique for finding an un-aerated simulant to aerated system with a similar elastic property was established.

4.6 ACKNOWLEDGEMENTS

The authors acknowledge South East Water support for providing sludge to carry out the research, and RMIT University to provide the Australian postgraduate scholarship for V. Bobade.

4.7 REFERENCES

Babaei, R., Bonakdarpour, B. and Ein-Mozaffari, F. (2015) Analysis of gas phase characteristics and mixing performance in an activated sludge bioreactor using electrical resistance tomography. Chemical Engineering Journal 279, 874-884.

Bajón Fernández, Y., Cartmell, E., Soares, A., McAdam, E., Vale, P., Darche-Dugaret, C. and Jefferson, B. (2015) Gas to liquid mass transfer in rheologically complex fluids. Chemical Engineering Journal 273, 656-667.

Baroutian, S., Eshtiaghi, N. and Gapes, D.J. (2013) Rheology of a primary and secondary sewage sludge mixture: Dependency on temperature and solid concentration. Bioresource Technology 140, 227-233.

Baudez, J.C. (2008) Physical aging and thixotropy in sludge rheology. Applied Rheology 18(1), 13495-13491-13495-13498.

Baudez, J.C. and Coussot, P. (2001) Rheology of aging, concentrated, polymeric suspensions: Application to pasty sewage sludges. Journal of Rheology 45(5), 1123-1140.

Brannock, M., Wang, Y. and Leslie, G. (2010) Mixing characterisation of full-scale membrane bioreactors: CFD modelling with experimental validation. Water Research 44(10), 3181-3191.

Curvers, D., Saveyn, H., Scales, P.J. and Van der Meeren, P. (2009) A centrifugation method for the assessment of low pressure compressibility of particulate suspensions. Chemical Engineering Journal 148(2-3), 405-413.

De Temmerman, L., Maere, T., Temmink, H., Zwijnenburg, A. and Nopens, I. (2015) The effect of fine bubble aeration intensity on membrane bioreactor sludge characteristics and fouling. Water Research 76, 99-109.

Dieude-Fauvel, E., Heritier, P., Chanet, M., Girault, R., Pastorelli, D., Guibelin, E. and Baudez, J.C. (2014) Modelling the rheological properties of sludge during anaerobic digestion in a batch reactor by using electrical measurements. Water Research 51, 104-112.

Ducloué, L., Pitois, O., Goyon, J., Chateau, X. and Ovarlez, G. (2015) Rheological behaviour of suspensions of bubbles in yield stress fluids. Journal of Non-Newtonian Fluid Mechanics 215, 31-39.

Eshtiaghi, N., Markis, F., Yap, S.D., Baudez, J.C. and Slatter, P. (2013) Rheological characterisation of municipal sludge: A review. Water Research 47(15), 5493-5510.

Estellé, P., Lanos, C. and Perrot, A. (2008) Processing the Couette viscometry data using a Bingham approximation in shear rate calculation. Journal of Non-Newtonian Fluid Mechanics 154(1), 31-38.

Fabiyi, M.E. and Novak, R. (2008) "Evaluation of the factors that impact successful membrane biological reactor operations at high solids concentration". p. 503 to 512.

Fransolet, E., Crine, M., Marchot, P. and Toye, D. (2005) Analysis of gas holdup in bubble columns with non-Newtonian fluid using electrical resistance tomography and dynamic gas disengagement technique. Chemical Engineering Science 60(22), 6118-6123.

Hao, L., Liss, S.N. and Liao, B.Q. (2016) Influence of COD:N ratio on sludge properties and their role in membrane fouling of a submerged membrane bioreactor. Water Research 89, 132-141.

Jones, P.D.G.M. and Sanks, P.P.R.L. (2008) Pumping Station Design: Revised 3rd Edition, Elsevier Science.

Markis, F., Baudez, J.-C., Parthasarathy, R., Slatter, P. and Eshtiaghi, N. (2014) Rheological characterisation of primary and secondary sludge: Impact of solids concentration. Chemical Engineering Journal 253, 526-537.

Meng, F., Shi, B., Yang, F. and Zhang, H. (2007) New insights into membrane fouling in submerged membrane bioreactor based on rheology and hydrodynamics concepts. Journal of Membrane Science 302(1–2), 87-94.

Menniti, Adrienne, Morgenroth and Eberhard (2010) The influence of aeration intensity on predation and EPS production in membrane bioreactors. Water Research 44(8), 2541-2553.

Menniti, A., Kang, S., Elimelech, M. and Morgenroth, E. (2009) Influence of shear on the production of extracellular polymeric substances in membrane bioreactors. Water Research 43(17), 4305-4315.

Mezger, T.G. (2011) The rheology handbook: for users of rotational and oscillatory rheometers, Vincentz Network, Hanover, Germany.

Monteiro, P.S. (1997) The influence of the anaerobic digestion process on the sewage sludges rheological behaviour. Water Science and Technology 36(11), 61-67.

Orvalho, S., Ruzicka, M.C., Olivieri, G. and Marzocchella, A. (2015) Bubble coalescence: Effect of bubble approach velocity and liquid viscosity. Chemical Engineering Science 134, 205-216.

Ratkovich, N., Horn, W., Helmus, F.P., Rosenberger, S., Naessens, W., Nopens, I. and Bentzen, T.R. (2013) Activated sludge rheology: A critical review on data collection and modelling. Water Research 47(2), 463-482.

Rice, E.W., Bridgewater, L., Association, A.P.H., Association, A.W.W. and Federation, W.E. (2012) Standard methods for the examination of water and wastewater., Washington, D.C. American Water Works Association, 2012.

Rosenberger, S., Kubin, K. and Kraume, M. (2002) Rheology of Activated Sludge in Membrane Bioreactors. Engineering in Life Sciences 2(9), 269-275.

Ruiz-Hernando, M., Labanda, J. and Llorens, J. (2015) Structural model to study the influence of thermal treatment on the thixotropic behaviour of waste activated sludge. Chemical Engineering Journal 262, 242-249.

Seyssiecq, I., Karrabi, M. and Roche, N. (2015) In situ rheological characterisation of wastewater sludge: Comparison of stirred bioreactor and pipe flow configurations. Chemical Engineering Journal 259, 205-212.

Seyssiecq, I., Marrot, B., Djerroud, D. and Roche, N. (2008) In situ triphasic rheological characterisation of activated sludge, in an aerated bioreactor. Chemical Engineering Journal 142(1), 40-47.

Seyssiecq., Ferrasse and Roche (2003) State-of-the-art: rheological characterisation of wastewater treatment sludge. Biochemical Engineering Journal 16(1), 41-56.

Slatter, P.T. (1997) The rheological characterisation of sludges. Water Science and Technology 36(11), 9-18.

Tabuteau, H., Baudez, J.C., Bertrand, F. and Coussot, P. (2004) Mechanical characteristics and origin of wall slip in pasty biosolids. Rheologica Acta 43(2), 168-174.

Tixier, N., Guibaud, G. and Baudu, M. (2003) Determination of some rheological parameters for the characterization of activated sludge. Bioresource Technology 90(2), 215-220.

Wang, Y. and McNeil, B. (1996) A study of gas hold-up, liquid velocity, and mixing time in a complex high viscosity, fermentation fluid in an airlift bioreactor. Chem. Eng. Technol. 19(2), 143-153.

Zhang, H., Yu, H., Zhang, L. and Song, L. (2015) Stratification structure of polysaccharides and proteins in activated sludge with different aeration in membrane bioreactor. Bioresource Technology 192, 361-366.

CHAPTER 5: IMPACT OF GAS INJECTION ON PHYSICOCHEMICAL PROPERTIES OF WASTE ACTIVATED SLUDGE: A LINEAR RELATIONSHIP BETWEEN THE CHANGE OF VISCOELASTIC PROPERTIES AND THE CHANGE OF OTHER PHYSIOCHEMICAL PROPERTIES

This chapter was published in Water Research

(Vol: 144, P: 246-253, 2018)

Keywords: Waste activated sludge, Viscoelastic properties, Suspended solids, Soluble COD, Zeta potential

V. Bobade, G. Evans, J.C. Baudez, N. Eshtiaghi, "Impact of gas injection on physicochemical properties of waste activated sludge: A linear relationship between the change of viscoelastic properties and the change of other physiochemical properties". Water Research 144 (2018) 246-253.

Graphical Abstract

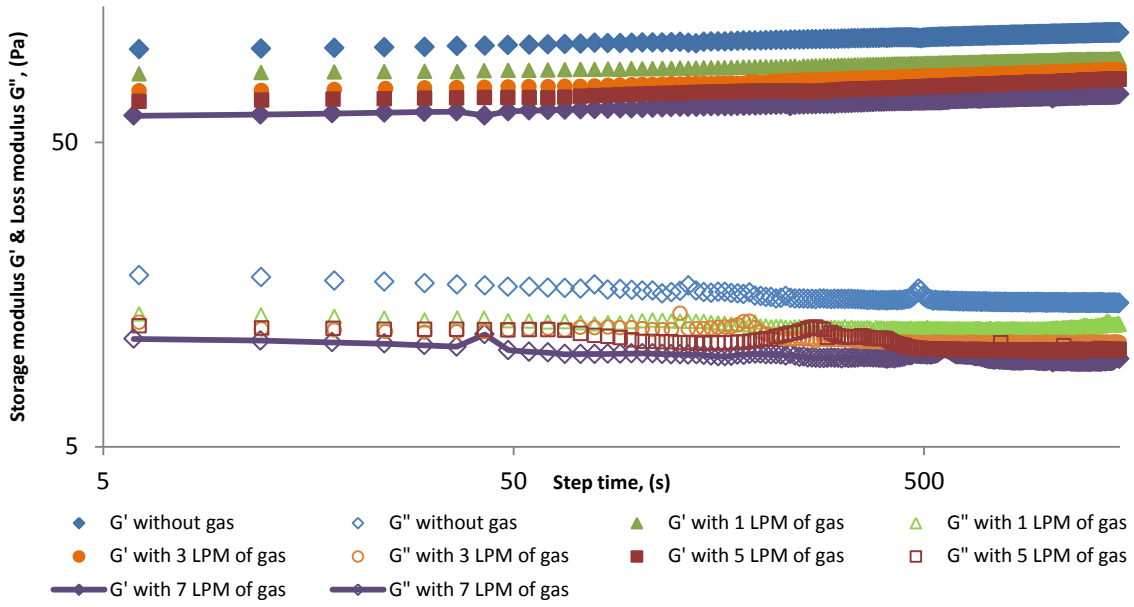

5.1 ABSTRACT

Aeration process in the waste activated sludge treatment accounts for 75% of total energy consumption of the treatment plant. The main purpose of the aeration process is to enhance the biodegradation of the liquid waste. Gas bubbles, rising through the liquid, improve mixing, reduce inhomogeneity in the treatment tank and enhance biological reactions. Thus aeration intensity and several physicochemical properties of feed such as viscosity, total suspended solids, and surface charge play a significant role in the biological reaction.

This paper examines the impact of the gas injection rate on some physicochemical properties of waste activated sludge namely rheological properties, suspended solids, soluble COD (sCOD), surface tension, and zeta potential. The impact of four different gas flow rates on four different concentrations of waste activated sludge properties was analysed.

The results showed that in linear viscoelastic regime the viscous and elastic modulus decreases linearly with an increase in gas flow rate. The amount of stress imposed by gas injection also showed a direct relationship with gas velocity. Gas injection also showed a substantial impact on soluble COD, suspended solids, and zeta potential. Additionally, a linear relationship was observed between the percentage change in the abovementioned physical properties and stress imposed by gas injection. These results confirm that gas injection produces additional shear impacting sludge physicochemical properties and therefore changes its rheological behaviour. The extra stress induced by gas injection can be predicted using a simple model based on sludge concentration and gas velocity

5.2 INTRODUCTION

The waste activated sludge process is the most versatile and commonly used biological treatment (Seyssiecq et al. 2008). The efficiency of the waste activated sludge process depends upon an aeration operation. Aeration provides oxygen to the micro-organisms to breakdown the complex organic compounds into carbon dioxide and water and reduces the volume of sludge produced (Bailey et al. 2002). However, the oxygen transfer rate in the aeration tank decreases with an increase in the total solid concentration of sludge and strongly influences the efficiency of the process (Rosenberger et al. 2002). This is because with increasing solid concentration of sludge results in an increased viscosity of sludge

that causes variations in system hydrodynamics as and impacts on bubble buoyancy, bubble shape and turbulence (Bajón Fernández et al. 2015).

Waste activated sludge is composed of water, microorganisms, and macromolecules grouped in bioflocs (Laspidou and Rittmann 2002). Hence its structure depends on many factors and can remarkably change when exposed to shear stress. Therefore, sludge is known to exhibit shear thinning behaviour (Eshtiaghi et al. 2013, Baudez and Coussot 2001, Baudez 2008). Thus, rheology plays a crucial role in optimising and designing the aeration system. Since the sludge characteristics and rheology affect each other, the impact of aeration on rheology and sludge physical properties should be considered when studying the sludge flow behaviour in the aeration tank.

Increase in aeration intensity results in a severe breakup of sludge flocs, and promotes the release of colloids and solutes from the microbial flocs to the bulk solution (Meng et al. 2008). Consequently, it influences the sludge physical properties like total suspended solids (TSS), sludge volume index (Vesvikar and Al-Dahhan), etc. and impacts on sludge settleability, filterability, and compressibility (Pollice et al. 2007). The impact of shear stress generated by aeration intensity increased the soluble contents of sludge (SMP, EPS) (Menniti et al. 2010, Menniti et al. 2009). Moreover, the induced shear stress by micro bubbles broke down the sludge that reduced the floc size and released the organic content such as EPS and it also changed the viscosity and surface tension of sludge (Liu et al. 2012). Almost all the studies that have conducted to date have only focused on membrane bioreactor to study the impact of aeration intensity on sludge physical properties and for the solid concentration less than 2%.

Provided that aeration intensity impacts on sludge physical properties and consequently changes its rheological properties, currently there isn't any study that showed the relationship between sludge rheology (especially in a linear viscoelastic region that can be measured online) and physiochemical properties of sludge.

As both the physical and rheological properties simultaneously change in the aeration process and impact on the efficiency of the waste activated sludge process, monitoring shear and its effect on complex physicochemical properties through online tools (e.g. rheometers) with any minor change provides useful information to adjust operating conditions accordingly. However, there is lack of detailed analysis on the change in

sludge rheology with an aeration rate and its impact on the sludge physicochemical properties. This study wants to elucidate and correlate the stress generated by aeration intensity with sludge physicochemical properties. Therefore, this research primarily aims at investigating the impact of gas injection on viscoelastic properties, zeta potential, soluble COD and surface tension to get the detailed insight of the shear induced by the gas intensity and its effect on sludge physicochemical properties. The second objective is to develop relationships between change in rheological properties and physical properties at the different gas flow rates.

5.3 MATERIALS AND METHODS

5.3.1 SAMPLE PREPARATION

Waste activated sludge with 3wt% (TS 30 g/L; TSS 26.833 g/L; sCOD 3720 mg/L; zeta potential -16.4mv; surface tension 46.04 mN/m) was collected from a wastewater treatment plant (Mt Martha Treatment Plant) in southern region of Victoria, Australia. Sewage sludge of 600,000 customers after grit removal and primary tank settling is aerated in ambient temperature. The sludge samples were collected after the dissolved air flotation tank before the polymer dosing. The sludge was thickened to higher concentration (6%) using a centrifuge at 7^{o}C and 8000 rpm (i.e., at 12,200 g maximum relative centrifugal force) for 30 minutes. The homogeneous samples of 3.0%, 4.0%, 5.0% & 5.5% total solids concentration (TS) were prepared by diluting the 6% concentrated sludge with the original sample.

5.3.2 APPARATUS

Rheological measurements were performed using commercially available hybrid stress controlled (HR3) rheometer from TA Instruments using a grooved bob geometry with an outer diameter of 14.9 mm, and 42 mm length. A custom designed plexiglass cup (inner diameter: 100 mm, length: 100 mm) with a stainless steel porous disk (outer diameter: 100 mm, thickness: 1.6 mm, porosity: 40%, from SINTEC Australia) at the bottom was used for sparging gas while it connected to rheometer (Bobade et al. 2017). The gas flow rate was varied from 0.001 m^3/min to 0.007 m^3/min using a gas mass flow meter from AALBORG at a pressure of 10 psi.

5.3.3 RHEOMETRIC TECHNIQUE

To monitor the evolution of structural changes in sludge due to gas injection, dynamic time sweep measurement was carried out. The experimental procedure for the time sweep measurement was carried out in the following pattern:

- Step 1: Pre shear the sludge at high shear rate (350 s^{-1}) for 900s to ensure that identical condition is achieved before each measurement.
- Step 2: The sludge was allowed to rest for a short time (120 s) to start the test in the same condition (Baudez 2008, Markis et al. 2014).
- Step 3: The dynamic time sweep test at 0.09% strain and 1 HZ frequency in a linear viscoelastic range was carried out for 1500 s.
- Step 4: Preshearing of sludge was repeated (step 1) and the nitrogen gas was injected for 1500s before repeating the time sweep measurement (step 3). Similar experimental procedure was repeated for four different sludge concentrations (3%, 4%, 5% & 5.5%) at four different gas flow rates (1 LPM – 7 LPM).

The experimental procedure to measure the extra stress induced by gas injection on sludge was carried out as follows:

- Step 1: Preshearing of sludge at 350 s^{-1} for 900 s; resting for 120 s;
- Step 2: Dynamic time sweep measurement at different strains and 1 HZ frequency without aeration;
- Step 3: Compare the viscoelastic response (G', G") of non-aerated sludge with the aerated sludge at 0.09% strain, the difference between the two strains showed the extra strain imposed. The detailed sketch diagram of the rheological measurement process is provided elsewhere, Bobade et al. (2017).

5.3.4 PHYSICOCHEMICAL PROPERTIES

Soluble COD (sCOD) and Zeta potential were examined to study the sludge solubilisation after gas injection. The sample collected for measuring the sCOD and Zeta potential was centrifuged at 10,000 rpm (i.e., 20913 g at maximum relative centrifugal force) for 20 min for separating the liquor from solid. The small volume of obtained liquor was used

directly for zeta potential measurement and rest of the liquor was filtered through a 0.45 μm filter membrane. The collected filtrate was used to determine sCOD following standard American methods (Eaton et al. 2005). All measurements were carried out in duplicate. To avoid any alteration of sludge properties the samples and liquor are stored in a fridge at 4^{o}C.

The zeta potential measurement was performed using zetasizer Nano Range from Malvern Instruments, using disposable folded capillary cells (DTS 1070). The measurement was carried out at 20^{o}C, keeping the time lag of 10s between each set of readings. Each measurement was repeated for three times. The standard maximum deviation is 5%.

A surface tension of fluid changes with any change of formulation at the molecular level and helps to know the dispersibility and adhesion of the fluid (Davies and Rideal 1963). The measurement of surface tension was performed by using Force Tensionmeter (K100) from Kruss (Germany) using plate method. Sludge being a non-Newtonian viscous fluid, the measurement was carried out using microscope glass slide for 1200 s at an immersion depth of 2 mm. For precise measurement of surface tension, the glass slide was activated using oxygen flame before each measurement. Different immersion depth and time of run was examined to find an optimum point to obtain reproducible data.

5.4 RESULTS AND DISCUSSION

5.4.1 INFLUENCE OF AERATION INTENSITY ON VISCOELASTIC PROPERTIES

The oscillatory time sweep carried out in the linear viscoelastic region at low applied sinusoidal strain helps to understand whether any change in structure is occurring during gas injection. Both the storage modulus (G') & loss modulus (G") are impacted by gas injection as they are decreasing when the gas flow rate is increasing. At different solid concentrations, viscoelastic modulus [storage modulus (G′) & loss modulus (G″)] vs. time was plotted. One sample graph is presented in Figure 5.1 (Bobade and Eshtiaghi 2018 Figshare-a). This figure indicates the impact of different gas flow rates on the modulus of sludge with 3wt% total solids.

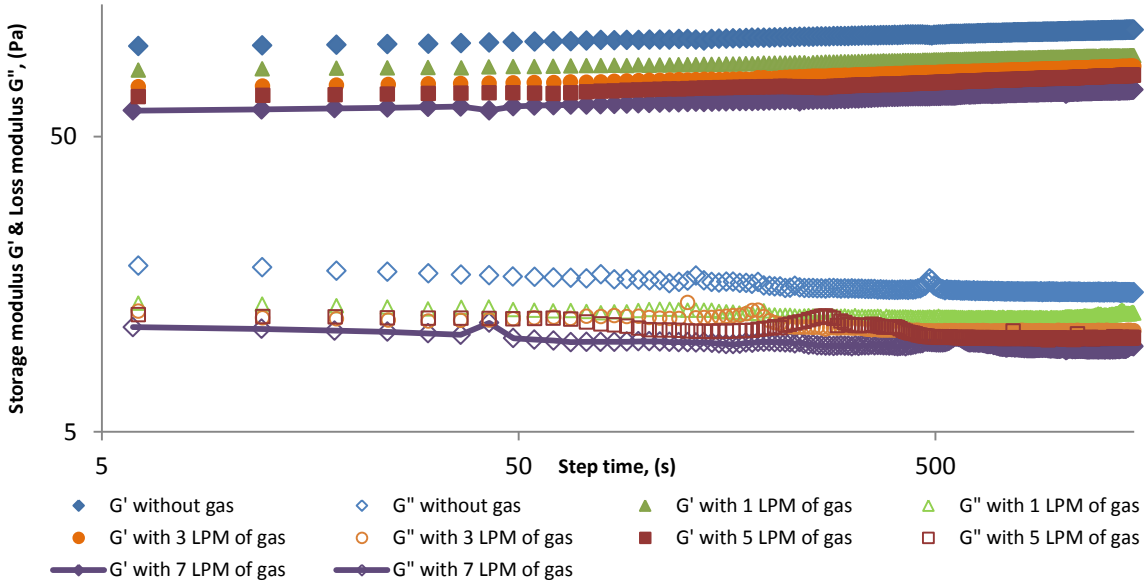

Figure 5.1: Impact of gas injection on 3% total solids concentration of WAS at four different gas flow rate (1–7 LPM) measured through time sweep test

A similar effect of gas intensity on sludge modulus was observed for all the four concentrations at four different gas flow rates during oscillatory time sweep (Bobade and Eshtiaghi 2018 Figshare-a) (see the supplementary material, Figures S1-S3). The percentage change of average sludge modulus due to aeration intensity $\left(\left(\frac{(Avg\ of\ G'\ at\ without\ \ gas\ -\ Avg\ of\ G'\ at\ given\ gas\ flowrate)}{(Avg\ of\ G'\ at\ without\ gas)}\right) * 100\right)$, obtained during the measurement for all the four concentrations by four different gas flow rates is shown in Table 5.1.

Table 5.1: Change of sludge elastic modulus (G') at four different (3%, 4%, 5%, and 5.5%) total solids concentration of waste activated sludge and at four different gas injection intensities (percentage of change in elastic modulus was calculated in comparison to non-aerated sludge at the similar solid concentrations)

Total solids concentration (%)	Percentage change in sludge elastic modulus (%)			
	1 LPM	3 LPM	5 LPM	7 LPM
3%	18%	25%	30%	37%
4%	13%	21%	27%	30%
5%	5%	11%	20%	26%
5.5%	2%	5%	7%	14%

This change in sludge modulus with gas intensity indicates that sludge structure is impacted by gas injection because the gas injection is applying additional shear (Bobade et al. 2017). Such modification of sludge structure may be attributed to the release of soluble components due to floc dissolution (Meng et al. 2008). Similarly, it was reported that the increase in aeration intensity enhances the release of soluble components, which further decreases the oxygen transfer efficiency (Meng et al. 2007, Menniti et al. 2010) by impacting on food to microorganism ratio. As, more soluble material means more food and less oxygen available for microorganism to consume.

5.4.2 Amount of Shear strain /stress imposed by gas injection

The extra strain imposed by gas injection showed that the imposed strain increases with increase in gas flow rate but decreases with increase in concentration as shown in Table 5.2. Furthermore, the equivalent shear stress imposed is calculated by using Equation 5.1 (Mezger 2011).

$$\tau = G' * \gamma \quad (5.1)$$

Where,

τ = shear stress (pa)

γ = strain (%)

G' = Average of the modulus of elasticity of unaerated sludge over 20min measurement time (Pa)

The amount of stress imposed by different gas velocities for different concentrations was plotted in Figure 5.2 (Bobade and Eshtiaghi 2018 Figshare-a). The linear increase of stress with gas velocity was observed for the entire concentration range. This result indicates that for a given concentration the stress imposed by gas injection increases linearly. In contrast for the same gas velocity, the amount of imposed stress decreases linearly with an increase in sludge concentration. Which means at high solid concentrations of sludge the shear caused by the gas injection decreases. The reduction in imposed stress by gas injection with an increase in solid concentration is because sludge becomes more viscous and possesses a strong force of attraction between particles as the concentration increases (Baroutian et al. 2013).

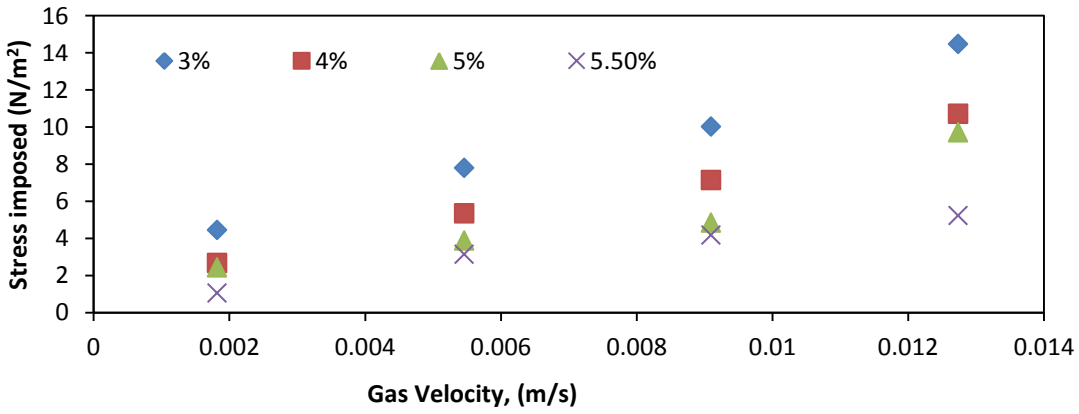

Figure 5.2: Stress imposed at different gas velocity for four different concentrations of waste activated sludge (3 %, 4%, 5% & 5.5% TS)

Table 5.2: Strain and stress imposed by four different gas velocities (1.82E-03 to 1.27E-02) at four different total solid concentrations of waste activated sludge (3%, 4%, 5% and 5.5%)

Total Concentration (TS) (g/g)	Gas flow rate (L/min)	Gas velocity (m/s)	Strain imposed (%)	Stress imposed calculated from Equation 5.1 (N/m^2)
0.03	1	1.82E-03	4.00E-02	4.4564
	3	5.46E-03	7.00E-02	7.7987
	5	9.10E-03	9.00E-02	10.0269
	7	1.27E-02	1.30E-01	14.4833
0.04	1	1.82E-03	1.50E-02	2.67855
	3	5.46E-03	3.00E-02	5.3571
	5	9.10E-03	4.00E-02	7.1428
	7	1.27E-02	6.00E-02	10.7142
0.05	1	1.82E-03	5.00E-03	2.42791
	3	5.46E-03	8.00E-03	3.884656
	5	9.10E-03	1.00E-02	4.85582
	7	1.27E-02	2.00E-02	9.71164
0.055	1	1.82E-03	2.00E-03	1.04614
	3	5.46E-03	6.00E-03	3.13842
	5	9.10E-03	8.00E-03	4.18456
	7	1.27E-02	0.01	5.2307

Also, to better understand the stress imposed by gas flow rate at the different concentration of sludge, the obtained data (refer Table 5.2) is analysed using linear multiple regression method and an equation is derived (Equation 5.2). In which its fitting parameters are linked to measurable parameters in the sludge to increase the applicability of this Equation 5.3 to other systems. The equation was also applicable with ±10% error to another waste activated sludge sample collected from Eastern Treatment plant in Eastern region of Victoria. Equation 5.3 is significant at 95% of confidence level with a P value much less than 0.05 and with an R^2 value of 0.88. The estimated error is ± 7 % within the range of concentration studied with 0.5% for lowest concentration and 7% for the highest concentration.

$$\sigma_{imposed} = 840.15 * U_g - 10.92 * TS \quad (5.2)$$

, where,

$\sigma_{imposed}$ = Stress (N/m^2)

Ug = Gas velocity (m/s)

TS = Concentration of total solids (g/g)

$$\sigma_{imposed} = \left(\frac{(0.0135 * TS^2)}{TSS^2 * D_p}\right) * \mu_{(water)} * U_g - \left(\frac{10 * TS^2}{TSS}\right) \quad (5.3)$$

Where,

TSS = Total suspended solids of unaerated sludge (g/g)

TS = Total solids concentration (g/g)

D_p = Diameter of the Pore of the membrane (in this study is 0.00002 m)

$\mu_{(Water\ @\ 20^oC)}$ = Viscosity of water = 1 Ns/m^2

5.4.3 Influence of Aeration Intensity on Total Suspended Solids (TSS)

Suspended solids mostly consist of colloidal and particulate particles (Meng et al. 2017, Trussell et al. 2007). Figure 5.3 illustrates the decreasing trend of suspended solids with increasing gas velocity. It means that as the gas velocity increases, the amount of solids that can pass through filter increases, i.e., gas intensity breaks the suspended particles into smaller fragments and a large number of smaller particles settle causing fouling issue.

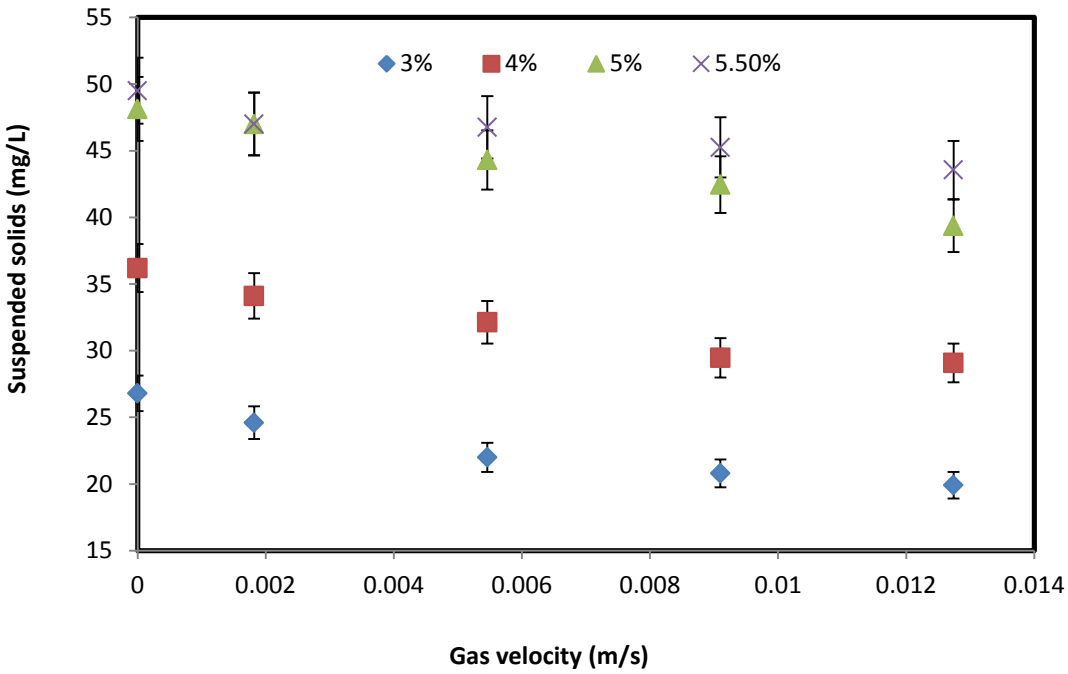

Figure 5.3: Impact of gas velocity on suspended solids of waste activated sludge at four different total solid concentrations (3%, 4%, 5% &5.5%)

However, it is also clear from Figure 5.3 that as the concentration increases, reduction in suspended solids decreases, i.e., at higher concentration and for the same gas velocity, the stress imposed by gas velocity is not sufficient to break down the suspended particles into submicron particles. Zhang et al. (2004) also found that suspended solids gradually decrease with increasing aeration intensity. This reduction in suspended solids due to aeration intensity is the consequence of the floc breakage and releasing EPS present inside the floc structure (Chang et al. 2002), which consequently decreases an oxygen transfer efficiency due to increase in food to microorganism ratio (Houghton and Quarmby 1999, Meng et al. 2006, Wilén et al. 2003).

Interestingly, there is a linear relationship between stress imposed by gas injection and the change in suspended solids at given condition and for given concentration (Equation 5.4). This linear relation has 95% of confidence level and p-value much less than 0.05 with ± 5% error which is the highest related to sludge with the highest concentration. Utilising an online rheometer and obtaining viscoelastic properties of sludge and the stress imposed by the gas injection can give us a better understanding of the influence of aeration intensity on suspended solids.

$$\%\Delta TSS = a * \sigma_{imposed} \quad (5.4)$$

Where,

$\sigma_{imposed}$ = Stress imposed by the gas velocity at any solids concentration studied (3-5.5%), (N/m^2)

% Δ TSS = Percentage change in suspended solids compared to non-aerated sludge (%)

a = Fitting parameter = 2.01 (m^2/N)

This decrease in suspended solids is due to change in floc structure caused by the aeration was also confirmed by measuring the viscoelastic properties of aerated sludge immediately after sparging and after resting the sludge for 40 mins as shown in Figure 5.4. It is obvious that after 20 mins of gas injection, G' reduced by (13%) also after stopping gas injection and giving 40 mins of rest time, the sludge structure was not returned to original structure as the G' is 8% less than the G' of the non-aerated system.

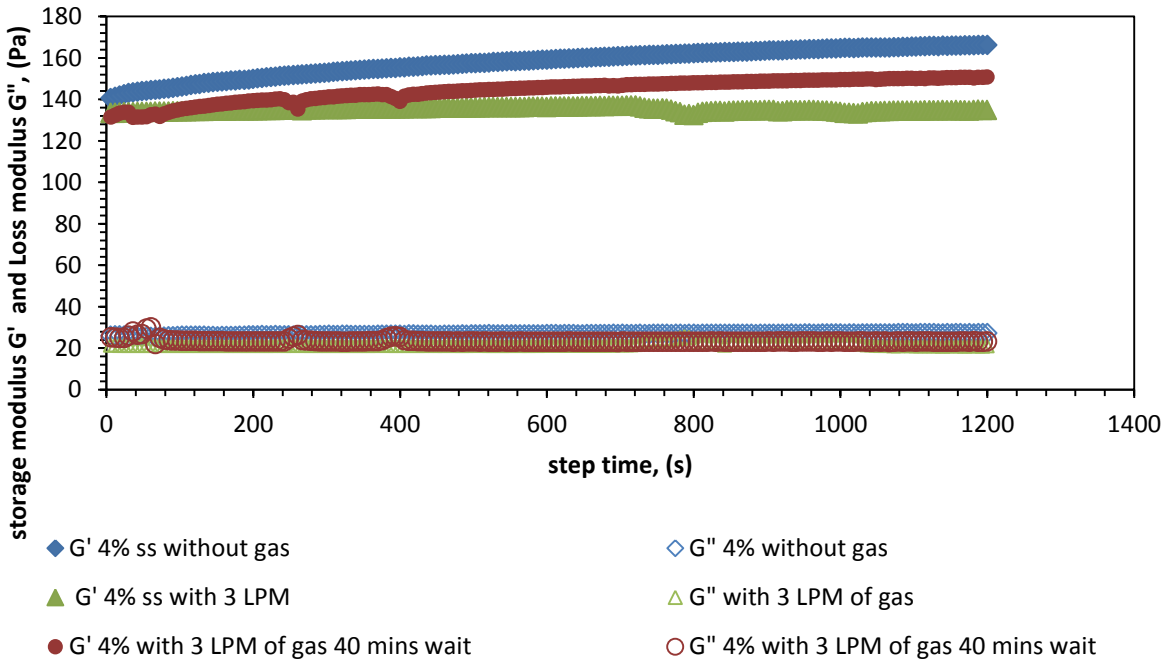

Figure 5.4: Comparison of storage and loss modulus of 4% waste activated sludge immediately after 20 mins of gas injection at 3 LPM and after the resting time for 40 mins

5.4.4 Influence of Aeration Intensity on Soluble COD (sCOD)

The soluble COD is one of the critical parameters for estimation and optimisation of the performance of the biological treatment process (Hayet et al. 2016). The sCOD content is

also used to determine the amount of oxygen required for the biodegradation in the aeration tank (Henze and Henze 1997). Thus the impact of aeration intensity on the soluble COD (sCOD) of the sludge sample was measured at different concentrations and at different gas injection rates as presented in Table 5.3.

A linear increase in sCOD was observed with an increase in gas velocity over the entire concentration range. Additionally, the results indicated that at 0.01274 m/s of gas velocity, more organic matter is released from solid phase to liquid phase. A similar increase in soluble COD with an increase in aeration intensity was also observed by Meng et al. (2008) and very well explained that the shear-induced by gas leads to floc breakage and increases the soluble contents in the sludge. Azami et al. (2012), Ladewig and Al-Shaeli (2016), Meng et al. (2006) have also highlighted that role of soluble microbial products (SMP), which is characterized as soluble chemical oxygen demand (sCOD) on the kinetic activity, flocculating and settling properties of sludge.

Table 5.3: Impact of gas velocity on soluble COD (sCOD) at four different total solid concentrations (3%, 4%, 5%, & 5.5%) of waste activated sludge

Gas velocity (m/s)	sCOD (mg/L)			
	3% TS	**4% TS**	**5% TS**	**5.5% TS**
0	3720	3960	4740	5090
0.00182	4060	4260	5390	5580
0.00546	4960	5050	6000	6260
0.0091	5340	5500	6520	6740
0.01274	6340	6680	7120	7290

The increase in sCOD, therefore confirms that the shear induced by gas injection impacts on floc structure releases EPS and increases the soluble contents causing a decrease in viscoelastic properties. Hence, it is necessary to consider the impact of shear force induced by the gas injection on the sludge and increase in sCOD together for efficient operation of the treatment plant. Additionally using multiple regression analysis, the

percentage change in sCOD has a linear relationship with stress imposed for all concentration studied (Equation 5.5). This equation has a confidence level of 95% with R square value of 0.96 and a P value much smaller than 0.05 with an error range of ± 15% for lower concentration and increases up to ±30% at higher concentrations.

$$\%\Delta sCOD = b * \sigma_{imposed} \quad (5.5)$$

, where,

σ = Stress imposed by the gas velocity at concentration range studied (3-5.5%) (N/m^2)

% Δ sCOD = Percentage change in soluble COD compared to non-aerated sludge (%)

b = Fitting parameter = 2.75 (m^2/N)

5.4.5 Influence of Aeration Intensity on Zeta potential

The zeta potential, which measures the surface charge / electrostatic interactions between the particles, represents the potential drop between the diffuse double layers of the surface. This analysis helps to get detailed insight into the cause of dispersion, aggregation, flocculation & sedimentation (Hunter 1981, Vold 1982, Yuan et al. 2011).

The zeta potential of waste activated sludge at given total solids concentration, linearly decreased (become more negative) with increasing gas velocity (Figure 5.5). The reduction in zeta potential i.e. the zeta potential value becoming more negative indicates that the sludge is becoming more stable because the repulsive force is more than the attractive force (Lu and Gao 2010). Thus the resistance to aggregation is increasing (Vold 1982). The zeta potential also increased with increasing total solid concentration and became less negative. The less negative zeta potential values confer that the attractive force is exceeding the repulsive force and decreasing the stability (resistance to aggregation/agglomeration) of the sample and increasing the coagulation & flocculation behaviour. Similarly, zeta potential value becomes less negative with an increase in solid concentration at a constant aeration rate of 0.2 m^3/h as reported by Meng et al. (2006). Interestingly, an increase in zeta potential with an increase in total suspended solids is also reported by (Su et al. 2014). Additionally, Sutherland (2001) also showed that EPS plays a crucial role in defining the stability of the system as each structural cell of polysaccharide forms intra-or inter-molecular associations that leads to gelation. However, this gelation varies greatly depending on the type of inter or intermolecular hydrogen bonding which contributes to floc formation, stability, etc.

Therefore, the more negative surface charge of sludge with an increase in gas velocity indicates that gas injection modifies the sludge characteristics because of increased solubilisation of loosely bound EPS (LB-EPS) (Zhang et al. 2013). A linear correlation between stress imposed by gas injection and the percentage change in zeta potential as presented in Equation 5.6 was found through multiple regression method with a P value less than 0.05 and R square value of 0.92. The percentage error is ± 5%. Zeta potential crucially reflects the stability of the system and affects the overall performance of the process. Moreover, the knowledge of zeta potential and hydrophobicity is important to understand the electrostatic interaction between SMPs with membrane surface and flocculation potential in activated sludge process (Azami et al. 2012, Chen et al. 2012). Thus the knowledge of a change in zeta potential with stress imposed by gas flow rate will help to optimise the operation of waste activated sludge process.

$$\% \, \Delta\zeta = c * \sigma_{imposed} \quad (5.6)$$

Where,

$\% \, \Delta\zeta$ = Percentage change in Zeta potential compared to the non-aerated system (%)

$\sigma_{imposed}$ = Stress imposed by gas injection at a given concentration (N/m^2)

c = Fitting parameter = 2.12 (m^2/N)

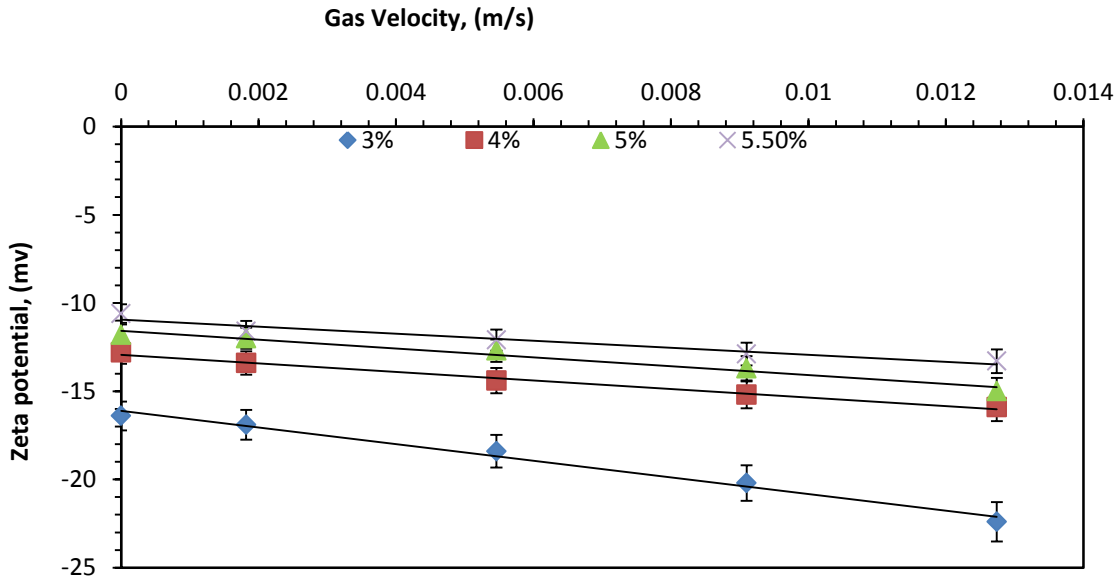

Figure 5.5: Impact of gas velocity on Zeta potential of waste activated sludge at four different total solid concentrations (3%, 4%, 5% & 5.5%)

5.4.6 INFLUENCE OF AERATION INTENSITY ON SURFACE TENSION

The change in interfacial surface tension of sludge with gas velocity is shown in Table 5.4. The interfacial surface tension is observed to increase linearly with increase in gas velocity for all the concentrations studied (R^2= 0.9). (Note: All the surface tension reported here are at the 1200 s of the time interval). As the concentration increases the time required by the surface tension curve to reach steady state increases, i.e., the surface tension curve has not reached the stable value at the 1200 s and hence shows a large difference in surface tension value even at no gas.) As the concentration increases, the intermolecular force in the sludge increases and results in bubble coalescence, thereby impacting more on surface tension. Hence the percentage change of surface tension is more at high concentration of sludge and low gas flow rate as shown in Figure 5.6. Interestingly it was also observed that gas velocity has a linear correlation with the percentage change in surface tension at a given concentration.

The surface tension is closely related to carbohydrates, and protein content of EPS as those are amphiphobic molecules and could change the surface tension of the fluid (Sheng et al. 2010). Moreover, a direct relationship was reported by Schonhorn (1965) between surface tension and cohesive energy of the molecule. And the cohesion of sludge increases with increasing the polysaccharide content of EPS (Ahimou et al. 2007). In addition, there is a direct relation between interfacial surface tension and bio flocculation i.e. when the fine dispersed particles are clumped together and a big agglomerated floc is formed, and settling of organic matter takes place more which then results in reducing the interfacial surface tension (Liss and Droppo 2005).

Table 5.4: Impact of gas velocity on surface tension at four different total solid concentrations (3%, 4%, 5%, & 5.5%) of waste activated sludge

Gas Velocity (m/s)	Surface Tension (mN/m)			
	3%	4%	5%	5.5%
0	46.04	46.4	59.45	60.04
0.00182	49.5	48.91	65.68	65.9
0.00546	52.68	54.43	67.72	67.9
0.0091	54.1	55.33	69.39	70.45
0.01274	56.62	56.32	72.68	73.9

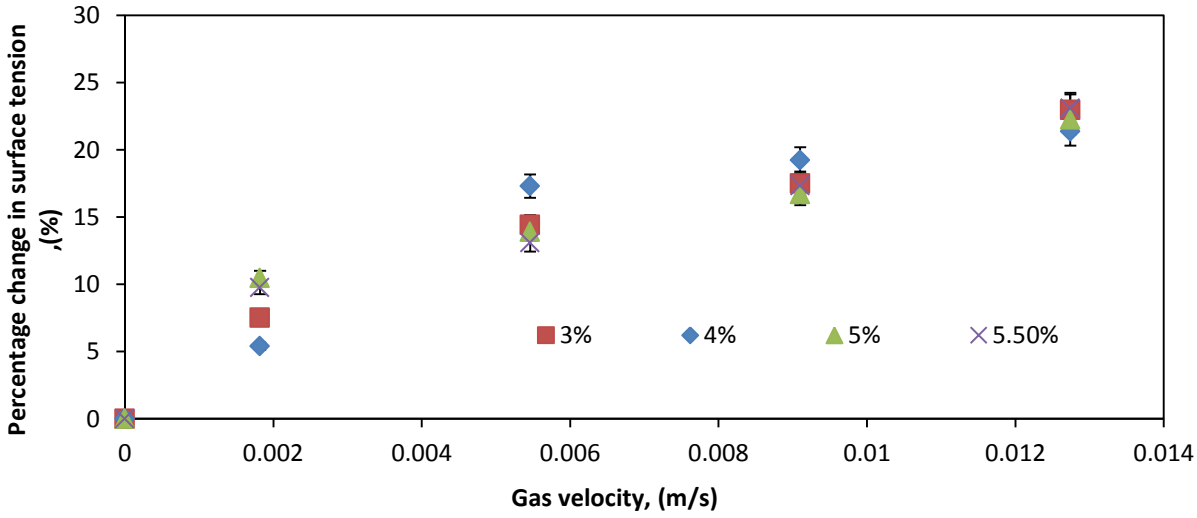

Figure 5.6: Impact of gas velocity on percentage change in surface tension of waste activated sludge at four different total solid concentrations (3%, 4%, 5% & 5.5%)

Thus, gas injection induces shear and increases the sludge stability which means resistance to aggregation increases (more negative Zeta potential) and results in measuring higher value for surface tension. This understanding of surface tension and gas flow rate at a given concentration will help to understand orientation time and growth time of bubble (Kulkarni and Joshi 2005). During the bubble formation and detachment process, two types of surface tension forces act on a bubble, dynamic and static. At the

initial growth phase, the surface tension is dynamic as its contact angle with the orifice changes continuously and in the later part, it reaches to a constant contact angle approaching to static. Thus although the surface tension forces are small, they vary significantly with gas flow rates and impacts on bubble formation. In addition, considering the surface tension change with the strain imposed by gas injection together is important to understand the bubble coalescence phenomena and gas distribution behaviour. This will further help to optimise the hydrodynamics of the system since bubble characteristics depend on the viscous property and the surface tension of the fluid (Sikorski et al. 2009).

5.5 CONCLUSION

The impact of gas injection on the physiochemical and rheological properties of sludge is elucidated. The viscoelastic modulus of sludge decreased with an increase in gas flow rate resulting in weakening of sludge structure. The gas flow rate induced shear, and the intensity of shear-induced linearly increased with increasing gas velocity. However, for the same gas flow rate, the shearing intensity decreased with increasing total solids concentration of sludge.

A linear relationship was observed between the change in suspended solids, soluble COD, and zeta potential with an increase in stress induced by gas injection. This change in physiochemical properties is because of breakdown of floc structure. The decrease in zeta potential values also proved that gas injection modifies the sludge surface by changing the stability of the system which in turn increases the surface tension linearly with increase in gas velocity. Thus observing the change in rheological properties due to gas injection intensity is also useful to understand the changes in physicochemical properties of sludge that are responsible for efficient and optimised operation of waste activated sludge treatment.

5.6 ACKNOWLEDGEMENTS

The authors acknowledge South East Water support for providing sludge to carry out the research, and RMIT University to provide Australian Government Research Training Program Scholarship for V. Bobade.

5.7 REFERENCES

Ahimou, F., Semmens, M.J., Haugstad, G. and Novak, P.J. (2007) Effect of protein, polysaccharide, and oxygen concentration profiles on biofilm cohesiveness. Applied and Environmental Microbiology 73(9), 2905-2910.

Azami, H., Sarrafzadeh, M.H. and Mehrnia, M.R. (2012) Soluble microbial products (SMPs) release in activated sludge systems: a review. Iranian Journal of Environmental Health Science & Engineering 9(1), 30-30.

Baroutian, S., Eshtiaghi, N. and Gapes, D.J. (2013) Rheology of a primary and secondary sewage sludge mixture: Dependency on temperature and solid concentration. Bioresource Technology 140, 227-233.

Baudez, J.C. (2008) Physical aging and thixotropy in sludge rheology. Applied Rheology 18(1), 13495-13491-13495-13498.

Bobade, V., Baudez, J.C., Evans, G. and Eshtiaghi, N. (2017) Impact of gas injection on the apparent viscosity and viscoelastic property of waste activated sewage sludge. Water Research 114, 296-307.

Bobade, V. and Eshtiaghi, N. (2018 Figshare) Dynamic time sweep measurement of sludge for four different concentrations (3%, 4%, 5% & 5.5%) at four different gas flow rates (1 Lpm to 7 LPM), https://figshare.com/s/87454a1b2f8b5ccaf03c.

Chang, I.-S., Le Clech, P., Jefferson, B. and Judd, S. (2002) Membrane fouling in membrane bioreactors for wastewater treatment.(Abstract). Journal of Environmental Engineering 128(11), 1018.

Chen, L., Tian, Y., Cao, C.-q., Zhang, J. and Li, Z.-n. (2012) Interaction energy evaluation of soluble microbial products (SMP) on different membrane surfaces: Role of the reconstructed membrane topology. Water Research 46(8), 2693-2704.

Davies, J.T. and Rideal, E.K. (1963) Interfacial phenomena, Academic Press, New York.

Eaton, A.D., American Public Health, A., American Water Works, A. and Water Environment, F. (2005) Standard methods for the examination of water and wastewater, APHA-AWWA-WEF, Washington, D.C.

Hayet, C., Saida, B.-A., Youssef, T. and Hédi, S. (2016) Study of biodegradability for municipal and industrial Tunisian wastewater by respirometric technique and batch reactor test. Sustainable Environment Research 26(2), 55-62.

Henze, M.A. and Henze, M. (1997) Wastewater treatment: biological and chemical processes, Springer, Berlin, Heidelberg, [Germany].

Houghton, J.I. and Quarmby, J. (1999) Biopolymers in wastewater treatment. Current Opinion in Biotechnology 10(3), 259-262.

Hunter, R.J. (1981) Zeta Potential in Colloid Science, pp. 1-10, Academic Press.

Kulkarni, A.A. and Joshi, J.B. (2005) Bubble Formation and Bubble Rise Velocity in Gas-Liquid systems -A Review. Industrial & Engineering Chemistry Research 44, 5873 - 5931.

Ladewig, B. and Al-Shaeli, M.N.Z. (2016) Fundamentals of Membrane Bioreactors: Materials, Systems and Membrane Fouling, Springer.

Liss, S.N. and Droppo, I.G. (2005) Flocculation in natural and engineered environmental systems, CRC Press, Boca Raton.

Liu, C., Tanaka, H., Ma, J., Zhang, L., Zhang, J., Huang, X. and Matsuzawa, Y. (2012) Effect of microbubble and its generation process on mixed liquor properties of activated sludge using Shirasu porous glass (SPG) membrane system. Water Research 46(18), 6051-6058.

Lu, G.W. and Gao, P. (2010) Handbook of Non-Invasive Drug Delivery Systems, pp. 59-94, William Andrew Publishing, Boston.

Markis, F., Baudez, J.-C., Parthasarathy, R., Slatter, P. and Eshtiaghi, N. (2014) Rheological characterisation of primary and secondary sludge: Impact of solids concentration. Chemical Engineering Journal 253, 526-537.

Meng, F., Shi, B., Yang, F. and Zhang, H. (2007) New insights into membrane fouling in submerged membrane bioreactor based on rheology and hydrodynamics concepts. Journal of Membrane Science 302(1–2), 87-94.

Meng, F., Yang, F., Shi, B. and Zhang, H. (2008) A comprehensive study on membrane fouling in submerged membrane bioreactors operated under different aeration intensities. Separation and Purification Technology 59(1), 91-100.

Meng, F., Zhang, H., Yang, F., Zhang, S., Li, Y. and Zhang, X. (2006) Identification of activated sludge properties affecting membrane fouling in submerged membrane bioreactors. Separation and Purification Technology 51(1), 95-103.

Meng, F., Zhang, S., Oh, Y., Zhou, Z., Shin, H.-S. and Chae, S.-R. (2017) Fouling in membrane bioreactors: An updated review. Water Research 114(Supplement C), 151-180.

Menniti, A., and Morgenroth, E. (2010) The influence of aeration intensity on predation and EPS production in membrane bioreactors. Water Research 44(8), 2541-2553.

Menniti, A., Kang, S., Elimelech, M. and Morgenroth, E. (2009) Influence of shear on the production of extracellular polymeric substances in membrane bioreactors. Water Research 43(17), 4305-4315.

Mezger, T.G. (2011) The rheology handbook: for users of rotational and oscillatory rheometers, Vincentz Network, Hanover, Germany.

Pollice, A., Giordano, C., Laera, G., Saturno, D. and Mininni, G. (2007) Physical characteristics of the sludge in a complete retention membrane bioreactor. Water Research 41(8), 1832-1840.

Schonhorn, H. (1965) Theoretical relationship between surface tension and cohesive energy density. The Journal of Chemical Physics 43(6), 2041-2043.

Sheng, G.-P., Yu, H.-Q. and Li, X.-Y. (2010) Extracellular polymeric substances (EPS) of microbial aggregates in biological wastewater treatment systems: A review. Biotechnology Advances 28(6), 882-894.

Sikorski, D., Tabuteau, H. and de Bruyn, J.R. (2009) Motion and shape of bubbles rising through a yield-stress fluid. Journal of Non-Newtonian Fluid Mechanics 159(1-3), 10-16.

Su, B., Qu, Z., Song, Y., Jia, L. and Zhu, J. (2014) Investigation of measurement methods and characterization of zeta potential for aerobic granular sludge. Journal of Environmental Chemical Engineering 2(2), 1142-1147.

Sutherland, I.W. (2001) Exopolysaccharides in biofilms, flocs and related structures. Water Science and Technology 43(6), 77.

Trussell, R.S., Merlo, R.P., Hermanowicz, S.W. and Jenkins, D. (2007) Influence of mixed liquor properties and aeration intensity on membrane fouling in a submerged membrane bioreactor at high mixed liquor suspended solids concentrations. Water Research 41(5), 947-958.

Vold, M.J. (1982) Zeta potential in colloid science. Principles and applications. Journal of Colloid and Interface Science 88(2), 608.

Wilén, B.-M., Jin, B. and Lant, P. (2003) The influence of key chemical constituents in activated sludge on surface and flocculating properties. Water Research 37(9), 2127-2139.

Yuan, H., Zhu, N. and Song, F. (2011) Dewaterability characteristics of sludge conditioned with surfactants pretreatment by electrolysis. Bioresource Technology 102(3), 2308-2315.

Zhang, Y., Zhang, P., Guo, J., Ma, W., Fang, W., Ma, B. and Xu, X. (2013) Sewage sludge solubilization by high-pressure homogenization. Water Science and Technology 67(11), 2399.

Zhang, Z., Zhu, J. and Park, K.J. (2004) Effects of Duration and Intensity of Aeration on Solids Decomposition in Pig Slurry for Odour Control. Biosystems Engineering 89(4), 445-456.

5.8 SUPPLEMENTARY FIGURES

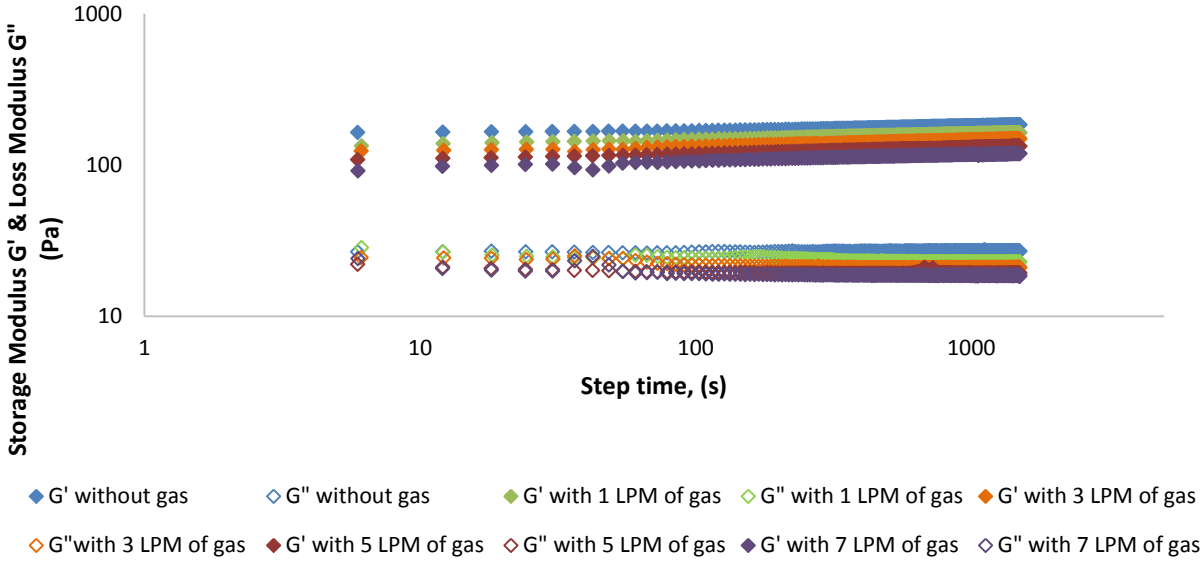

Figure S 5.1: Impact of gas injection on 4% total solids concentration at four different gas flow rates measured through Time sweep test

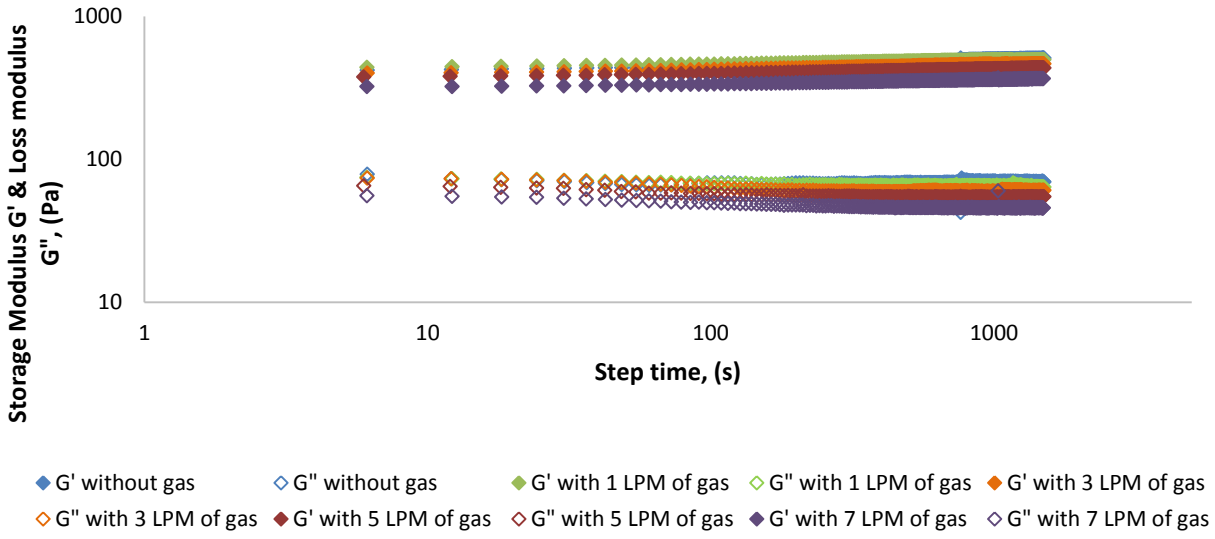

Figure S 5.2: Impact of gas injection on 5 % total solids concentration at four different gas flow rates measured through Time sweep test

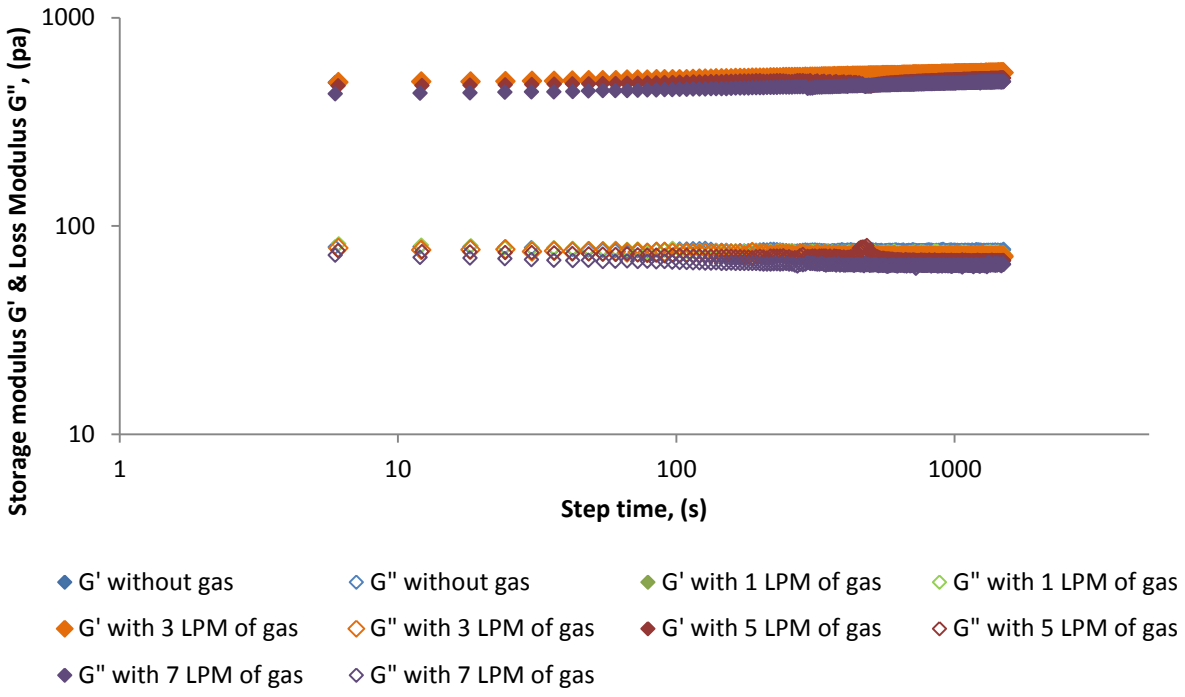

Figure S 5.3: Impact of gas injection on 5.5 % total solids concentration at four different gas flow rates measured through Time sweep test

CHAPTER 6: INFLUENCE OF GAS INJECTION ON VISCOUS AND VISCOELASTIC PROPERTIES OF XANTHAN GUM

This chapter was published in Water Research

(Vol: 134, P: 86-91, 2018)

Keywords: Gas injection; Xanthan gum; Viscoelastic Properties; Flow behaviour; Herschel-Bulkley Model

Bobade, V., Cheetham, M., Hashim, J. and Eshtiaghi, N. "Influence of gas injection on viscous and viscoelastic properties of Xanthan gum". Water Research 134 (2018) 86-91.

Graphical Abstract

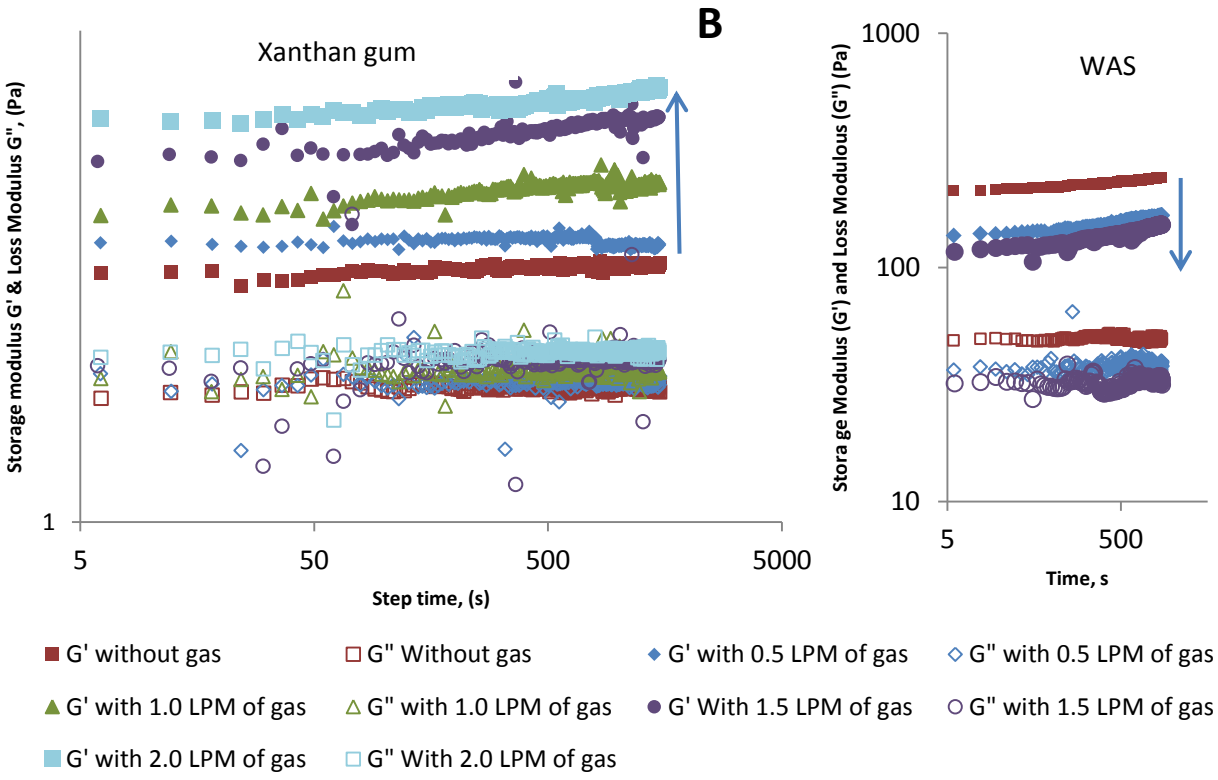

6.1 ABSTRACT

Xanthan gum is widely used as a model fluid for sludge to mimic the rheological behaviour under various conditions including impact of gas injection in sludge. However, there is no study to show the influence of gas injection on rheological properties of xanthan gum specifically at the concentrations at which it is used as a model fluid for sludge with solids concentration above 2%.

In this paper, the rheological properties of aqueous xanthan gum solutions at different concentrations were measured over a range of gas injection flow rates. The effect of gas injection on both the flow and viscoelastic behaviour of Xanthan gum (using two different methods - a creep test and a time sweep test) was evaluated. The viscosity curve of different solid concentrations of digested sludge and waste activated sludge were compared with different solid concentrations of Xanthan gum and the results showed that Xanthan gum can mimic the flow behaviour of sludge in flow regime.

The results in linear viscoelastic regime showed that increasing gas flow rate increases storage modulus (G'), indicating an increase in the intermolecular associations within the material structure leading to an increase in material strength and solid behavior. Similarly, in creep test an increase in the gas flow rate decreased strain%, signifying that the material has become more resistant to flow. Both observed behaviour is opposite to what occurs in sludge under similar conditions.

The results of both the creep test and the time sweep test indicated that choosing Xanthan gum aqueous solution as a transparent model fluid for sludge in viscoelastic regime under similar conditions involving gas injection in a concentration range studied is not feasible. However Xanthan gum can be used as a model material for sludge in flow regime; because it shows a similar behaviour to sludge.

6.2 INTRODUCTION

Xanthan gum is a naturally occurring polysaccharide, produced by fermenting glucose with the bacteria Xanthomonas campestris, with a backbone of β-(1,4)τ-D-glucose (Kennedy et al. 2015). The primary structure of the material is shown in Figure 6.1.

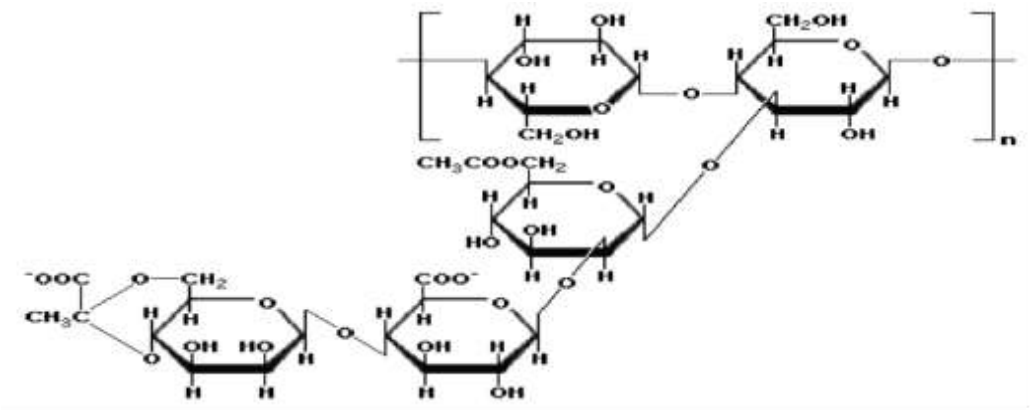

Figure 6.1: Molecular structure of Xanthan gum (García-Ochoa et al. 2000)

The structure consists of repetitive pentasaccharide units formed with two glucose units, two mannose units, and one glucuronic acid unit, with the molar ratio being 2.8:2.0:2.0 (García-Ochoa et al. 2000).

When mixed in aqueous solution, xanthan gum exists in an ordered helical conformation, either single or double stranded. The molecular structure of the material actively contributes to its rheological properties, with the structuration pattern of the solutions being related to hydrogen-bridging between lateral chains and binding networks formed by molecular entanglement (Laneuville et al. 2013). Additionally, Figure 6.2 shows that dehydration can affect the conformation of molecules, in which the intra and intermolecular ester bonds cause crosslinking with an extended polymer structure (Bueno et al. 2013). Xanthan solutions are known to have a non-Newtonian rheology, with a shear-thinning behaviour under increasing shear rate. It has been widely reported that an initial yield stress is exhibited by xanthan solutions must be overcome for the solution to start flowing (García-Ochoa et al. 2000, Marcotte et al. 2001, Song et al. 2006). Only when the magnitude of stress reaches above the yield stress, the structure is broken down, orienting the polymer chains to align with flow stream. The yield stress is attributed to the molecular structure of the material and a large number of hydrogen bonds which exist in the solution (Bradshaw et al. 1983).

Xanthan gum is widely used as a model fluid for sludge to mimic sludge shear thinning behaviour (García-Ochoa et al. 2000, Kennedy et al. 2015, Saha and Bhattacharya 2010). Sludge is the residual, semi-solid slurry produced from waste water treatment process. It is also well known that sludge is a mixture of complex biological material and difficult to characterize (Eshtiaghi et al. 2013, Ratkovich et al. 2013, Seyssiecq. et al. 2003).

Moreover, the opaque nature of sludge makes it difficult to estimate the accurate bubble behaviour and impacts on hydrodynamics of the process. As well as the complex rheological behaviour of sludge changes over time because of aging and microbial activity exhibit variations in sludge viscosity making it difficult to optimize the process performance (Bajón Fernández et al. 2015, Baudez and Coussot 2001).

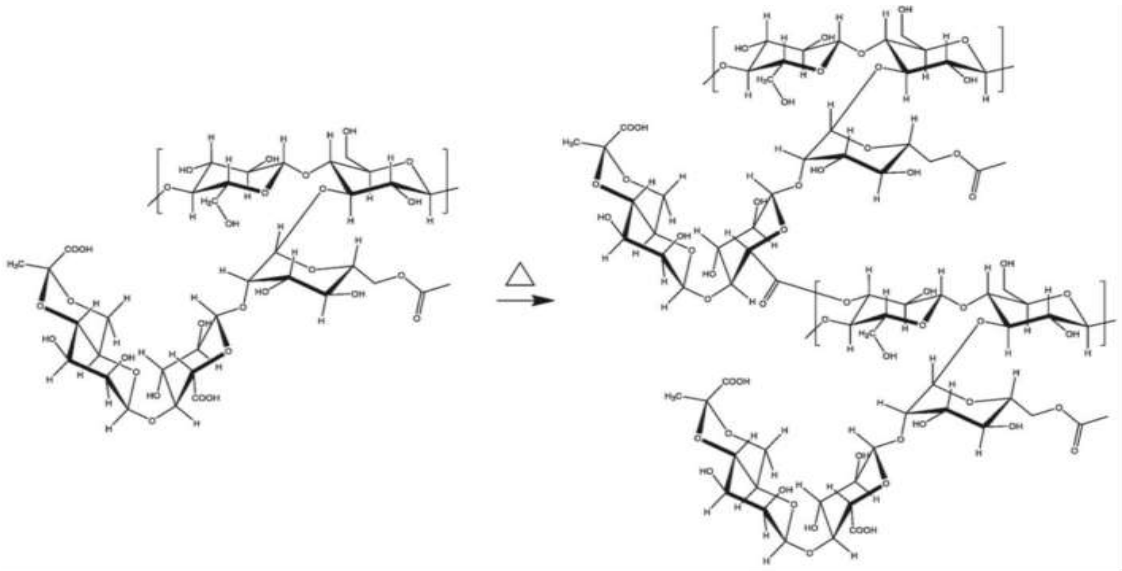

Figure 6.2: Intra- & Inter-molecule ester bonds crosslinking causing extended Xanthan gum structure (Bueno et al. 2013)

The variations in sludge rheological properties can have a significant impact on the design parameters of the equipment used in the process, that potentially affects energy consumption, and the cost of operation (Yang et al. 2009). Hence, Xanthan gum is used as a model fluid for sludge under gas injection for optimising and modelling of process equipment in sludge treatment plant (Bhattacharjee et al. 2015, Cao et al. 2016). Gas injection in sludge is recognized to play a significant role in oxygen transfer, mixing efficiency and energy consumption in membrane bioreactor and waste activated sludge process (Åmand and Carlsson 2012, Bobade et al. 2017, Ratkovich et al. 2013, Seyssiecq et al. 2008). The gas injection also has a major impact on sludge physical properties like extra cellular polymeric substances (EPS), soluble COD, particle size, etc., and changes its rheological properties influencing the efficiency of the process (Drews 2010, Meng et al. 2006).

Although the rheological properties of xanthan gum have been extensively studied under varying conditions of pressure (Laneuville et al. 2013), temperature (Marcotte et al. 2001), gum concentration and ionic strength (Vega et al. 2015); there is no study reporting the impact of gas injection on rheological properties of xanthan gum.The objective of this work is to investigate the effect of gas injection on the rheological properties (apparent viscosity and viscoelastic modulus) of xanthan gum at different solids concentrations and gas flow rates by using dynamic time sweep test and creep test.

6.3 MATERIALS AND METHODS

6.3.1 SAMPLE PREPARATION

Xanthan gum solutions of 0.3wt%, 0.4wt%, 0.5% and 0.6wt% were prepared by mixing xanthan gum powder (supplied by Sigma Aldrich) in deionized water to form a homogenous solution. Solutions were mixed using a stirrer at approximately 700 rpm until the solution became homogenous. The solution was allowed to rest for one day, to remove air bubbles from the solution.

6.3.2 APPARATUS

Rheological measurements were performed using a commercially available hybrid stress controlled (HR3) rheometer from TA Instruments equipped with Grooved bob geometry with an outer diameter of 0.0149 m and 0.042 m length. A custom designed plexi glass cup (inner diameter: 0.1 m, length: 0.1 m) was used. A stainless steel porous disk (outer diameter: 0.1 m, thickness: 0.0016 m, porosity: 40%, from SINTEC Australia) was used at the bottom for the gas sparging. The gas flow rate was varied from 0.5 litres per minute (LPM) to 2 LPM, i.e., 0.00091 m/s to 0.00364274 m/s gas superficial velocity, using a gas mass flow meter from AALBORG at a pressure of 10 psi. All measurements were carried out at room temperature.

6.3.3 RHEOLOGICAL MEASUREMENTS

To understand the impact of gas injection on apparent viscosity of Xanthan gum, a flow curve measurement was carried out using following procedure. The sample was pre sheared at high shear rate "310 s^{-1}" [the maximum shear rate without turbulence in this cup with grooved bob geometry] for 300 s and then allowed to rest for 120 s, to obtain an identical sample before each flow curve measurement. The viscosity of the sample was then measured at the shear rate from 0.001 s^{-1} to 100 s^{-1}. Further, the preshearing stage

was repeated and the gas was injected with 0.5 LPM for 1200 s, and then the flow curve was measure. The above procedure is repeated for all the gas flow rates and all concentrations.

Since grooved bob geometry with a wide gap (0.042 m) was used, the flow curves were recalculated using Equations (6.1) and (6.2) (Estellé et al. 2008)

$$\tau_{Ri} = \frac{M}{(2\pi H R_i^2)} \quad (6.1)$$

$$\dot{\gamma} = 2M \frac{d\Omega}{dM}, \tau_c \leq \tau_y \leq \tau_b \quad (6.2)$$

Where,

M = Torque (N.m),

H = Height of the bob (m),

R_i = Radius of the bob,

$d\Omega/dM = (\Omega_j - \Omega_{j-1}) / (M_j - M_{j-1})$,

τ_y; τ_c ; τ_b = yield stress, stress at the cup and stress at the bob, respectively (Pa).

To understand the macro or micro structural changes occurring in Xanthan gum due to gas dispersion, a time sweep measurement was performed using following pattern: preshear the Xanthan gum at a high shear rate of 310 s^{-1} and allow the short rest period of 120 s to remove the history of the sample and obtain the identical sample for each test. Afterward, oscillation time sweep test at 0.15% strain and 1 Hz frequency for 1500 seconds is carried out and preshearing step is repeated. After repeating the preshearing step, the gas is injected for 20 mins and time sweep test is carried out again. This procedure is repeated for all the four concentrations and 4 gas flow rates. Similarly, to understand the impact of gas injection on elastic deformation of xanthan gum, a creep test at very low stress of 3 Pa was carried out using the same procedure. This procedure is similar to gas injection procedure into sludge which was done by Bobade et al. (2017).

6.4 RESULT AND DISCUSSION

6.4.1 IMPACT OF GAS INJECTION ON FLOW BEHAVIOUR (APPARENT VISCOSITY) OF XANTHAN GUM

The stress response over a range of shear rates was measured to understand the flow behaviour of Xanthan gum. For different solids concentration viscosity curves were

plotted at different gas flow rates. One sample graph is presented in Fig 6.3. The figure shows that at 0.3wt% xanthan gum for different gas flow rates there is negligible change in viscosity at given shear rate. Similar trend in viscosity curve was observed for all the 4 concentrations at 4 different gas flow rates (See supplementary Figure S.6.1).

It is interesting to note that similar negligible change in viscosity of sludge with gas injection was also observed by Bobade et al. (2017). The reason for negligible change in viscosity can be bubble coalescence occurring in Xanthan gum because of its high viscosity (Bobade et al. 2017, Fransolet et al. 2005). Thus the results clearly indicated that gas injection has no impact on viscosity of xanthan gum.

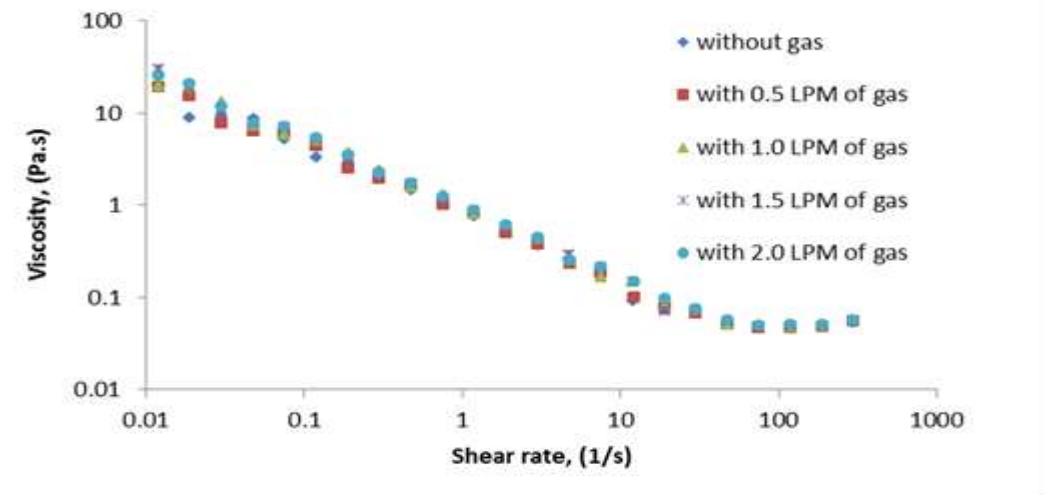

Figure 6.3: Viscosity curve of 0.3% Xanthan gum at 4 different gas flow rates

In addition, to find the xanthan gum simulant for the sludge the flow behaviour of xanthan gum was also compared with the waste activate sludge (WAS) and digested sludge flow behaviour as shown in Figure 6.4.

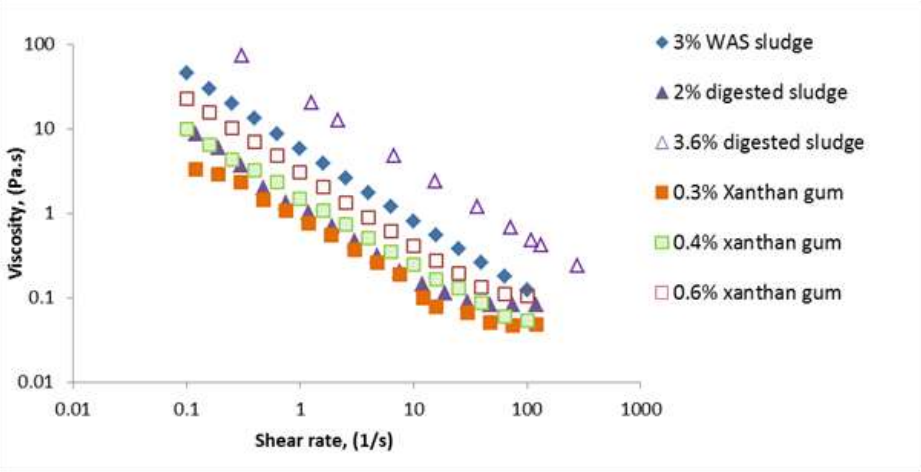

Figure 6.4: Comparison of 3% WAS viscosity curve & 2% and 3.6% digested sludge viscosity curve with 0.3% & 0.6% xanthan gum viscosity curve

The digested sludge data in Figure 6.4 was extracted from Eshtiaghi et al. (2016). The figure clearly shows that 2wt % digested sludge is close to 0.3 wt% and 0.4wt% Xanthan gum. However, there was a significant difference between the viscosity curves for both 3wt% WAS and 3.6wt% Digested sludge with 0.6wt% xanthan gum. The Herschel Bulkley parameters for 3wt% WAS and 3.5wt% digested sludge were much greater than xanthan gum for all the concentrations as shown in Figure 6.5.

The value of Herschel–Bulkley parameters for each concentration of Xanthan gum; WAS and digested sludge is presented in Table 6.1. It is clear from the table that much higher concentration of xanthan gum is needed to use Xanthan gum as a simulant for digested sludge at 3.6wt% and 3wt% WAS in liquid regime.

Table 6.1: Herschel–Bulkley parameters for Xanthan gum, waste activated sludge & digested sludge

Fluid Name	Concentrations (%)	Yield stress, τ_o (Pa)	Consistency index, K ($Pa.s^n$)	Flow index, n (-)
Xanthan gum	0.3	0.199	0.6017	0.3712
Xanthan gum	0.4	0.529	0.956	0.31415
Xanthan gum	0.5	1.097	1.052	0.3000
Xanthan gum	0.6	1.719	1.275	0.283
WAS	3	3.29	2.5	0.278
Digested Sludge	2	0.53	0.65	0.35
Digested Sludge	3.6	18.57	6.788	0.35

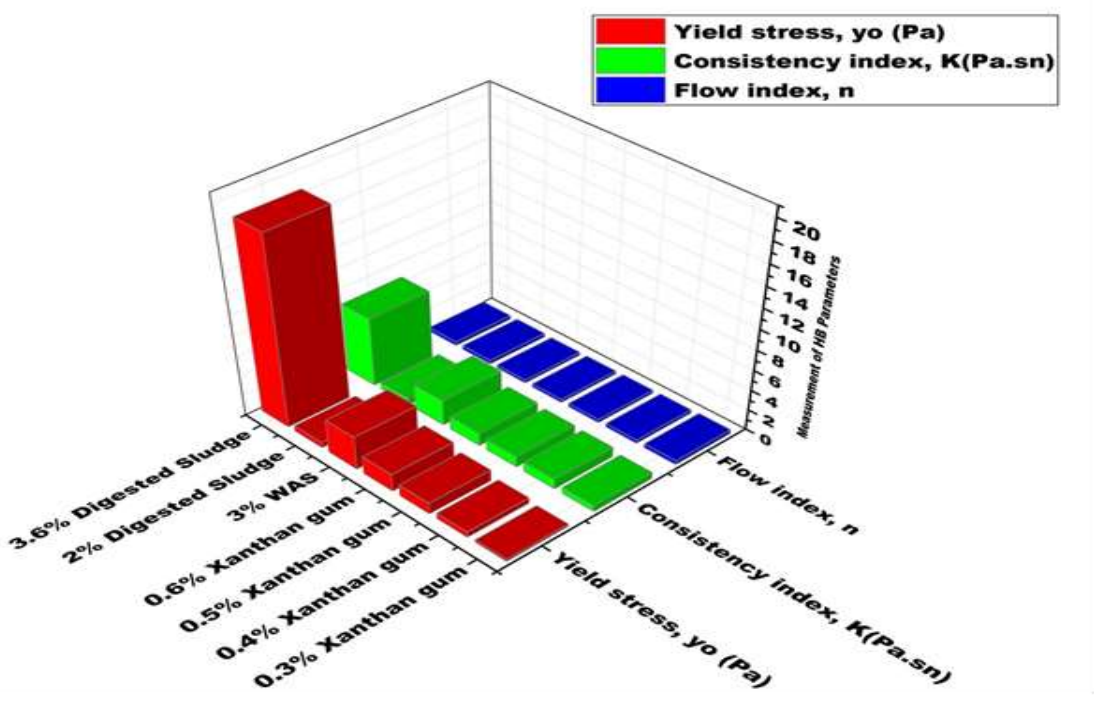

Figure 6.5: Comparison of Herschel–Bulkley parameters of Xanthan gum (0.3%, 0.4%, 0.5% & 0.6%) with3% WAS & digested sludge (1.8% & 3.6%)

6.4.2 *Influence of gas injection on viscoelastic property of Xanthan gum in linear viscoelastic region (Solid regime)*

To investigate the impact of gas injection on the viscoelastic property of xanthan gum in the linear region, the influence of gas was studied by both (1) creep test, and (2) time sweep test as shown in Figure 6.6. Figure 6.6A demonstrates that, during creep test, the strain % for 0.3wt% xanthan gum decreased by increasing the gas flow rate. The decreasing values for strain % indicate more resistance to the constant load and a lower degree of deformation of material. The less strain % values means more solid behaviour and difficult to deform as a result of being stronger material (Saha and Bhattacharya 2010). Thus, xanthan gum solidifies and becomes harder to deform as the gas injection rate is increases.

Similarly, Figure 6.6B reveals that, as the gas flow rate increased both the viscous (loss) modulus (G") and elastic (storage) modulus (G') are increased. However, an increase in G" at different gas flow rates is negligible as compared to G'. But on comparing G' with G" for all gas flow rate showed G' is higher than G" which means that, the solid behaviour of xanthan gum has dominant impact compared to the liquid behaviour of xanthan gum, indicating that material is still in solid regime. A similar observation was observed for all the four solid concentrations at four different gas flow rates in both creep test and time sweep test (see supplementary Figure S.6.2 and Figure S.6.3). Thus, together these results suggest that Xanthan gum solidified in the linear viscoelastic regime as the gas injection rate increased.

The main possible reason behind xanthan gum solidifying behaviour can be, change in molecular structure at a micro or macro level due to the injection of nitrogen gas, which results in a more entangled structure by altering crosslinking. In the same way, the thickening behaviour has been observed in similar polysaccharide materials such as mamaku gum (Jaishankar et al. 2015), whereby the material exhibits thickening behaviour when sheared below yield stress. Jaishankar et al. 2015 explained that thickening behaviour of polysaccharide at low shear rate occurs because of an interaction between intra and intermolecular associations. It means at low shear rates the molecule remains in equilibrium due to the disentanglement time being longer, because of which molecule gets elongated and results into thickening behaviour.

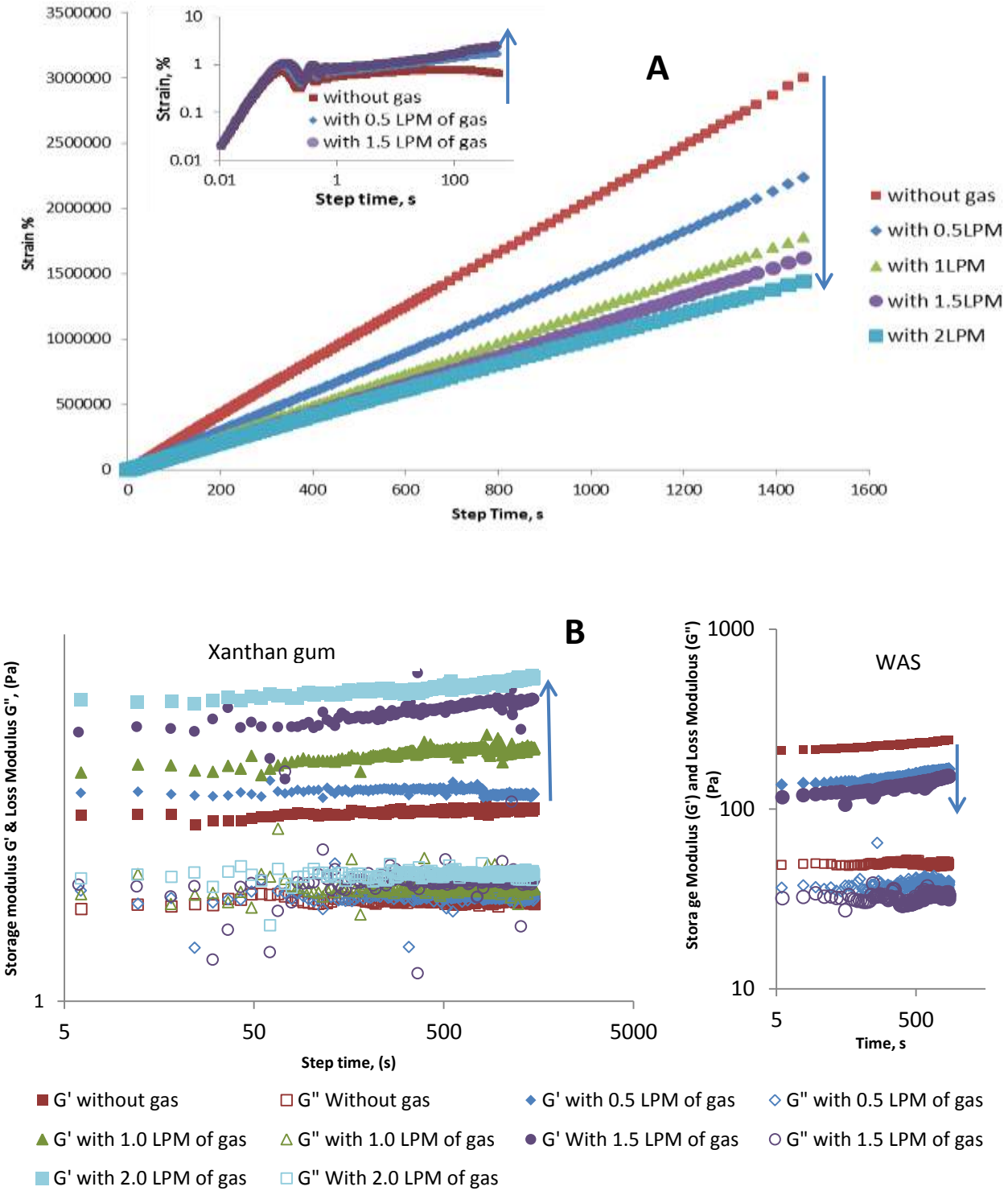

Figure 6.6: Impact of gas injection on the viscoelastic modulus of 0.3 % xanthan gum at four different gas flow rates 0.5 LPM, 1.0 LPM, 1.5 LPM & 2.0 LPM and for 4.2% WAS at 0.5 LPM & 1.5 LPM (inset) through (A) creep test (3Pa) and (B) time sweep test (0.15% strain & 1 Hz)

Thus in the same way, when the gas is injected in the xanthan gum solution, the stress developed by gas injection is minimal and not sufficient to disentangle the molecular

structure. Hence, the polymer chains became extensionally deformed and partially elongated, increasing exposure for local molecular interactions and physical crosslinking to form helices. The presence of helix structure and hydrogen bonds in xanthan gum show resistance to stress and flow is suggested by Bradshaw et al. (1983).

Furthermore, as the gas velocity increases with increased flow rate, there is an increase in the shear stress between the bubble-liquid interface (Majumder et al. 2007). The increase in shear stress increases molecular elongation and thus the exposure for further molecular interactions, therefore contributing to an increased material strength, solution viscosity, and solid behaviour. Surprisingly, this behaviour of xanthan gum was not consistent with the sludge behaviour under similar conditions i.e., at low strain and stress corresponding to linear region. Bobade et al. (2017) have shown that increase in gas injection rate reduces the viscoelastic properties of sludge due to breakdown of structure as a result of imposed shear by gas injection using same experimental setup and with the same gas velocity at strain and stress corresponding to linear region. Moreover, the creep tests done under similar condition showed that sludge deforms more by increasing gas injection flow rate. This means weaker structure (see insets in Fig 6.6). Bobade et al. (2017) proved weakening of sludge structure through environmental scanning electron microscopic analysis by observing more porous structure.

6.5 CONCLUSION

In this present study, we investigated how the rheological properties of xanthan gum at different solids concentration changes due to gas injection.

In flow region, the flow curve of xanthan gum showed negligible change in the apparent viscosity of in xanthan gum solution as gas injection flow rate increased. However, in linear viscoelastic region, the creep test and time sweep test proved that gas injection increased the storage and loss modulus which is an indication of strengthening of molecular structure. This could be due to deformation of the molecular structure of xanthan gum and increasing the crosslinking within an extended structure which will result in higher resistance to stress and showing more solid like behaviour in the linear viscoelastic region. Thus although xanthan gum behaves similar to the sludge in the liquid regime, the behaviour of xanthan gum contradicts with the sludge behaviour in the solid

regime which means Xanthan gum is not suitable as a model fluid for sludge under gas injection below yield stress point.

6.6 ACKNOWLEDGEMENTS

The authors acknowledge RMIT University for providing the Australian postgraduate scholarship to V. Bobade to carry out the research.

6.7 REFERENCES

Åmand, L. and Carlsson, B. (2012) Optimal aeration control in a nitrifying activated sludge process. Water Research 46(7), 2101-2110.

Bajón Fernández, Y., Cartmell, E., Soares, A., McAdam, E., Vale, P., Darche-Dugaret, C. and Jefferson, B. (2015) Gas to liquid mass transfer in rheologically complex fluids. Chemical Engineering Journal 273, 656-667.

Baudez, J.C. and Coussot, P. (2001) Rheology of aging, concentrated, polymeric suspensions: Application to pasty sewage sludges. Journal of Rheology 45(5), 1123-1140.

Bhattacharjee, P.K., Kennedy, S., Eshtiaghi, N. and Parthasarathy, R. (2015) Flow regimes in the mixing of municipal sludge simulant using submerged, recirculating jets. Chemical Engineering Journal 276(Supplement C), 137-144.

Bobade, V., Baudez, J.C., Evans, G. and Eshtiaghi, N. (2017) Impact of gas injection on the apparent viscosity and viscoelastic property of waste activated sewage sludge. Water Research 114, 296-307.

Bradshaw, I.J., Nisbet, B.A., Kerr, M.H. and Sutherland, I.W. (1983) Modified xanthan—its preparation and viscosity. Carbohydrate Polymers 3(1), 23-38.

Bueno, V.B., Bentini, R., Catalani, L.H. and Petri, D.F.S. (2013) Synthesis and swelling behavior of xanthan-based hydrogels. Carbohydrate Polymers 92(2), 1091-1099.

Cao, X., Zhao, Z., Cheng, L. and Yin, W. (2016) Evaluation of a Transparent Analog Fluid of Digested Sludge: Xanthan Gum Aqueous Solution. Procedia Environmental Sciences 31(Supplement C), 735-742.

Cui, S.W. and Wang, Q. (2005) 4 Functional Properties of Carbohydrates: Polysaccharide Gums.

Drews, A. (2010) Membrane fouling in membrane bioreactors—Characterisation, contradictions, cause and cures. Journal of Membrane Science 363(1), 1-28.

Eshtiaghi, N., Markis, F., Yap, S.D., Baudez, J.C. and Slatter, P. (2013) Rheological characterisation of municipal sludge: A review. Water Research 47(15), 5493-5510.

Eshtiaghi, N., Markis, F., Zain, D. and Mai, K.H. (2016) Predicting the apparent viscosity and yield stress of digested and secondary sludge mixtures. Water Research 95, 159-164.

Estellé, P., Lanos, C. and Perrot, A. (2008) Processing the Couette viscometry data using a Bingham approximation in shear rate calculation. Journal of Non-Newtonian Fluid Mechanics 154(1), 31-38.

Fransolet, E., Crine, M., Marchot, P. and Toye, D. (2005) Analysis of gas holdup in bubble columns with non-Newtonian fluid using electrical resistance tomography and dynamic gas disengagement technique. Chemical Engineering Science 60(22), 6118-6123.

García-Ochoa, F., Santos, V.E., Casas, J.A. and Gómez, E. (2000) Xanthan gum: production, recovery, and properties. Biotechnology Advances 18(7), 549-579.

Jaishankar, A., Wee, M., Matia-Merino, L., Goh, K.K.T. and McKinley, G.H. (2015) Probing hydrogen bond interactions in a shear thickening polysaccharide using nonlinear shear and extensional rheology. Carbohydrate Polymers 123, 136-145.

Kennedy, J.R.M., Kent, K.E. and Brown, J.R. (2015) Rheology of dispersions of xanthan gum, locust bean gum and mixed biopolymer gel with silicon dioxide nanoparticles. Materials science & engineering. C, Materials for biological applications 48, 347-353.

Laneuville, S.I., Turgeon, S.L. and Paquin, P. (2013) Changes in the physical properties of xanthan gum induced by a dynamic high-pressure treatment. Carbohydrate Polymers 92(2), 2327-2336.

Majumder, S.K., Kundu, G. and Mukherjee, D. (2007) Pressure drop and bubble–liquid interfacial shear stress in a modified gas non-Newtonian liquid downflow bubble column. Chemical Engineering Science 62(9), 2482-2490.

Marcotte, M., Taherian Hoshahili, A.R. and Ramaswamy, H.S. (2001) Rheological properties of selected hydrocolloids as a function of concentration and temperature. Food Research International 34(8), 695-703.

Meng, F., Zhang, H., Yang, F., Zhang, S., Li, Y. and Zhang, X. (2006) Identification of activated sludge properties affecting membrane fouling in submerged membrane bioreactors. Separation and Purification Technology 51(1), 95-103.

Ratkovich, N., Horn, W., Helmus, F.P., Rosenberger, S., Naessens, W., Nopens, I. and Bentzen, T.R. (2013) Activated sludge rheology: A critical review on data collection and modelling. Water Research 47(2), 463-482.

Saha, D. and Bhattacharya, S. (2010) Hydrocolloids as thickening and gelling agents in food: a critical review. Journal of food science and technology 47(6), 587-597.

Seyssiecq, I., Marrot, B., Djerroud, D. and Roche, N. (2008) In situ triphasic rheological characterisation of activated sludge, in an aerated bioreactor. Chemical Engineering Journal 142(1), 40-47.

Seyssiecq., Ferrasse and Roche (2003) State-of-the-art: rheological characterisation of wastewater treatment sludge. Biochemical Engineering Journal 16(1), 41-56.

Song, K.-W., Kim, Y.-S. and Chang, G.-S. (2006) Rheology of concentrated xanthan gum solutions: Steady shear flow behavior. Fibers and Polymers 7(2), 129-138.

Vega, E.D., V¨¢squez, E., Diaz, J.R.A. and Masuelli, M.n.A. (2015) Influence of the Ionic Strength in the Intrinsic Viscosity of Xanthan Gum. An Experimental Review. Journal of Polymer and Biopolymer Physics Chemistry 3(1), 12-18.

Yang, F., Bick, A., Shandalov, S., Brenner, A. and Oron, G. (2009) Yield stress and rheological characteristics of activated sludge in an airlift membrane bioreactor. Journal of Membrane Science 334(1–2), 83-90.

6.8 SUPPLEMENTARY FIGURES

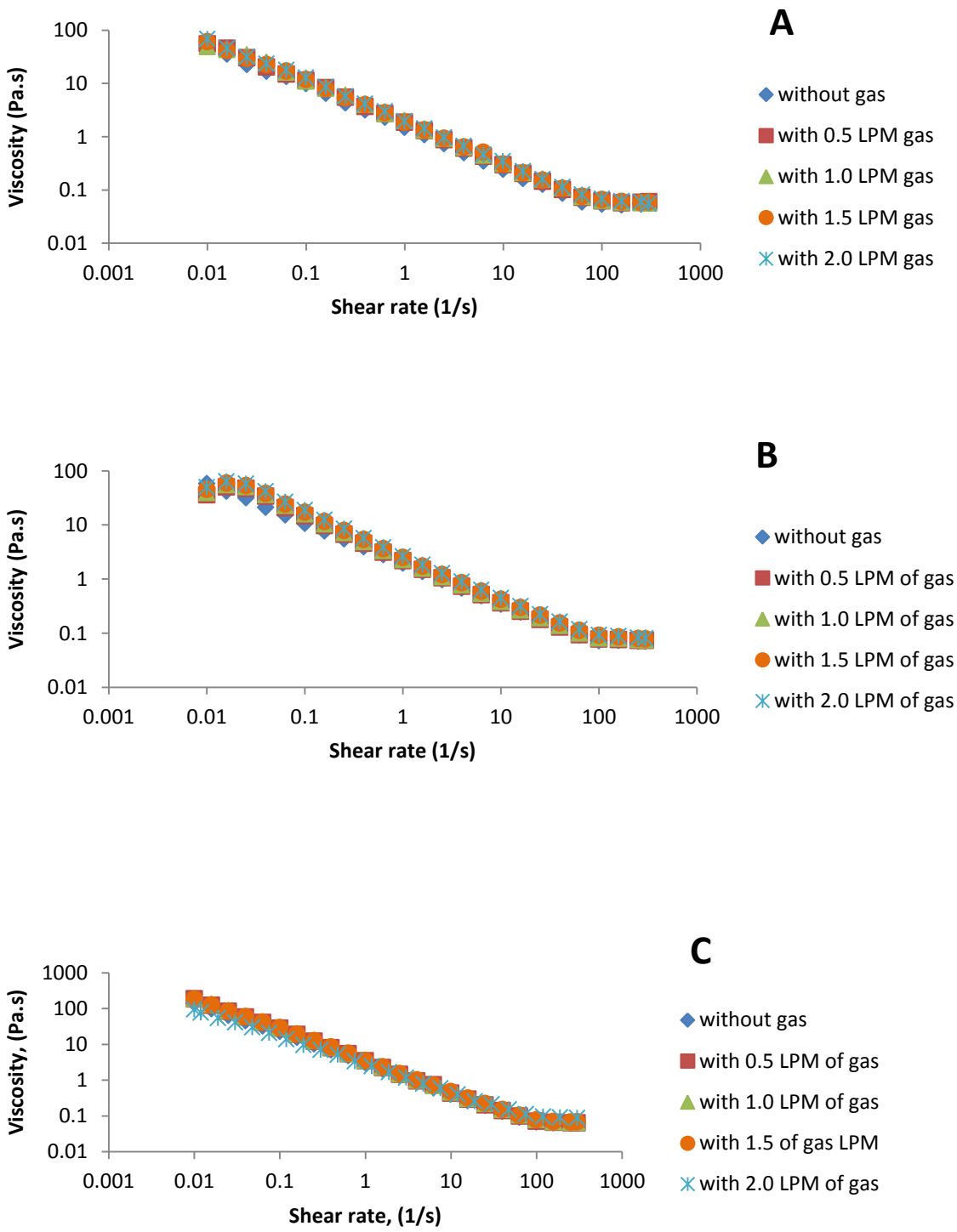

Figure S.6.1: Viscosity curve of Xanthan gum at 4 different gas flow rates 0.5 LPM – 2 LPM for (A) 0.4%, (B) 0.5% and (C) 0.6%

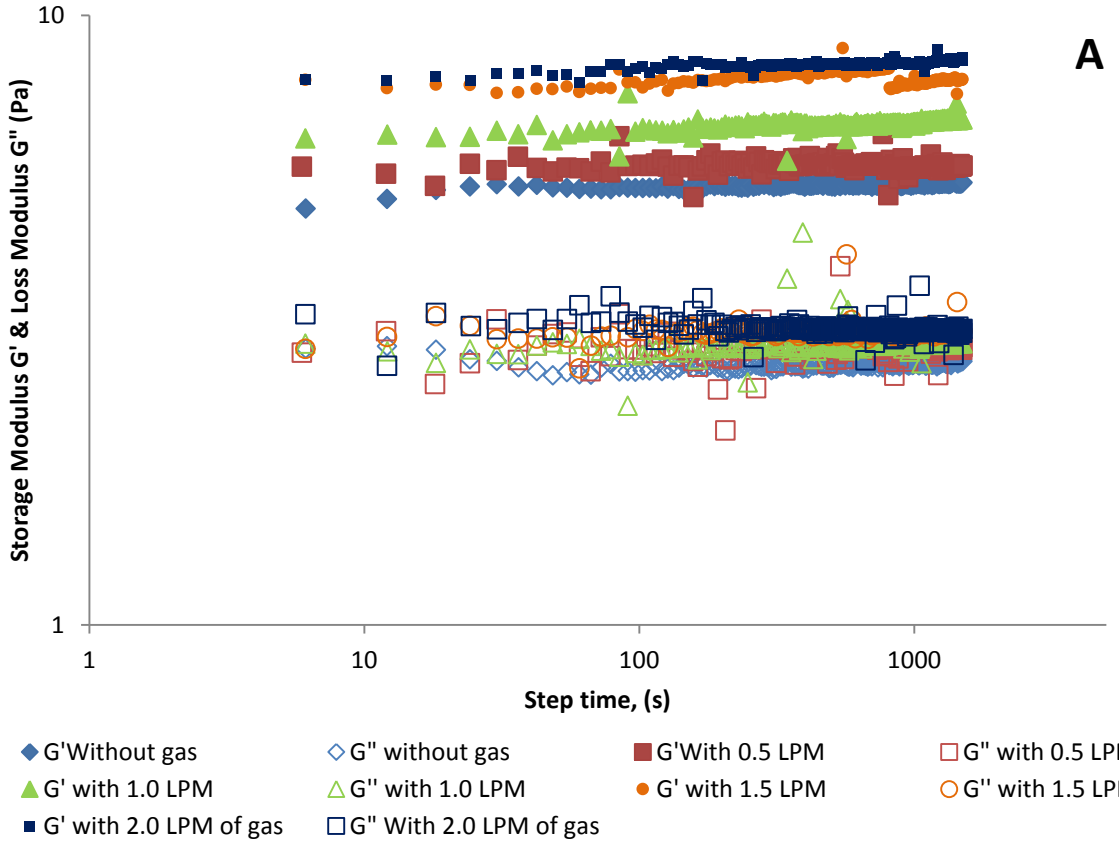
A
10
1
Storage Modulus G' & Loss Modulus G'' (Pa)
1
10
100
1000
Step time, (s)
G'Without gas
G'' without gas
G'With 0.5 LPM
G'' with 0.5 LPM of gas
G' with 1.0 LPM
G'' with 1.0 LPM
G' with 1.5 LPM
G'' with 1.5 LPM
G' with 2.0 LPM of gas
G'' With 2.0 LPM of gas

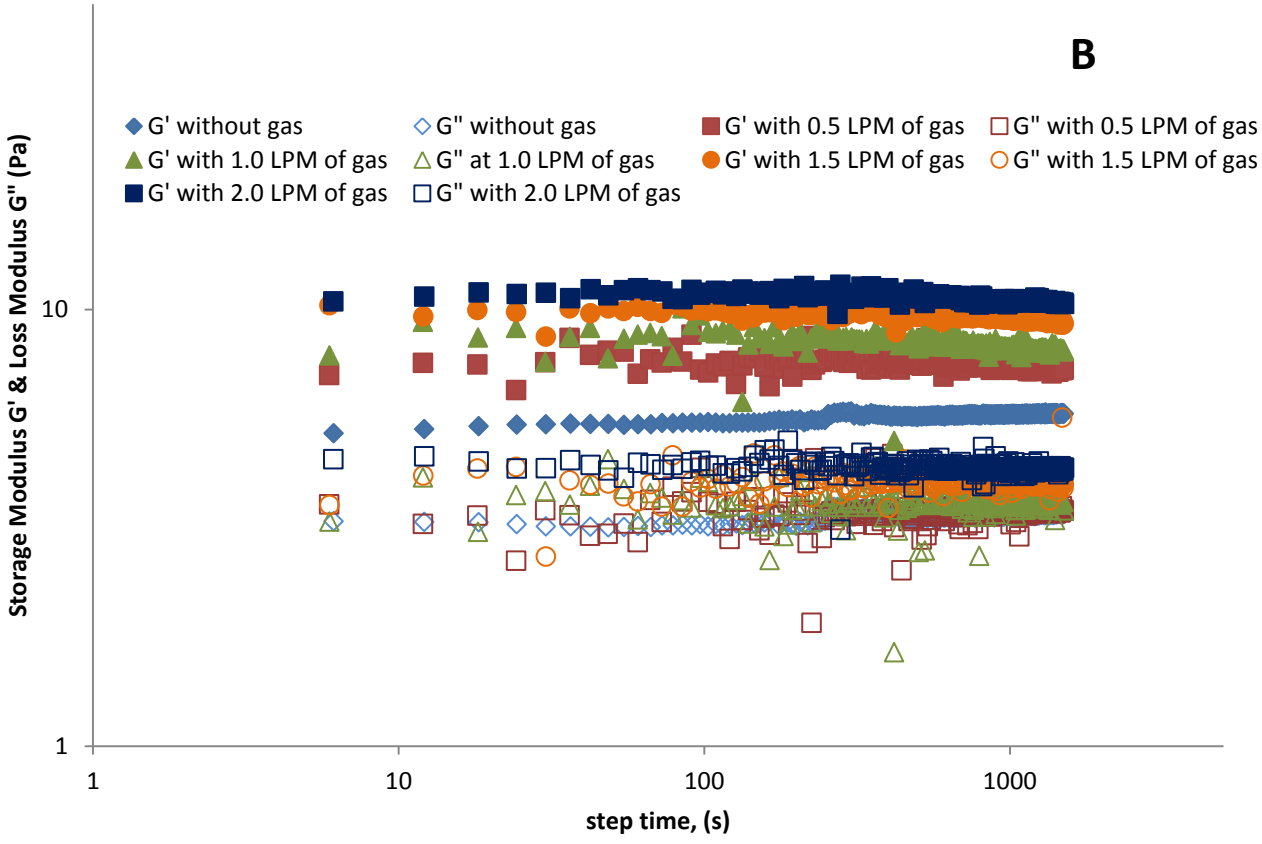
B
G' without gas
G'' without gas
G' with 0.5 LPM of gas
G'' with 0.5 LPM of gas
G' with 1.0 LPM of gas
G'' at 1.0 LPM of gas
G' with 1.5 LPM of gas
G'' with 1.5 LPM of gas
G' with 2.0 LPM of gas
G'' with 2.0 LPM of gas
10
1
Storage Modulus G' & Loss Modulus G'' (Pa)
1
10
100
1000
step time, (s)

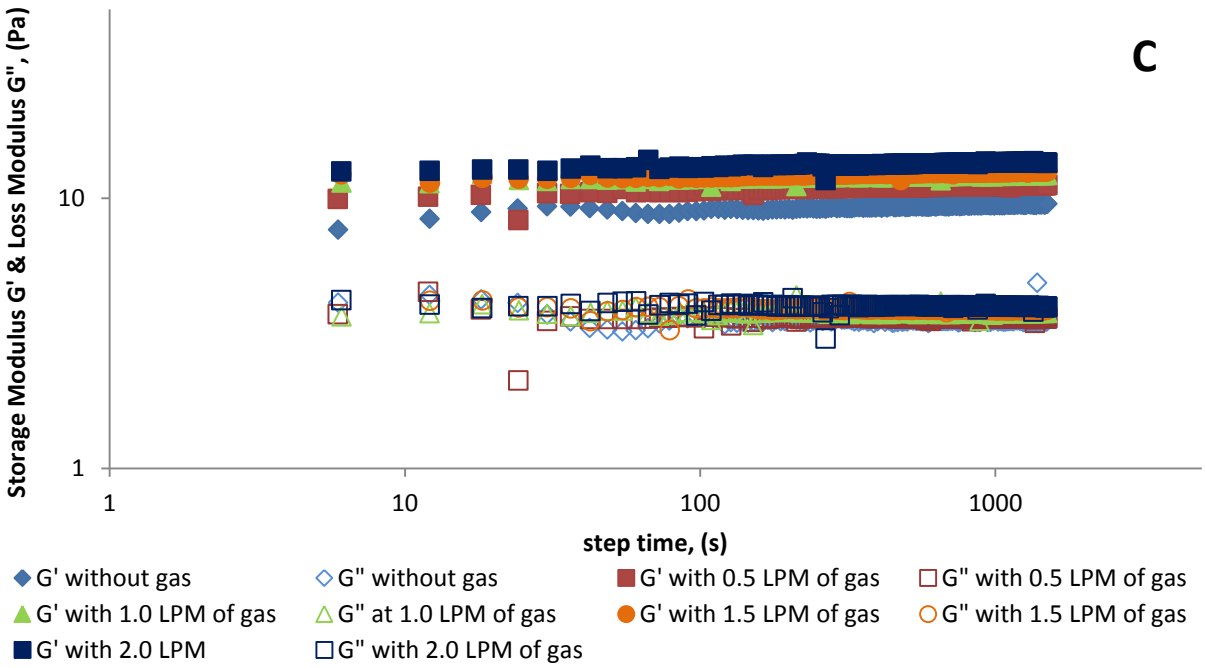

Figure S.6.2: Impact of gas injection on viscoelastic modulus of Xanthan gum during time sweep test (0.15% strain & 1 Hz) at four different gas flow rates 0.5 LPM – 2 LPM at (A) 0.4%, (B) 0.5% and (C) 0.6%.

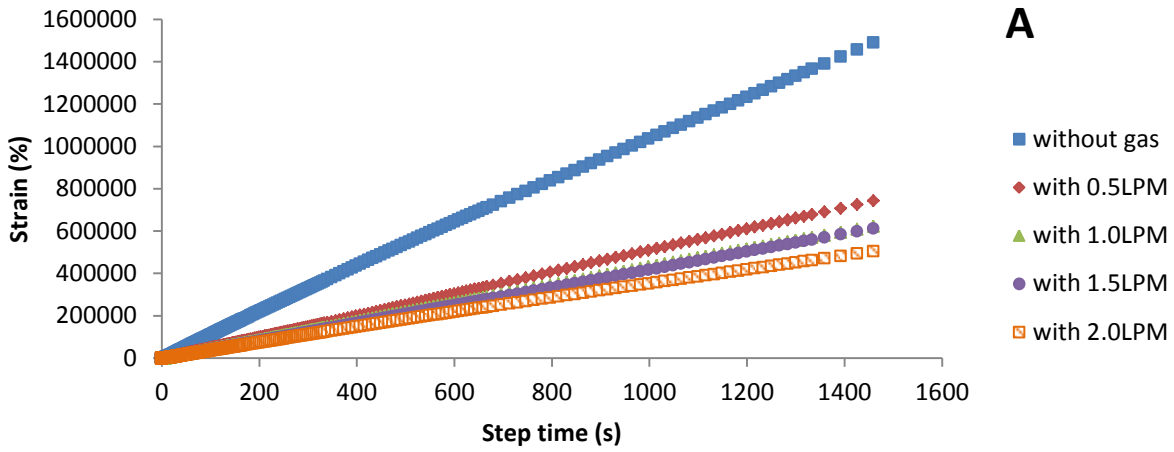
A
Strain (%)
1600000
1400000
1200000
1000000
800000
600000
400000
200000
0
0
200
400
600
800
1000
1200
1400
1600
Step time (s)
without gas
with 0.5LPM
with 1.0LPM
with 1.5LPM
with 2.0LPM

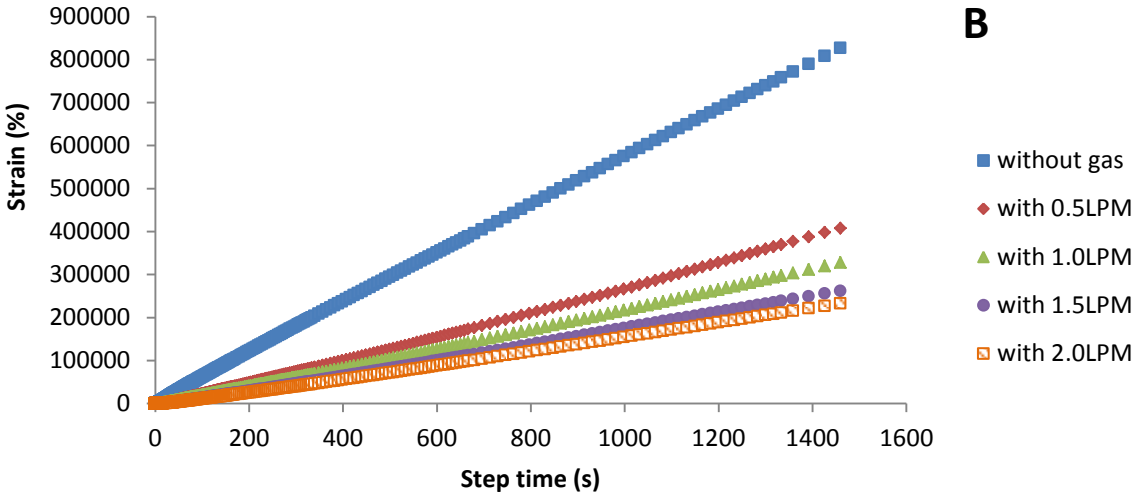
B
Strain (%)
900000
800000
700000
600000
500000
400000
300000
200000
100000
0
0
200
400
600
800
1000
1200
1400
1600
Step time (s)
without gas
with 0.5LPM
with 1.0LPM
with 1.5LPM
with 2.0LPM

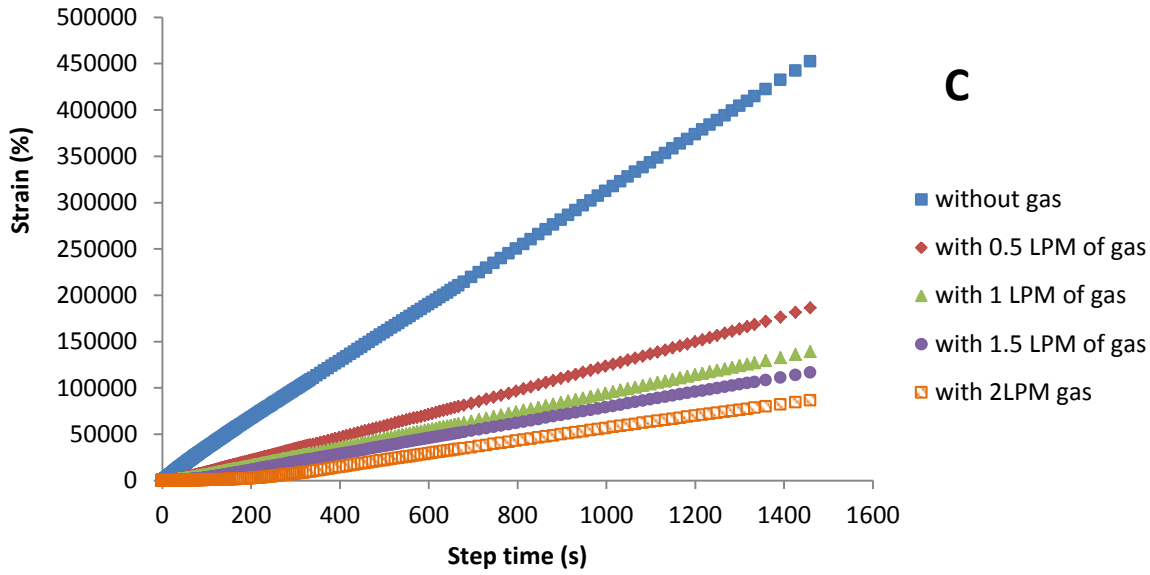

Figure S.6.3: Impact of gas injection on viscoelastic modulus of Xanthan gum in creep test (at applied stress of 3 Pa) at four different gas flow rates 0.5 LPM – 2 LPM at (A) 0.4%, (B) 0.5% and (C) 0.6%.

CHAPTER 7: BUBBLE RISE VELOCITY AND BUBBLE SIZE IN THICKENED WASTE ACTIVATED SLUDGE: UTILISING ELECTRICAL RESISTANCE TOMOGRAPHY (ERT)

This chapter was published in Chemical Engineering Research and Design

(Vol: I48, Page: 119-128, 2019)

Keywords: Waste activated sludge, Gas holdup, Bubble rise velocity, Bubble size, effective shear rate.

Bobade, V., Evans, G. and Eshtiaghi, N. Bubble rise velocity and bubble size in thickened waste activated sludge: Utilising electrical resistance tomography (ERT). Chemical Engineering Research and Design, I48 (2019) 119-128

Graphical Abstract

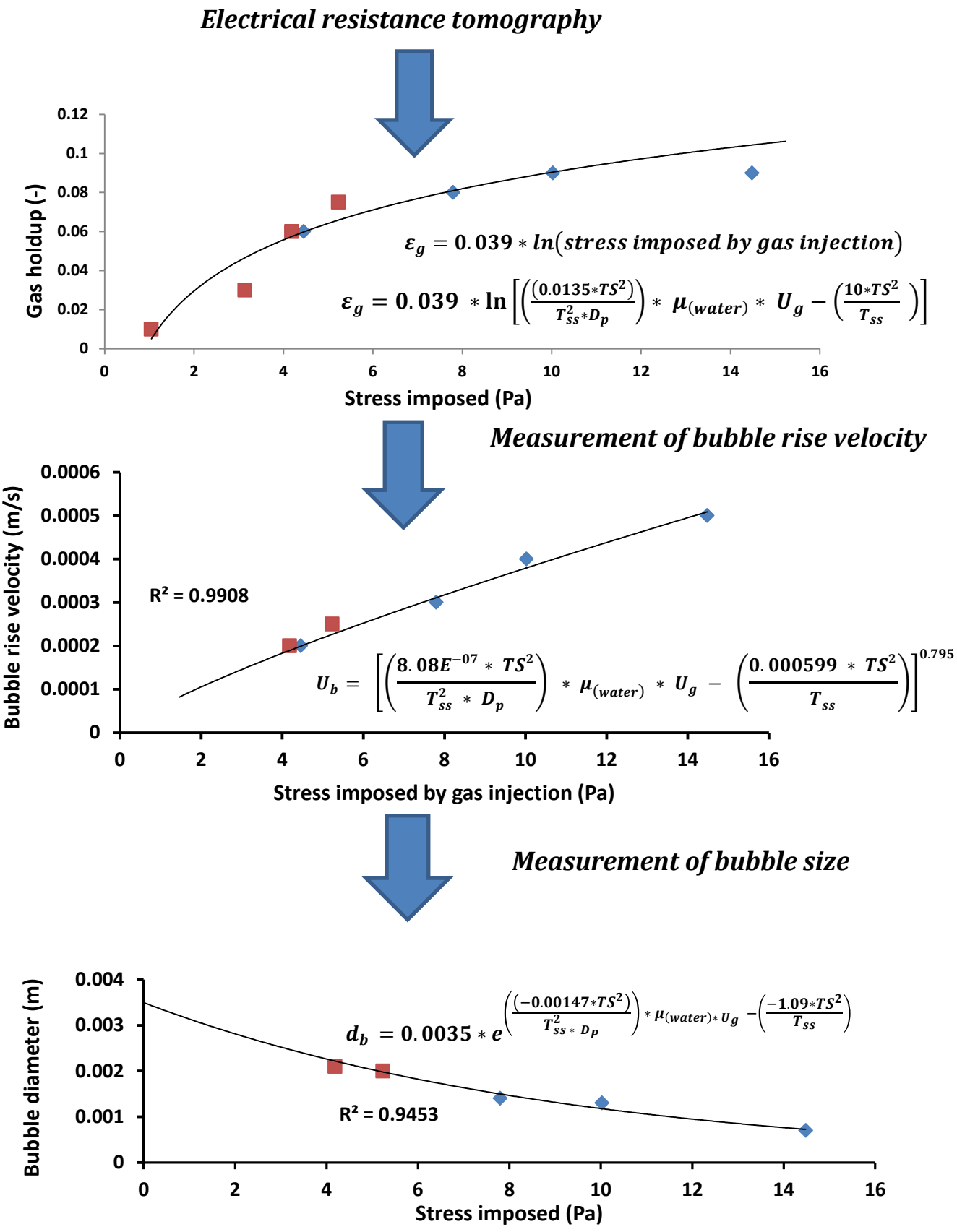

7.1 ABSTRACT

Bubble columns are intensively used in many different industries as multiphase contactors. The gas phase properties in the bubble column significantly impact on the hydrodynamics of the column which effects on heat and mass transfer rates within the column. In this paper, electrical resistance tomography together with dynamic gas disengagement technique is used to determine the gas holdup and bubble rise velocity within the column at four different gas flow rates (1 to 7 L/min) and two different total solids concentrations of waste activated sludge (3% & 5.5%). For the first time, effective shear rate and bubble size are calculated based on the Herschel-Bulkley model. A linear relation was observed for the bubble rise velocity with stress imposed and between gas holdup and natural logarithm of stress imposed by gas injection.

7.2 INTRODUCTION

Increasing volume of wastewater is becoming a crucial problem for the industries (Fatone et al. 2011). Among the available different treatment methods waste activated sludge treatment is the most widely used treatment (Seyssiecq et al. 2008). Aeration operation is known to be the heart of waste activated sludge process (Bailey et al. 2002). Aeration provides oxygen to bacteria for treating the wastewater. Oxygen is essential for the bacteria to allow biodegradation to take place. The supplied oxygen is utilised by bacteria in the wastewater to break down the organic matter to form carbon dioxide and water. Without the presence of sufficient oxygen, bacteria cannot biodegrade the incoming organic matter in a reasonable time (Henze and Henze 1997). Thus adequate and evenly distributed oxygen supply is required in an aeration system for the rapid, economically viable and efficient treatment. However, the efficiency of the aeration depends on the hydrodynamics of the gas phase characteristic, i.e., gas holdup, bubble rise velocity and bubble size (Jamshidi and Mostoufi 2017). Therefore measuring and understanding the gas phase properties like gas holdup and bubble rise velocity and bubble size in sludge is vital to increase the overall efficiency of the waste activated sludge process.

The number of studies has measured the gas phase characteristics and shown how rheology plays a crucial role in gas phase properties. Lind and Phillips (2010) estimated the viscous and viscoelastic properties of the fluid and reported that viscoelastic properties of fluid have a remarkable impact on bubble shape, size and rise velocity. The

elasticity of fluid increases both the gas bubble collision and coalescence time because; elasticity decreases the size of the toroid wake behind a moving spherical bubble, thus making the detachment of the next bubble slower (Acharya and Ulbrecht 1978, Dekée et al. 1986). However, most of these studies have been done on clear non-Newtonian model fluid as it is convenient to use the optical system of measurement. Furthermore, most of these fluids have a stable rheological behaviour, i.e., the rheology does not change with time (Bajón Fernández et al. 2015, Esmaeili et al. 2015, Fransolet et al. 2005).

Recently non-intrusive methods such as X-ray tomography, electrical resistance tomography (ERT), electrical impedance tomography (EIT) and electrical capacitance tomography (ECT) are being used for measuring the gas phase characteristics in opaque system such as sludge (Babaei et al. 2015a, b, Dziubiński et al. 2003, Fransolet et al. 2005, Jin et al. 2007, Warsito and Fan 2001). ERT is a method that calculates the subsurface distribution of electrical resistivity from a large number of resistance measurements made from electrodes (Daily et al. 2004). It is a comparatively new imaging tool which is applied to the opaque system along with dynamic gas disengagement method to measure the gas phase characteristics in waste activated sludge (e.g. (Babaei et al. 2015a), Babaei et al. (2015b)). However, the concentration of sludge (WAS) used in the abovementioned studies was very low (0.07 to 1.5%). Other researchers (Fransolet et al. 2005, Jin et al. 2007, Khalili et al. 2018a) have also successfully implemented electrical resistance tomography technique coupled with dynamic gas disengagement to measured bubble phase characteristics in the two-phase gas-liquid system and agitated systems of transparent liquids like Xanthan gum (1 g/L to 5 g/L). However, for economical treatment in the upcoming decentralised system, it is important to focus on high solids concentration of sludge. As the decentralised system capacity must relate to the local household and community and should not put excessive financial burden on the users (Capodaglio 2017). Thus, operating in high solid concentration is imperative for decentralised sewage treatment plant. Sludge being a complex rheological fluid, gas phase characteristics varies significantly with concentration.

Since, no study has been done on the measurement of gas characteristics at high solid concentration of sludge greater than 30 g/L, and no study has been reported on relationship between stress imposed by gas injection and bubble characteristics. The

current study aims to investigate the gas phase characteristics in the concentrated waste activated sludge. In addition, the role of viscoelastic properties on the gas phase characteristics was analysed.

7.3 MATERIALS AND METHODS

7.3.1 SAMPLE PREPARATION

Waste activated sludge was sampled from one of the waste water treatment plant in Victoria, Australia. The samples were stored at 4^{o}C for 30 days to reduce the microbial activity inside the sludge. This procedure helps with the stability of samples which results in reproducible data (Curvers et al. 2009). To prepare different concentration sludge samples, the sludge was thickened to higher concentration (6%) using centrifuge at 8000 rpm (i.e., at 12,200 g maximum relative centrifugal force) for 30 minutes, and mixed with original sludge to prepare the homogeneous sample of desired concentrations (3% & 5.5%).

7.3.2 APPARATUS

The gas holdup measurements were carried out using the Electrical resistance tomography from Industrial Tomography Systems which was equipped with a specially designed plexiglass cup (105 mm inside diameter and 100 mm length) with a stainless steel porous disk (outer diameter: 100 mm, thickness: 1.6 mm, porosity: 40%, from SINTEC Australia) at the bottom of the cup for gas sparging as shown in Figure 7.1. The actual volume of cup used in the experiment was 5.89 x 10^{5} mm^{3} (68 mm length and 105 mm inside diameter).

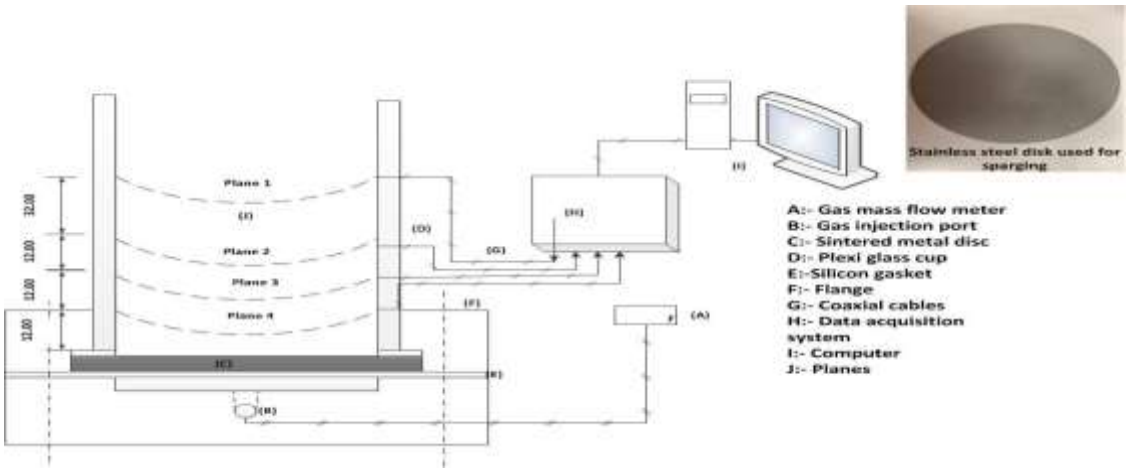

Figure 7.1: Schematic drawing of experimental setup with ERT

7.3.3 ERT MEASUREMENT TECHNIQUE

Electrical resistance tomography is used to acquire the conductivity distribution across different sensor planes. Four sensor planes were located across the cup. Each plane was mounted with 16 equally spaced rectangular electrodes (10 mm X 7 mm). Three major components of ERT are data acquisition system (DAS) and an image reconstruction system. The electrodes are connected to the DAS using coaxial cables. The DAS applies a current between the two adjacent electrodes and measures the returning voltage between all other electrode pairs. The same procedure was repeated for all other combination of adjacent electrode pairs until a full rotation was obtained. The frequency of 9600 Hz and injection current of 15 mA was given as input in all of the experiments. The DAS was connected to the computer which processed the data using image reconstruction algorithm. Therefore, a total 316 pixels of non-invasive conductivity measurements were obtained in each plane per frame.

The conductivity distribution measured by ERT was then used to determine the gas phase distribution in the column. The Maxwell equation is used to convert the conductivity data to the gas holdup (Babaei et al. 2015b) (Equation 7.1).

$$\varepsilon_g = \frac{2\sigma_1 + \sigma_2 - 2\sigma_{mc} - \frac{\sigma_{mc}\sigma_2}{\sigma_1}}{\sigma_{mc} - \frac{\sigma_2}{\sigma_1}\sigma_{mc} + 2(\sigma_1 - \sigma_2)} \quad (7.1)$$

Since the gas phase (Nitrogen) is non-conductive, substituting $\sigma_2 = 0$ in Equation 7.1, the equation is modified as shown in Equation 7.2.

$$\varepsilon_g = \frac{2(\sigma_1 - \sigma_{mc})}{2\sigma_1 + \sigma_{mc}} \quad (2)$$

The sludge concentration is varied from 3% to 5.5% and the gas injection rate is varied from 1 LPM to 7 LPM, i.e.; $1.82E^{-03}$ m/s to $1.27E^{-02}$ m/s. All the experiments were carried out at room temperature. This ERT raw data was stored in (Bobade and Eshtiaghi 2018 Figshare-b).

7.3.4 DYNAMIC GAS DISENGAGEMENT TECHNIQUE (DGD)

DGD technique was used to measure the bubble rise velocity inside the bubble column and to understand the bubble size classes within the column. The process used for DGD technique is as follows: Step 1) Start measuring the conductivity distribution using ERT.

Step 2) at frame 10 starts injecting the gas at desired gas flow rate for 20 mins. Step 3) After 20 mins stop the gas flow rate. Step 4) Continue to measure the conductivity distribution after stopping the gas injection for another 20 mins. Step 5) Calculate the gas holdup for an average of 20 frames, and step 6) plot the gas holdup against time. The bubble rise velocity for different bubble size class is calculated by using Equations 7.3, 7.4 and 7.5 (Babaei et al. 2015a). The large size bubbles disengage first (t_2) and the small size bubbles disengage last (t_4).

$$u_{b,small} = \frac{H_{liquid}}{(t_4 - t_1)} \quad (7.3)$$

$$u_{b,medium} = \frac{H_{liquid}}{(t_3 - t_1)} \quad (7.4)$$

$$u_{b,large} = \frac{H_{liquid}}{(t_2 - t_1)} \quad (7.5)$$

7.3.5 RHEOLOGICAL MEASUREMENTS

Rheological measurements were performed using commercially available hybrid stress controlled (HR3) rheometer from TA Instruments. A custom designed plexiglass cup (inner diameter: 100 mm, length: 100 mm) with a stainless steel porous disk (outer diameter: 100 mm, thickness: 1.6 mm, porosity: 40%, from SINTEC Australia) at the bottom for the gas sparging and grooved bob geometry with outer diameter of 14.9 mm, and 42 mm length. The Flow curve measurement was carried out for the non-aerated sludge for a shear rate range of 0.1 s^{-1} to 100 s^{-1} after preshearing the sludge at 300 s^{-1} for 600 s and giving a short rest time of 120 s.

7.4 RESULTS AND DISCUSSION

7.4.1. RHEOLOGICAL BEHAVIOUR AND MODELING

Among the various models Power law, Bingham law, and Herschel-Bulkley; Herschel Bulkley model (Equation 7.6) is the best fitting model to describe the sludge flow behaviour (Baudez and Coussot 2001, Baudez et al. 2011, Eshtiaghi et al. 2013, Feng et al. 2016) for sludge above 3% solid concentrations. The three parameters, i.e. yield stress (τ_o, Pa), the consistency index (K), Pa.s^n), and the flow behaviour index (n) calculated for both the concentrations studied are reported in Table 7.1.

$$\tau = \tau_o + K\dot{\gamma}^n \quad (7.6)$$

Table 7.1: Herschel–Bulkley Model parameters for different solids concentration of waste activated sludge

Concentration of sludge (%)	Yield stress, τ_o (Pa)	Consistency index, K ($Pa.s^n$)	Flow behaviour index, n
3%	7.25	0.668	0.7672
5.5%	28.84	4.603	0.536

7.4.2. GAS HOLDUP IN THE COLUMN

The reconstructed images of gas holdup obtained from ERT at same gas flow rate (7 LPM) but at two different concentrations (3% & 5.5%) are shown in Figure 7.2(A&B) both at the start of gas injection and when the gas injection is stopped. The colour in the ERT mammograms represents the different region of conductivity. The low conductivity region is represented by blue colour whereas red colour in mammograms represents the high conductivity region. Additionally, as the conductivity increases from low conductive region to high conductive region it is represented by light blue, green and yellow colour as shown in the Fig 7.2(A&B) colour line at the bottom of each mammogram. The impact of gas injection on sludge structure is represented by the light blue, green and yellow colour. This is because immediately after starting gas injection, gas breaks down the suspended particles into smaller fragments and a large number of smaller particles starts settling down and be present at Plan 4. That is why a higher conductivity was measured at Plane 4 right at the start of gas injection compared to other planes. However, conductivity in Plane 4 at the end of injection is less than conductivity at the start of injection at Plane 4 because smaller particles settled down within 20 min of injection time on the membrane and fewer particles are present at Plane 4. Considering thickness of 5.5% sludge, there is no gas trapped at Plane 4 and all escaped from this area.

Considering, the conductivity of the gas is zero the low conductivity region in mammograms represents the gas holdup. Thus from Figure 7.2 you can clearly see that, the low conductivity area i.e. blue in colour which represents the gas hold up decreases as the concentration increases from 3% to 5.5%. Moreover it is clear from Figure 7.2B that, at 5.5% at 7 LPM when the gas injection is stopped the low conductivity area is mainly at the center. Whereas, in Figure 7.2A at 3% when the gas injection is stopped the low

conductivity area is seen to be extended from the centre to the circumference. The possible explanation is that by increasing the elasticity of concentrated sludge, it takes longer bubbles to be formed and detached which promotes bubble coalescences. As a result, gas is distributed in small area after 20 minutes of gas injection. Whereas, at 3% WAS the elastic properties of sludge is less than 5.5% WAS's elasticity and hence a better distribution of gas was observed. Thus at 3% solid concentration of WAS and at 7 LPM of gas flow rate, the gas holdup is more than the gas holdup at 5.5% at same gas flow rate.

To evaluate the influence of aeration rate on gas holdup, the average gas holdup of 250 frames (20 mins of gas injection) was calculated using Equation 7.2. The average gas holdup versus gas flow rate at two different concentrations of WAS (3% and 5.5%) is shown in Figure 7.3 (Bobade and Eshtiaghi 2018 Figshare-b). It is clear from the figure that at given aeration rate, the gas holdup decreases as the concentration increases; because the sludge structure at higher concentration becomes more viscous and possesses a strong force of attraction between particles (Baroutian et al. 2013, Bobade et al. 2018). This is in line with the reconstructed image obtained from the ERT. Bo and Lant (2004) stated the increase in solids concentration reduces the contact area of the gas and liquid phases. As a result, bubble coalescence increases and the gas holdup decreases. A similar reduction in the gas holdup with an increase in solids concentration was also observed by Fransolet et al. (2005), Hwang and Cheng (1997), Shimizu et al. (2001).

However, as the aeration rate increases the gas holdup also increases for both the concentration because, the aeration intensity impacts on sludge structure and decreases the attractive force that makes the sludge an easier material to flow i.e., the stress imposed by the gas injection increases with an increase in aeration intensity and decreases the elasticity of the sludge (Bobade et al. 2018). Thus as the aeration intensity increases the gas holdup increases irrespective of the concentration. Interestingly a logarithmic correlation (Equation 7.7) with an error range of ± 20% for 5.5% at low gas flow rate and ± 2% for 3% concentration at low gas flow rate along with 95% confidence level and P value much less than 0.05 between the stress imposed and gas holdup is observed for both the concentration as shown in Figure 7.4 (Bobade and Eshtiaghi 2018 Figshare-b). Data for stress imposed is obtained from Bobade et al. (2018) at the same gas flow rate.

$$\varepsilon_g = 0.039 * \ln(stress\ imposed\ by\ gas\ injection) \quad (7.7)$$

Where, the fitting constant has a unit of (1/Pa).

Therefore, replacing the stress imposed by gas injection as shown in the Equation 7.8 (Bobade et al. 2018), Equation 7.7 is modified to Equation 7.9.

$$\sigma_{imposed} = \left(\frac{(0.0135 * TS^2)}{TSS^2 * D_p}\right) * \mu_{(water)} * U_g - \left(\frac{10 * TS^2}{TSS}\right) \quad (7.8)$$

$$\varepsilon_g = 0.039 * \ln\left[\left(\frac{(0.0135 * TS^2)}{TSS^2 * D_p}\right) * \mu_{(water)} * U_g - \left(\frac{10 * TS^2}{TSS}\right)\right] \quad (7.9)$$

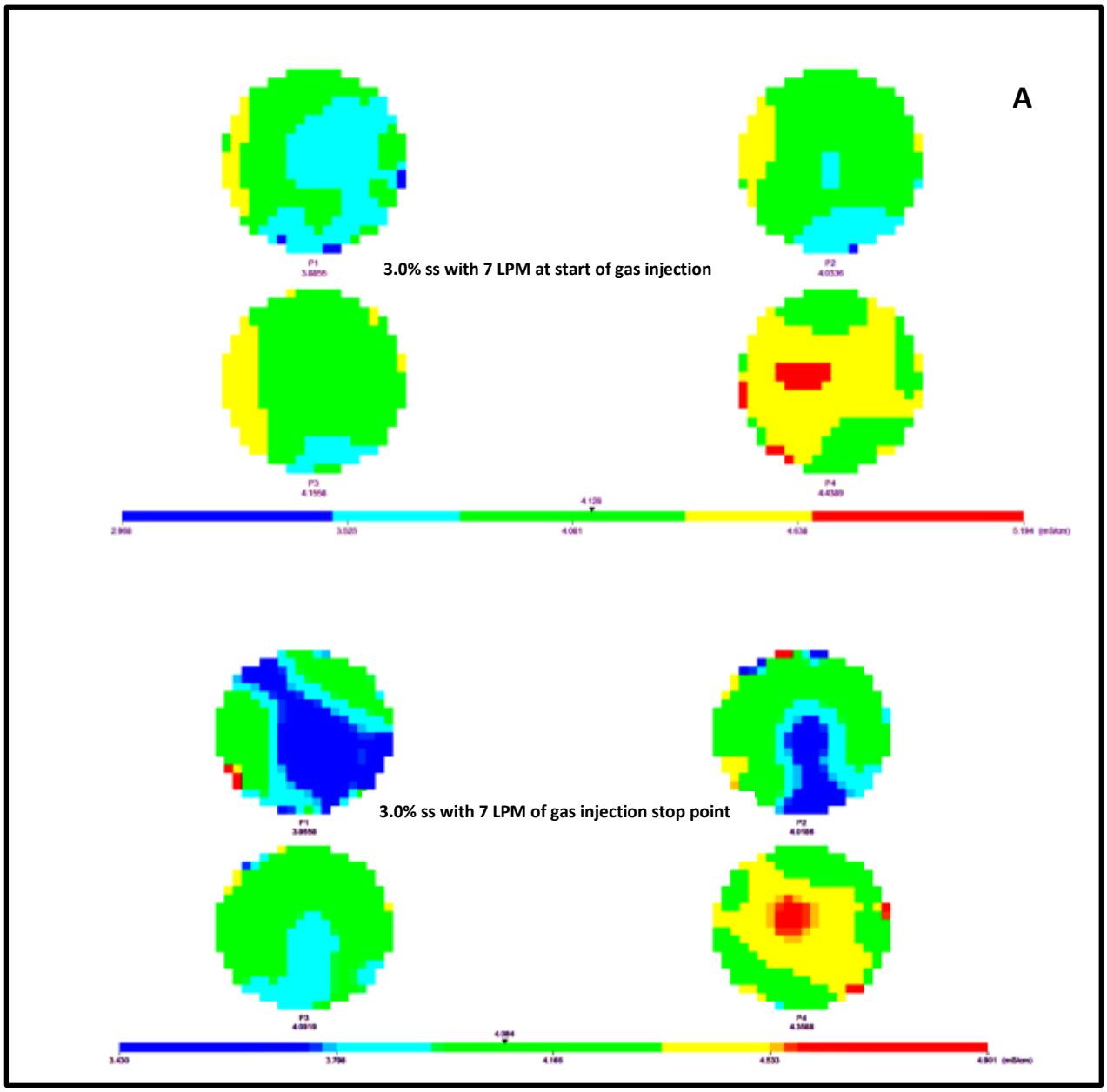

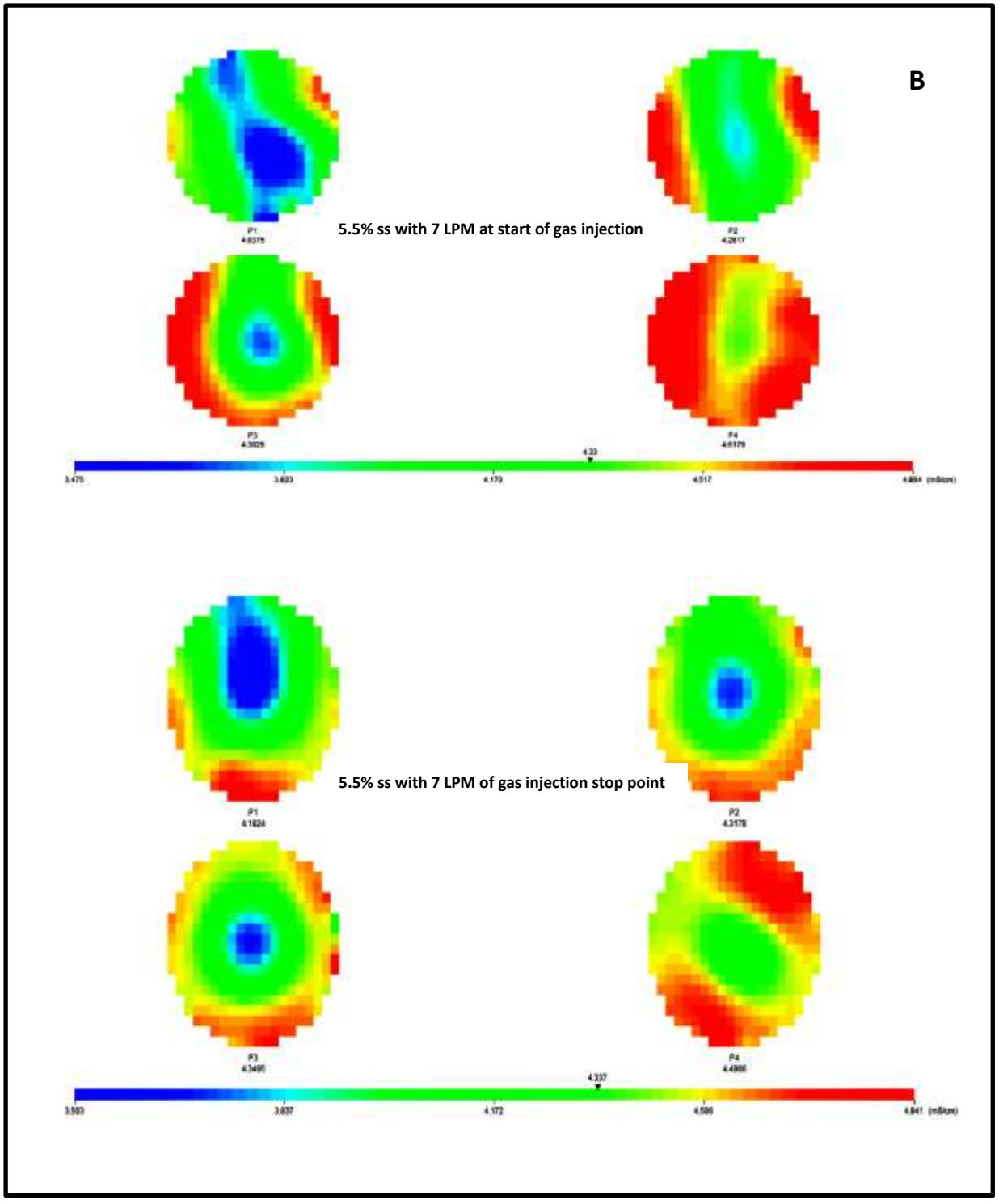

Figure 7.2: Reconstructed images of gas holdup obtained from ERT at the gas injection start point and when the gas injection is stopped at (A) 3% and (B) 5.5% solids concentrations of waste activated sludge

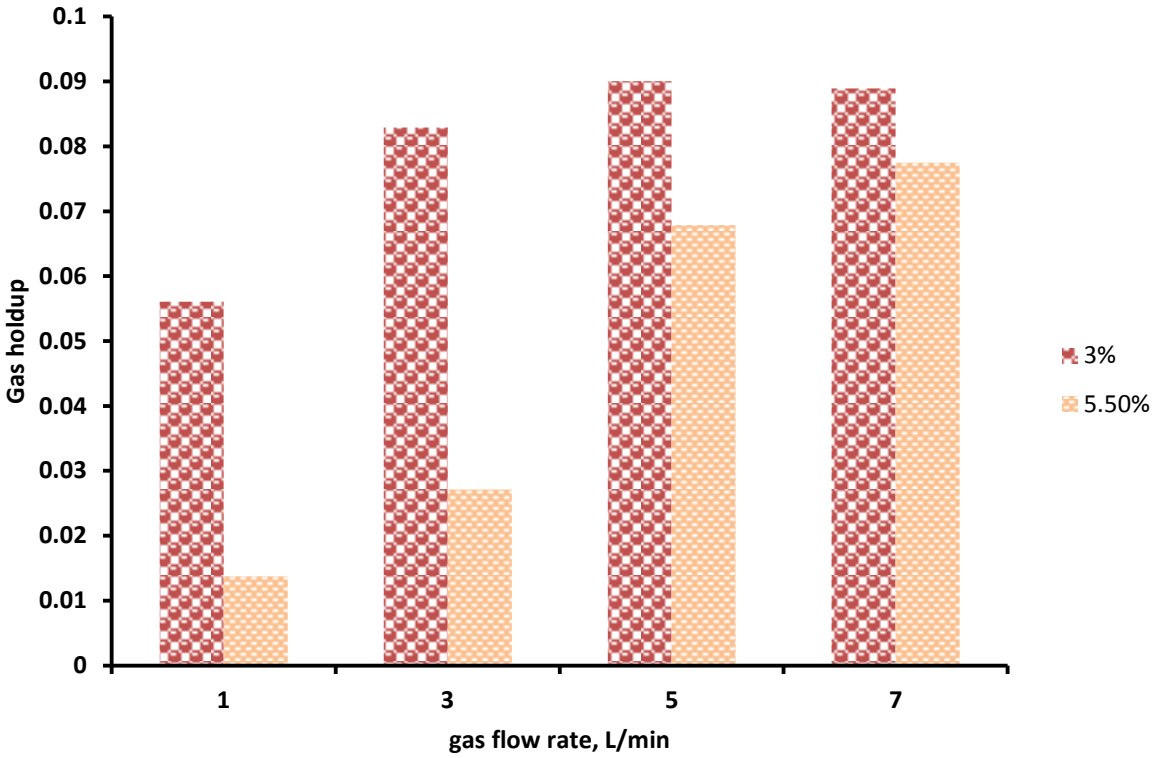

Figure 7.3: Impact of four different aeration rate on gas holdup at two different solid concentrations (3% and 5.5%) of WAS

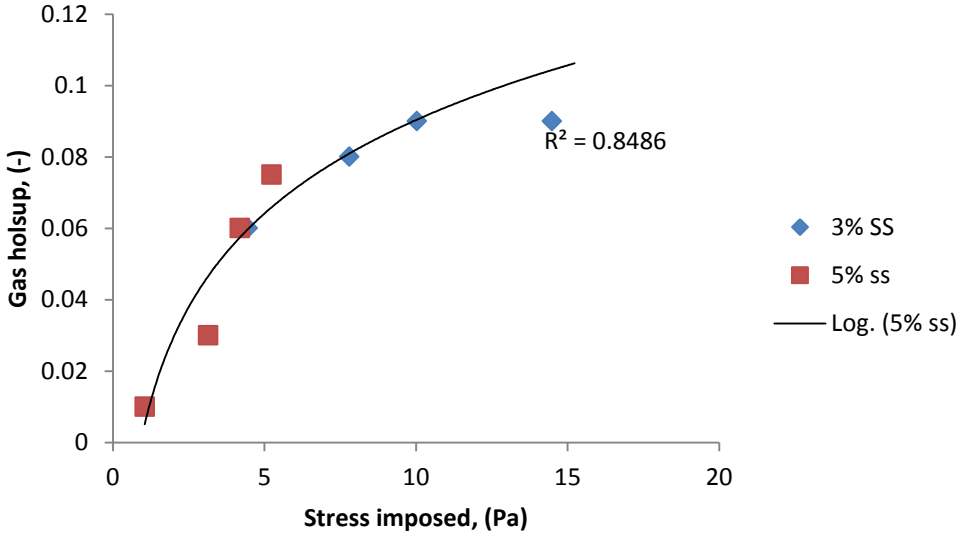

Figure 7.4: Impact of stress imposed by four different gas flow rate (1 LPM, 3 LPM, 5 LPM & 7 LPM) on gas holdup at 3% and 5.5% solids concentrations of sludge

7.4.3. *BUBBLE RISE VELOCITY (DGD TECHNIQUE)*

Dynamic gas disengagement (DGD) technique along with ERT is used to get information on bubble rise velocity and on different bubble sizes present in the column. Disengagement gas technique can determine gas holdup structure by stopping the gas supply and measuring the average gas holdup of 20 frames. DGD technique for 3% and 5.5% WAS with 4 different gas flow rates is shown in Figure 7.5 (A & B).

It is very interesting to see that at 5.5% solid concentration of sludge with 1 LPM and 3 LPM, the gas holdup for DGD technique decreases even before the gas injection is stopped. This is because at 5.5% solid concentration, the sludge is so thick that the gas couldn't overcome sludge yield stress to bubble through samples. Thus when the gas is injected, it causes lifting the sludge bed lifts up until its structure break down suddenly and entire bed drops which forms a channel in the middle of sample for gas to escape. Since the gas suddenly escapes from the sludge bed, we can see that the average gas holdup of 20 frames began to decrease even before the gas injection stopped, i.e. before 1200 s of time.

(A)

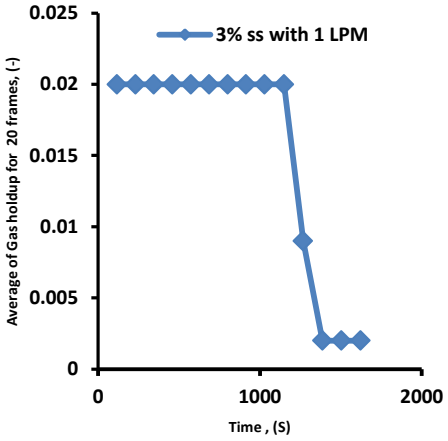
3% ss with 1 LPM
Average of Gas holdup for 20 frames, (-)
0.025
0.02
0.015
0.01
0.005
0
0
1000
2000
Time , (S)

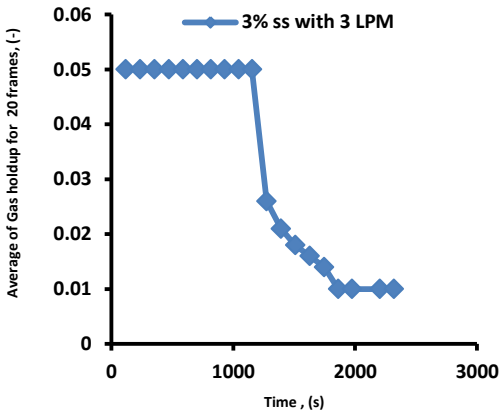
3% ss with 3 LPM
Average of Gas holdup for 20 frames, (-)
0.06
0.05
0.04
0.03
0.02
0.01
0
0
1000
2000
3000
Time , (s)

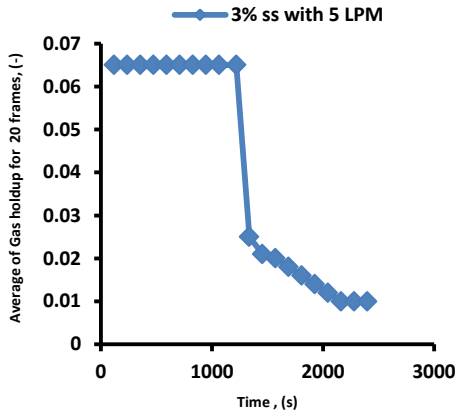
3% ss with 5 LPM
Average of Gas holdup for 20 frames, (-)
0.07
0.06
0.05
0.04
0.03
0.02
0.01
0
0
1000
2000
3000
Time , (s)

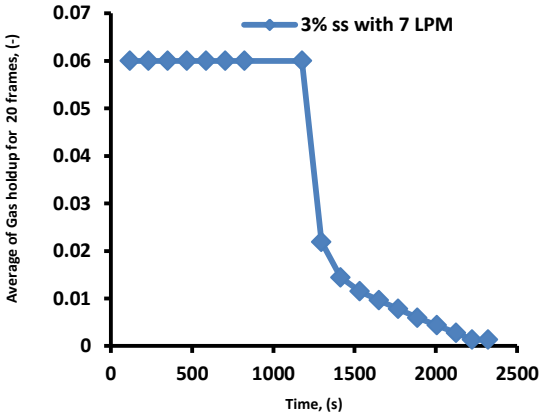
3% ss with 7 LPM
Average of Gas holdup for 20 frames, (-)
0.07
0.06
0.05
0.04
0.03
0.02
0.01
0
0
500
1000
1500
2000
2500
Time, (s)

(B)

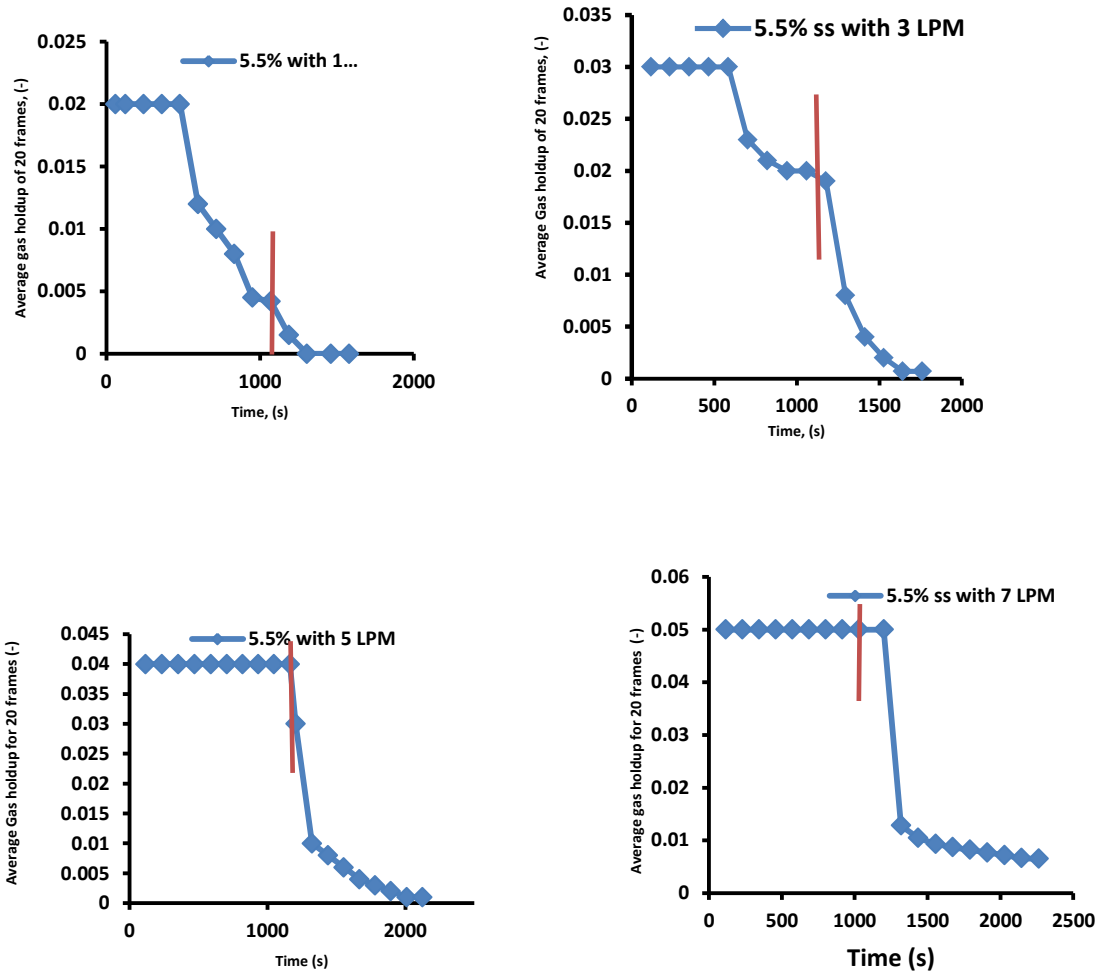

Figure 7.5: Dynamic gas disengagement technique at four different gas flow rates (1, 3, 5 & 7 LPM) for (A) 3% WAS & (B) 5% WAS

However, as the gas flow rate increases to 5 LPM, the average gas holdup only decreases when the gas injection is stopped, i.e. after 1200 s of time. This information tells us that at 5.5% of solids concentration, 5 LPM is the minimum required gas flow rate required to trap the gas bubbles within the sludge samples.

The calculated average bubble rise velocity ($U_{b(average)} = \frac{\sum_{i=!}^{N} \varepsilon_{g,i} U_{b,i}}{\varepsilon_{g\ overall}}$) for both the concentrations and for all the gas flow rates is shown in Table 7.2 (Bobade and Eshtiaghi 2018 Figshare-b). From the table it is clear that for 3% and 5.5% WAS, bubble rise velocity increases with an increase in gas flow rate. At 5.5% solid concentration of WAS and at 1 LPM and 3 LPM, the gas holdup decreases even during gas injection due to bed lifting and sudden bubble escaping. So as soon as the gas injection is stopped, gas holdup

decreases to minimum. Hence, the bubble rise velocity is not calculated for 1 LPM and 3 LPM of gas flow rate. By further increase in gas flow rates, bubble rise velocity also increases.

Additionally, once all bubble rise velocity for both solid concentrations was plotted against different gas flow rates, a linear correlation was observed between the gas flow rate and bubble rise velocity for both the solids concentration of sludge. Similarly, a linear power correlation between stress imposed by gas and bubble rise velocity for waste activated sludge was observed as shown in Figure 7.6. Furthermore on applying multiple regression analysis, Equation 7.10 is obtained with 95% of confidence level and P -value much less than 0.05 having an error range of ± 20% for 5.5% and ± 3% for 3% concentration at gas flow rate above 3 LPM. In addition, similar to Equation 7.9, replacing stress imposed by

Table 7.2: Bubble rise velocity for 3% WAS and 5.5% WAS at 4 different gas flow rates

Gas flow rate (L/min)	Bubble rise velocity for 3% WAS (m/s)	Bubble rise velocity for 5.5% WAS (m/s)
1	0.0002	-
3	0.0003	-
5	0.0004	0.0002
7	0.0005	0.00025

gas injection in Equation 7.10 from Equation 7.8, Equation 7.11 is obtained. From Figure 7.6, it is clear that the rise velocity of bubble depends upon the stress imposed by the gas injection for the given concentration of sludge. In the same way a linear correlation of gas flow rate and bubble rise velocity was also observed by Jin et al. (2012) and Jamshidi and Mostoufi (2017). However, as shown in Equation 7.7, gas holdup is also related to stress imposed, a correlation between bubble rise velocity and gas holdup was obtained as shown in Equation 7.12 with P – value 6.14049E-06.

$$u_b = 5.99E^{-05}.(\sigma_{imposed}) \quad (7.10)$$

Where the fitting constant has a unit of (m^3/N.s)

$$\therefore\ u_b = \left[\left(\frac{(8.08E^{-07}.TS^2)}{TSS^2\ .D_p}\right).\ \mu_{(water)}\ .\ U_g - \left(\frac{0.000599\ .TS^2}{TSS}\right)\right]^{0.795} \quad (7.11)$$

$$u_b = 0.00394 * \varepsilon_g \quad (7.12)$$

Where the fitting constant has a unit of (m/s)

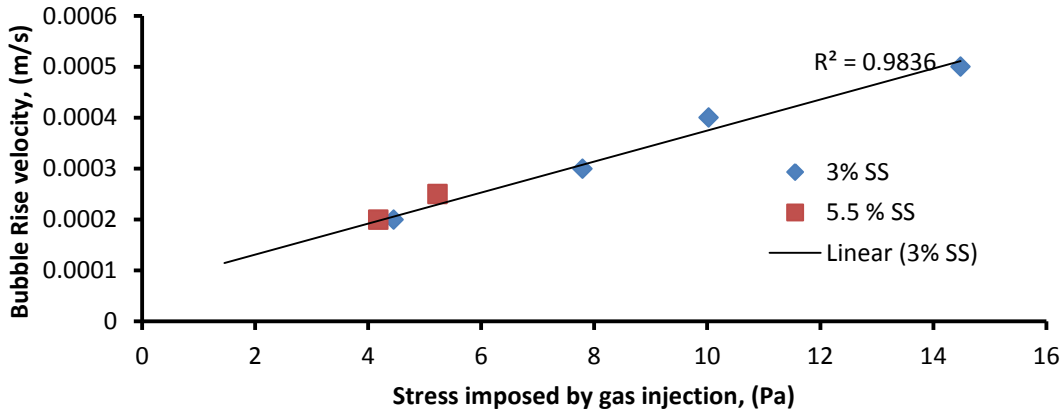

Figure 7.6: Impact of stress imposed on bubble rise velocity of 3% and 5.5% of WAS

7.4.4. Effective shear rate calculation in bubble column using Herschel-Bulkley fluid

Effective viscosity (μ_{eff}) is one of the most commonly used design parameters for bubble columns to correlate mass transfer and hydrodynamic parameters of the system. In order to calculate the effective viscosity, the average shear rate in the bioreactor must be known. There are many differences in the literature regarding the effective viscosity of a fluid (Al-Masry and Chetty 1997) due to massive discrepancy of the effective shear rate calculation (see Table 7.3). Furthermore, these equations were developed for Newtonian system such as water-air. A commonly used equation for calculating the effective shear rate is presented in Equation 7.13, which was developed by Nishikawa et al. (1977).

$$\dot{\gamma} = 5000U_g \quad (7.13)$$

However, Chisti and Moo-Young (1989) step by step proved that this equation was derived only by considering the input power by gas in the bubble column. However, the turbulence in the bubble column (or the shear) depends on both the input power and on the rheological behaviour of the fluid itself. Additionally the comparison of several other

equations that are available for the shear rate calculation in the bubble column showed a massive discrepancy for the shear rate calculation as shown in Table 7.3.

Table 7.3: Average shear rate in bubble columns as a function of gas superficial velocity for air water system

Effective shear rate formula	shear rate range (s^{-1})	Velocity range x 10^2 (m/s)	Reference
$\dot{\gamma} = \left(\frac{\rho_L\, g\, U_G}{\mu_L}\right)^{0.5}$	450 - 900	2 – 10	(Henzler and Kauling 1985)
$\dot{\gamma} = 5000\, U_G$	200 – 500	4 – 10	(Nishikawa et al. 1977)
$\dot{\gamma} = 2800\, U_G$	100 – 150	4 – 10	(Schumpe and Deckwer 1987)
$\dot{\gamma} = 1500\, U_G$	60 – 90	4 – 10	(Henzler 1980)
$\dot{\gamma} = \left(\frac{U_G}{d_c}\right)$ $(for\ d_c = 0.20\ m)$	0.2 – 40	3.5 - 10	(Kawase and Moo-Young 1986)

In recent years for non-Newtonian shear thinning fluid the effective shear rate was calculated by using power law model. For Xanthan gum solution and assuming a power law behaviour for this solution, Fransolet et al. (2005) showed that effective shear rate is equivalent to 2800 of gas velocity. Babaei et al. (2015b) used the power law model for sludge and proved that effective shear rate is equivalent to 28 of gas velocity. Despite the fact that it is known that sludge with solid concentrations above 3% behave as Herschel-Bulkley model (Eshtiaghi et al. 2013), there is no equation available for that which we aim to develop one.

The effective shear rate in bubble column based on Herschel-Bulkley model considering the energy dissipation rate in a stirred tank can be calculated as follows,

$$\frac{P}{v} = \tau\dot{\gamma} \quad (7.14)$$

Therefore substituting shear stress from Equation 7.6 to Equation 7.14, we get

$$\frac{p}{v} = \dot{\gamma}\,(\tau_o + k\dot{\gamma}^n) \quad (7.15)$$

However, for bubble columns power energy dissipation rate is given as

$$\frac{p}{v} = g\rho u_g \quad (7.16)$$

Therefore substituting $\frac{p}{v}$ from Equation 7.16 to Equation 7.15 and rearranging the equation, we get

$$\dot{\gamma} = \frac{g\rho u_g}{(\tau_o + k\dot{\gamma}^n)} \quad (7.17)$$

Since, the shear rate is on both the sides of equation, solving Equation 7.17 using trial and error method by substituting the Herschel-Bulkley parameters to get RHS = LHS. Thus, the effective shear rate calculated for 3% and 5% total solids of WAS is as shown in Table 7.4. It is very interesting to see that the effective shear rate calculated using the Equation 7.13 is same for all concentrations as it is based on gas flow rate only. However, the effective shear rate calculated using Equation 7.17 considering the rheological properties of the sludge changes with change in concentration. Similarly, the effective shear rate depends on rheological behaviour of the fluid along with operating conditions and geometry of the bioreactor was shown by Cerri et al. (2008).

7.4.5. BUBBLE SIZE CALCULATION

The bubble size plays an important role in the gas liquid contact in bubble columns. There exist different bubble size classes at higher liquid viscosity and low gas flow rate (Kulkarni and Joshi 2005). Moreover for system with different bubble size, the calculation of bubble sauter mean diameter and its relation to gas velocity and bubble coalescence phenomena has been very well explained by Babaei et al. (2015a). However, all the empirical equations that have been used in the literature to calculate the average bubble size are based on power law model and by using dimensionless equations (Babaei et al. 2015a, Fransolet et al. 2005, Jamshidi and Mostoufi 2017, Lind and Phillips 2010).

Thus, the bubble size calculation using the Herschel-Bulkley model is calculated as shown below.

Table 7.4: Effective shear rate in the column for 3% & 5% of WAS at different gas flow rates

Concentration of WAS (%)	Gas flow rate (L/min)	Effective shear rate within the column, (1/s), calculated using Equation 7.17.	Effective shear rate calculated using commonly used Equation 7.13. $\dot{\gamma} = 5000\, u_g$
3	1	2.1	9.1
	3	5.5	17.73
	5	8.4	29.55
	7	11	356
5.5	1	0.5	9.1
	3	1.5	17.73
	5	2.5	29.55
	7	3.3	356

From Equation 7.6, we know that

$$\mu = \frac{\tau_o}{\dot{\gamma}} + k\dot{\gamma}^{n-1} \quad (7.18)$$

However,

$$\dot{\gamma} = \frac{u_b}{d_h} \quad (7.19)$$

(Margaritis et al. 1999) Thus, the bubble horizontal diameter dh is calculated using Equation 7.19.

Now to calculate the average bubble size db in the column, Reynolds number for Herschel-Bulkley model is calculated using Equation 7.20 (Madlener et al. 2009).

$$R_e = \frac{\rho {u_b}^{2-n} {d_h}^n}{\left(\frac{\tau_o}{8}\right)\left(\frac{d_h}{u_b}\right)^n + k\,(\frac{3m+1}{4m})^n\, 8^{n-1}} \quad (7.20)$$

Where,

$$m = \frac{nk(\frac{8u_b}{d_h})^n}{\tau_o + k(\frac{8u_b}{d_h})^n}$$

For non-Newtonian, shear thinning fluids, the drag coefficient (White and McDougall) (White and McDougall) is calculated using Equations 7.21 or 7.22 (Margaritis et al. 1999):

$$C_D = \frac{24}{R_e}\left(1 + 0.173\, {R_e}^{0.657}\right) + \frac{0.413}{1 + 16300 {R_e}^{-1.09}} \quad (R_e < 60) \quad (7.21)$$

$$C_D = 0.95 \quad (R_e > 60) \quad (7.22)$$

Now assuming CD∞= CD, the bubble size is calculated as

$$d_b = \sqrt[3]{\frac{3\, C_{D\infty}\, {d_h}^2 {u_b}^2}{4g}} \quad (7.23)$$

Thus, the calculated bubble diameter using Equation 7.23 for both the sludge concentration is shown in Table 7.5 (Bobade and Eshtiaghi 2018 Figshare-b).

Table 7.5: Average bubble diameter (m) for both 3% & 5% WAS at different gas flow rates

Gas flow rate, (L/min)	stress imposed at 3% WAS (Pa)	3% WAS Bubble diameter (db, mm)	Stress imposed at 5.5% WAS (Pa)	5.5% WAS Bubble diameter (db, mm)
1	4.5	1.42	1.0	-
3	7.8	1.4	3.1	-
5	10.0	1.3	4.1	2.1
7	14.5	0.7	5.2	2

From Table 7.5 it is clearly seen that bubble size decreases as the gas flow rate and stress imposed increases. However, at 5.5% because of sludge bed lifting the bubble size is not calculated for 1 LPM and 3 LPM of gas flow rate. Since, 5 LPM of gas flow rate was strong enough to escape without the bed lifting, we can see similar trend of decrease in bubble size with increase in gas flow rate from 5 LPM to 7 LPM. Moreover on plotting the bubble size against stress imposed by the gas injection (Figure 7.7), we can see that bubble size decreases exponentially with the stress and is given by Equation 7.24 with an error range of ± 5% Thus replacing the stress imposed by gas injection by Equation 7.8, a more simple equation for bubble diameter is developed as shown in Equation 7.25.

$$d_b = 0.035e^{-0.109(stress\ imposed)} \quad (7.24)$$

$$d_b = 0.0035 * e^{\left(\frac{\left(-0.00147*TS^2\right)}{TSS^2 * D_p}\right) * \mu_{(water)} * U_g - \left(\frac{-1.09*TS^2}{TSS}\right)} \quad (7.25)$$

Similar decrease in bubble size for sludge (0.05% solids concentration) with increase in superficial gas velocity was also observed by Jamshidi and Mostoufi (2017). Thus, the results presented in Table 7.5 and in Figures 7.4, 7.6 and 7.7 together also show that fluid rheology plays an important role in gas holdup, bubble rise velocity and bubble size. The increase in gas holdup also helps to decrease the mixing time within the bubble column

and increase efficiency. As the stress induced by gas injection in shear thinning fluid decreases the rheological properties and contribute to reduce mixing time was shown by Babaei et al. (2015a).

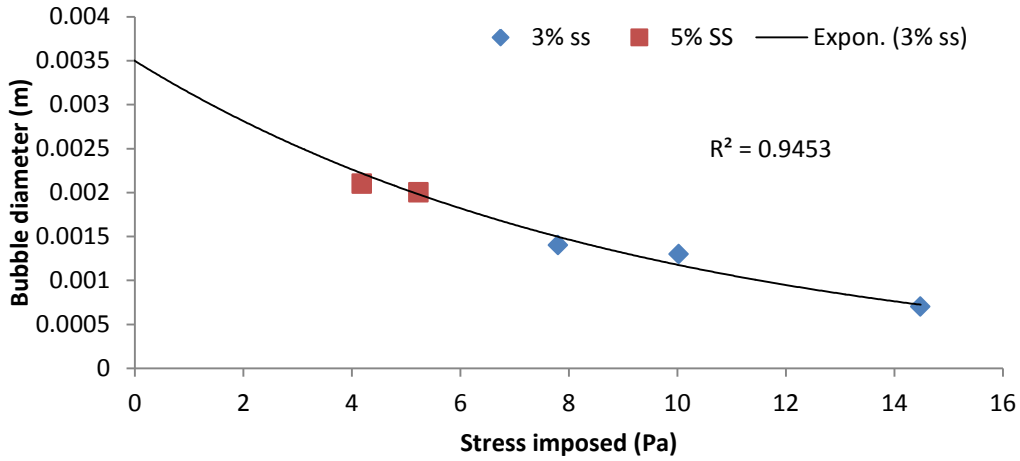

Figure 7.7: Impact of stress imposed on bubble size for 3% & 5% WAS

7.5 CONCLUSION

The impact of gas injection rate on bubble size at high solid concentration of waste activated sludge is explained. Gas holdup increases with increase in gas flow rate is shown. This increase in gas holdup is because stress imposed gas injection modifies the sludge and increases the gas liquid contact. However, as the total solids concentration increases the gas holdup decreases due to coalescence.

For the first time an effective shear rate calculation for the Herschel–Bulkley fluid using HB model is shown. Effective shear rate within the column increases with the increase in gas flow rate for the given concentration is observed. Additionally, a method is developed to calculate the bubble size in the fluid that best fits the Herschel–Bulkley model. A decrease in bubble size is observed with an increase in gas flow rate and with the stress imposed by gas. Moreover, a linear relation was seen for bubble rise velocity with gas holdup; also a linear correlation between the gas holdup and natural logarithm of stress imposed by gas injection was observed.

Thus knowledge of change in bubble size and bubble rise velocity with gas holdup in a bubble column of complex opaque fluid will help the design engineers to understand the

hydrodynamics at high concentration of sludge and optimised process for efficient operation effectively using ERT.

7.6 ACKNOWLEDGEMENT

The authors acknowledge South East Water support for providing sludge to carry out the research, and RMIT University to provide Australian Government Research Training Program Scholarship for V. Bobade.

7.7 NOMENCLATURE

u_b Bubble rise velocity (m/s)

H Height of the column (m)

t Time (s)

u_g Gas superficial velocity (m/s)

g gravitational constant, 9.81 (m/s^2)

ρ density (kg/m^3)

P Power Input (W),

v Volume (m^3)

K Consistency index (Pa.s^n)

n Flow behaviour index (-)

C_D Drag coefficient (-)

R_e Reynolds number (-)

d_b Bubble diameter (mm)

Greek Letters

τ Shear Stress (Pa)

τ_o Yield stress (Pa)

$\dot{\gamma}$ Shear rate (s^{-1})

$\sigma_{imposed}$ Stress imposed by gas injection (Pa)

μ Viscosity

d_h bubble horizontal diameter (m)

ε_g Gas holdup

σ_1 Conductivity of continuous phase (mS/cm)

σ_2 Conductivity of dispersed phase (mS/cm)

σ_{mc} average reconstructed conductivity by ERT measurements (mS/cm)

7.8 REFERENCES

Acharya, A. and Ulbrecht, J.J. (1978) Note on the influence of viscoelasticity on the coalescence rate of bubbles and drops. AIChE Journal 24(2), 348-351.

Ahimou, F., Semmens, M.J., Haugstad, G. and Novak, P.J. (2007) Effect of protein, polysaccharide, and oxygen concentration profiles on biofilm cohesiveness. Applied and environmental microbiology 73(9), 2905-2910.

Babaei, R., Bonakdarpour, B. and Ein-Mozaffari, F. (2015a) Analysis of gas phase characteristics and mixing performance in an activated sludge bioreactor using electrical resistance tomography. Chemical Engineering Journal 279, 874-884.

Babaei, R., Bonakdarpour, B. and Ein-Mozaffari, F. (2015b) The use of electrical resistance tomography for the characterization of gas holdup inside a bubble column bioreactor containing activated sludge. Chemical Engineering Journal 268, 260-269.

Bailey, R.A., Clark, H.M., Ferris, J.P., Krause, S. and Strong, R.L. (2002) Chemistry of the Environment (Second Edition). Bailey, R.A., Clark, H.M., Ferris, J.P., Krause, S. and Strong, R.L. (eds), pp. 415-442, Academic Press, San Diego.

Bajón Fernández, Y., Cartmell, E., Soares, A., McAdam, E., Vale, P., Darche-Dugaret, C. and Jefferson, B. (2015) Gas to liquid mass transfer in rheologically complex fluids. Chemical Engineering Journal 273, 656-667.

Baroutian, S., Eshtiaghi, N. and Gapes, D.J. (2013) Rheology of a primary and secondary sewage sludge mixture: Dependency on temperature and solid concentration. Bioresource Technology 140, 227-233.

Baudez, J.C. and Coussot, P. (2001) Rheology of aging, concentrated, polymeric suspensions: Application to pasty sewage sludges. Journal of Rheology 45(5), 1123-1140.

Baudez, J.C., Markis, F., Eshtiaghi, N. and Slatter, P. (2011) The rheological behaviour of anaerobic digested sludge. Water Research 45(17), 5675-5680.

Bo, J. and Lant, P. (2004) Flow regime, hydrodynamics, floc size distribution and sludge properties in activated sludge bubble column, air-lift and aerated stirred reactors. Chemical Engineering Science 59(12), 2379-2388.

Bobade, V., Baudez, J.C., Evans, G. and Eshtiaghi, N. (2017) Impact of gas injection on the apparent viscosity and viscoelastic property of waste activated sewage sludge. Water Research 114, 296-307.

Bobade, V. and Eshtiaghi, N. (2018) ERT data for 3% and 5.5% WAS, https://doi.org/10.6084/m9.figshare.7159040.

Bobade, V. and Eshtiaghi, N. (2018 Figshare) Dynamic time sweep measurement of sludge for four different concentrations (3%, 4%, 5% & 5.5%) at four different gas flow rates (1 Lpm to 7 LPM), https://figshare.com/s/87454a1b2f8b5ccaf03c.

Bobade, V., Evans, G., Baudez, J.C. and Eshtiaghi, N. (2018) Impact of gas injection on physicochemical properties of waste activated sludge: A linear relationship between the change of viscoelastic properties and the change of other physiochemical properties. Water Research 144, 246-253.

Capodaglio, A.G. (2017) Integrated, decentralized wastewater management for resource recovery in rural and peri-urban areas. Resources 6(2), 22.

Cerri, M.O., Futiwaki, L., Jesus, C.D.F., Cruz, A.J.G. and Badino, A.C. (2008) Average shear rate for non-Newtonian fluids in a concentric-tube airlift bioreactor. Biochemical Engineering Journal 39(1), 51-57.

Chisti, Y. and Moo-Young, M. (1989) On the calculation of shear rate and apparent viscosity in airlift and bubble column bioreactors. Biotechnology and Bioengineering 34(11), 1391-1392.

Curvers, D., Saveyn, H., Scales, P.J. and Van der Meeren, P. (2009) A centrifugation method for the assessment of low pressure compressibility of particulate suspensions. Chemical Engineering Journal 148(2-3), 405-413.

Dai, X., Gai, X. and Dong, B. (2014) Rheology evolution of sludge through high-solid anaerobic digestion. Bioresour Technology 174, 6-10.

Daily, W., Ramirez, A., Binley, A. and LeBrecque, D. (2004) Electrical resistance tomography. The Leading Edge 23(5), 438-442.

Dekée, D., Carreau, P.J. and Mordarski, J. (1986) Bubble velocity and coalescence in viscoelastic liquids. Chemical Engineering Science 41(9), 2273-2283.

Dziubiński, M., Orczykowska, M. and Budzyński, P. (2003) Comments on bubble rising velocity in non-Newtonian liquids. Chemical Engineering Science 58(11), 2441-2443.

Eshtiaghi, N., Markis, F., Yap, S.D., Baudez, J.C. and Slatter, P. (2013) Rheological characterisation of municipal sludge: A review. Water Research 47(15), 5493-5510.

Esmaeili, A., Guy, C. and Chaouki, J. (2015) The effects of liquid phase rheology on the hydrodynamics of a gas–liquid bubble column reactor. Chemical Engineering Science 129, 193-207.

Fatone, F., Di Fabio, S., Bolzonella, D. and Cecchi, F. (2011) Fate of aromatic hydrocarbons in Italian municipal wastewater systems: An overview of wastewater treatment using conventional activated-sludge processes (CASP) and membrane bioreactors (MBRs). Water Research 45(1), 93-104.

Feng, X., Tang, B., Bin, L., Song, H., Huang, S., Fu, F., Ding, J., Chen, C. and Yu, C. (2016) Rheological behavior of the sludge in a long-running anaerobic digestor: Essential factors to optimize the operation. Biochemical Engineering Journal 114, 147-154.

Fransolet, E., Crine, M., Marchot, P. and Toye, D. (2005) Analysis of gas holdup in bubble columns with non-Newtonian fluid using electrical resistance tomography and

dynamic gas disengagement technique. Chemical Engineering Science 60(22), 6118-6123.

Henze, M.A. and Henze, M. (1997) Wastewater treatment : biological and chemical processes, Springer, Berlin, Heidelberg, [Germany].

Henzler, H.-J. (1980) Begasen höherviskoser Flüssigkeiten. Chemie Ingenieur Technik 52(8), 643-652.

Henzler, H. and Kauling, J. (1985) Scale-up of mass transfer in highly viscous liquids. Wurzberg, Germany. BHRA, Cranfield. p, 303-312.

Jamshidi, N. and Mostoufi, N. (2017) Measurement of bubble size distribution in activated sludge bubble column bioreactor. Biochemical Engineering Journal 125(Supplement C), 212-220.

Jin, H.-R., Lim, D.H., Lim, H., Kang, Y., Jung, H. and Kim, S.D. (2012) Demarcation of large and small bubbles in viscous slurry bubble columns. Industrial & Engineering Chemistry Research 51(4), 2062-2069.

Jin, H., Wang, M. and Williams, R.A. (2007) Analysis of bubble behaviors in bubble columns using electrical resistance tomography. Chemical Engineering Journal 130(2–3), 179-185.

Kawase, Y. and Moo-Young, M. (1986) Liquid phase mixing in bubble columns with Newtonian and non-Newtonian fluids. Chemical Engineering Science 41(8), 1969-1977.

Khalili, F., Jafari Nasr, M.R., Kazemzadeh, A. and Ein-Mozaffari, F. (2018a) Analysis of gas holdup and bubble behavior in a biopolymer solution inside a bioreactor using tomography and dynamic gas disengagement techniques. Journal of Chemical Technology & Biotechnology 93(2), 340-349.

Kulkarni, A.A. and Joshi, J.B. (2005) Bubble Formation and Bubble Rise Velocity in Gas-Liquid systems -A Review. Industrial & Engineering Chemistry Research 44, 5873 - 5931.

Lind, S.J. and Phillips, T.N. (2010) The effect of viscoelasticity on a rising gas bubble. Journal of Non-Newtonian Fluid Mechanics 165, 852-865.

Madlener, K., Frey, B. and Ciezki, H.K. (2009) Generalized reynolds number for non-newtonian fluids. EUCASS Proceedings Series – Advances in AeroSpace Sciences 1, 237-250.

Margaritis, A., Te Bokkel, D.W. and Karamanev, D.G. (1999) Bubble rise velocities and drag coefficients in non-Newtonian polysaccharide solutions. Biotechnology and Bioengineering 64(3), 257-266.

Nishikawa, M., Kato, H. and Hashimoto, K. (1977) Heat transfer in aerated tower filled with non-Newtonian liquid. Industrial & Engineering Chemistry Process Design and Development 16(1), 133-137.

Sánchez Pérez, J.A., Rodríguez Porcel, E.M., Casas López, J.L., Fernández Sevilla, J.M. and Chisti, Y. (2006) Shear rate in stirred tank and bubble column bioreactors. Chemical Engineering Journal 124(1–3), 1-5.

Schumpe, A. and Deckwer, W.-D. (1987) Viscous media in tower bioreactors: Hydrodynamic characteristics and mass transfer properties. Bioprocess Engineering 2, 79 - 94.

Shimizu, K., Takada, S., Takahashi, T. and Kawase, Y. (2001) Phenomenological simulation model for gas hold-ups and volumetric mass transfer coefficients in external-loop airlift reactors. Chemical Engineering Journal 84(3), 599-603.

Warsito, W. and Fan, L.S. (2001) Measurement of real-time flow structures in gas–liquid and gas–liquid–solid flow systems using electrical capacitance tomography (ECT). Chemical Engineering Science 56(21), 6455-6462.

White, P. and McDougall, F.R. (2001) Integrated solid waste management : a life cycle inventory, Blackwell Science, Oxford, UK ; Malden, MA.

CHAPTER 8: INDUSTRIAL IMPLICATIONS

8.1 INTRODUCTION

The rheological properties of sludge are significant parameters in the design and optimisation of wastewater pumping and mixing systems and membrane bioreactor operation, as highlighted in many studies (Dentel 1997, Eshtiaghi et al. 2013, Feng et al. 2016, Laera et al. 2007, Meng et al. 2009, Menniti et al. 2009, Ratkovich et al. 2013, Rosenberger et al. 2002, Sanin et al. 2011, Van Kaam et al. 2006, Yang et al. 2009). Aeration is the key to WAS treatment, accounting for 60–75% of the total energy consumption of wastewater treat plants. This study was designed to reveal how gas injection affects concentrated sludge rheology and any relationship between the rheology and physicochemical properties of sludge and gas phase characteristics. An online rheometer measures shear stress vs. shear rate and the viscoelastic properties of sludge (Konigsberg et al. 2013), and it is possible to use these data to control the aeration system in a WAS process.

As shown in the results and discussion chapters, gas injection imposes extra stress and affects the viscoelastic properties of sludge. This extra stress imposed by gas injection has a linear relation with the percentage change in physicochemical properties such as sCOD, zeta potential, and suspended solids. In the same way, gas phase characteristics such as bubble size and bubble rise velocity were shown to have a linear relationship with the stress imposed, whereas gas holdup was shown to have a linear relationship with the natural log of the stress imposed by gas injection. Therefore, online rheometer that can provide data on imposed stress can be utilised to control important parameters such as TSS and sCOD for a better and more efficient WAS treatment process. The following sections describe the relationship between important physiochemical properties of sludge and the operation of wastewater treatment plants.

8.2 CHANGE IN VISCOELASTIC PROPERTIES

In the results and discussion chapters, it was shown that gas injection significantly alters the viscoelastic properties of sludge through structural changes. Many materials exhibit a viscoelastic behaviour and the area of study is relevant to many applications in different industries such as concrete technology, geology, polymers and composites, plastic

processing, paint flow, cosmetics, and adhesives (De Vicente 2012). Viscoelastic properties are important to predict the physical-chemical stability of the fluid.

Sludge viscoelastic properties have a significant impact on sludge management and treatment. Viscoelastic properties are important to understand the sludge physico-chemical properties, dewaterability and filterability, permeability and compressibility that are related to sludge settling, drying and mixing applications in waste water industry (Wang et al. 2017).

Furthermore, viscoelastic properties are inversely related to the water activity in the sludge structure; a decrease in the viscoelastic properties of sludge means an increase in the water activity – the amount of free water[2] available within the sludge structure (Agoda-Tandjawa et al. 2013). Thus, knowing the percentage change in viscoelastic properties with change in the gas injection intensity enables understanding of the amount of water activity and its use as a parameter to evaluate sludge structural strength and its foaming and dewaterability potential. Decrease in viscoelastic properties (storage and loss modulus) indicates that water is becoming more accessible (i.e. some water is released from flocs). Miryahyaei et al. (2018) showed that dewaterability improves when storage and loss modulus decreases. Therefore, at any solid concentration of sludge, an increase in the gas injection rate improves dewaterability. Furthermore, decreases in the storage and loss modulus indicate change in sludge structure at micro and macro level, which happens as a result of the solubilisation. Increased content of extracellular components in liquor as a result of solubilisation increases the likelihood of foaming.

8.3 STRESS IMPOSED BY GAS INJECTION

That gas injection imposes extra shear on sludge was proved in this research by observing significant changes in the viscoelastic properties of sludge. This extra stress imposed increased with increase in gas injection intensity, as discussed in chapter 5. Additionally, a simple model was developed, based on the sludge concentration and gas velocity, to calculate the stress imposed by gas injection. Knowledge of the stress imposed by gas injection (or in other words, the corresponding shear rate) is important because the shear

[2] The types of water in sludge are free water (water which is not associated with solid particles); bound water (water molecules that are bound to each other due to strong electrical polarity); interstitial water (water trapped in the sludge floc space and organisms); and surface water (water held on the surface of solid particles due to adhesion or adsorption), in amounts depending on the type of sludge and its consistency

rate influences power consumption, mixing characteristics and mass transfer phenomena in aerators. Energy consumption changes in a power relationship with shear imposed either through aeration or mechanical mixing (Buzatu et al. 2017). In addition, Buzatu et al. (2017) showed that the energy demand changes with the change in rheological properties for power law fluids.

8.3.1 STRESS IMPOSED BY GAS INJECTION AND CHANGE IN SUSPENDED SOLIDS

Percentage change in suspended solids due to gas injection has a linear relation with the stress imposed, as demonstrated in chapter 5. In waste activated sludge treatment, suspended solids (TSS) are important parameters that are measured to ensure that the biological treatment process runs efficiently. If the solid content is too high, then there is a risk that the system will become overloaded, requiring more oxygen to be provided. Moreover, when the system is overloaded, the oxygen flow rate is insufficient for adequate mixing, and some kind of mechanical mixing is required, which requires more energy. If the solid content drops too low, the biological agents will run out of "food" and start to die, leading to a fall in the efficiency of the process (Angus Fosten 2016). Additionally, insufficient dissolved oxygen (DO) and overloading causes foaming in the activated sludge process. Thus, knowing the change in suspended solids with the stress imposed by gas injection helps wastewater treatment engineers to optimise the aeration rate, minimise energy consumption and increase oxygen transfer efficiency.

8.3.2 STRESS IMPOSED BY GAS INJECTION AND CHANGE IN SCOD

Soluble organic matter (sCOD) is a critical parameter for estimating and optimising the performance of a biological wastewater treatment process (Hayet et al. 2016). The sCOD content is also used to determine the amount of oxygen required for biodegradation in the aeration tank (Henze and Henze 1997), so knowing the change in sCOD due to gas injection will assist in optimising the aeration rate. This is because the shear induced by gas injection affects floc structure and releases EPS, which eventually increases the soluble contents within the sludge. Moreover, as the increase in sCOD indicates an increase in soluble contents, it plays a crucial role in the kinetic activity, flocculating and settling properties of sludge (Azami et al. 2012, Ladewig and Al-Shaeli 2016). The released sCOD is also used as a measure of foulants in membrane bioreactors (Meng et al. 2007, Meng et al. 2006). Thus, monitoring the change in sCOD with the stress imposed

can help to improve the oxygen transfer efficiency and efficiency of the membrane bioreactor.

8.3.3 STRESS IMPOSED BY GAS INJECTION AND CHANGE IN ZETA POTENTIAL

Zeta potential is a key factor in the performance of physical processes such as flocculation and sedimentation (Sze et al. 2003). A more negative zeta potential value indicates a solution which is more dispersed and may require a long time for the particles to settle. Thus, zeta potential measurements can be used successfully to monitor plant coagulant dosages. Understanding the change in zeta potential with the stress imposed by gas injection will assist in understanding the coagulation and flocculation ability of sludge within the aeration tank and allow optimisation of the coagulant dosages needed for clarification.

8.4 IMPACT OF STRESS IMPOSED ON GAS PHASE CHARACTERISTICS

Gas phase characteristics are important because they directly affect the mass transfer and fluid flow pattern within the aeration tank. Most of the studies in the literature were carried out using a model fluid for sludge like Xanthan gum in order to obtain flow behaviour similar to that of sludge. Additionally, Xanthan gum is used to identify stagnant zones and mixing in large industrial vessels (anaerobic digesters, thickeners). However, when the researcher compared the rheological behaviour of the linear viscoelastic region for aerated Xanthan gum with that of sludge, they were observed to be Very different. Thus, although measurement of gas phase characteristics is much easier and accurate using Xanthan gum than sludge due to the former being a stable and clear fluid, its different behaviour in the linear viscoelastic region indicates that it is not a suitable model fluid for sludge below yielding point.

Gas holdup measurement in sludge is an important parameter in aerobic waste water treatment processes. If it is too high or too low, it can adversely affect the process efficiency of aerobic biochemical reactors (Hofmeester 1988). The increase in gas injection rate increases the gas holdup in sludge; that is, gas holdup increases the stress imposed. Effective shear rate is another parameter used in the design of aerobic fermenters for viscous non-Newtonian systems (Cerri et al. 2008). If the effective shear rate, which is a function of fluid physical properties and the intensity of mixing, is not selected correctly, it may cause physical damage to delicate micro-organisms and reduce

the efficiency of the process. In aerobic fermenters, micro-organisms utilise oxygen to break down complex organic compounds into simpler compounds, but their ability to do this in impaired by high shear.

Effective viscosity (μ_{eff}), which is calculated at effective shear rate, is a design parameter widely used in the literature to correlate mass transfer and hydrodynamics, such as mixing and pumping parameters in viscous non-Newtonian systems (Al-Masry and Chetty 1997). The research described in this thesis included an effective shear rate calculation for the HB fluid using the HB model –the first time this has ever been performed. It was shown that the effective shear rate within the column increases with the increase in the gas flow rate at a given concentration and decreases with increasing solid concentrations. Thus, knowing the change in the effective shear rate with the change in the gas flow rate and solids concentration will enable engineers to accurately optimise the hydrodynamic parameters for the HB fluid to maintain good mass transfer as well as healthy micro-organisms.

In addition, the researcher developed a method for calculating the bubble size in the fluid that best fits the HB model. Calculating the effective shear rate using the HB model eliminates the disparity among the predictions of $\dot{\gamma}$ that are based on either the power-law model or the assumption that the fluid behaves as a Newtonian fluid. This is because the degree of turbulence in a reactor depends not only on the power input but the momentum transport characteristics of the fluid itself, that is, the motion of dispersed fluid within the stationary fluid. Moreover, the fluid flow pattern in a bubble column is affected by the rheological properties of the liquid, especially when using highly viscous non-Newtonian fluids, and strongly influences phase mixing and transfer parameters.

The researcher observed a linear correlation between the gas holdup and the natural logarithm of stress imposed by gas injection, and a linear relation between bubble rise velocity and gas holdup. These results are important due to the multifold significance of gas phase characteristics in the aeration tank. The gas holdup determines the residence time of the gas in the liquid, and in combination with the bubble size, it controls the gas–liquid interfacial area available for mass transfer. It also predetermines the reactor design, because the total volume of the reactor for any range of operating conditions depends on the maximum holdup that must be accommodated. Similarly, bubble rise velocity determines the operation time of the column, contact time of the gas and liquid phase.

8.5 CONCLUSION

This chapter shows how the knowledge developed in this research and described in this thesis can be utilised by the wastewater industry to design and optimise wastewater treatment processes. A procedure outlined in this thesis enables calculation of the stress imposed by gas injection using rheological measurements in the linear viscoelastic region. Additionally, this thesis provides information about the physiochemical properties of sludge, and the relationship between gas phase characteristics and the stress imposed for concentrated waste activated sludge. For example, it was shown how from the correlation between the stress imposed by gas injection and the percentage change in physicochemical properties like suspended solids and sCOD, the speed of an aerator can be automatically controlled to optimise the energy requirements of pumps and mixers to increase the efficiency of the treatment process.

8.6 REFERENCES

Agoda-Tandjawa, G., Dieudé-Fauvel, E., Girault, R. and Baudez, J.C. (2013) Using water activity measurements to evaluate rheological consistency and structure strength of sludge. Chemical Engineering Journal 228, 799-805.

Al-Masry, W.A. and Chetty, M. (1997) On the estimation of effective shear rate in external loop airlift reactors: non-Newtonian fluids*. Studies in Environmental Science 66, 153-166.

Angus Fosten (2016) How & why we measure suspended solids, https://www.partech.co.uk/how-why-we-measure-suspended-solids/, Britain.

Azami, H., Sarrafzadeh, M.H. and Mehrnia, M.R. (2012) Soluble microbial products (SMPs) release in activated sludge systems: a review. Iranian Journal of Environmental Health Science & Engineering 9(1), 30-30.

Buzatu, P., Qiblawey, H., Nasser, M. and Judd, S. (2017) Comparative power demand of mechanical and aeration imposed shear in an immersed membrane bioreactor. Water Research 126, 208-215.

Cerri, M.O., Futiwaki, L., Jesus, C.D.F., Cruz, A.J.G. and Badino, A.C. (2008) Average shear rate for non-Newtonian fluids in a concentric-tube airlift bioreactor. Biochemical Engineering Journal 39(1), 51-57.

Choi, M., Park, K. and Oh, T. (2016) Viscoelastic properties of fresh cement paste to study the flow behavior. International Journal of Concrete Structures and Materials 10(3), 65-74.

De Vicente, J. (2012) Viscoelasticity: From Theory to Biological Applications, BoD–Books on Demand.

Dentel, S.K. (1997) Evaluation and role of rheological properties in sludge management. Water Science and Technology 36(11), 1-8.

Eshtiaghi, N., Markis, F., Yap, S.D., Baudez, J.C. and Slatter, P. (2013) Rheological characterisation of municipal sludge: A review. Water Research 47(15), 5493-5510.

Feng, X., Tang, B., Bin, L., Song, H., Huang, S., Fu, F., Ding, J., Chen, C. and Yu, C. (2016) Rheological behavior of the sludge in a long-running anaerobic digestor: Essential factors to optimize the operation. Biochemical Engineering Journal 114, 147-154.

Hayet, C., Saida, B.-A., Youssef, T. and Hédi, S. (2016) Study of biodegradability for municipal and industrial Tunisian wastewater by respirometric technique and batch reactor test. Sustainable Environment Research 26(2), 55-62.

Henze, M.A. and Henze, M. (1997) Wastewater treatment: biological and chemical processes, Springer, Berlin, Heidelberg, [Germany].

Jones, P.D.G.M. and Sanks, P.P.R.L. (2008) Pumping Station Design: Revised 3rd Edition, Elsevier Science.

Konigsberg, D., Nicholson, T., Halley, P., Kealy, T. and Bhattacharjee, P. (2013) Online process rheometry using oscillatory squeeze flow. Applied Rheology 23(3).

Kumar, B. (2010) Energy dissipation and shear rate with geometry of baffled surface aerator. Chemical Engineering Research Bulletin 14(2), 92-96.

Ladewig, B. and Al-Shaeli, M.N.Z. (2016) Fundamentals of Membrane Bioreactors: Materials, Systems and Membrane Fouling, Springer, Singapore, Singapore.

Laera, G., Giordano, C., Pollice, A., Saturno, D. and Mininni, G. (2007) Membrane bioreactor sludge rheology at different solid retention times. Water Research 41(18), 4197-4203.

Meng, F., Chae, S.-R., Drews, A., Kraume, M., Shin, H.-S. and Yang, F. (2009) Recent advances in membrane bioreactors (MBRs): Membrane fouling and membrane material. Water Research 43(6), 1489-1512.

Meng, F., Shi, B., Yang, F. and Zhang, H. (2007) New insights into membrane fouling in submerged membrane bioreactor based on rheology and hydrodynamics concepts. Journal of Membrane Science 302(1–2), 87-94.

Meng, F., Zhang, H., Yang, F., Zhang, S., Li, Y. and Zhang, X. (2006) Identification of activated sludge properties affecting membrane fouling in submerged membrane bioreactors. Separation and Purification Technology 51(1), 95-103.

Menniti, A., Kang, S., Elimelech, M. and Morgenroth, E. (2009) Influence of shear on the production of extracellular polymeric substances in membrane bioreactors. Water Research 43(17), 4305-4315.

Miryahyaei, S., Olinga, K., Muthalib, F.A.A., Das, T., Aziz, M.S.A., Othman, M., Baudez, J.C., Batstone, D. and Eshtiaghi, N. (2018) Impact of rheological properties of substrate on anaerobic digestion and digestate dewaterability: New insights through rheological and physico-chemical interaction. Water Research 150, 56-67.

Ratkovich, N., Horn, W., Helmus, F.P., Rosenberger, S., Naessens, W., Nopens, I. and Bentzen, T.R. (2013) Activated sludge rheology: A critical review on data collection and modelling. Water Research 47(2), 463-482.

Rosenberger, S., Kubin, K. and Kraume, M. (2002) Rheology of activated sludge in membrane bioreactors. Engineering in Life Sciences 2(9), 269-275.

Sanin, F.D., Clarkson, W.W. and Vesilind, P.A. (2011) Sludge engineering: the treatment and disposal of wastewater sludges, DEStech Publications, Inc.

Sze, A., Erickson, D., Ren, L. and Li, D. (2003) Zeta-potential measurement using the Smoluchowski equation and the slope of the current–time relationship in electroosmotic flow. Journal of Colloid and Interface Science 261(2), 402-410.

Van Kaam, R., Anne-Archard, D., Alliet, M., Lopez, S. and Albasi, C. (2006) Aeration mode, shear stress and sludge rheology in a submerged membrane bioreactor: some keys of energy saving. Desalination 199(1-3), 482-484.

Wang, H.-F., Ma, Y.-J., Wang, H.-J., Hu, H., Yang, H.-Y. and Zeng, R.J. (2017) Applying rheological analysis to better understand the mechanism of acid conditioning on activated sludge dewatering. Water Research 122, 398-406.

Yang, F., Bick, A., Shandalov, S., Brenner, A. and Oron, G. (2009) Yield stress and rheological characteristics of activated sludge in an airlift membrane bioreactor. Journal of Membrane Science 334(1–2), 83-90.

CHAPTER 9: CONCLUSION AND RECOMMENDATIONS

9.1 CONCLUSIONS

Aeration is an integral part of the WAS treatment process. It provides oxygen to microorganisms to enable them to degrade pollutant components and promotes microbial growth in the wastewater. An ample and evenly distributed oxygen supply in an aeration system is the key to rapid, economically viable and effective wastewater treatment. Thus, the aim of this study was to understand the influence of the gas injection rate on sludge rheological properties; physicochemical properties like suspended solids, surface tension, sCOD and zeta potential; and gas phase characteristics like bubble rise velocity, gas holdup and bubble size. Additionally, the researcher strove to identify relationships between the changes in rheological properties and gas phase characteristics.

This chapter summarises the major findings of this research project and provides ideas for future study in this field of research. The major findings of this thesis are described in the following sections.

- The research showed that the in situ method is not an accurate technique for measuring rheological properties in aerated systems, leading to the development of a world-first method for rheological measurement while gas is injected into a fluid. In study 1, which investigated how gas injection affects the apparent viscosity and viscoelastic properties of WAS, the viscosity curves of in situ and after sparging measurement showed a huge difference in viscosity values at low shear rate range. Rising gas bubbles close to the rotating bob cause slippage and thus yields a much lower viscosity measurement with the in situ method than the after sparging method.

  A creep test and dynamic measurement (time sweep) proved that gas injection induces shear in sludge. The increase in tan (delta) and the decrease in the elastic and viscous modulus of sludge by increasing the gas flow rate indicate weakening sludge structure. This was also proved by ESEM images of sludge showing that bubbling modified the sludge structure.

- The results suggest that although gas bubbling induces extra shear, it is not enough to break down the structure completely and reduce the viscosity of sludge significantly. However, the impact of bubbles on the viscoelastic properties of sludge was notable.

Also, for the first time, a technique for finding an unaerated simulant of an aerated system with a similar elastic property was established. The gas flow rate induced shear, and the intensity of the induced shear increased linearly with increasing gas velocity. However, for the same gas flow rate, the shearing intensity decreased with increasing total solids concentration of sludge. Additionally, it was shown that the extra stress induced by gas injection can be predicted using a simple model based on sludge concentration and gas velocity (chapters 4 and 5).

- In study 2, the impact of gas injection on the physiochemical properties of sludge was explained. Gas injection had a substantial impact on sCOD, suspended solids and zeta potential, with a linear relationship observed between the percentage change in these parameters and the increase in stress induced by gas injection. This change in physiochemical properties is due to breakdown of the floc structure. The decrease in zeta potential values also proved that gas injection modifies the sludge surface by changing the stability of the system, which in turn increases the surface tension linearly with increase in gas velocity (chapter 5).

- Study 3 compared the rheological behaviour of a model fluid of sludge (Xanthan gum) after aeration with the behaviour of aerated WAS. The flow curve showed negligible change in the apparent viscosity of Xanthan gum solution as the gas injection flow rate increased. However, in the linear viscoelastic region, the creep test and time sweep test proved that gas injection increased the storage and loss modulus, which is an indication of the strengthening of molecular structure. This could be due to deformation of the molecular structure of Xanthan gum and increased crosslinking within an extended structure, resulting in higher resistance to stress and more solid-like behaviour in the linear viscoelastic region. Thus, although Xanthan gum behaves similarly to the sludge in the liquid regime, its behaviour is unlike that of sludge in the solid regime during gas injection, which means Xanthan gum is unsuitable as a model fluid for sludge under gas injection below the yield stress point (Chapter 6).

- In study 4, the impact of the solids concentration and gas flow rate on gas phase characteristics such as gas holdup, bubble rise velocity and bubble size was investigated. The results showed that gas holdup increases with increasing gas flow rate, because stress imposed by gas injection modifies the sludge structure and increases the gas–liquid contact. However, as TS increases, the gas holdup decreases due to coalescence.

This part of the research involved the first ever use of an effective shear rate calculation for a HB fluid. It showed that effective shear rate within the column increases with increased gas flow rate for a given concentration and decreases with increased solid concentration. Additionally, a method was developed to calculate the bubble size in the fluid that best fits the Herschel–Bulkley fluids. A decrease in bubble size was observed to occur as the gas flow rate and the stress imposed by the gas increased. Finally, the research showed that gas holdup, bubble rise velocity and bubble size have a natural log, linear, and exponential relationship with the stress imposed by gas injection, respectively.

9.2 RECOMMENDATIONS FOR FURTHER RESEARCH

- The research presented herein constitutes the most detailed study to date of the impact of gas injection on WAS. However, it is also important to study the impact of gas injection on the rheology and physicochemical properties of digested sludge, because gas mixing is done in digesters to increase biogas production efficiency. Gas mixing helps to reduce the dead zone volume of reactors. Thus, research on the impact of gas injection on digested sludge rheology and physicochemical properties can be used to optimise digester design.

- Future researchers could extend this study to investigate the impact of higher gas flow rates, equivalent to actual industrial aeration rates, on sludge rheology, physicochemical properties and gas phase characteristics. This will help to optimise aeration rates and reduce energy consumption, which is 50–90% of the total electrical consumption in wastewater plants.

- While nitrogen gas was used in this study for calculating the stress imposed and its impact on the physical properties of sludge, it would be useful to measure the amount of stress imposed at different gas flow rates and solids concentrations of sludge using oxygen injection. Measurement and calculation of oxygen transfer efficiency with different gas flow rates would be of interest to the wastewater treatment industry. This knowledge would improve understanding of processes within aeration tanks and digesters if oxygen is utilised instead of nitrogen and linked to the stress imposed by gas.

- In this study the bed lifting issue was observed at higher concentration and low gas flow rate, which is very similar to the problem that is observed in wastewater treatment lagoons. Thus, the current study could be extended by modifying the reactor design, for example, its height, to see at what gas flow rate bed lifting does not take place, or to

observe the height at which the bed falls back at different concentrations and gas flow rates.

- In the linear viscoelastic regime, Xanthan gum showed an increase in G' with an increase in the gas flow rate. This study could be extended at higher gas flow rates to see if G' still increases or if there is a critical flow rate at which G' will start to reduce. This would provide an understanding of whether Xanthan gum behaves similarly to sludge after the critical gas flow rate is reached.

- In this study, Xanthan gum was shown to be unsuitable as a model fluid for sludge during gas injection. Future researchers could examine the rheological properties of other clear model fluids – such as Carbopol® gel – in the linear viscoelastic region after gas injection. Transparency enables more accurate correlations and observations of bubble behaviour in complex non-Newtonian fluids.

- This study could also be extended by modifying the wastewater aeration process, for example, using spray drying. Spraying the sludge in the air instead of injecting air into it might reduce energy consumption and increase the efficiency of the aerobic digestion process.

APPENDIX I: METHOD USED TO DETERMINE THE OPTIMUM DURATION OF GAS INJECTION

The impact of gas injection on viscosity was measured because viscosity is a very common parameter for wastewater treatment process design and directly affects the efficiency of the aeration process. However, using the after sparging method, 20 minutes of gas injection had negligible impact on viscosity. To ensure that the duration of injection was sufficient to reach the conclusion that gas injection has negligible impact on gas injection; the test was repeated after injecting gas for 40 minutes. Further, in comparing the viscosity curve of 3% WAS aerated sludge (for 20 and 40 minutes of gas injection) to the viscosity curve for non-aerated sludge, negligible change in viscosity was observed, as shown in Figure A1. Thus, 20 minutes of gas injection was proved to be the optimum time of gas injection.

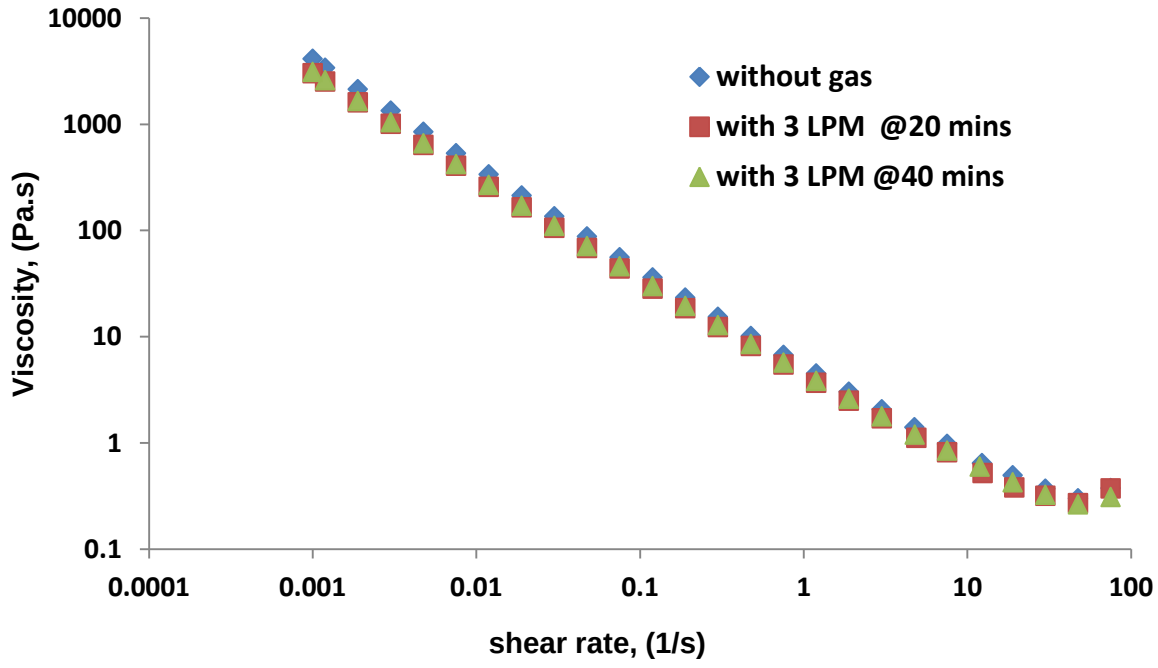

FIGURE A1: COMPARISON OF VISCOSITY CURVES OF AERATED 3% WASTE ACTIVATED SLUDGE AT 20 MINUTES AND 40 MINUTES OF GAS INJECTION WITH THAT OF NON-AERATED SLUDGE.

APPENDIX II: MEASUREMENT OF IMPACT OF GAS INJECTION ON DIGESTED SLUDGE RHEOLOGY AND PHYSICOCHEMICAL PROPERTIES

A2.1 INTRODUCTION

In recent years, environmental engineers and scientists have gradually developed anaerobic digestion technology that produces biogas from solid waste as a source of clean and green energy. Sufficient mixing is essential to increase the efficiency and the quality of product sludge (Monteith and Stephenson 1978). Proper mixing or agitation is vital to homogenise the contents of digesters, to ensure uniform distribution of substrates and microorganism cultures, to avoid settling of the heavy solid particles to the bottom, to avoid flotation of biomass at the surface of the slurry, and to maintain the pH and temperature of the slurry at optimal levels for microbial processes (Vesvikar and Al-Dahhan 2005). Therefore, it is important to understand the impact of gas injection on the physicochemical properties of digested sludge (such as sCOD and zeta potential), because this allows determination of the sludge's stability and settleability and eventually how its rheological properties will change. To confirm that gas injection imposes extra shear on digested sludge and affects the physicochemical properties of sludge, this study focused on measurement of rheological and physicochemical properties. Rheological measurements (the time sweep test), sCOD measurement and zeta potential measurement were carried out as described in chapter 3.

A2.2 SAMPLE PREPARATION

Digested sludge with 2 wt% was collected from a wastewater treatment plant (Melbourne Water Treatment Plant) in eastern Victoria, Australia. The sludge was thickened to a higher concentration (6%) using a centrifuge at 7^{o}C and 8000 rpm (i.e., at 12,200g maximum relative centrifugal force) for 40 minutes. Homogeneous samples of 4.0%, & 5.0% TS concentration were prepared by diluting the 6% concentrated sludge with the original sample.

A2.3 RESULTS AND DISCUSSION

A2.3.1 Influence of gas injection on the viscoelastic properties of digested sludge

The oscillatory time sweep test was carried out in the linear viscoelastic region at low applied sinusoidal strain at different gas injection rates. Both the storage modulus (G') and loss modulus (G″) decreased when the gas flow rate increased. The viscoelastic modulus [storage modulus (G′) & loss modulus (G″)] vs. time at two solid concentrations was plotted as shown in Fig. A2.1 (A&B). The decrease in storage and loss modulus indicated that gas injection influenced the sludge structure and imposed additional shear similar to that of WAS.

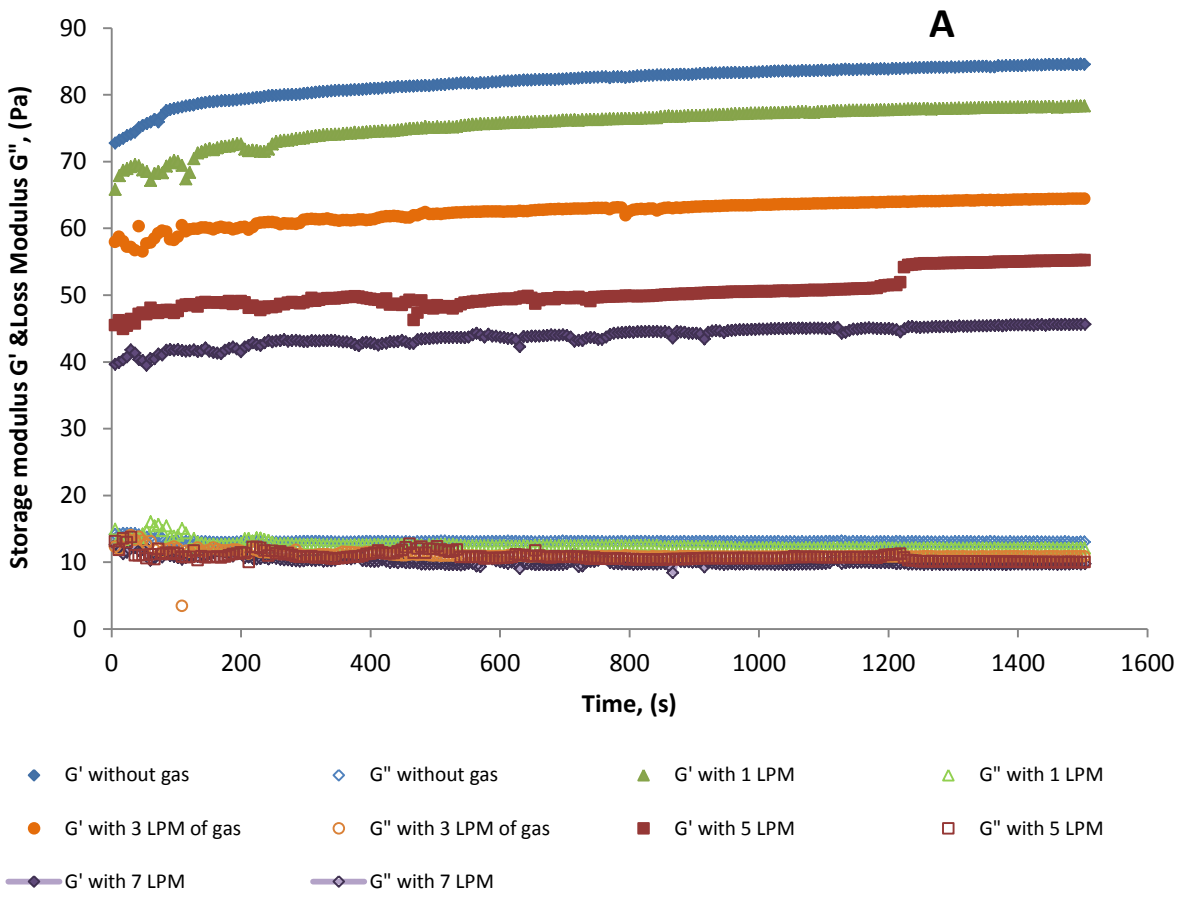

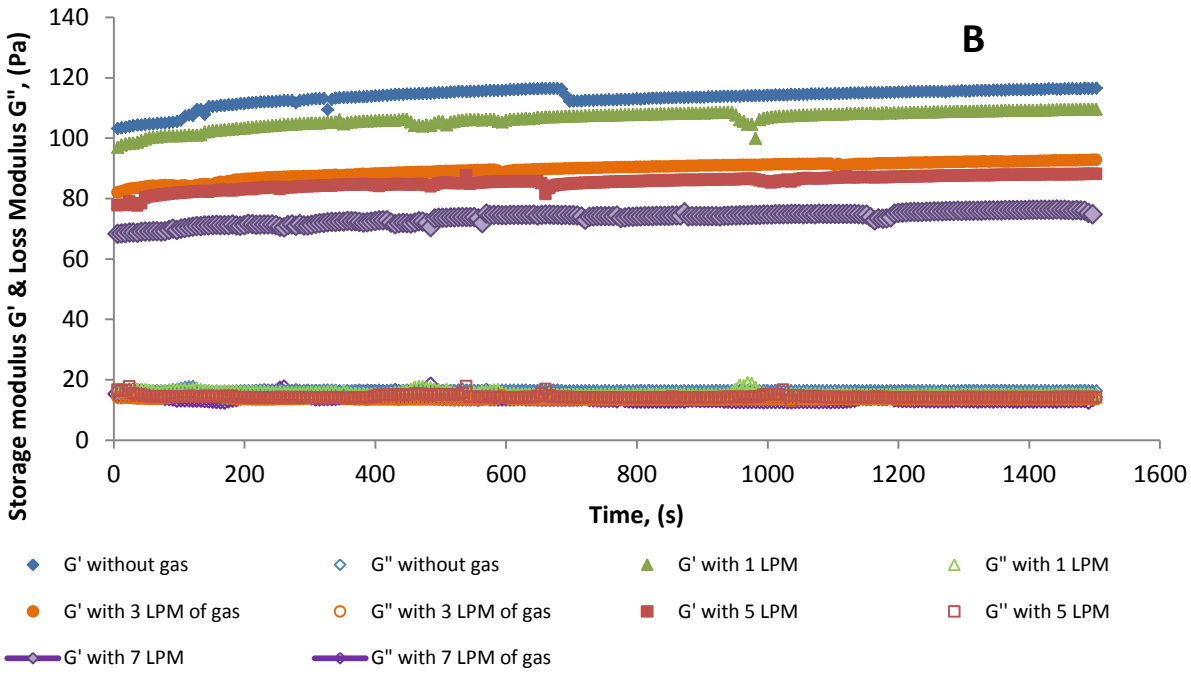

FIGURE A2. 1: IMPACT OF GAS INJECTION ON DIGESTED SLUDGE AT FOUR DIFFERENT GAS FLOW RATES (1–7LPM) MEASURED USING A TIME SWEEP TEST WITH (A) 4% & (B) 5% TOTAL SOLIDS CONTENT.

A2.3.2 Stress imposed by gas injection

Since gas injection was proved to influence the viscoelastic properties of the digested sludge, similar to that of WAS, the stress imposed by gas injection on digested sludge was calculated, using Equation A2.1.

$$\tau = G' * \gamma \quad (A2.1)$$

Where:

τ = shear stress (Pa)

γ = strain (%)

G' = Average of the modulus of elasticity of unaerated sludge over 20 mins of measurement time (Pa)

The amounts of stress imposed at two concentrations of digested sludge and four gas flow rates were calculated. Further the stress imposed on digested sludge was compared with the stress imposed by gas injection on WAS at the same concentration and at similar gas flow rate, as shown in Table A2.1.

Table A2.1 suggests that stress imposed by gas injection increases with increasing gas flow rate and decreases with increasing concentration for both types of sludge. However, it also shows that the stress imposed by gas injection is higher for digested sludge than WAS at the same concentration and similar gas flow rate. The reason for this difference in the stress imposed at the same solids concentration and gas flow rate could be related to the different natures of these sludges: digested sludge behaves like an emulsion, and WAS behaves like a gel (Baudez et al. 2013a). This is because colloidal gels have a strong force of attraction between fluid and solid and mostly look like semi-solid to solid material. Moreover, during rheological measurements of colloidal gel, the shear modulus increases with time, indicating a stiffening of the gel, similar to what Guo et al. (2010) reported. Emulsions have a relatively weak force of attraction between solid and liquid and mostly look like liquid materials (Barnes 1994). Thus, because digested sludge behaves like an emulsion, the attraction force between the particles is lower and as a result the stress imposed by gas injection on digested sludge is more than imposed on WAS at the same concentration and gas flow rate.

TABLE A2.1: COMPARISON OF STRESS IMPOSED BY GAS INJECTION ON DIGESTED SLUDGE AND WAS FOR 4% AND 5% OF TOTAL SOLIDS CONCENTRATION AT FOUR GAS FLOW RATES.

Total solids concentration (TS) (g/g)	Gas flow rate (L/min)	Gas velocity (m/s)	Strain imposed (%)	Stress imposed on digested sludge (N/m^2)	Stress imposed on waste activated sludge (N/m^2)
0.04	1	1.82E-03	0.06	4.91	2.67
	3	5.46E-03	0.13	10.65	5.35
	5	9.10E-03	0.2	16.38	7.14
	7	1.27E-02	0.22	18.02	10.71
0.05	1	1.82E-03	0.03	3.40	2.42
	3	5.46E-03	0.09	10.2	3.88
	5	9.10E-03	0.11	12.485	4.85582
	7	1.27E-02	0.15	17.025	9.71164

A2.3.3 Influence of aeration intensity on sCOD

Soluble COD is an important parameter in the performance of an anaerobic digester (Miryahyaei et al. 2018), necessitating the measurement of the impact of gas velocity on sCOD in this research. The percentage change in sCOD at different gas velocities was plotted for two concentrations, as shown in Figure A2.2. An increase in sCOD with an increase in the stress imposed was observed. This increase in sCOD indicates that the stress imposed by gas injection breaks down the digested sludge structure and changes its solubilisation. A similar increase in sCOD with change in sludge structure due to an increase in temperature was observed by Farno et al. (2014).

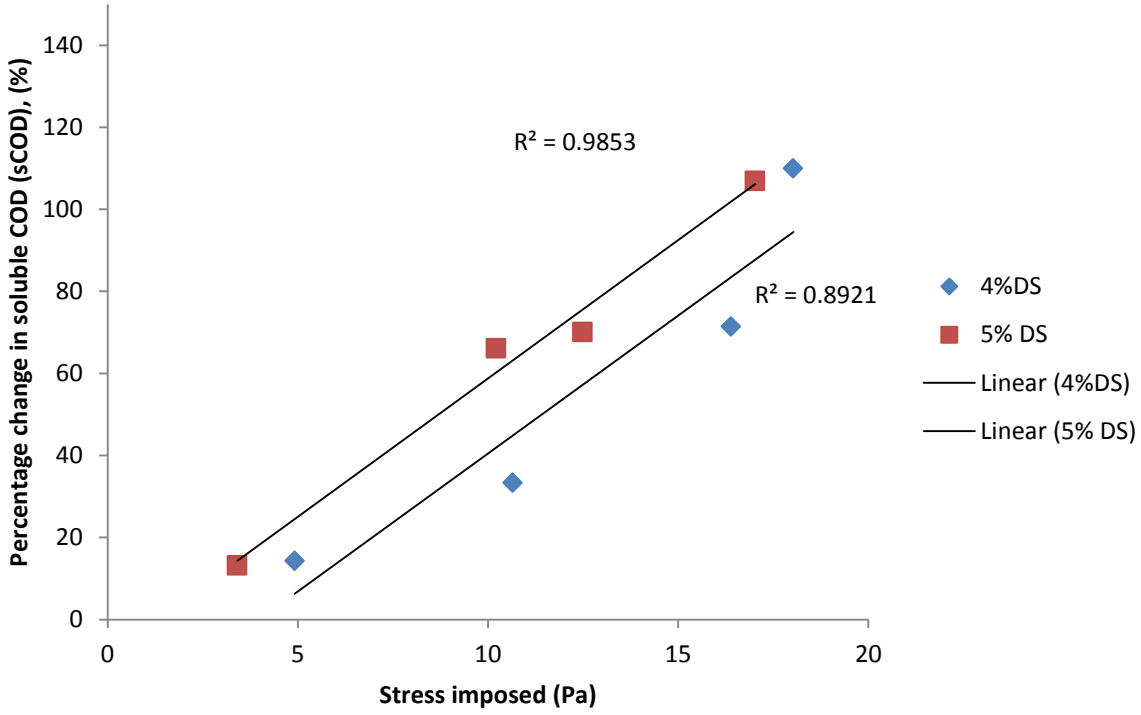

FIGURE A2. 2: PERCENTAGE CHANGE IN SOLUBLE COD DUE TO STRESS IMPOSED BY GAS INJECTION ON DIGESTED SLUDGE WITH TOTAL SOLIDS CONTENT OF 4% AND 5%.

A2.3.4 Influence of aeration intensity on zeta potential

The stability of sludge plays a major role in its settleability within the digester, which in turn affects biogas production and the efficiency of the digester (Rytwo et al. 2014). Thus, the impact of gas injection on the zeta potential of digested sludge was measured for two concentrations and four gas flow rates, as shown in Figure A2.3.

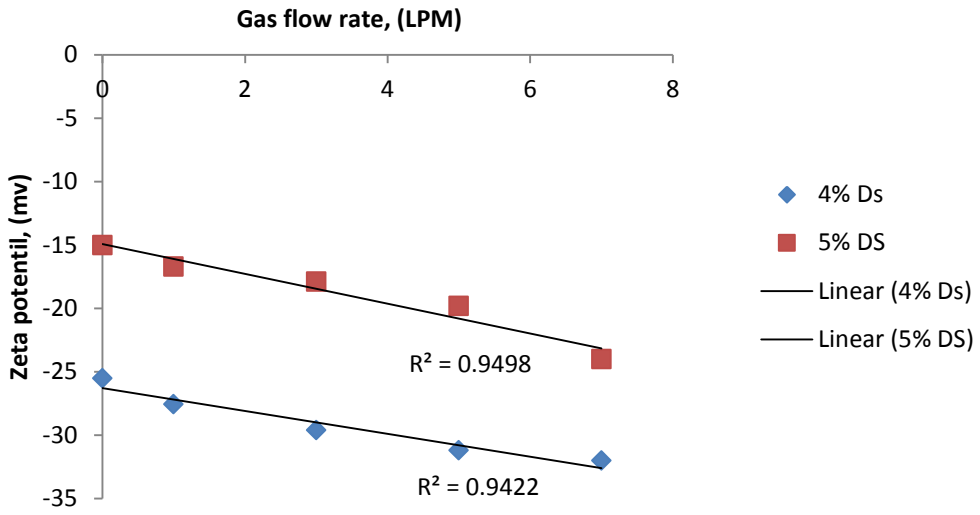

FIGURE A2. 3: IMPACT OF GAS INJECTION ON ZETA POTENTIAL OF DIGESTED SLUDGE WITH SOLIDS CONTENT OF 4% AND 5%.

The zeta potential of digested sludge decreases (becomes more negative) linearly with gas flow rate. This decrease in zeta potential indicates that the sludge is becoming more stable and that the repulsive force is stronger than the attractive force (Lu and Gao 2010). Thus, gas injection alters the sludge structure and changes the stability and settleability of the sludge significantly. Knowledge of how zeta potential changes with gas injection will help to optimise wastewater treatment process parameters, such as mixing speed, to increase the efficiency of the digester.

A2.4 CONCLUSION

Gas injection has substantial impacts on the physiochemical and rheological properties of digested sludge. The viscoelastic modulus of sludge decreased as the gas flow rate increased, resulting in weakening of the sludge structure. The gas flow induced greater shear in digested sludge than WAS, indicating that digested sludge is an easier material to flow than WAS. Moreover, the induced stress increases with increasing gas flow rate for the same concentration, and for the same gas flow rate, shearing intensity decreases with increasing total solids concentration of sludge.

A linear relationship was observed between the change in sCOD and zeta potential of sludge, due to an increase in the stress induced by gas injection. This change in physiochemical properties is due to breakdown of the floc structure. The decrease in zeta

potential values also proved that gas injection modifies the sludge surface by changing the stability of the system. Thus, observing the change in rheological properties due to gas injection intensity improves understanding of the changes in the physicochemical properties of sludge that are responsible for efficient and optimised digester operation.

A2.5 REFERENCES

Barnes, H.A. (1994) Rheology of emulsions — a review. Colloids and Surfaces A: Physicochemical and Engineering Aspects 91, 89-95.

Baudez, J.-C., Gupta, R.K., Eshtiaghi, N. and Slatter, P. (2013) The viscoelastic behaviour of raw and anaerobic digested sludge: Strong similarities with soft-glassy materials. Water Research 47(1), 173-180.

Farno, E., Baudez, J.C., Parthasarathy, R. and Eshtiaghi, N. (2014) Rheological characterisation of thermally-treated anaerobic digested sludge: Impact of temperature and thermal history. Water Research 56, 156-161.

Guo, H., Ramakrishnan, S., Harden, J.L. and Leheny, R.L. (2010) Connecting nanoscale motion and rheology of gel-forming colloidal suspensions. Physical Review E 81(5), 050401.

Lu, G.W. and Gao, P. (2010) Handbook of Non-Invasive Drug Delivery Systems, pp. 59-94, William Andrew Publishing, Boston.

Miryahyaei, S., Olinga, K., Muthalib, F.A.A., Das, T., Aziz, M.S.A., Othman, M., Baudez, J.C., Batstone, D. and Eshtiaghi, N. (2018) Impact of rheological properties of substrate on anaerobic digestion and digestate dewaterability: New insights through rheological and physico-chemical interaction. Water Research.

Monteith, H.D. and Stephenson, J.P. (1978) Mixing Efficiencies in Full-Scale Anaerobic Digesters by Tracer Methods. Water Quality Research Journal 13(1), 135-148.

Rytwo, G., Lavi, R., König, T.N. and Avidan, L. (2014) Direct Relationship Between Electrokinetic Surface-charge Measurement of Effluents and Coagulant Type and Dose. Colloids and Interface Science Communications 1, 27-30.

Vesvikar, M.S. and Al-Dahhan, M. (2005) Flow pattern visualization in a mimic anaerobic digester using CFD. Biotechnology and bioengineering. 89(6), 719-732.